Benzo (Aza) Di- and Tripyrrins, and Their Metal Complexes

Ala Alturk

This thesis is submitted in fulfilment of the requirements of the degree of

Doctor of Philosophy at the University of East Anglia

School of Chemistry

University of East Anglia, Norwich, United Kingdom

January 2025

Declaration

The research described in this thesis is, to the best of my knowledge, original except where due reference is made.

Ala Alturk

2025

Abstract

This thesis continues the investigation of our group's synthesis of benzo-fused aza di- and tripyrrins. The main focus of this work is the complexation of these ligands with various metals. Therefore, symmetrical and unsymmetrical benzo azadipyrrins were successfully synthesised. The synthesis of benzo azatripyrrin was optimised in this work. The success of this objective led to the preparation of these compounds and various derivatives. The path to producing homoleptic complexes faced several obstacles. To solve this problem, many experiments were attempted with various purification techniques.

Complexation of azatripyrrn was not achieved. A range of reaction conditions failed to reach our goal. These conditions were gradually modified until a breakup and decomposition were observed. On the other hand, the complexation of symmetrical and unsymmetrical benzo azadipyrrins proposed other difficulties. The main problems in this path were the produced complexes' purification and stability. Several attempts were made using different metals. Unlike azatripyrrin, successful complexation of azadipyrrin was achieved using palladium metal.

The unsymmetrical azadipyrrin palladium complex was the first to be successfully synthesised and characterised in 1:1. Through ligand modification, a range of complexes containing ferrocene and thiophene groups were synthesised. While these derivatives are highly interesting in the organometallic field, the goal was to study the insertion behaviour of palladium metal. Modifying this successful technique led to the preparation of symmetrical azadipyrrin palladium complexes and their derivatives.

Due to time constraints, these palladium complexation procedures were briefly tested with other metals in the preparation of azadipyrrin complexes. Additionally, test reactions were made to synthesise azatripyrrin palladium complexes. While the results are not conclusive, these tests are the seeds of further work.

This work is dedicated to my parents,

beloved wife and sons

Acknowledgements

First, I would like to express my gratitude to my supervisor, Prof. Andrew N. Cammidge, for his unlimited support during my PhD. I am very grateful for his advice and patience during these years. I have gained more knowledge and experience by dealing with a great scientist and leader. I want to extend my thanks to Dr. Isabelle Fernandes for her time, advice, and support. It has been my pleasure working and learning from you every day. I would also like to acknowledge Dr. David Hughes for his help in the X-ray crystallography service. I would also like to thank the examiners, Prof. Mark Searcey and Dr. G Dan Pantos, for their time and suggestions.

A special thanks to my parents for their unlimited support to my family and me. I would also like to thank my beloved wife. Her unmatched bravery and responsibility during a challenging time for our son made this achievement possible. I thank my sons for providing love and joy during the limited time we spent while achieving this goal. My thanks are extended to my brothers and sisters for their continuous encouragement and support.

I would like to acknowledge all the past and current members of Cammidge's group. I deeply appreciate the time we worked together at the lab and the experiences we shared during the last four years. My thanks are extended to all the members of the chemistry department at UEA.

I am very grateful to Taibah University for the opportunity to obtain this degree and to the Saudi Arabian Cultural Bureau for funding my PhD project.

Contents

List of Figures

List of Schemes

List of Tables

List of Abbreviations

Abs	Absorption
aq.	Aqueous
Ar	aromatic/ aryl
AcOEt	ethyl acetate
b.p	boiling Point
BINAP	2,2′-bis(diphenylphosphino)-1,1′-binaphthyl
Bu	butyl
Conc.	Concentrated
^{o}C	Celsius
d	doublet
dd	doublet of doublets
DBU	1,8-diazabicyclo [5.4.0] undec-7-ene
DCM	Dichloromethane
DMF	N, N-dimethylformamide
DMSO	Dimethyl sulfoxide
Eq.	Equivalent
h	Hour
Hz	Hertz
IR	Infrared
J	coupling constant in NMR spectroscopy
λ	lambda (wavelength)
m	Multiplet
MALDI	matrix assisted laser desorption ionisation
m.p	melting point
Me	Methyl
mmol	milli mole
mol	Mole
MS	mass spectrometry
MW	Microwave
OMe	methoxy
OPh	Phenoxy

PE	petroleum ether
Ph	Phenyl
ppm	parts per million
py	Pyridine
rt	room temperature
s	singlet
SubTBDAP	Sub tri benzo di aza porphyrin
TBTAP	Tetra benzo tri aza porphyrin
t	Triplet
tBu	tertiary butyl
THF	Tetrahydrofuran
UV-Vis	Ultraviolet/Visible spectroscopy
δ	chemical shift in parts per million (ppm)
ε	molar extinction coefficient
λ	Wavelength

1. Introduction

1.1. Dipyrrins

Dipyrrins can be described as "half-porphyrins" because of their electronic, geometric, and structural similarities to porphyrins (figure 1.1).[1] Dipyrromethenes (dpm), pyrromethenes, and dipyrrylmethenes are common names of dipyrrins. The presence of π-conjugation in these bis-pyrrolic systems is an interesting characteristic of these organic chromophores due to the absorption of visible light via π – π* transition.[2-4]

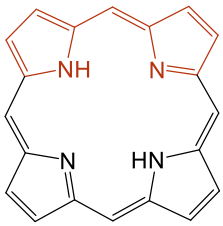

Figure 1.1 free base porphyrin structure with "half-porphyrins" red highlighted as a dipyrrin.[1]

A dipyrrin molecule comprises two pyrrole rings connected via a methine carbon bridge at *α, α'*-position. Based on the recommended IUPAC (1987) nomenclature, positions 1-, 4-, 6-, and 9-, and 2-,3-, 7-, and 8-, are referred to as *α*- and *β*- respectively. By following the naming pattern of porphyrins, position 5- is referred to as *meso*- position (figure 1.2).[5]

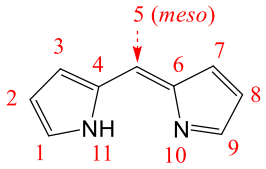

Figure 1.2 IUPAC numbering scheme of dipyrrin unit.[5]

Dipyrrins can be classified into three categories based on the linking position of pyrrole rings (figure 1.3).[5]

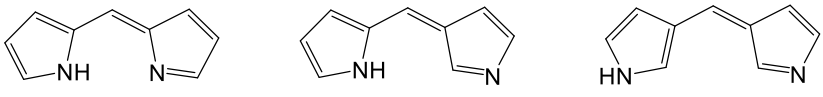

α,α'-linked dipyrrin α,β'-linked dipyrrin β,β'-linked dipyrrin

Figure 1.3 types of dipyrrine.[5]

Also, the oxidation of dipyrromethanes can yield three different possible isomers of dipyrrins (figure 1.4).[5] The geometric isomer (I) was found to be the most stable due to the intramolecular hydrogen bonding (N–H···H). The tautomerization of this highly conjugated system, the proton

transfer between the nitrogen atoms, is strongly affected by the substituents present on the pyrrole ring (figure 1.5).[6]

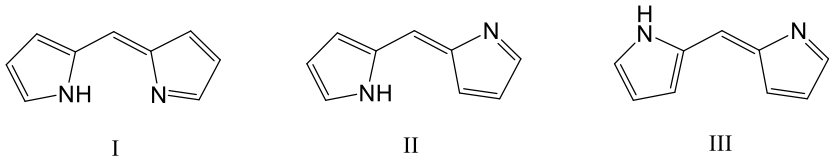

I II III

Figure 1.4 Geometrical isomers of dipyrrins.[5]

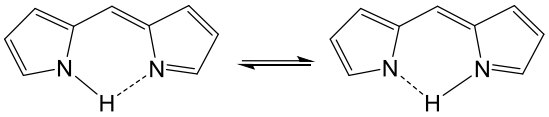

Figure 1.5 Tautomeric structures of dipyrrins.[6]

In 1914, dipyrrins were first reported by Piloty.[7] Hans Fischer advanced the chemistry of these compounds in the synthesis of porphyrins.[8] Because of their ease of synthesis, interesting photophysical properties, and diverse architectures, dipyrrin is an essential field in chemical research.[9] Moreover, dipyrrins' monoanionic and bidentate ligand scaffold provided stable, highly crystalline, and neutral complexes with different metals. 4,4-difluoro-4-bora-3a,4a-diaza-s-indacene (BODIPY) is the most stable and popular dipyrrin complex with exceptional optical properties (figure 1.6).[10] The unique chemical properties of this compound have found many applications in the development of photovoltaics, bio-imaging, and dynamic therapy.[11-13]

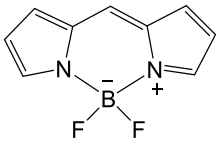

Figure 1.64,4-difluoro-4-bora-3a,4a-diaza-s-indacene (BODIPY).[10]

Because of facile reactions, the development of metal dipyrrin complexes research has advanced over BODIPY. This advancement led to various investigations in supermolecules, coordination polymers, and metal-organic frameworks (MOFs).[14-19] These complexes were found to have great potential as catalysts,[20, 21] sensors,[22] staining agents,[23] MOFs,[19, 24, 25] and light harvesting materials.[26]

1.1.1. Synthesis of dipyrromethene

The literature is rich with synthesis methods to prepare substituted and unsubstituted dipyrrins starting from pyrroles. By reacting 2-formylpyrrole with 2-unsubstituted pyrrole in

the presence of a strong acid, asymmetrical 5-unsubstituted dipyrrins can be formed (scheme 1.1 a).[27, 28] Additionally, the synthesis of asymmetrical 5-unsubstituted dipyrrins was achieved under acidic conditions by reacting suitably substituted pyrrole carbinyl cation with 2-unsubstituted pyrrole. This method involves an oxidation step of dipyrromethane to obtain the targeted dipyrrin (scheme 1.1 b).[29, 30]

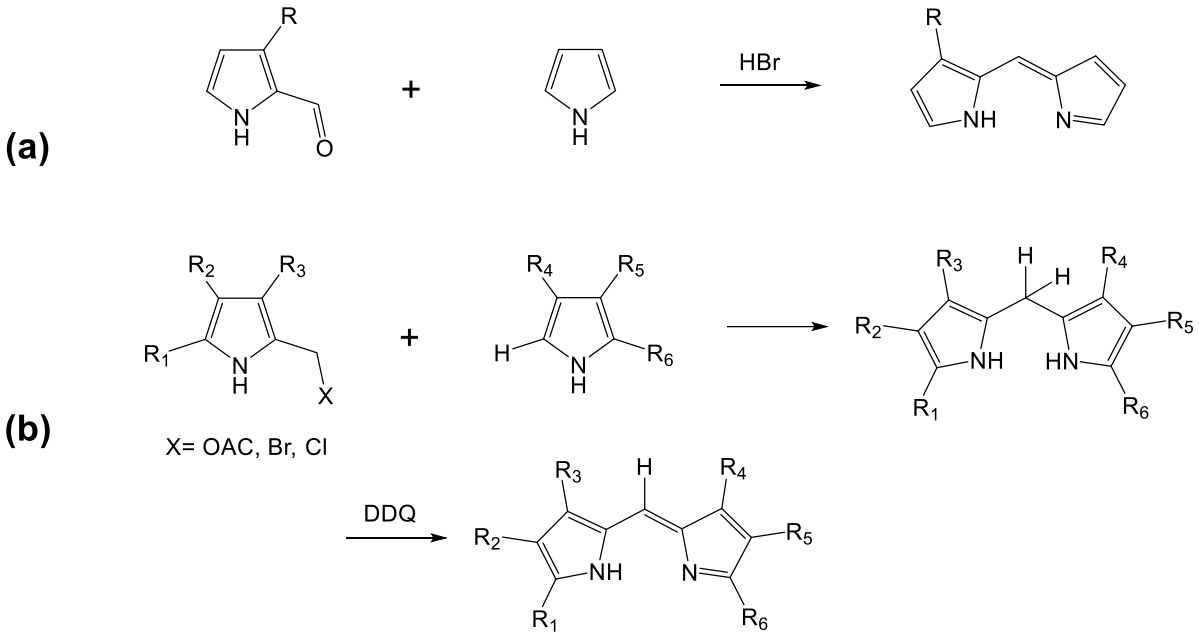

Scheme 1.1 Synthesis of 3- and 5-unsubstituted dipyrrins.[27-30]

5-substituted dipyrrins were achieved by condensation reaction of two equivalents of 2-unsubstituted pyrrole with carboxylic acid or acid halide while using a catalytic amount of HBr (Scheme 1.2 a).[31] 5-aryl substituted dipyrrins were also prepared by condensation of aldehydes with an excess of pyrrole and catalytic amounts of Lewis acid catalysts ($InCl_3$, CF_3COOH). The product of this step was then oxidized to obtain the targeted dipyrrin (Scheme 2.1 b).[32, 33] Lindsey and co-workers were the first to report N-confused (α,β'- linked) and doubly N-confused dipyrrins (β, β'- linked). By acid-catalyzed condensation reaction of benzaldehyde in excess of pyrrole, dipyrromethane, N-confused dipyrromethane, and tripyrrane were obtained (Scheme 1.3).[34]

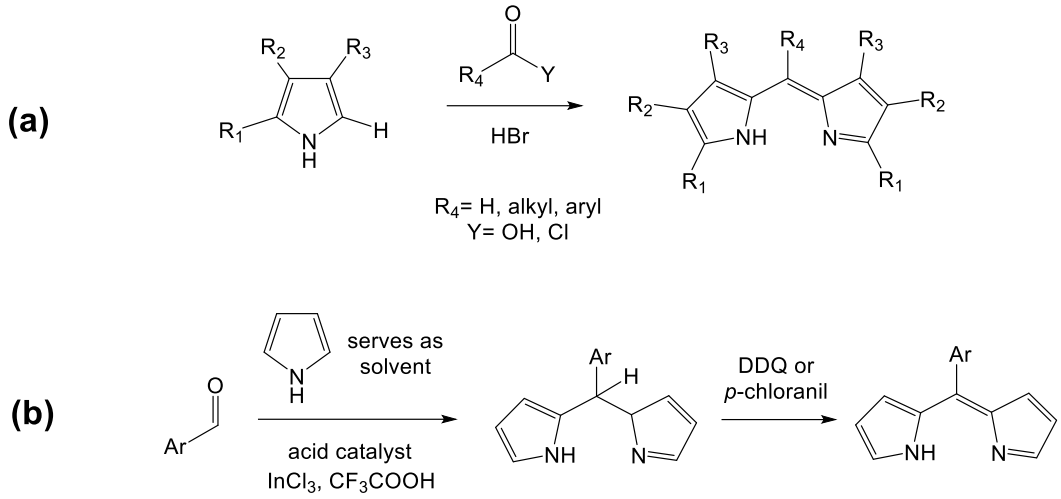

Scheme 1.2 Synthesis of 5-aryl/alkyl substituted dipyrrins.[31-33]

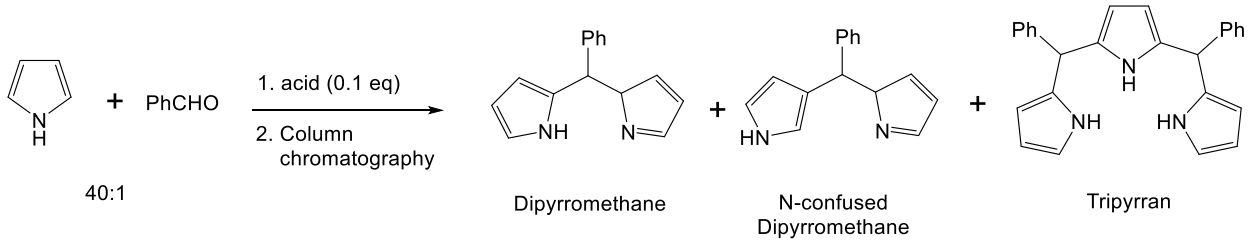

Scheme 1.3 synthesis of N-confused dipyrromethene.[34]

1.1.2. Synthesis of benzo-fused dipyrromethene

Several strategies have been developed to prepare benzo-fused dipyrromethene to synthesize BODIPYs (figure 1.7).[35] BODIPYs are known for their remarkable photophysical properties and are an essential class of fluorophores discovered in 1968 by Treibs and Kreuzer.[9, 36]

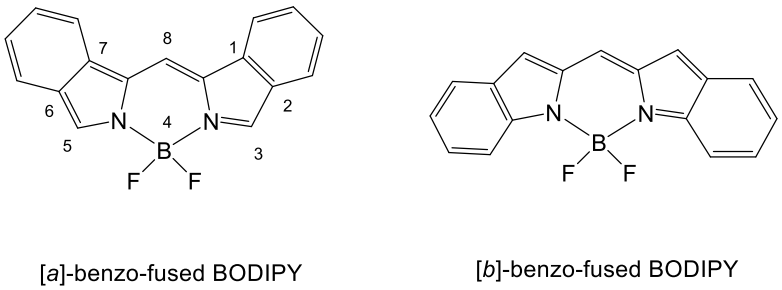

Figure 1.7 Structures of [*a*]- and [*b*]-benzo-fused BODIPYs.[35]

In 1995, Kand and Hangland reported the synthesis of diisoindole BODIPYs.[37] The benzo-fused dipyrrin was prepared according to the Paal-Knorr procedure. 2-acylacetophenone was synthesized by the reaction of o-hydroxy-acetophenone derivatives with N-arylhydrazones

followed by the treatment with lead(IV) salt.[38, 39] A condensation reaction of the resulting compound in the presence of ammonia or ammonium salts produced [*a*]-benzo-fused dipyrrin (Scheme 1.4).[40] Kand and Hangland reported several BODIPYs using this method of preparing benzo-fused dipyrrin (figure 1.8).

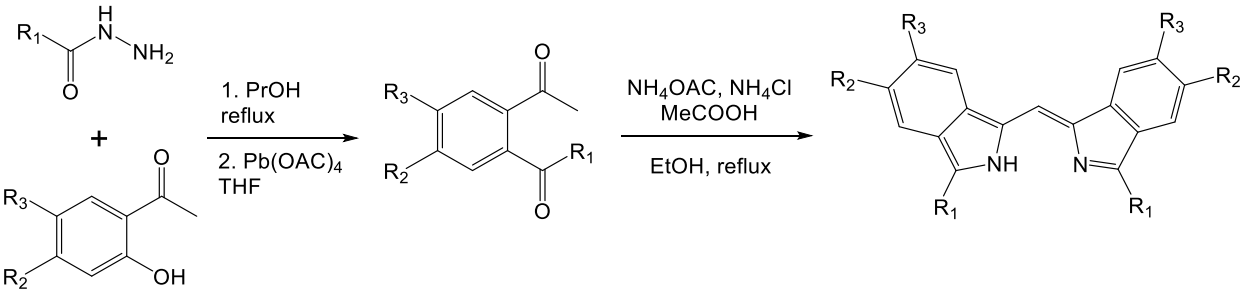

Scheme 1.4 synthesis of [a]-benzo-fused dipyrrin.[40]

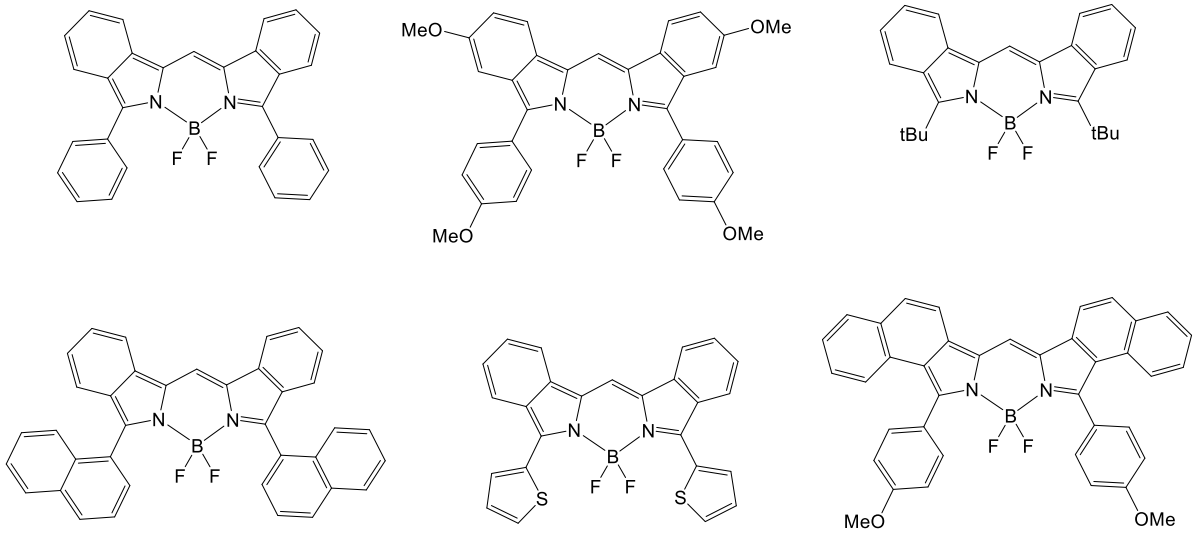

Figure 1.8 Examples of some diisoindole-BODIPYs synthesized by Kand and Haugland using the Paal–Knorr strategy.[35]

Kubo and co-worker reported their benzo-fused dipyrrin in the synthesis of BODIPY by using Paal–Knoor strategy. Tetramethoxy-substituted and benzo-fused dipyrrin was successfully synthesized via a multi-step procedure according to Scheme 1.5.[41]

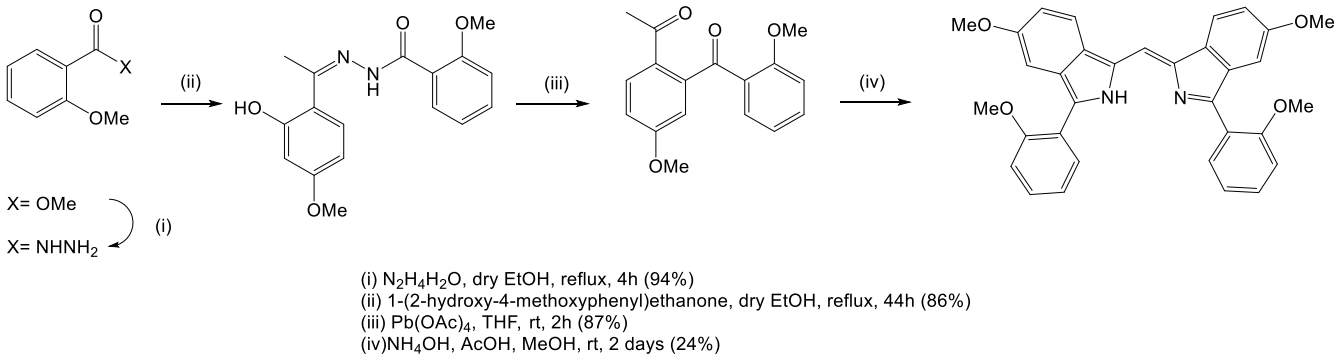

Scheme 1.5 Synthesis of tetramethoxy-substituted and benzo-fused dipyrrin by Kubo and co-workers.[41]

Many examples of preparing *meso*-free benzo-fused dipyrrin were reported using the Paal-Knorr strategy.[42, 43] The synthesis of benzo-fused dipyrrin was reported via a modified Barton-Zard reaction strategy. The Barton-Zard reaction involves the reaction of isocyanoacetate esters and activated arenes/alkenes in the presence of a non-nucleophilic base (Scheme 1.6).[44]

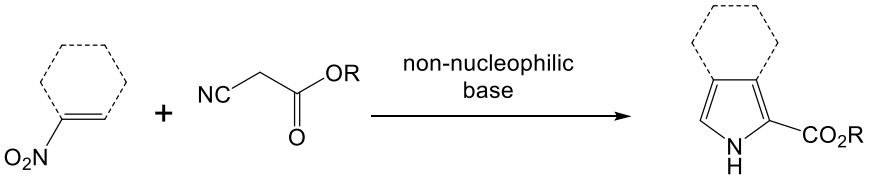

Scheme 1.6 Barton-Zard reaction.[44]

A disadvantage of this method is that it is expensive and malodorous because of the isocyanide. Also, the low reactivity of nitrobenzene prevents the attainment of the targeted 9-nitrophenanthrene.[45] In 2007, Vinogradov, Cheprakov, and co-workers reported successfully synthesizing 2-Substituted-4,7-dihydroisoindoles via a modified Barton-Zard reaction starting from 1-tosyl-1,4-cyclohexadiene.[46] The successful synthesis of dibenzo-dipyrrin was reported in 2010 by the subsequent oxidization of the obtained idoindoline (Scheme 1.7).[22]

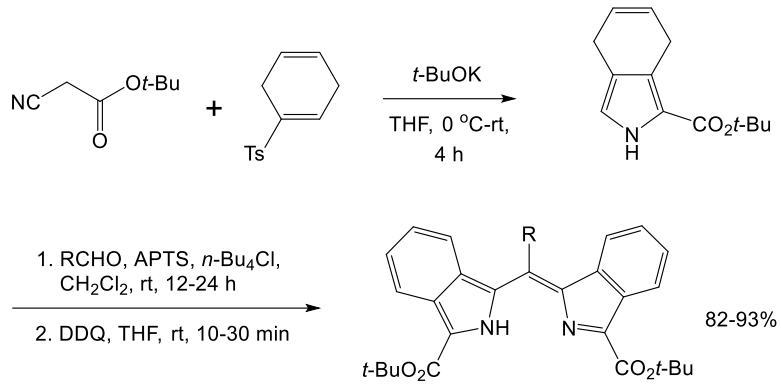

Scheme 1.7 Synthesis of dipyrrins starting from 4,7-dihydroisoindole obtained via the Barton-Zard reaction.[22]

In the development of π-extended diisoindole-BODIPY, Shen, You, Rurack, and co-workers used Barton-Zard methodology.[47] The starting dibenzo-isoindole was successfully prepared with a 78% yield from isocyanoacetate.[48] The π-extended dipyrrin was obtained by condensation reaction with various aromatic aldehydes followed by oxidation with DDQ and treatment with $BF_3.Et_2O/NEt_3$ (Scheme 1.8).

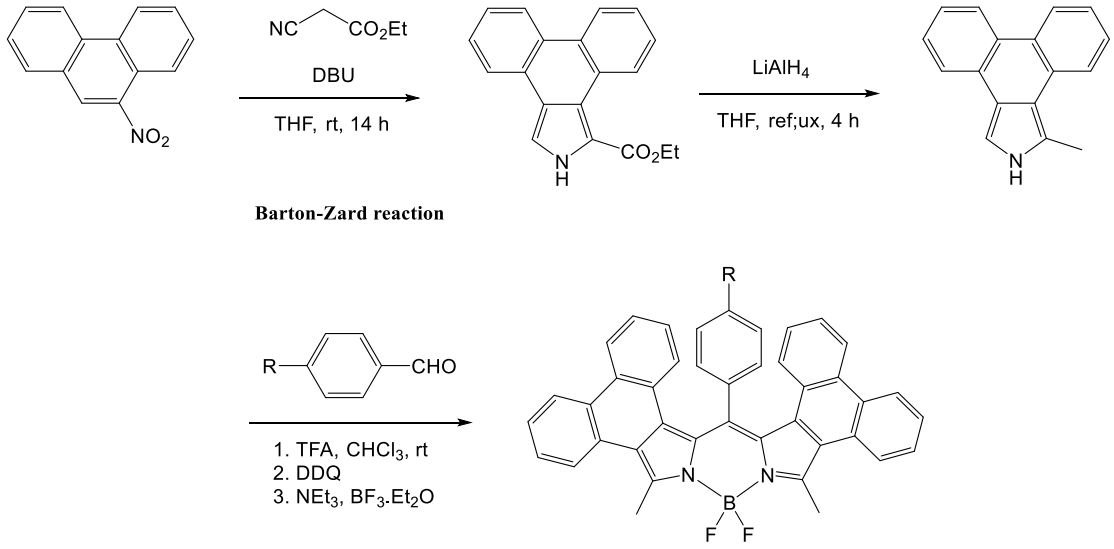

Scheme 1.8 phenanthrene-fusedBODIPY by Rurack and co-workers.[47,48]

The instability of some isoindoles has challenged the synthesis of benzo-fused dipyrrin via a straightforward condensation of the isoindole moiety. Therefore, precursors of "masked" isoindoles were utilized to overcome the instability issues.[35] This strategy of preparing benzo-fuzed dipyrrin is referred to as the retro Diels-Alder reaction on a ''masked'' isoindole precursor. In the late 90s, Ono and co-workers reported the synthesis of a ''masked'' isoindole by a Diels-Alder reaction between cyclopentadiene or cyclohexadiene and *β*-sulfonylnitroethylene followed by a Barton–Zard reaction with ethyl isocyanoacetate.[49] In

2001, Ono and co-workers applied this method to prepare diisoindole-BODIPY. By the reduction of the ester on the ‘‘masked’’ isoindole using $LiAlH_4$, the reaction with acyl chloride, and treatment with Et_2N and $BF_3.Et_2O$, BODIPYs with fused bicyclo[2.2.2]octadiene units were obtained. The compound then converted to diisoindole-BODIPYs via retro Diels-Alder reaction (Scheme 1.9).[50]

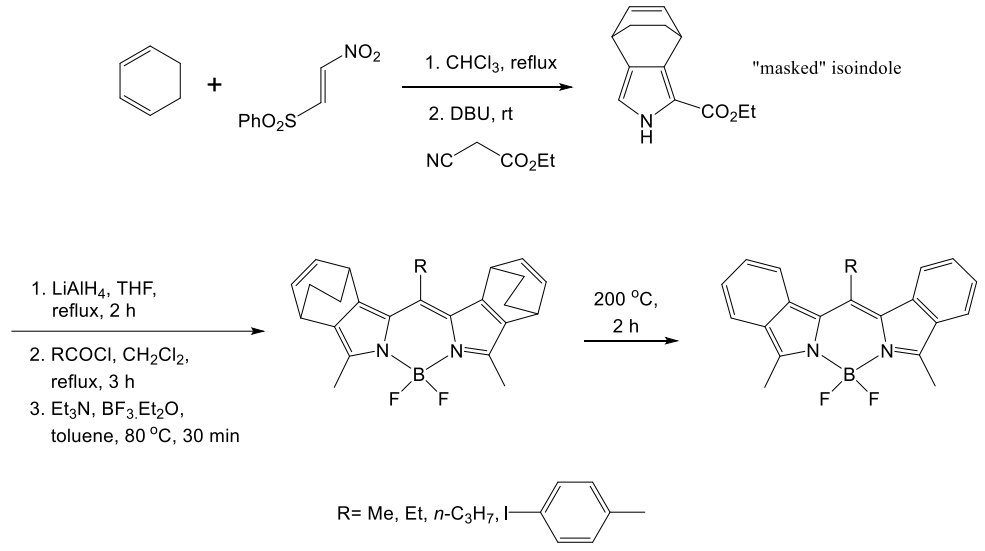

Scheme 1.9 Synthesis of diisoindole-BODIPYs by a retro Diels-Alder reaction.[50]

Another example of utilizing “masked” isoindole in a retro Diels-Alder strategy was reported by Okujima and co-workers. They reported good yields for the reaction of isoindole precursor with aromatic boronic acids using Suzuki-Miyaura reactions. The condensation with aromatic aldehyde and complexation with boron of the obtained product were followed by thermal treatment successfully produced diisoindole-BODIPYs (Scheme 1.10).[51]

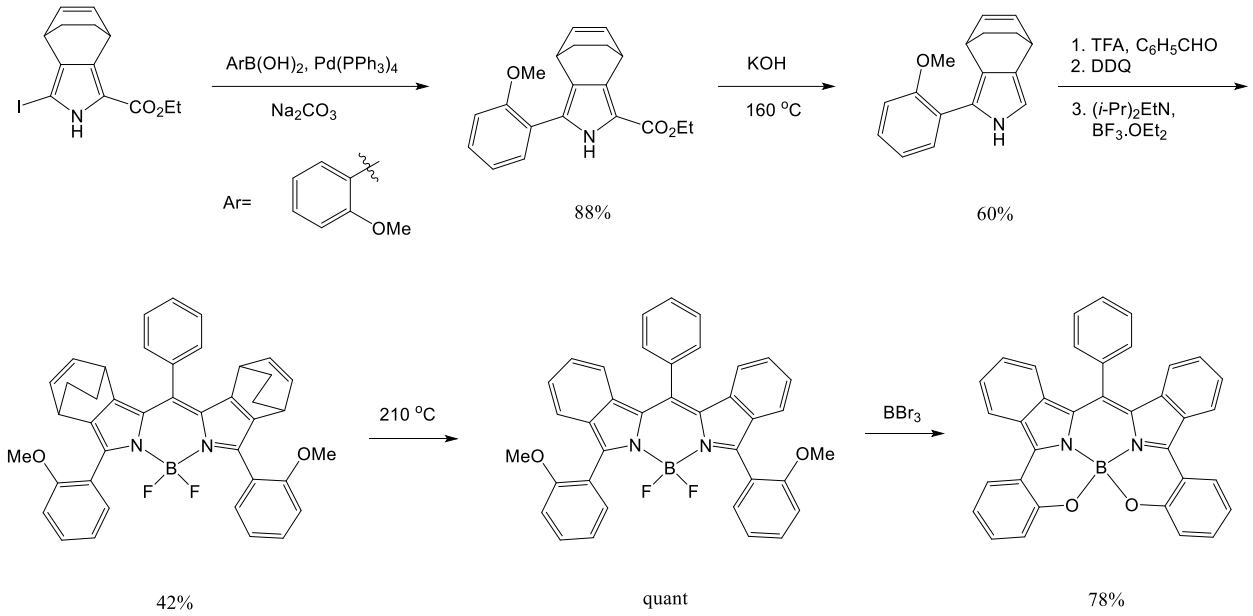

Scheme 1.10 Functionalization of the ‘‘masked’’ isoindole and synthesis of the O-chelated diisoindole-BODIPY reported by Okujima and co-workers.[51]

Another strategy for preparing benzo-fused dipyrrin is the Vilsmeier-Haack method. This synthesis route utilizes disubstituted isoindoles, originally proposed by Von Dobeneck in 1969 and later used for synthesizing benzoporphyrins and phthalocyanines.[52, 53] The halogen atom in the α-position provided the functionalization options via cross-coupling or nucleophilic substitution reactions (Scheme 1.11).

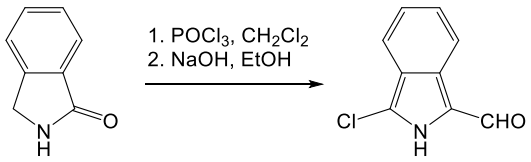

Scheme 1.11 Synthesis of disubstituted isoindole using Vilsmeier-Haack reaction.[52,53]

This method provided the opportunity to synthesize unsymmetrical benzo-fused dipyrrins to prepare isoindole BODIPYs. Jiao and co-workers reported the successful synthesis of unsymmetrical isoindole-BODIPYs using the Vilsmeier-Haack reaction starting from 3-halogeno-1-formylisoindole. Further functionalization by Sonogashira coupling and nucleophilic substitution reactions were efficiently performed, obtaining several unsymmetrical isoindole-BODIPYs derivatives (Scheme 1.12).[54]

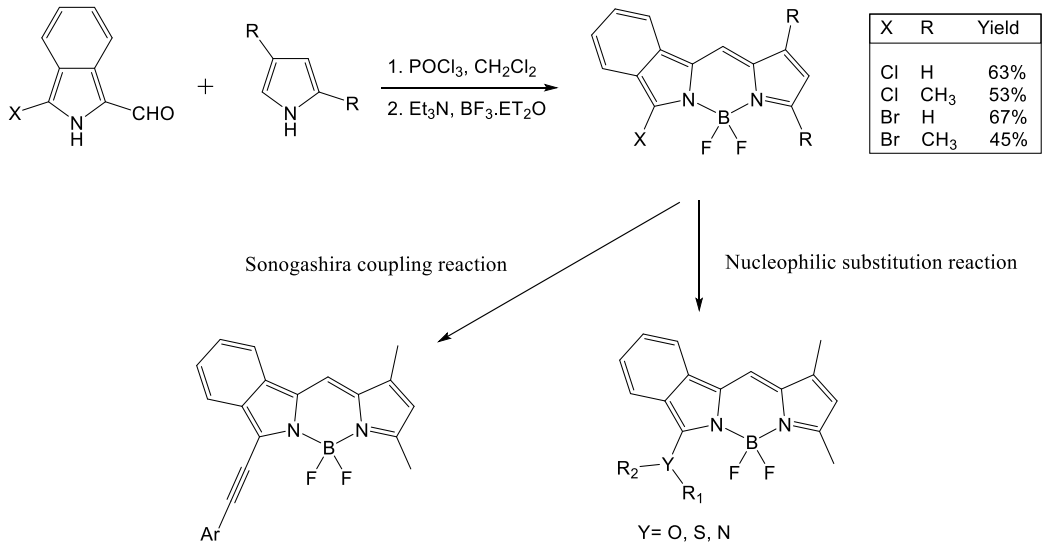

Scheme 1.12 Synthesis and Functionalization of 3-halogenated unsymmetrical isoindole BODIPYs.[54]

The same author reported *meso*-substituted unsymmetrical isoindole-BODIPYs with a pyrrole group on position 3. The formation of a carbon-carbon bond at the 3-position was performed in one step via non-metal catalyzed nucleophilic aromatic substitution reaction (Scheme 1.13).[55, 56]

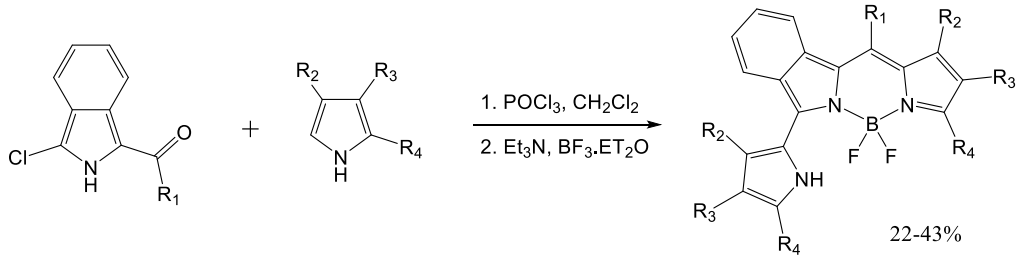

Scheme 1.13 Metal-free catalyzed one-step syntheses of 3-pyrrole substituted unsymmetrical isoindole-BODIPYs.[55,56]

Maeda, Ema, and co-workers reported another unsymmetrical benzo-fused dipyrrin starting from carbazole derivatives. They selectively functionalized the 1-position of the carbazole via Ir-catalyzed direct borylation. The unsymmetrical dipyrrin was then synthesized by reacting the functionalized carbazole with disubstituted isoindoles via Suzuki-Miyaura cross-coupling reaction. Followed by complexation with boron, carbazole-BODIPY was obtained (Scheme 1.14).[57]

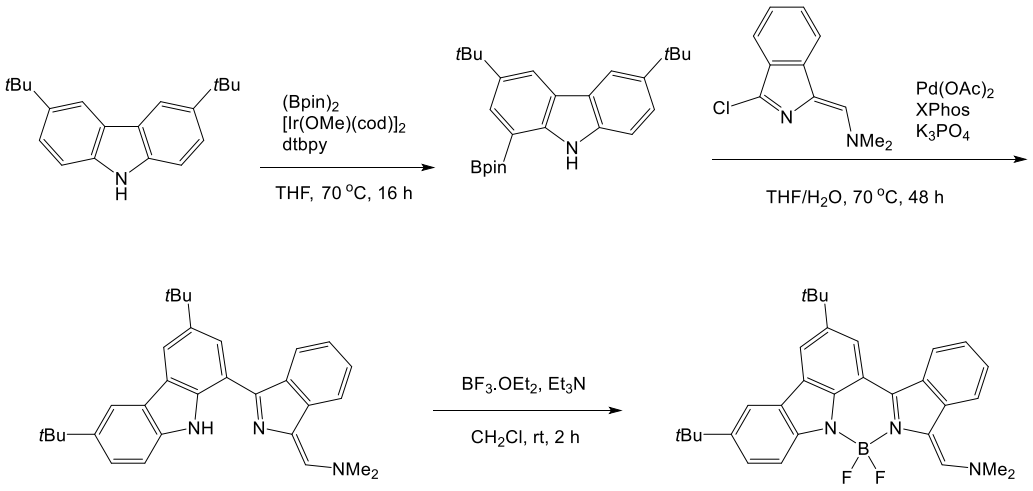

Scheme 1.14 Synthesis of carbazole-BODIPY.[57]

Hao, Jiao, and co-workers reported the synthesis of symmetrical 3,5-diarylbenzo dipyrrins and their boron complexes. These symmetrical compounds were prepared from commercial isoindoline-1-one via Vilsmeier–Haack, Suzuki coupling, and $POCl_3$-promoted self-condensation reactions (Scheme 1.15).[58]

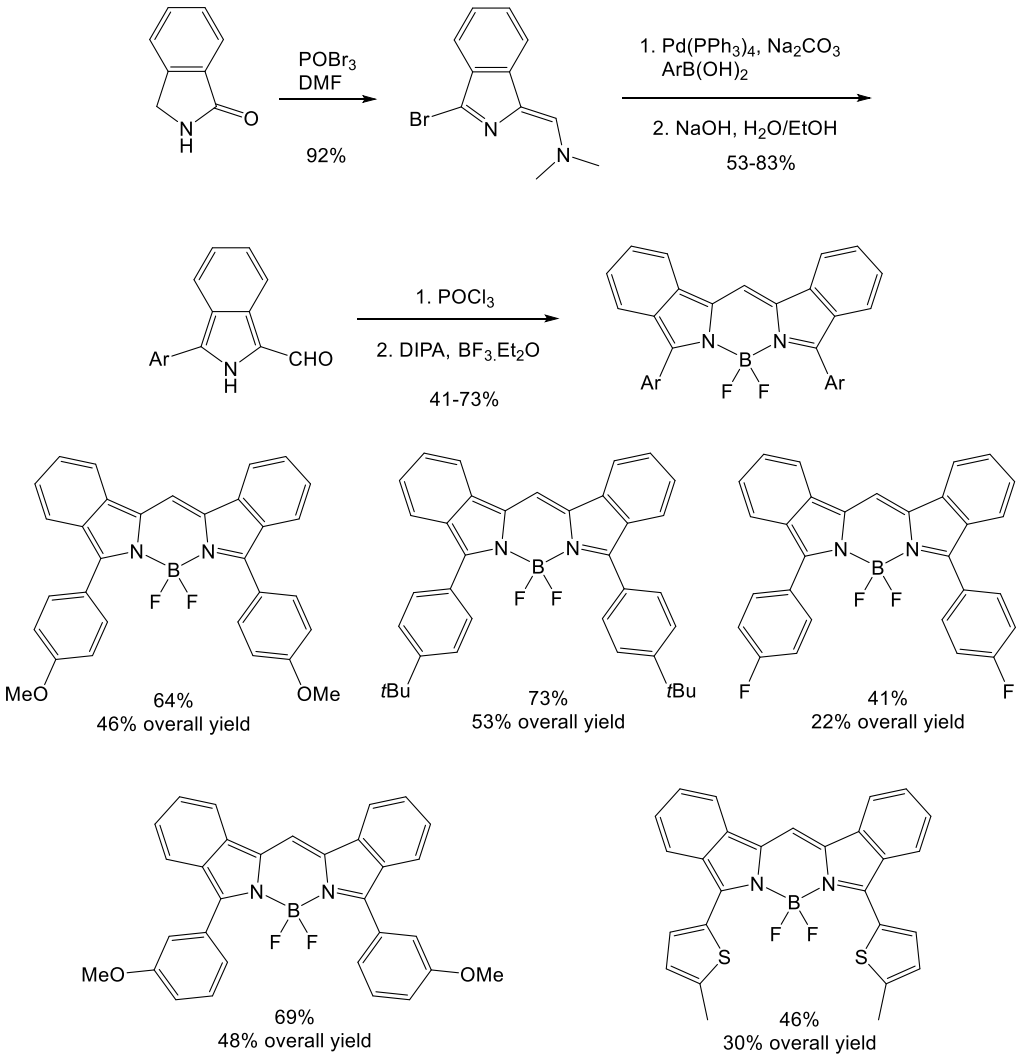

Scheme 1.15 Synthesis of 3,5-diarylbenzoBODIPYs from commercial isoindolin-1-one.[58]

Different strategies were developed to synthesize benzo-fused dipyrrins in the research of BODIPY. Barton-Zard reaction is used mainly for the construction of aromatic-fused pyrroles. Retro Diels-Alder reaction is performed on ‘‘masked’’ isoindole precursor. *Meso*-free BODIPYs are commonly prepared by the Paal-Knorr reaction. The Vilsmeier-Haack reaction allows the preparation of unsymmetrical BODIPYs.

1.2. Azadipyrrins

Also known as aza dipyrromethene, azapyrrin consists of two pyrrole rings connected via a nitrogen bridge (figure 1.9). It was first reported in the 1940s but was not extensively explored.[59] However, the interest in finding compounds with far-red or NIR region surged the research into the application of aza dipyrromethenes over the last few decades.[60]

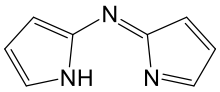

Figure 1.9 Structure of azapyrrin

Rogers reported the first synthetic method in 1943 by attempting a Leuckart reaction.[61] Ammonium formate was heated with 4-nitro-1,3-diphenylbutan-1-one under solventless conditions, producing an intense blue-coloured material. A similar result was observed when using 4-oxo-2,4-diphenyl butane nitrile. The new chromophoric system has a formal relationship to the phthalocyanines (Scheme 1.16).[62]

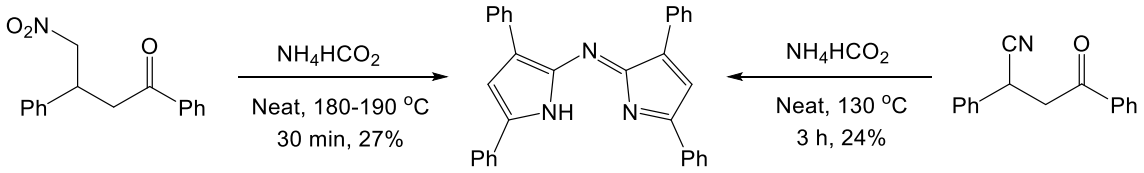

Scheme 1.16 Synthesis of azadipyrrin by Rogers.[62]

The O'Shea group optimized the synthesis of azadipyrrins using different ammonium sources. Aryl-substituted 4-nitro-1,3-diphenylbutan-1-one was refluxed in either ethanol or butanol in the presence of ammonium acetate instead of ammonium formate. This procedure improved the yield, while the precipitation of the formed azapyrrin in alcohol solvents enabled easier product isolation. Several derivatives were successfully synthesized using this method (Scheme 1.17).[63, 64]

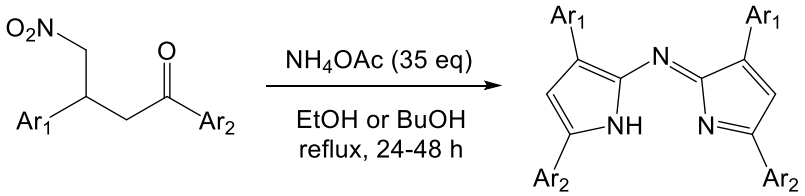

Ar_1	Ar_2	Time	yield%
Ph	Ph	48 h	42%
Ph	p-OMePh	24 h	47%
p-OMePh	Ph	48 h	48%
p-BrPh	Ph	48 h	24%

Scheme 1.17 The synthesis of azadipyrrins by the O'Shea group.[63,64]

A method to synthesize unsymmetrical azadipyrrins was developed on a condensation reaction of diaryl pyrroles and nitroso diaryl pyrroles in a mixture of acetic anhydride/acetic acid at 100 °C. By cooling the reaction mixture with ice, extracting with DCM, and slowly

evaporating the solvent at room temperature, pure unsymmetrical azadipyrrin was obtained as dark blue material (Scheme 1.18).[65]

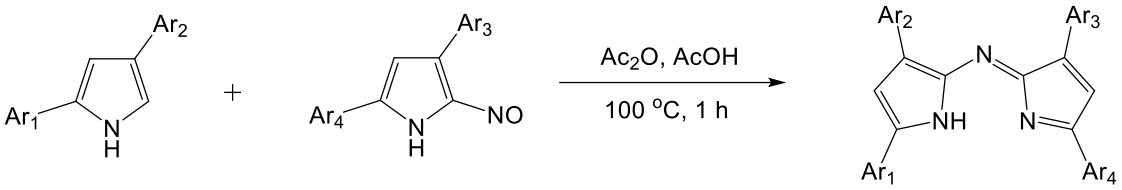

Ar_1	Ar_2	Ar_3	A_4	yield%
Ph	Ph	p-$MeNC_6H_4$	Ph	35%
Ph	Ph	p-BrC_6H_4	Ph	92%
Ph	Ph	p-$Et_2NCH_2C_6H_4$	Ph	94%
p-$MeOC_6H_4$	Ph	Ph	p-$MeOC_6H_4$	72%
Ph	p-FC_6H_4	p-$Et_2NCH_2C_6H_4$	p-$MeOC_6H_4$	88%
Ph	p-FC_6H_4	Ph	p-$MeOC_6H_4$	94%

Scheme 1.18 Synthesis of unsymmetrical azadipyrrins.[65]

1.2.1. Synthesis of benzo-fused aza dipyrromethene

In 1972, Vollman reported the first synthesis of benzo-fused aza dipyrromethene. This method relied on reacting phthalonitrile with 2.5 equivalents of aryl magnesium bromides in dry benzene at room temperature. Low to moderate benzo-fused aza dipyrromethenes yields were obtained using steam distillation and recrystallisation from pyridine (Scheme 1.19).[66]

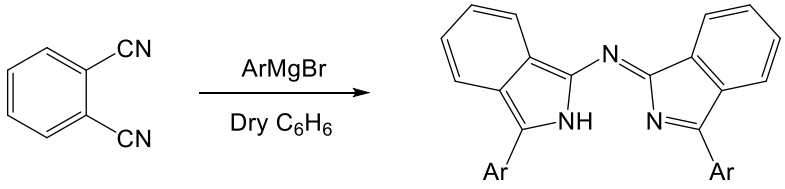

Ar= phenyl 34%
4-CH_3 phenyl 24%
4-OCH_3 phenyl 7%

Scheme 1.19 Vollman Synthesis of benzo-fused azadipyrrin.[66]

Carreira and co-workers reported, in 2005, a method using a ring-fused pyrrole precursor to synthesize a new azadipyrrin. This compound was developed to prepare aza-BODIPY. While the boron complex was obtained with a high yield, this method was considered inefficient due to the multiple-step synthesis of ring-fused pyrroles (Scheme 1.20).[67, 68]

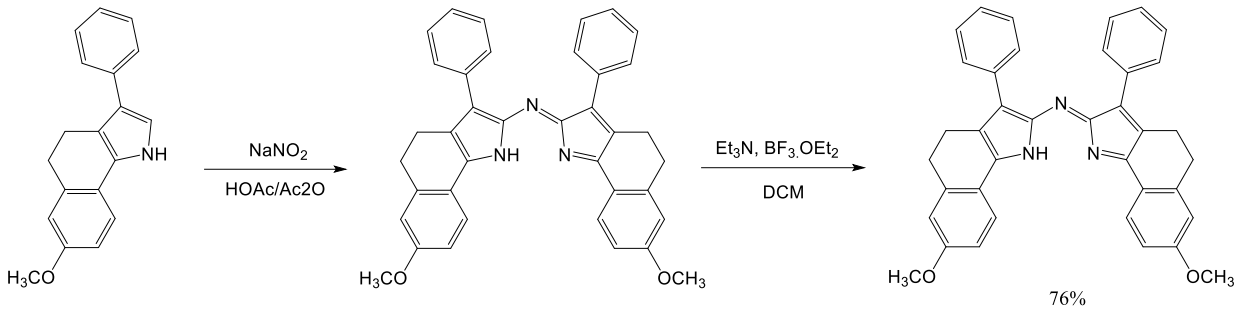

Scheme 1.20 Ring-fused azadipyrrin and aza-BODIPY.[67,68]

Mack et al. reported another example of applying this route of synthesis. In their work, 1,2-dicyanoacenaphthylene was prepared according to Rieke and co-workers' method.[69] This dinitrile was then used to prepare acenaphthalene fused-ring-expanded azadipyrrin and the boron complex (Scheme 1.21).[70]

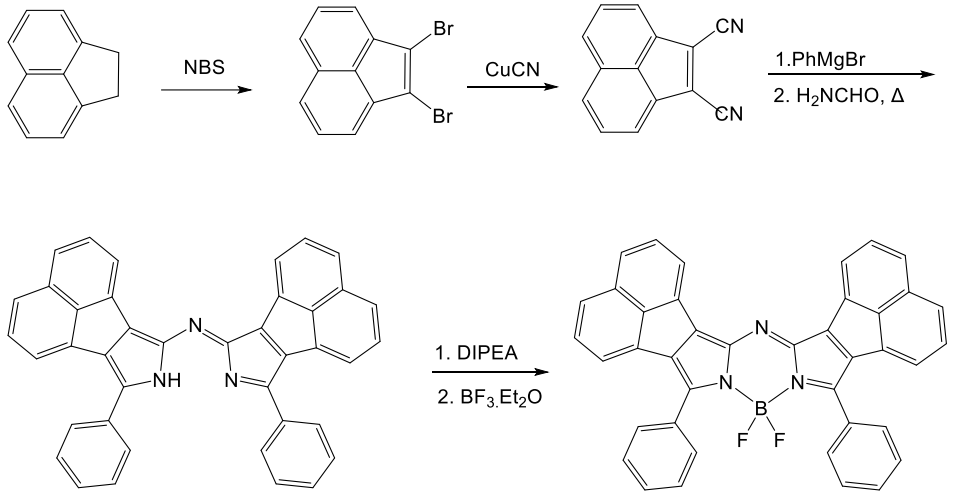

Scheme 1.21 Synthesis of the acenaphthalene fused-ring-expanded aza-BODIPY by Mack et al.[70]

Another strategy for preparing benzo-fused azapyrrins was designed around a lithiated benzonitrile in the *ortho*-position to the cyano group. This procedure was performed by using LDA at low temperatures.[71] The produced lithiated benzonitrile was subsequently coupled with a second benzonitrile molecule. The targeted benzo-fused aza dipyrromethenes were obtained by a condensation reaction of the intermediate, followed by reduction with formamide (Scheme 1.22).[72]

Shen and co-workers reported the synthesis of unsymmetric aza diisoindolylmethenes and their boron complexes. They established the synthesis by treating phthalonitrile with a solution of potassium *tert*-butoxide in dry dimethylformamide (DMF) for 3 hours at 0 °C. Then, the primary amine of the obtained compound was converted to a tertiary amine through

treatment with dimethylamine in tetrahydrofuran (THF). The targeted unsymmetric aza diisoindolylmethenes was successfully synthesized with a 69 % yield (Scheme 1.23).[73]

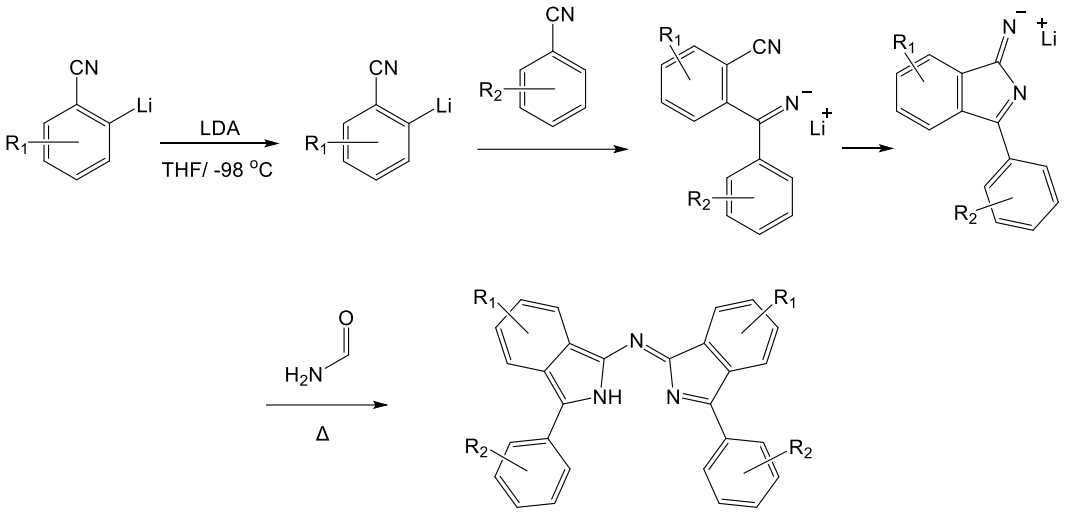

Scheme 1.22 New synthesis of benzo-fused aza dipyrromethene from aromatic nitriles.[72]

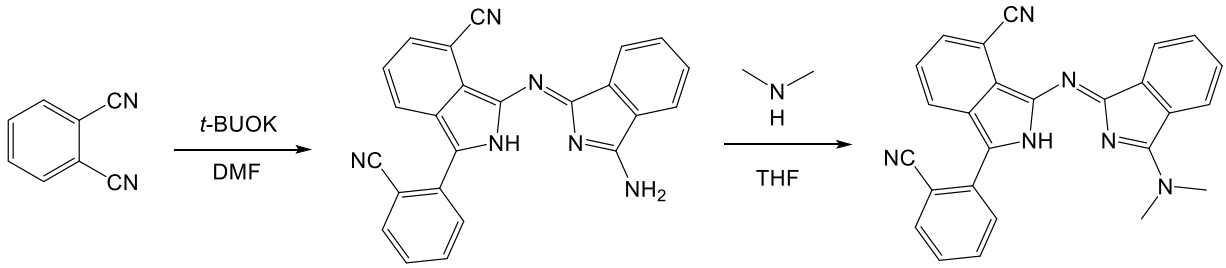

Scheme 1.23 Synthesis of unsymmetric aza diisoindolylmethene by Shen and co-workers.[73]

Our group has developed a new pathway to synthesize aza diisoindolylmethenes and their corresponding aza-BODIPY derivatives. Aminoisoindolines were prepared through a palladium-catalyzed cross-coupling reaction of a precursor amidine with various aryl acetylenes.[74] Then, synthesizing π extended aza (dibenzo) dipyrromethene derivatives was successfully achieved through efficient self-condensation of the obtained aminoisoindolines.[75] The self-condensation procedure was performed by heating the aminoisoindoline under reflux in toluene. The product of deep red crystals was recovered by crystallization from dichloromethane and methanol with high yield. Additionally, corresponding aza (dibenzo) BODIPY analogues were successfully obtained in moderate yield by a treatment with $BF_3 \cdot OEt_2$ (Scheme 1.24).[76]

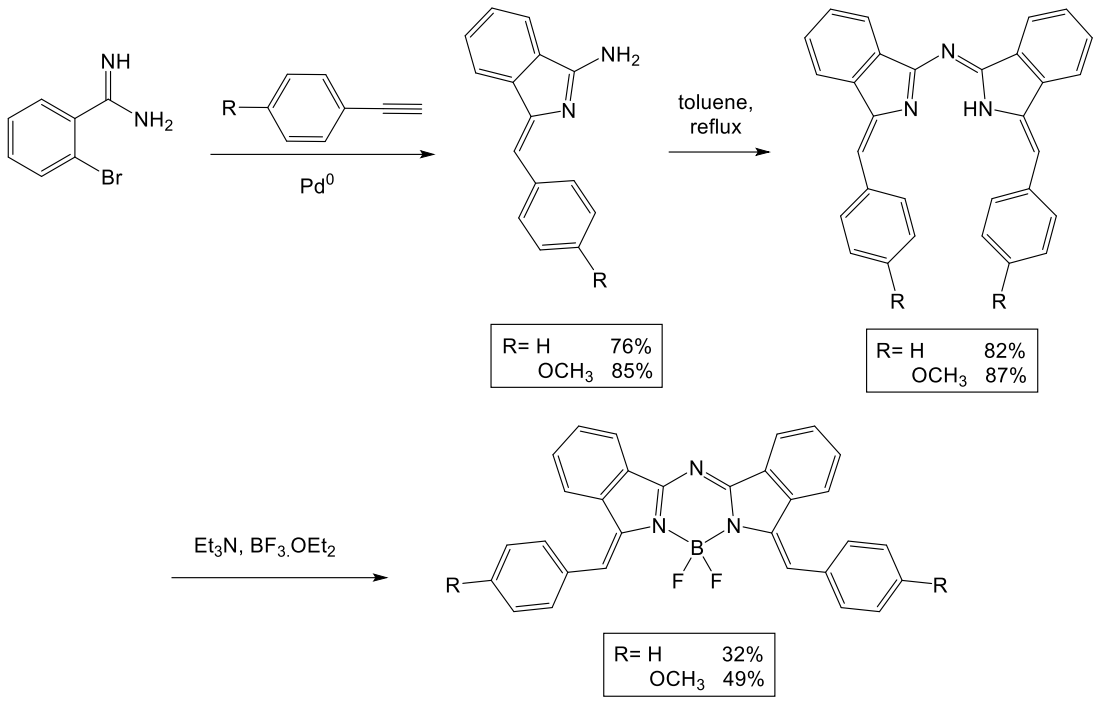

Scheme 1.24 Synthesis of aza diisoindolylmethene aza BODIPYs from aminoisoindolines.[76]

1.3. Complexation of dipyrrins

The dipyrrin scaffold, being fully conjugated and monoanionic, provides access to various metal ions to form homo and heteroleptic complexes (Scheme 1.25).[8] The structure of these complexes displayed diverse geometries affected by the nature of central metal. Moreover, the geometry of $M(dpm)_2$ complexes depends on the steric interaction between α-substituents on the dipyrrin core. These geometries range from square planar to tetrahedral or distorted tetrahedral.[33]

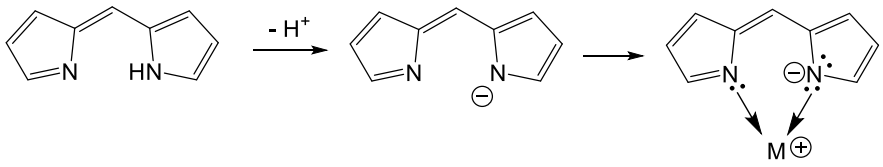

Scheme 1.25 Depicting deprotonation of dipyrrin and metal binding.[8]

Fergusson et al. reported a Pd(II) complex displaying an almost square planar geometry. While palladium metal promotes a square planar geometry, the steric repulsion between α-methyl groups on the dipyrrin forced a stepped arrangement around the central metal to avoid overcrowding.[77] $Zn(dpm)_2$ was found to have a tetrahedral environment, while Cu(II) and Ni(II) complexes with dipyrromethenes adopted distorted tetrahedral geometry.[16, 78-80]

However, a square planer $Ni(dpm)_2$ was reported by Pogozhev et al. despite the repulsion between α-CH of two dipyrrin units.[81]

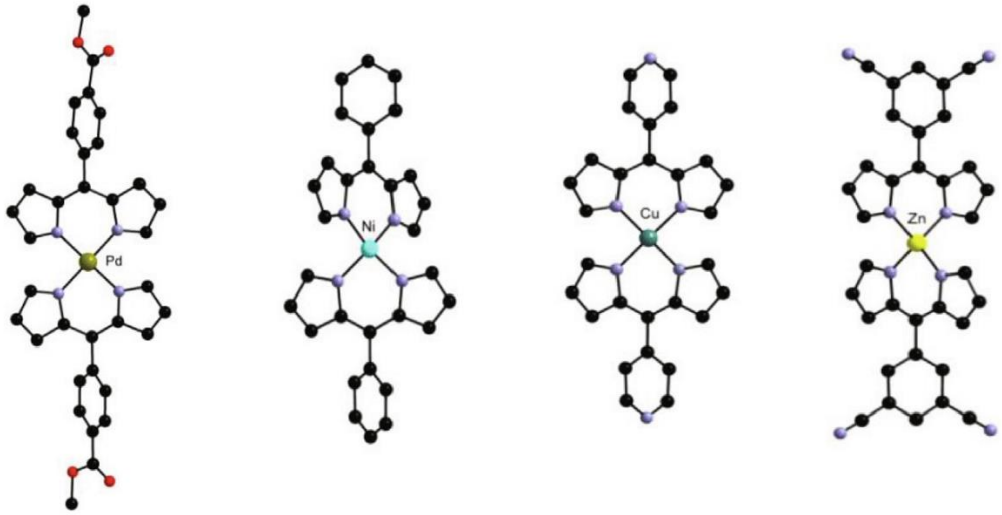

Figure 1.10 Examples of homoleptic dipyrromethenes complexes [51,79,80]

Dolphin and Cohen et al. reported the $M(dpm)_3$ complexes. These homoleptic complexes showed octahedral geometry with Fe(III), Mn(III), Co(III), Ga(III), In(III) (figure 1.10).[78, 82-85] On the other hand, the attempts at preparing $[Co(Ph\text{-}dpm)_2]$ (Ph-dpm = phenyldipyrrin) led to a Co(III) tris-dipyrrinato derivative due to $[Co(Ph\text{-}dpm)_2]$ being air-sensitive. To overcome the oxidation process, a methyl group was introduced at the α-positions of the dipyrrin to prevent the formation of tris-chelated complexes (figure 1.11).[86]

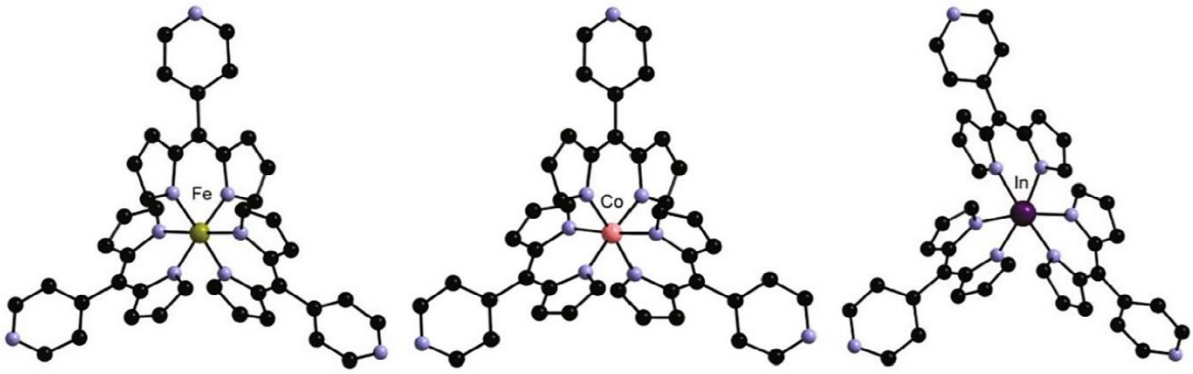

Figure 1.11 Examples of trivalent metal ions dipyrrins homoleptic complexes [83-87]

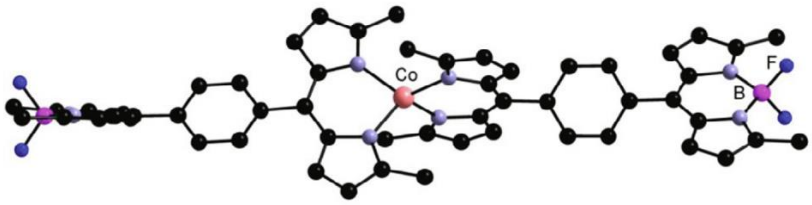

Figure 1.12 Co(II) dipyrrin complex [88]

Several heteroleptic dipyrrin complexes were reported by Thomson and co-workers. The minimum steric interaction near the central metal promoted square planar geometry (scheme 1.26).[9]

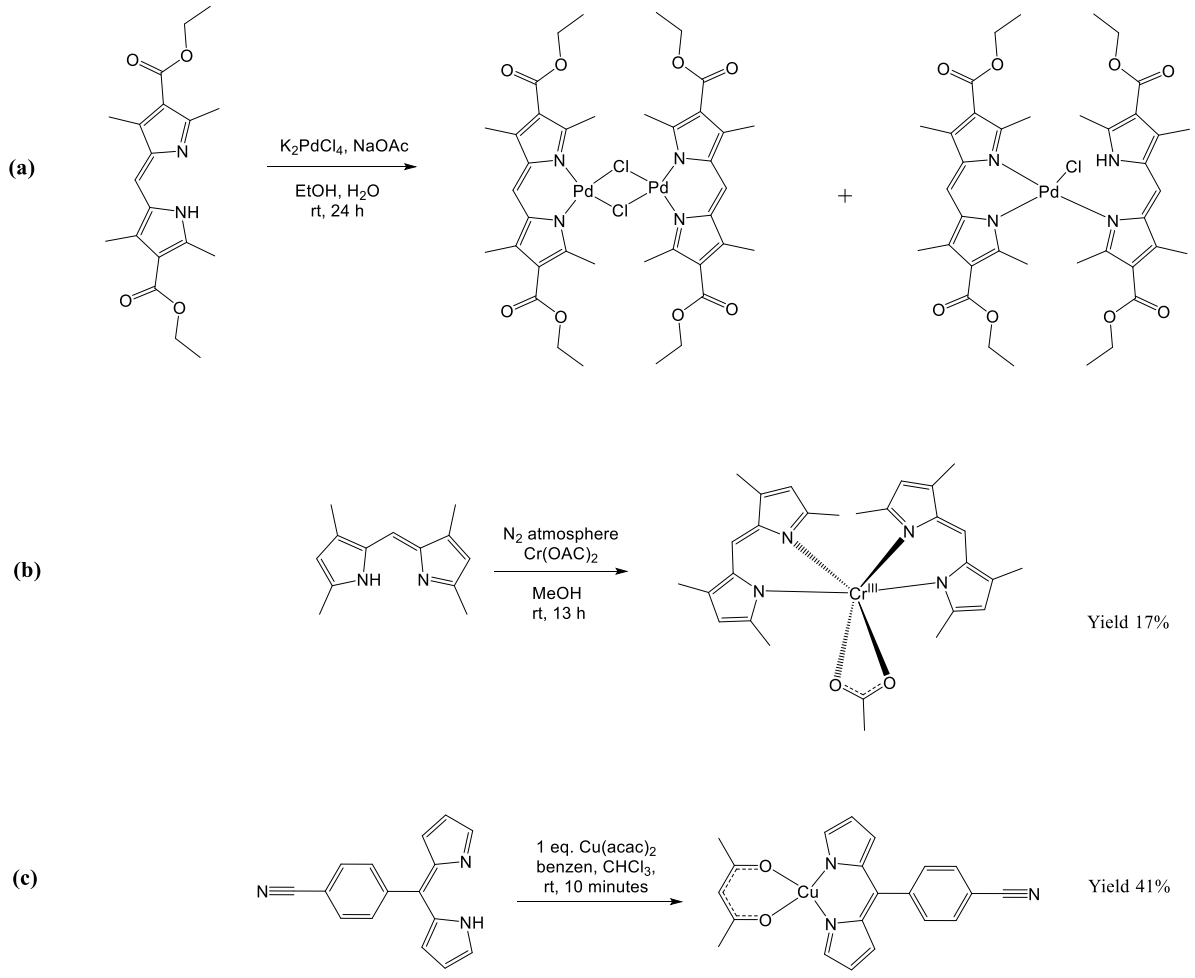

Scheme 1.26 Synthesis of; (a) bridged dimer and heteroleptic palladium(II), (b) heteroleptic chromium(III), (c) heteroleptic copper(II) dipyrrinato complexes.[9]

In 2011, Betley and co-workers reported heteroleptic Fe(II) dipyrromethene complexes. The pathway included the synthesis of dipyrromethene followed by deprotonation with phenyllithium in thawing benzene which afford a high yield of the lithium salts (88-92%). The reaction of lithio dipyrromethene species with a thawing slurry of $FeCl_2$ in an ethereal solvent

produced iron dipyrromethene complexes (Scheme 1.27). The geometry of the obtained complexes was related to the nature of *meso*-substituted groups (aryl or alkyl). The presence of a bulky aryl group (2,4,6-$Ph_3C_6H_2$ ligand) metal centre promoted trigonal planar geometry (figure 1.13 a). On the other hand, the presence of an alkyl group (i.e., adamantly) at the *meso*-position resulted in a four-coordinated trigonal-pyramidal geometry (figure 1.13 b).[14]

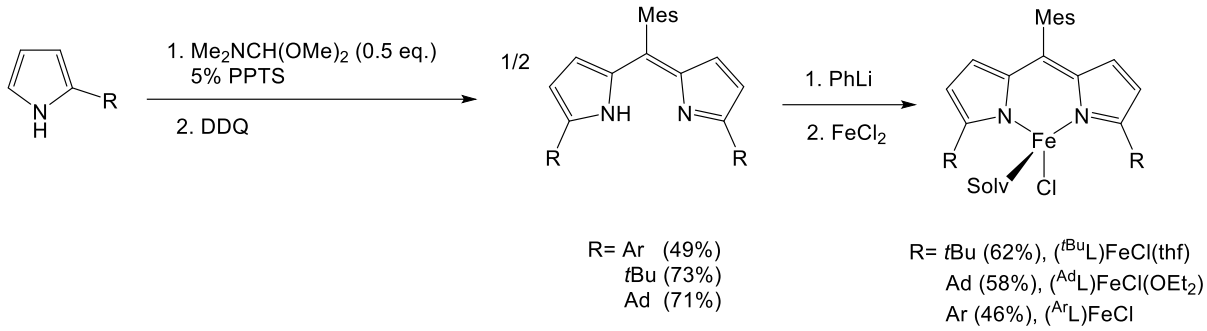

Scheme 1.27 Synthesis of Fe(II) complexes of dipyrromethene.[14]

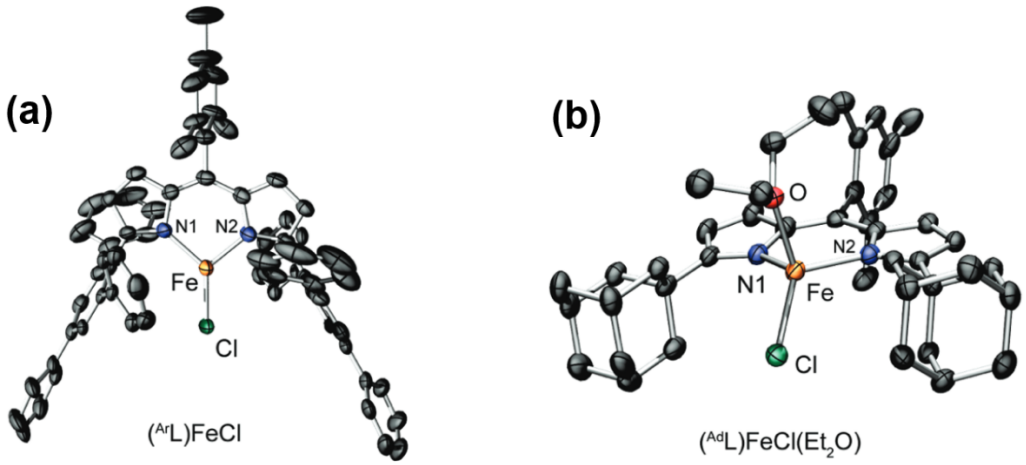

Figure 1.13 Structures of Fe(II) complexes of dipyrromethene; (a) trigonal planar geometry, (b) trigonal-pyramidal geometry.[14]

1.3.1. Azadipyrrin complexes

The progression in the syntheses and studies on azadipyrrins witnessed great interest after explorations of the excited state properties of aza-BODIPY. These BF_2^+ chelates are often used in photodynamic therapy, chemosensors, and luminescent probes.[63, 87, 88] On the other hand, metal complexes of azadipyrrins are relatively scarce.[10] Gray and co-workers reported the first development of azadipyrrin complexes in 2007. Tetraphenyl-substituted azadipyrromethene was successfully utilized to prepare Cu(I), Ag(I), and Au(I) complexes from their triphenylphosphine precursors (Scheme 1.28).[89] These new tri-coordinated

complexes were found to have absorption behavior comparable to aza-BODIPYs; nevertheless, they showed weak emission in solution.[90]

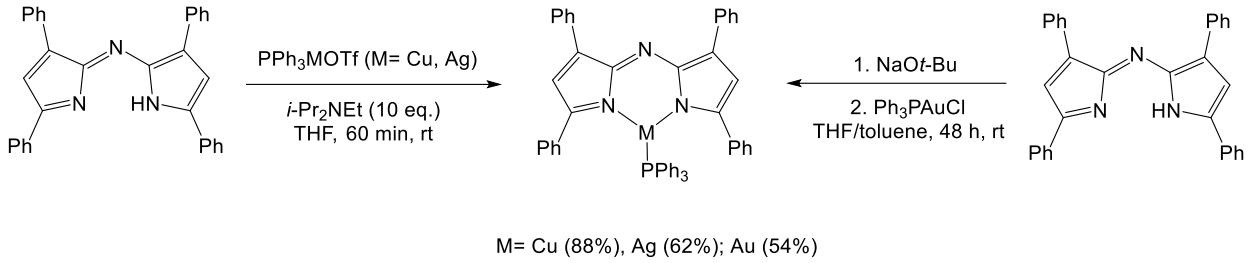

Scheme 1.28 Synthesis of Cu(I), Ag(I), and Au(I) aza dipyrrin complexes.[89]

The same author also reported four-coordinated azadipyrromethene complexes of Zn(II), Hg(II), and Re(I). These complexes were synthesized in a 2:1 fashion (L: M). Each zinc and mercury is coordinated with two azadipyrrins (Scheme 1.29).[91] Rhenium coordinated with one azadipyrrin and a THF molecule, while other ligands were introduced by exchanging the coordinated THF (Scheme 1.30).[92] These complexes exhibited octahedral geometry.[93, 94]

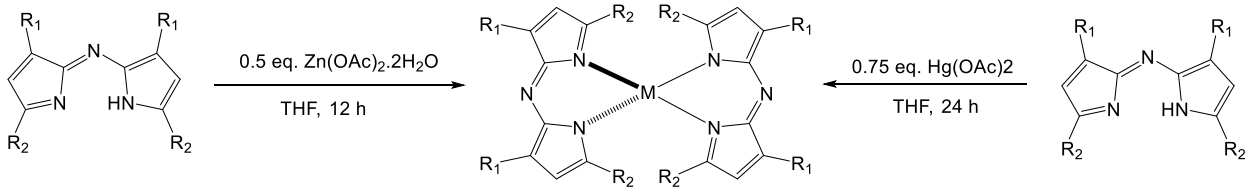

M	R1	R2	Yield
Zn	Ph	Ph	84%
Zn	Ph	*p*-C_6H_4OMe	90%
Zn	*p*-C_6H_4OMe	Ph	54%
Hg	Ph	Ph	61%

Scheme 1.29 Synthesis of Zn(II) and Hg(II) azadipyrromethene complexes.[91]

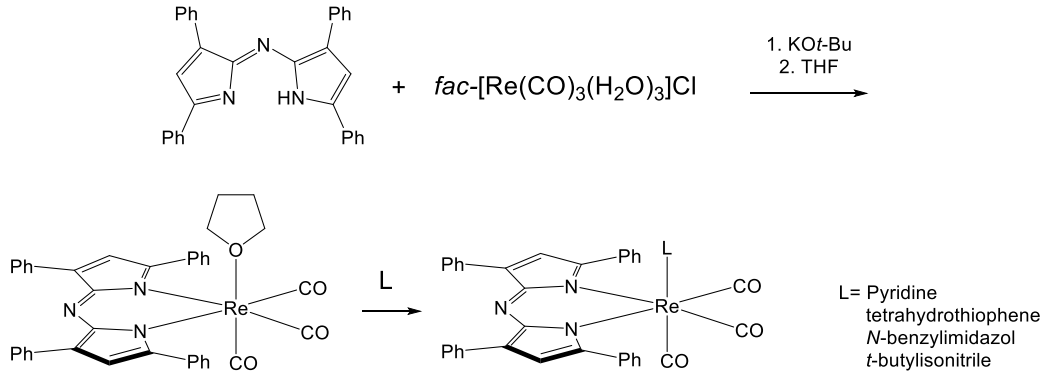

Scheme 1.30 Synthesis of *fac*-tricarbonyl rhenium(I) azadipyrromethene complexes.[92-94]

In 2011, Gresser and co-workers reported the synthesis of homoleptic Co(II), Ni(II), Cu(II), Zn(II), and Hg(II) benzo-fused azadipyrrin complexes (Scheme 1.31).[95]

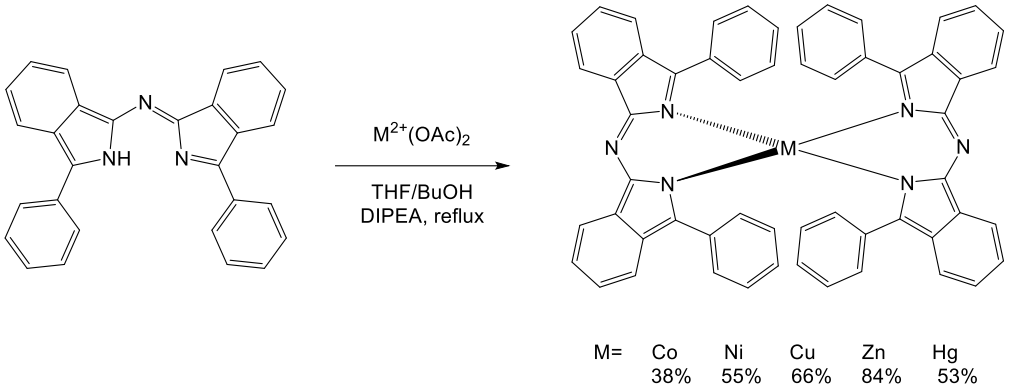

Scheme 1.31 Synthesis of benzo-fused azadipyrrin complexes.[95]

Also, microwave-assisted synthesis of a series of tetrakis(*p*-methoxyphenyl)-azadipyrrin Co(II), Ni(II), Cu(II), and Zn(II) complexes were reported by Hanan and co-workers (Scheme 1.32).[96]

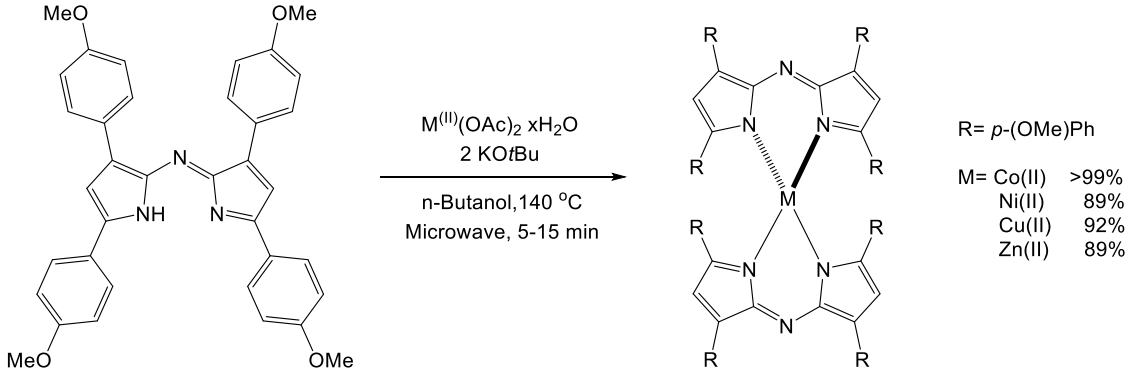

Scheme 1.32 Microwave-assisted synthesis of azadipyrrin complexes.[96]

Sauvé et al. reported the synthesis of homoleptic azadipyrromethene complexes containing di(phenylacetylene). The author presented that these complexes can transport charges in 3-D because of the delocalization of negative charge over the entire structure (Scheme 1.33).[97]

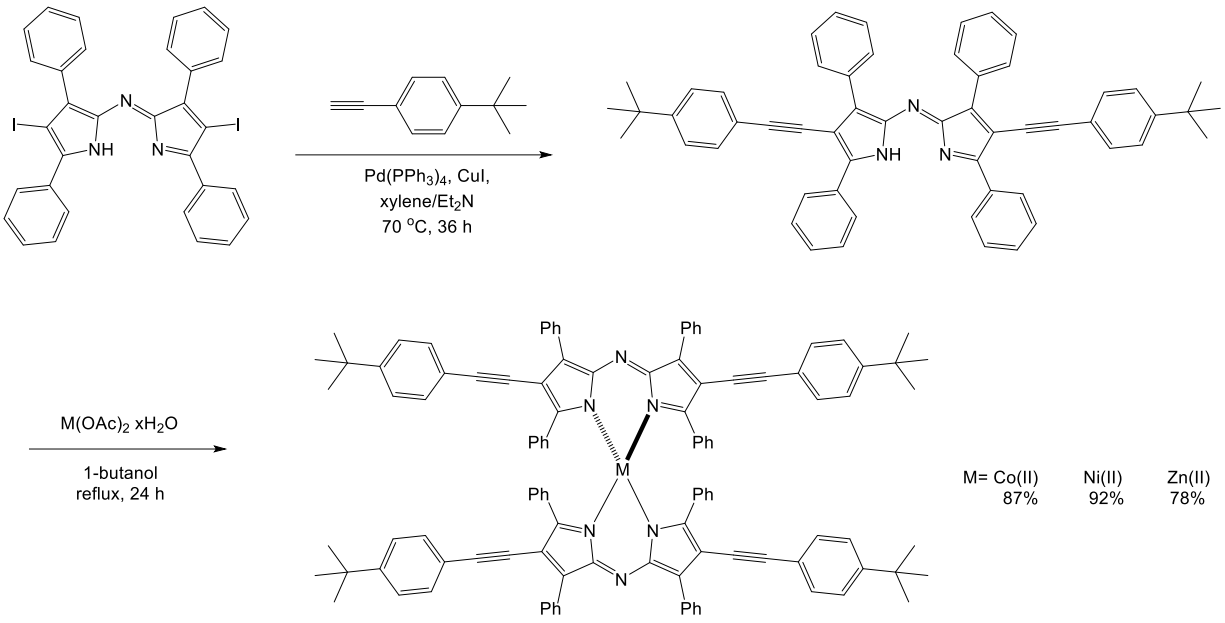

Scheme 1.33 Synthesis of homoleptic metal(II) complexes of di(phenylacetylene) azadipyrromethene.[97]

Transition metal complexes of dipyrrins demonstrating a catalytic potential motivated the synthesis of azadipyrromethene complexes of heavy d^8 metal.[35] Gray et al. successfully synthesized rhodium(I), iridium(I), palladium(II), and platinum(II) azadipyrromethene complexes in 2013 (Scheme 1.34). The new complexes were found to exhibit a square planer geometry.[98] In 2014, the same group reported cyclometalated Ir(III) complexes. revealing azadipyrromethene as a chromophore. The synthesis was achieved by transmetalation between bis(aquo)Ir(III) complexes and aza-BODIPY. The new complexes were found to have absorption in the red region and oxidative and reductive electrochemistry (figure 1.14).[99]

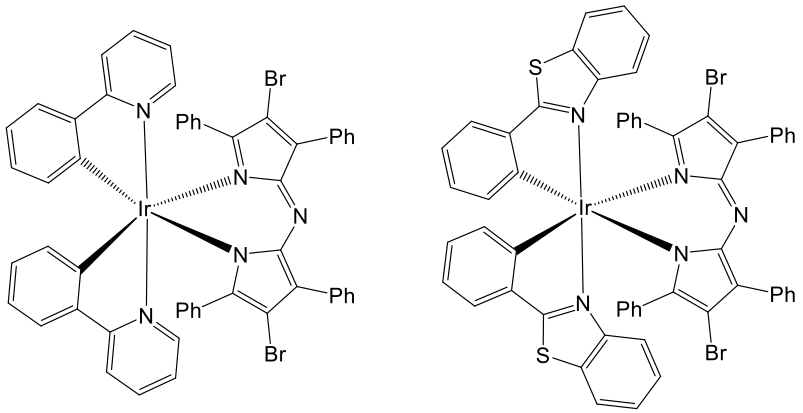

Figure 1.14 cyclometalated Ir(III) azadipyrromethene complexes.[99]

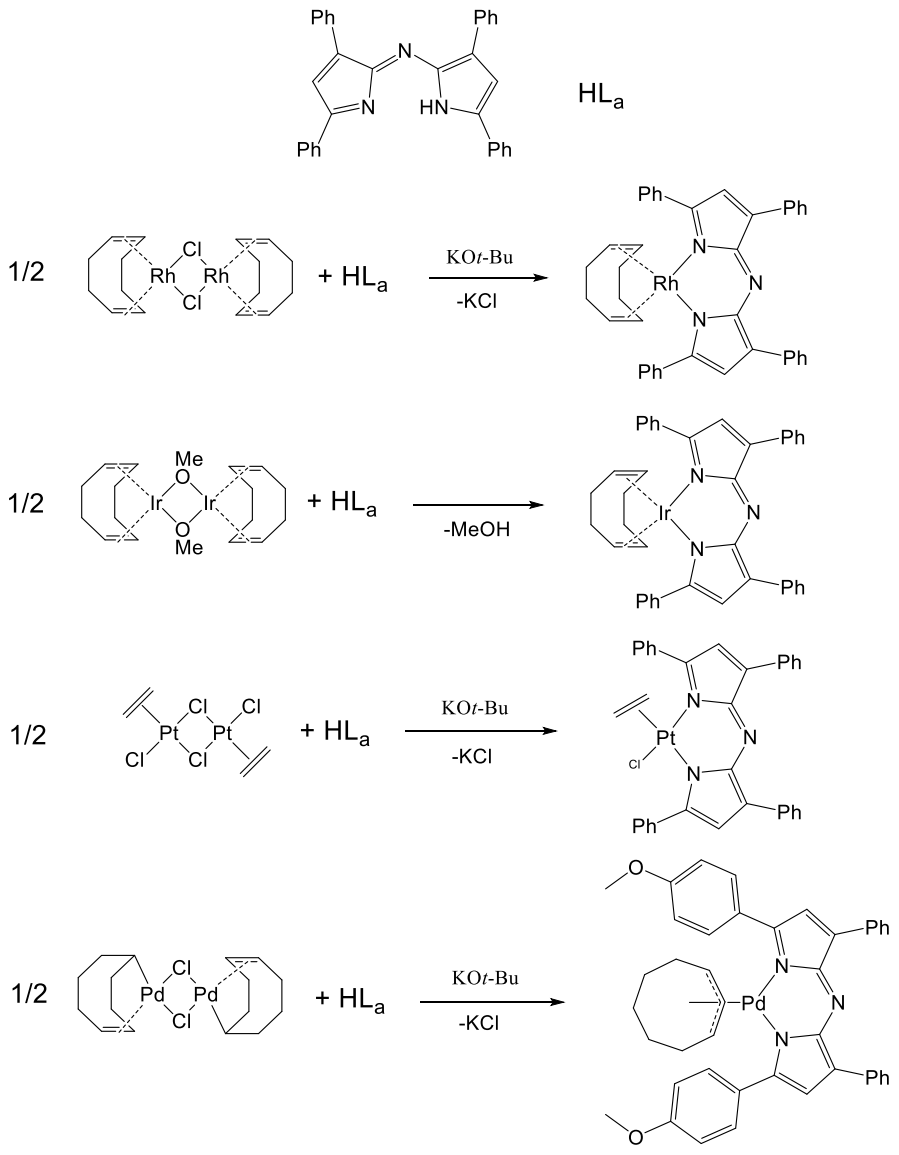

Scheme 1.34 Synthesis of azadipyrromethene complexes of d^8 metal centers.[98]

1.4. Applications of dipyrrin metal complexes

In general, dipyrrins metal complexes were found to have several applications. The manufacturing of silicon-based solar cells requires the use of toxic chemicals. Also, the main challenges in this field are the high cost and low power conversion efficiency (poor collection of photons at $\lambda > 800$ nm). Developing dipyrrin complexes as sensitizers in dye-sensitized solar cells (DSSCs) is one of the promising applications.[10] The research showed that DSSCs photoelectric conversion efficiency (PCE) ranges from 0.13-10.4%.[100-103] Unlike silicon-based solar cells, DSSCs are environment-friendly but have not yet succeeded in the global market.

The breakthrough in luminescent dipyrrin complexes advanced the use of dipyrrins as probes for various analytes. Variation in fluorescence promoted by a change in the

physicochemical properties upon interaction with analytes led to the development of dipyrrin-based chemosensors. Thus, several cation sensors were developed detecting Zn(II), Ca(II), Y(III), La(III), Gd(III), Sn(IV), Cd(II), Lu(III), Mn(II), In(III), Co(II), Hg(II), and Pb(II).[22, 104-109] The development of di-/ tripyrrins as anion sensors is worth noting. It has been found that cyclic and acyclic oligopyrroles, containing polarized-NH groups, have great potential for anion sensing.[110-112]

The self-assembled architectures of dipyrrins have gained enormous interest from the scientific community. These dipyrrin-based supramolecular structures are characterised by multiple coordination sites and a high tendency to bind with various metal centres of dipyrrins. Therefore, the supramolecular architectures have advanced over other scaffolds.[113, 114] Additionally, the application of dipyrrin complexes led to a development in metal-organic frameworks (MOFs) and porous coordination polymers (PCPs) based on bis/tris dipyrrinato metal complexes.[115-119]

Furthermore, researchers have also found many other applications for these interesting compounds and complexes. Such applications in electron and energy transfer systems,[120] thermoelectric conversion,[121] photoelectric conversion,[122] anticancer agents,[123, 124] nanoparticle synthesis,[125, 126] and active redox catalysts[127, 128] have propelled the scientific community to further development of dipyrrins and their complexes.

1.5. Isoindoline-based trimeric compounds

Linstead and co-workers are the first to report isoindoline-based trimeric compounds. A condensation reaction of 1,3-diiminoisoindoline with 2,6-diaminopyridine produced 2,6-Bis(1-imino-3-isoindolinylidenamino)pyridine (figure 1.15 a).[129] The same author synthesised another type of trimeric compound consisting of one isoindoline-1,3 ring and two pyridine units (figure 1.15 b)[130]

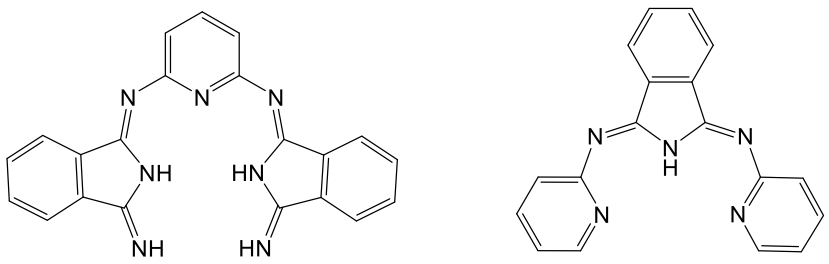

(a) (b)

Figure 1.15 Isoindoline-based trimeric compounds by Linstead et al.[129,130]

The synthetic strategy was developed by activating nitrile groups of phthalonitrile by the salts of alkali-earth metals.[131] The influence of the catalyst, temperature, and nature of amine and solvent on the condensation was investigated. The study suggested that using the analogous molecular ratio of phthalonitrile and arylenamine can obtain various products.[132] In 1996, the synthesis of a trimeric compound was reported as a precursor in the preparation of triazoleporphyrazines (Scheme 1.35).[133]

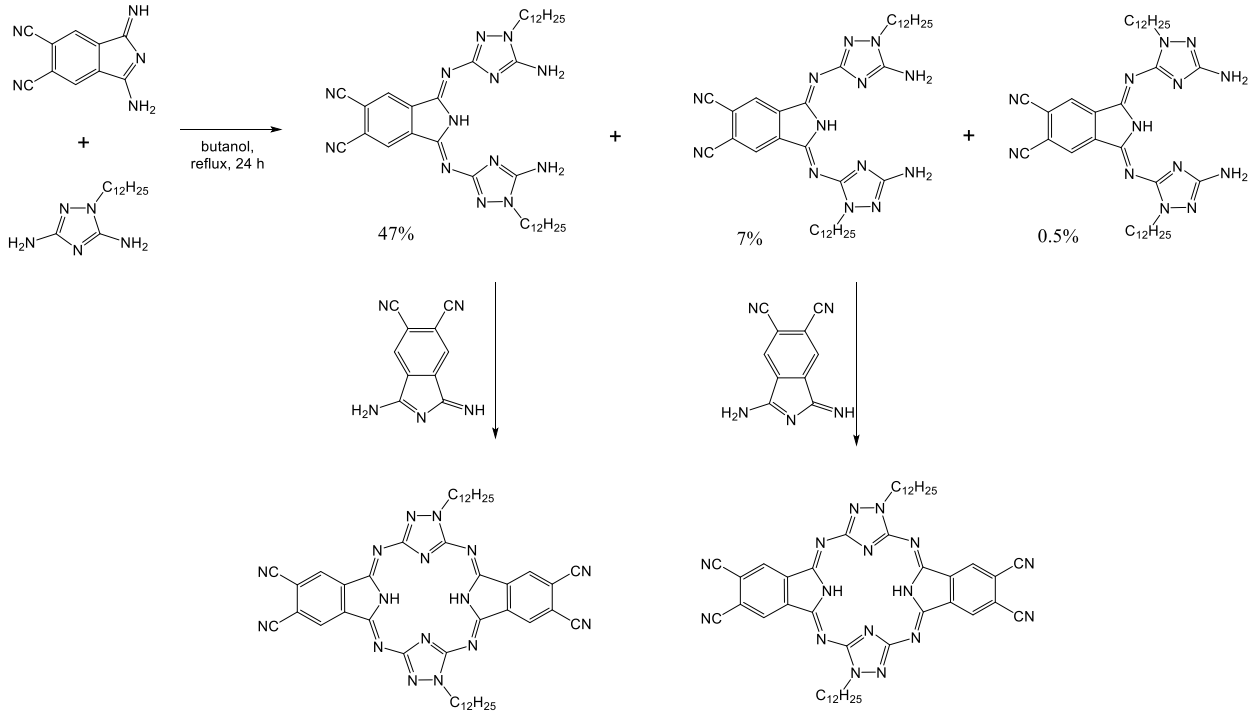

Scheme 1.35 Synthesis of triazoleporphyrazines via trimeric precursors.[133]

In 2009, the synthesis of three-unit products was reported by condensation of 3-alkylsubstituted 2,5-Diamino-1,3,4-thiadiazoles with 1,1-Dimethoxy-3-iminoisoindoline (Scheme 1.36).[134]

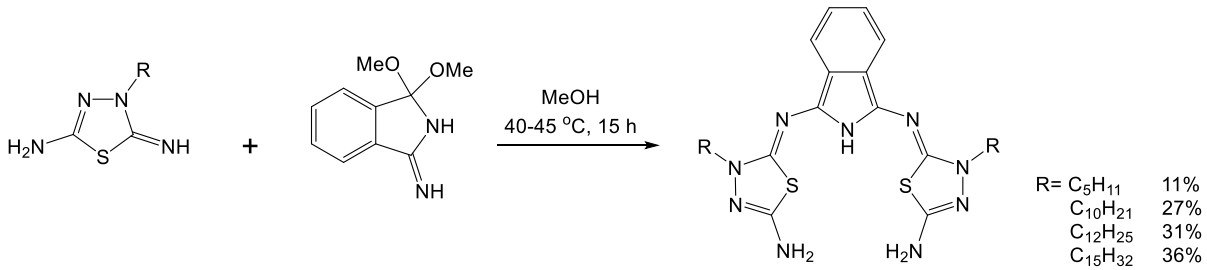

Scheme 1.36 Condensation of 3-alkylsubstituted 2,5-diamino-1,3,4-thiadiazoles with 1,1-dimethoxy-3-iminoisoindoline.[134]

In the literature, the development of isoindoline-based trimeric compounds is associated with synthesising porphyrinoids (Scheme 1.37).[135] Furthermore, their synthetic strategies were applied to prepare several macroheterocyclic compounds.[136]

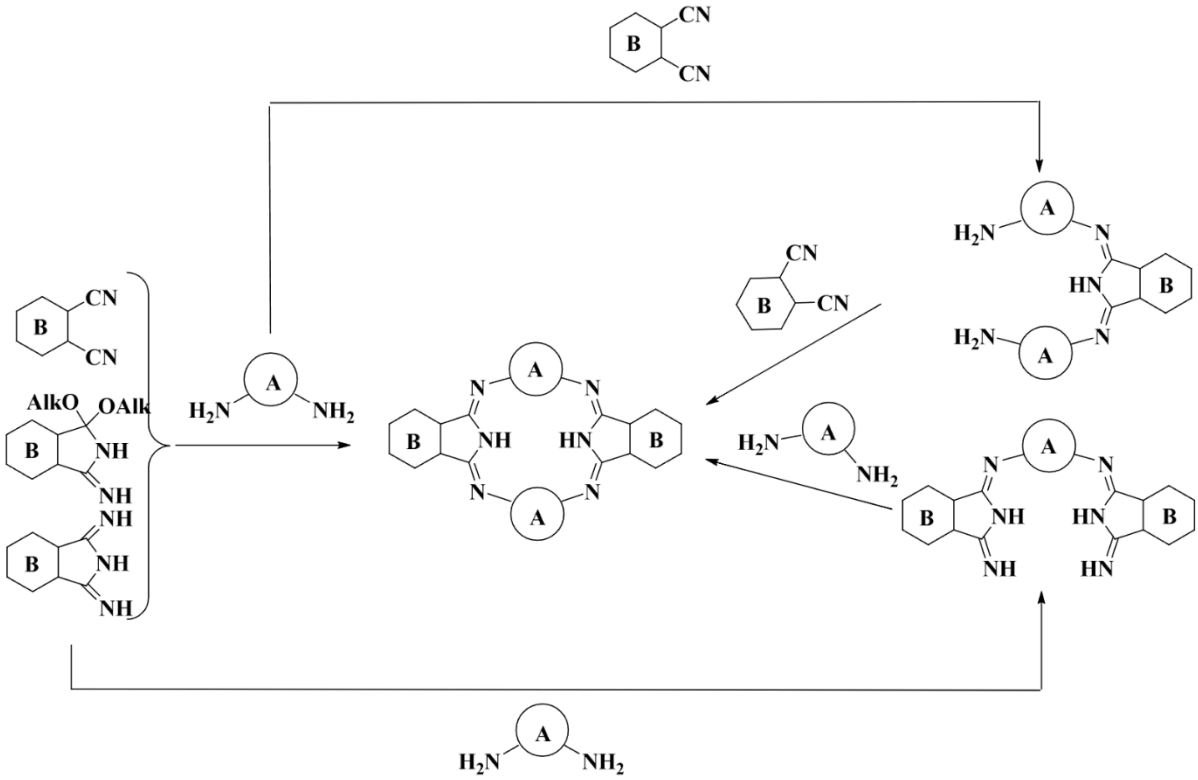

Scheme 1.37 The routes for the synthesis of hemiporphyrazines[137]

Scientists have been reporting the complexation of these isoindoline-based trimeric compounds with various metals. Following are examples of these complexes.

1.5.1. Complexation of isoindoline-based trimeric compounds

A homoleptic iron(II) complex was successfully synthesised by a reaction of two molar equivalents of 1,3-bis(20-pyridylimino)isoindoline (indH) in a solution of $Fe(ClO_4)_2$ in acetonitrile. The reaction was performed at room temperature for a day in the presence of Et_3N.

The product was filtered and washed. The complex was prepared in a 2:1 ratio (L: M) and exhibited an octahedral geometry (figure 1.16 a).[137]

The synthesis of palladium (II) bis(2-pyridylimino)isoindolate complex was reported in 2005. A 1:1 ratio (L: M) complex was prepared in benzene using [(*Ph*CN)$_2$PdCl$_2$] in the presence of Et$_3$N. The coordination geometry of the obtained complex deviates slightly from the ideal square planar arrangement (figure 1.16 b).[138]

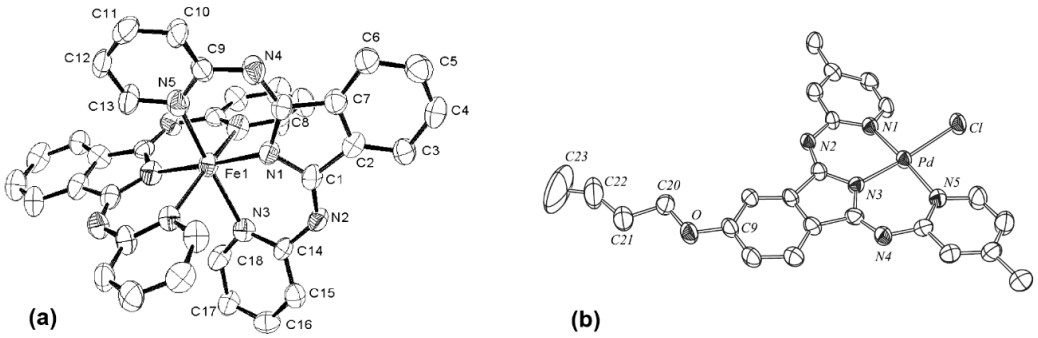

Figure 1.16 Isoindoline-based trimeric complexes (a) Pd(II), (b) Fe(II).[137,138]

A paper in 2013 reported the complexation of 1,3-bis(2-pyridylimino)isoindoline (BPI) with boron, aluminium, gallium, and indium. The BPI·BF$_2$, BPI·AlCl$_2$, BPI·GaCl$_2$, and BPI·InCl$_2$ complexes were prepared by heating the BPI ligand, formed from the condensation reaction of o-phthalonitrile and 2-aminopyridine, with the appropriate group 13 halide in the presence of Et$_3$N (Scheme 1.38). The yield of obtained products varied from batch to batch. The highest observed yields were 19, 25, 17, and 27% for BPI·BF$_2$, BPI·AlCl$_2$, BPI·GaCl$_2$, and BPI·InCl$_2$, respectively. The purification of these complexes was challenging. Aqueous workup led to a loss in products due to their solubility in water. Purification by silica gel column chromatography was also ineffective. The salt products and the desired complexes were stuck on the column and, thus, could not be separated.[139]

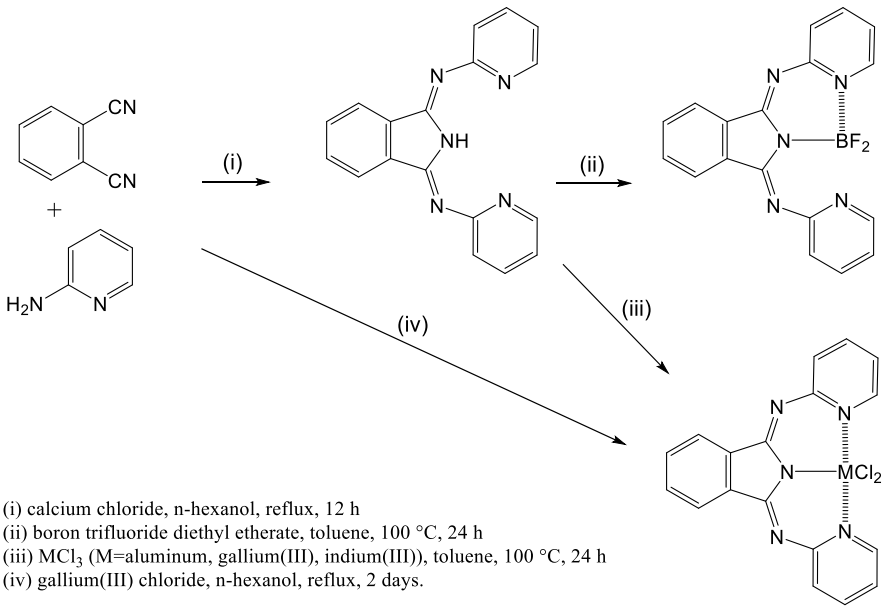

Scheme 1.38 Synthesis of BPI·BF_2, BPI·$AlCl_2$, BPI·$GaCl_2$, and BPI·$InCl_2$.[139]

A series of homoleptic and heteroleptic 3d transition metal complexes were reported in 2021. The synthesis was accomplished by reacting appropriate metal precursors with 1,3-bis(2-pyridylimino)isoindolate (BPIH). The heteroleptic complexes were synthesised in a 1:1 molar ratio by a dropwise addition of BPIH solution in methanol to the corresponding transition metal chloride in methanol. The solution mixture was refluxed for four hours. The mixture was then allowed to cool to room temperature. Upon cooling, the complex formed a solid that was filtered and washed with hot methanol. On the other hand, homoleptic complexes were prepared in a 2:1 molar ratio (L: M). The synthesis was performed in a similar manner to the heteroleptic procedure. However, a few drops of 25% ammonia solution (or 0.1 N potassium hydroxide) were added to the reaction mixture before heating. The reaction proceeded overnight under reflux in a water bath. The product was filtered and washed, similar to heteroleptic complexes. The homoleptic complexes exhibited a distorted octahedral structure containing two coordinating BPI ligands. Heteroleptic complexes showed a highly distorted square pyramidal geometry, with a planar tridentate BPI ligand coordinating with the metal centre and chloro and aqua ligands (figure 1.17).[140]

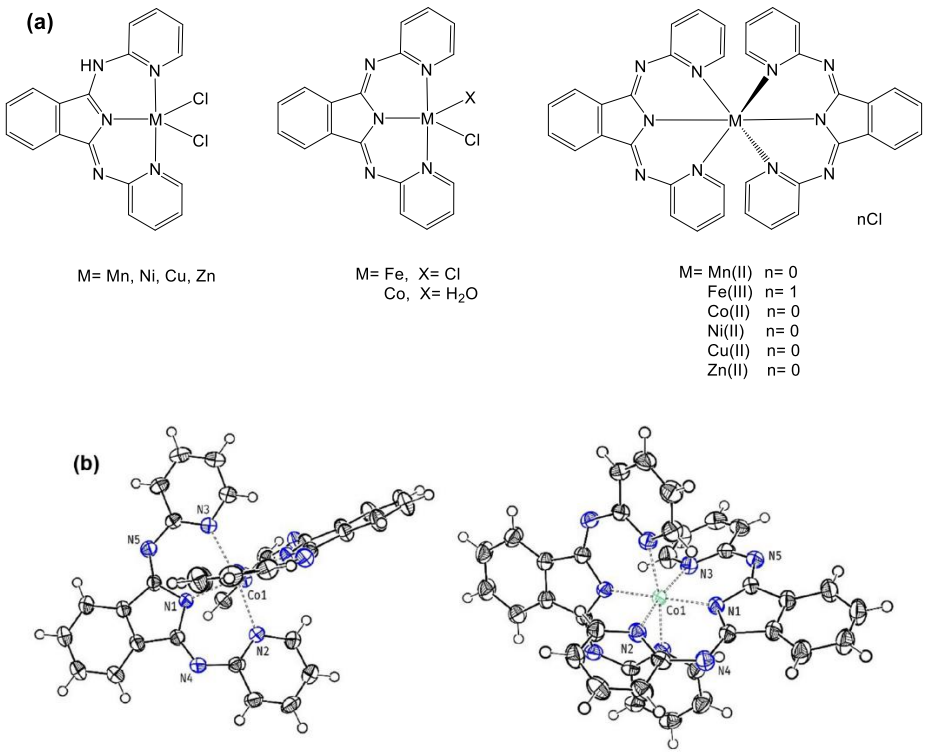

Figure 1.17(a) Projected structures of the homoleptic and heteroleptic complexes, (b) Molecular structure of the homoleptic cobalt complex.[140]

1.6. Aim of the project

This project investigates the complexation of benzo (aza) di- and tripyrrins. Using methods developed by our group, the project will start by synthesising symmetrical and non-symmetrical benzo-fused azadipyrrins starting from aminoisoindoline. Moreover, azatripyrrin will be synthesised from the same aiminoisoindoline precursor while optimising the reaction conditions. The project's primary goal after successfully synthesising these compounds is to prepare homoleptic complexes with various metals (figure 1.18).

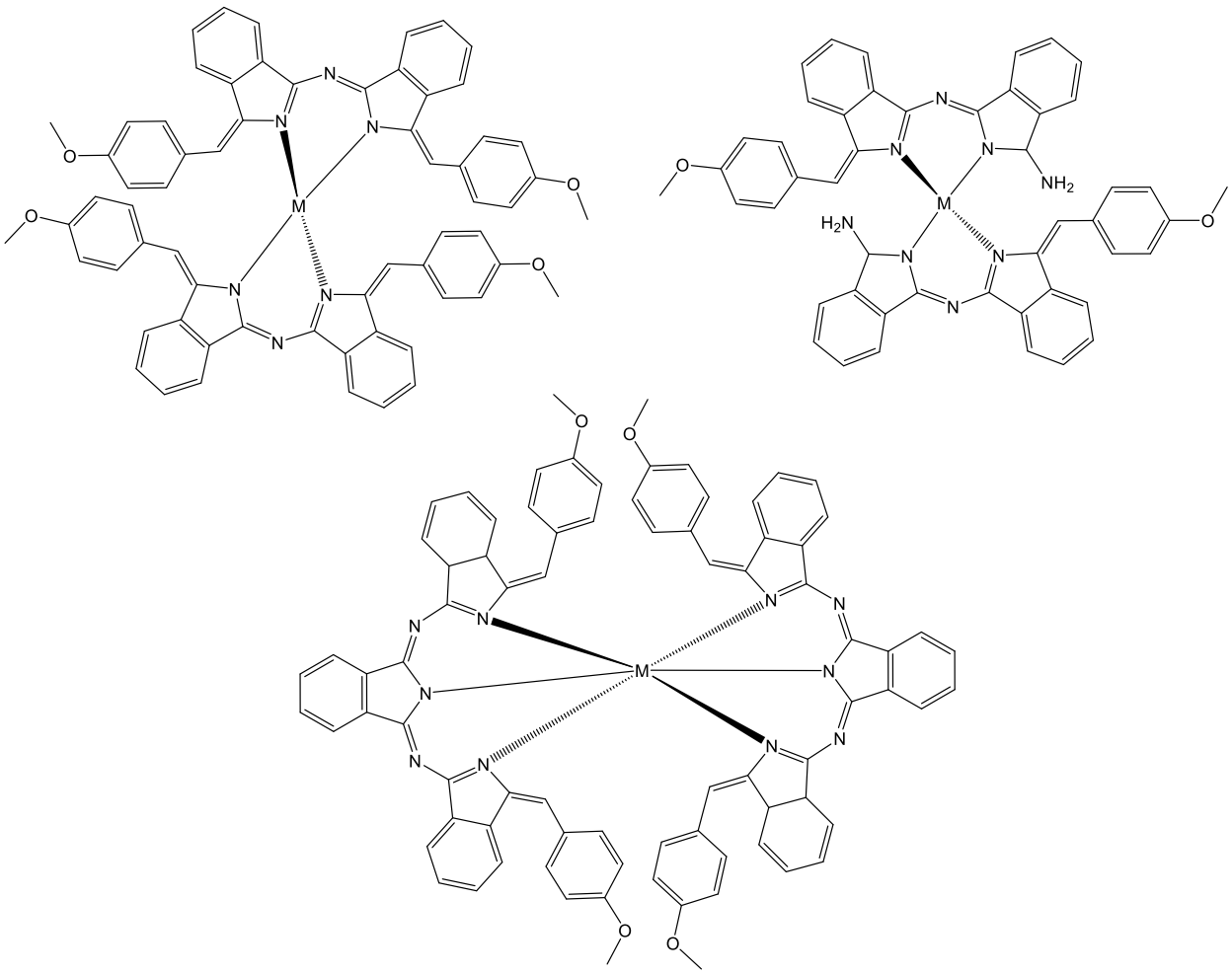

Figure 1.18 The targeted homoleptic complexes of benzo (aza) di- and tripyrrins

2. Results and discussion

2.1. Synthesis of aminoisoindoline

A precursor of 2-bromobenzamidine hydrochloride was obtained via the Dalai et al. procedure.[141] In this method, lithium bis(trimethylsilyl)amide was added to a solution of 2-bromobenzonitrile in THF at room temperature. The reaction proceeded for 4 hours and was quenched by a solution of isopropanol and HCl. The product (80% yield) was filtered, washed, and characterised by ^{1}H NMR (Figure 2.1 a). Then, the produced amidine salt was reacted with 4-methoxyphenylacetylen in the presence of palladium catalyst and irradiated by microwave to produce the aminoisoindoline via copper-free Sonogashira cross-coupling according to Hellal and Cuny procedure (scheme 2.1).[74] After liquid-liquid extraction and crystallisation in a DCM and petroleum ether mixture, the targeted aminoisoindoline was obtained (77% yield). The synthesis was confirmed by ^{1}H NMR (Figure 2.1 b).

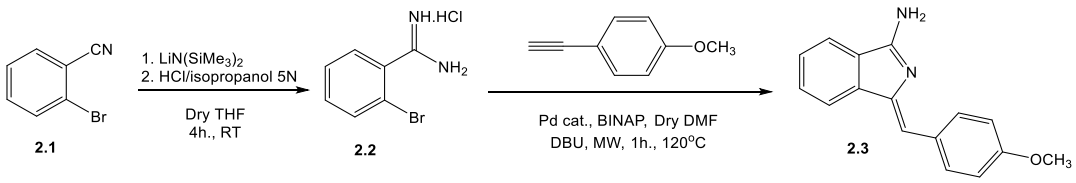

Scheme 2.1 Synthesis of aminoisoindoline

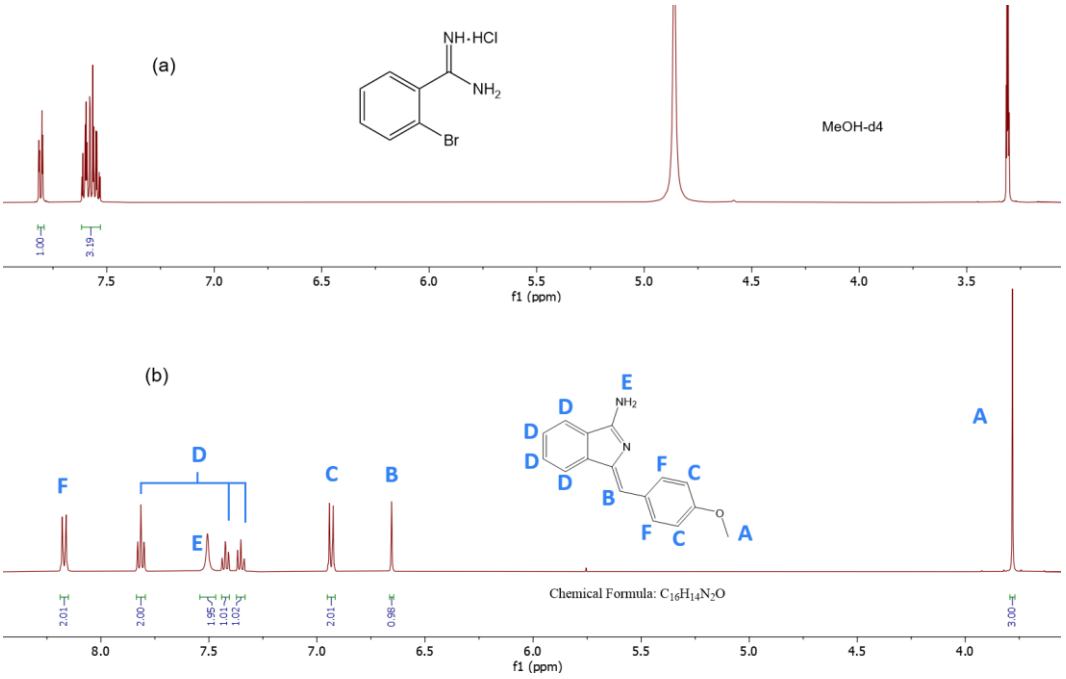

Figure 2.1 ^{1}H NMR of (a) 2-bromobenzamidine hydrochloride, (b) 4-methoxyphenyl aminoisoindoline

^{1}H NMR analysis confirmed the synthesis, showing peaks integrations corresponding to the total number of protons present in the aminoisoindoline. The spectrum indicates that the

peak of the methoxy group has a corresponding integration of 3 protons (3.8 ppm). In addition to the alkene proton at 6.7 ppm (figure 2.1 b). In this copper-free cross-coupling reaction, the BINAP ligand and DBU base were utilized in the cyclization reaction. Scheme 2.2 illustrates the proposed mechanism of preparing aminoisoindoline (**2.3**).

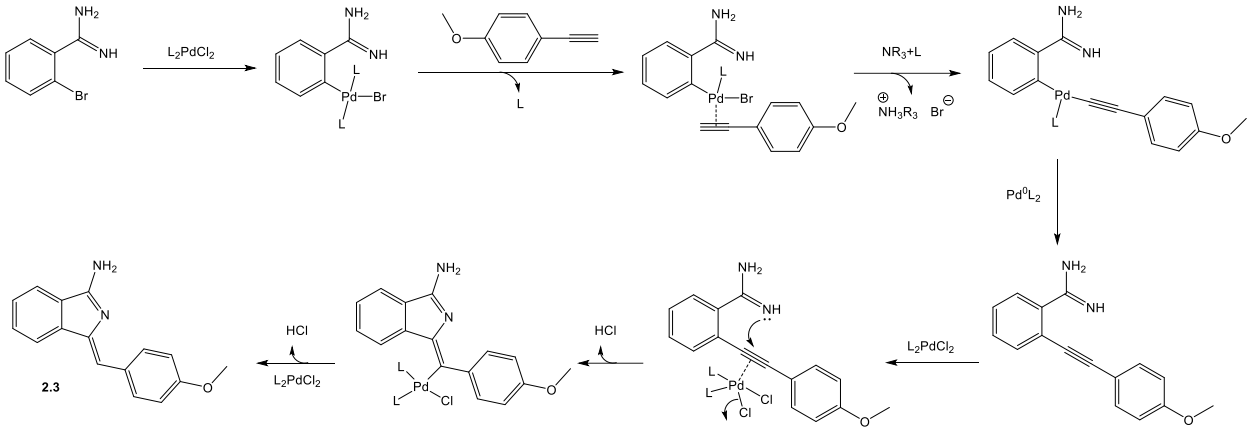

Scheme 2.2 supposed mechanism of preparing aminoisoindoline

While this reaction was performed on a small scale in a microwave vessel, a large-scale reaction was successfully performed, using the same molar ratios, in a round-bottom flask at 120 ^{o}C for 6 hours (70 yield%).

2.2. Dinitriles

The benzo (aza) di- and tripyrrins were prepared by condensation with different dinitriles. Phthalonitrile **(2.4)**, 4-*tert*-butylphthalonitrile **(2.5)**, and naphthalonitrile **(2.6)** will be utilised. The first two were directly purchased from suppliers, while the latter was synthesised. The synthesis was reported in the literature by reacting *α,α,α',α'*-tetrabromo-o-xylene with fumaronitrile in the presence of sodium iodide in DMF at 75 ^{o}C. After 5.5 h., the reaction mixture was quenched with sodium bisulfite in an ice-water mixture (Scheme 2.3).[142] The solid product was then filtered, washed, and recrystallised from a mixture of DCM and PE and characterized by ^{1}H NMR.

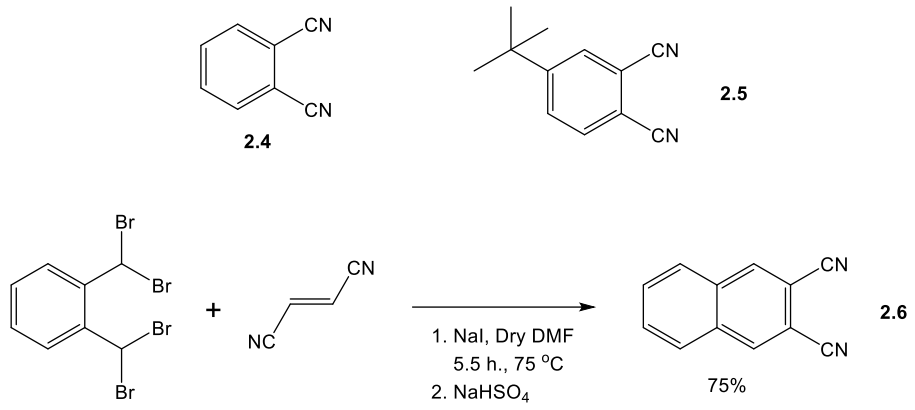

Scheme 2.3 The utilized dinitriles and the synthesis of naphthalonitrile

During the discussion in this chapter, aminoisoindoline will be referred to as **A** unit, while the dinitrile is **B** unit. Thus, symmetrical benzo-fused azadipyrromethene is **AA**, while **AB** is the unsymmetrical compound. Azatripyrrin is labeled as **ABA** (figure 2.2).

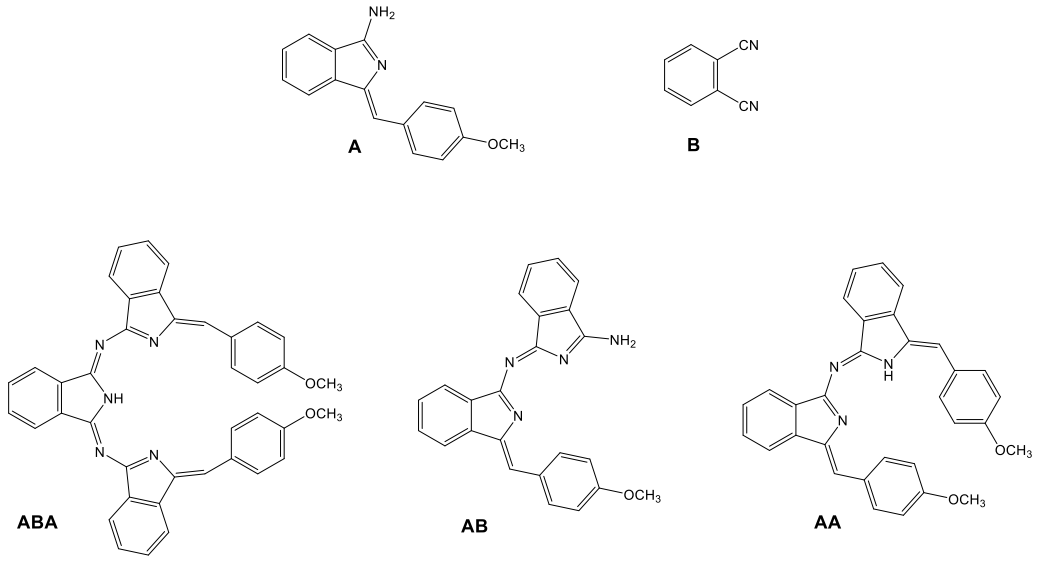

Figure 2.2 compounds labeling

2.3. Synthesis of benzo azadippyrrins

2.3.1. Symmetrical **AA**

Our group reported the synthesis of aminoisoindoline by self-condensation at elevated temperatures via removing NH_3 (Scheme 2.4).[75] The reaction was performed in toluene at reflux. The targeted azadipyrrin **AA** was purified using column chromatography, and a 73% yield was obtained after crystallisation in a mixture of DCM and methanol. The symmetry was confirmed by ^{1}H NMR, showing a single peak for the methoxy groups with an integration corresponding to six protons (Figure 2.3).

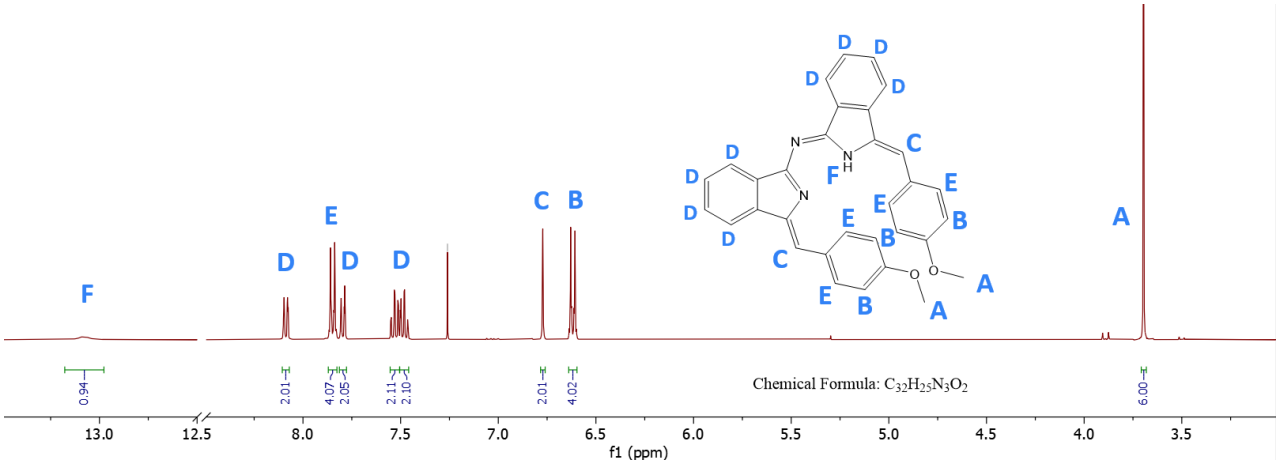

Figure 2.3 ^{1}H NMR of symmetrical azadipyrrin (2.7)

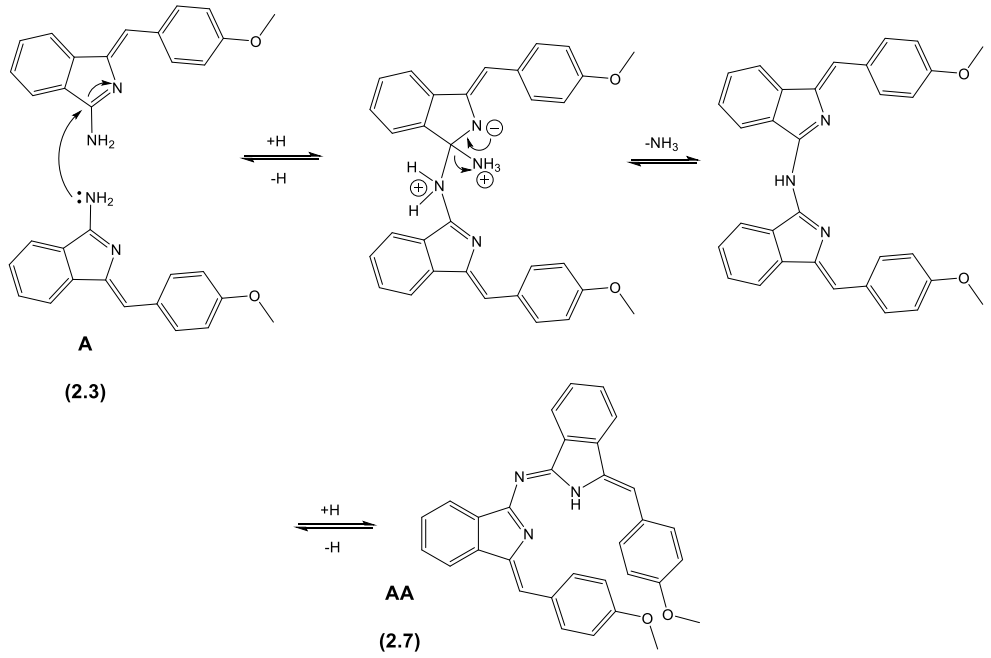

Scheme 2.4 proposed dimerisation mechanism of aminoisoindoline

2.3.2. Unsymmetrical **AB**

Our group developed a method for synthesising unsymmetrical benzo-fused azadipyrrin while investigating the synthesis of phthalocyanine analogues (e.g. tetrabenzotriazaporphyrins (TBTAP)).[143-147] Aminoisoindoline **A** was added to a mixture of methanol and a dinitrile in the presence of NaOMe. The reaction mixture was refluxed overnight to form a precipitating solid of the targeting compound (Scheme 2.5).The obtained products are poorly soluble in most solvents. NMR analysis was performed using deuterated DMSO (Figure 2.4).

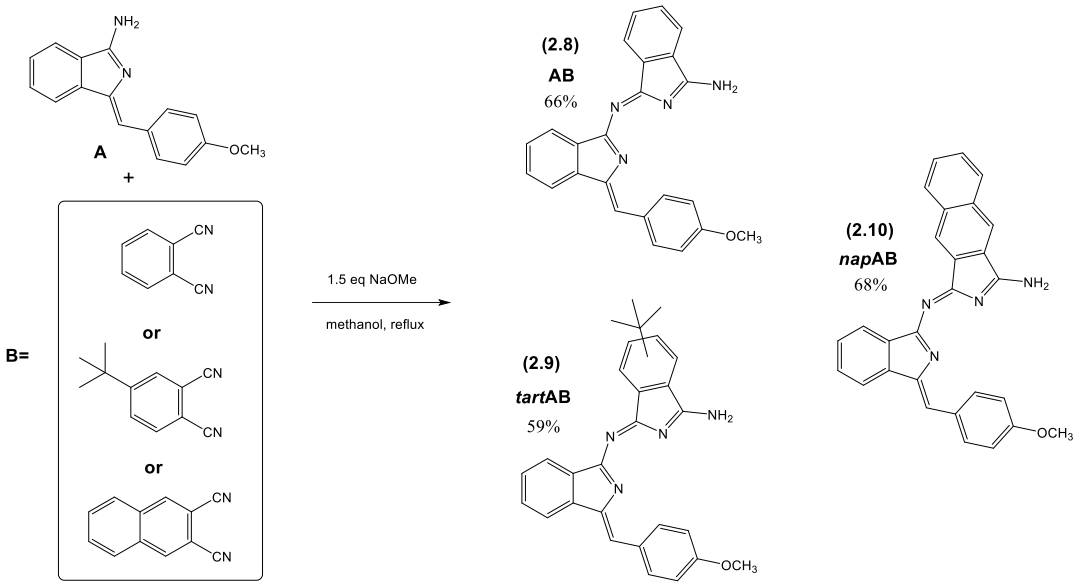

Scheme 2.5 Synthesis of unsymmetrical benzo-fused azadipyrrins

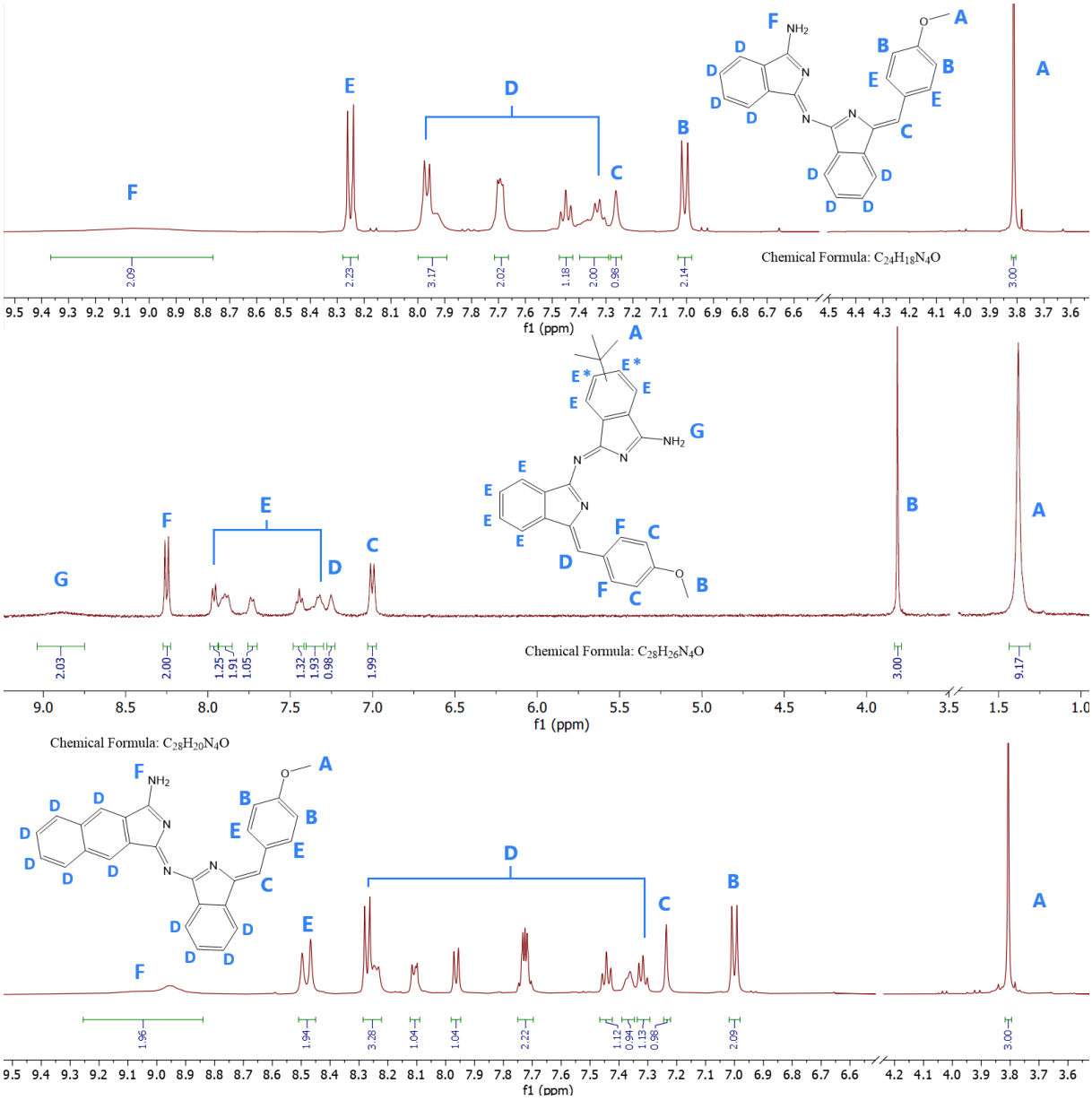

Figure 2.4 ^{1}H NMR of unsymmetrical benzo azadipyrrins

2.4. Benzo azatripyrrin

During the PhD work of Sonia Remiro's PhD work with Prof. Cammidge at UEA, an intermediate was observed in the synthesis of SubTBDAP hybrids (Scheme 2.6).[148]

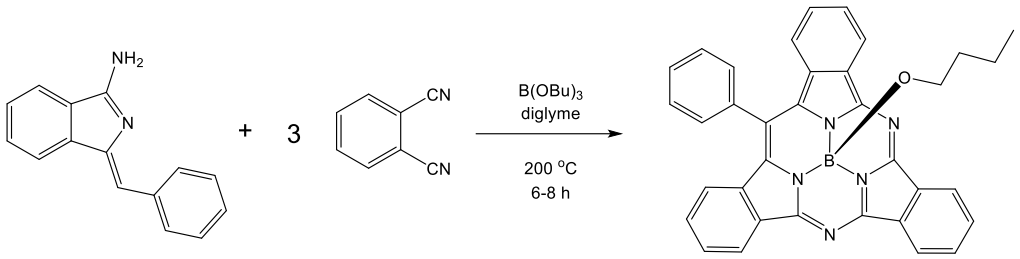

Scheme 2.6 Synthesis of SubTBDAP hybrid.[148]

The new compound **(2.11)** was found to be a brown spot that appeared on TLC after 30 minutes of reaction time. However, the spot disappeared with reaction progression. Using preparative TLC, Sonia was able to isolate and characterise the intermediate but could not report a yield. The compound was found to consist of two aminoisoindoline units and one phthalonitrile; hence, it was described as a trimer-like compound. MALDI-TOF (551 m/z) confirmed the mass. X-ray spectroscopy also imaged the structure using crystals successfully grown using a mixture of distilled dichloromethane and distilled petroleum ether. The intermediate showed a hydrogen bond that stabilizes the compound's helical (non-planer) conformation. This non-planer geometry is similar to hexahelicene compounds introduced by Newman et al. (figure 2.5).[149, 150]

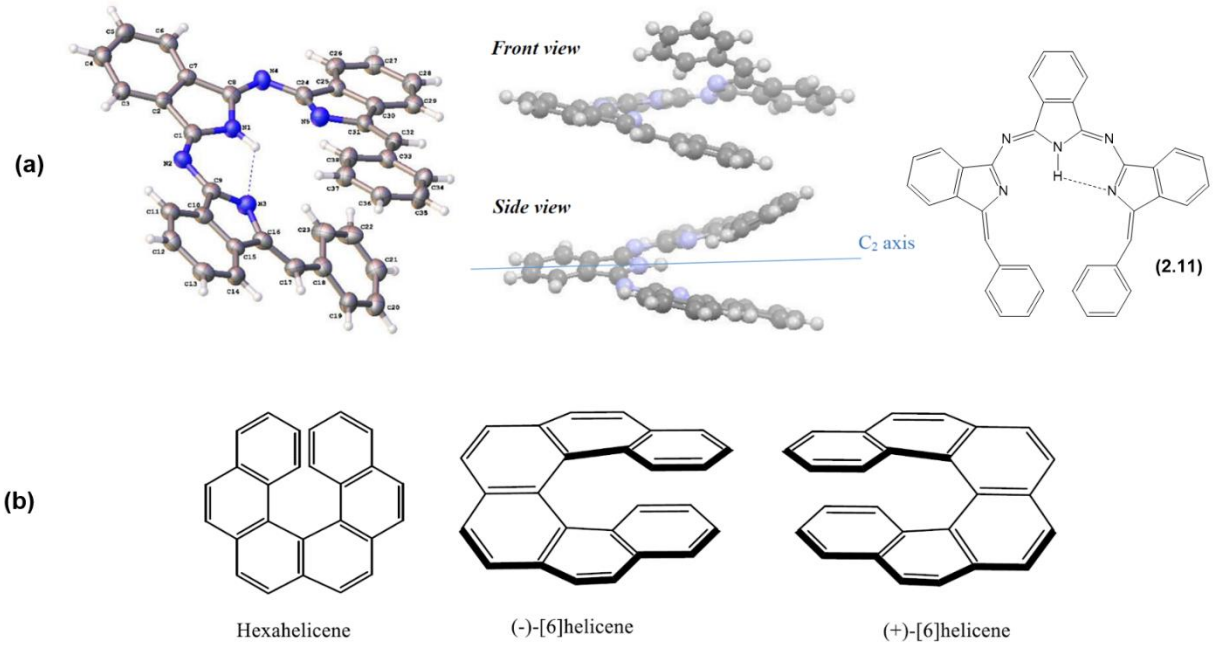

Figure 2.5(a) X-ray structure of trimer as presented in Sonia's thesis; (b) Enantiomers of [6]helicene.[149,150]

The intermediate trimer was described as a brown compound. The UV-Vis showed a broad spectrum with maximum absorption at 334 nm and $1.28x10^4$ M^{-1} cm^{-1} molar extinction coefficient.[148]

2.4.1. Synthesis of benzo-fused azatripyrrin

The first attempt at the synthesis was a procedure comparable to the reaction conditions used to synthesise unsymmetrical aza dipyrrin **AB**. The reaction was performed using two equivalents of (aminoisoindoline) **A** and one equivalent of (dinitrile) **B**. The reaction was performed in methanol at reflux in the presence of sodium methoxide (Scheme 2.7). By monitoring the reaction progression using TLC and ^{1}H NMR, the reaction proceeded by forming an **AB** intermediate that reacts with the excess of **A** to produce **ABA**. While the reaction proceeded for 8 days, the targeted compound was produced. However, the yield was significantly low. This condition was limited by the precipitation of **AB** in alcohol solvents.

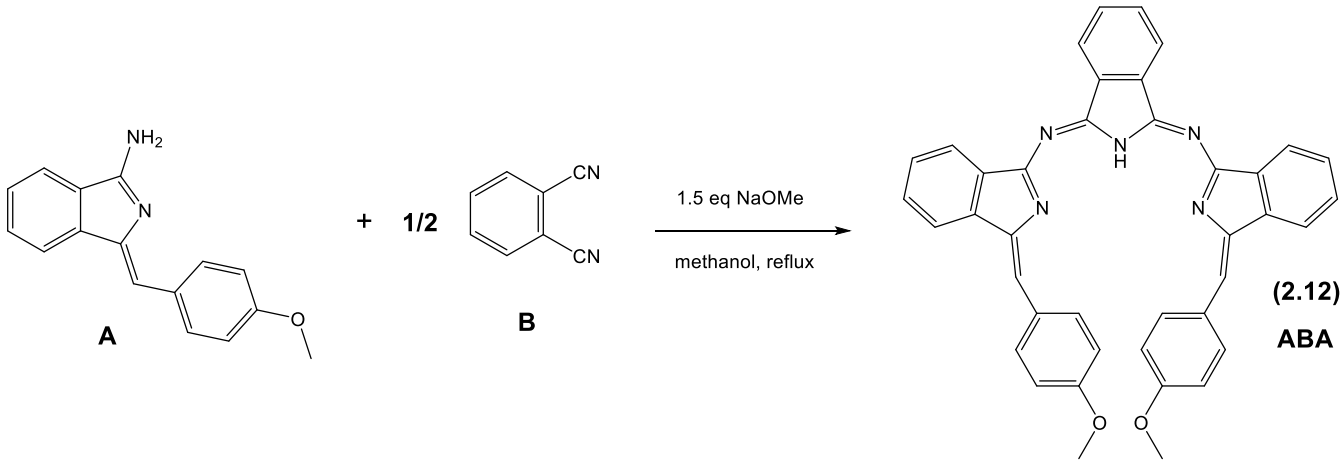

Scheme 2.7 synthesis of benzo azatripyrrin (method A)

This reaction condition showed that the synthesis of **ABA** proceeded through the formation of **AB** as an intermediate of the condensation reaction. Other solvents were tested to improve the solubility of the **AB**. The highest obtained yield was 10% of **ABA** using toluene at reflux. While toluene enhanced the solubility of the generated **AB**, the production of **ABA** competed against the dimerisation of aminoisoindoline, where **AA** was previously synthesised in toluene at reflux. Therefore, a new strategy was planned to prepare **ABA** starting from **AB**.

The strategy is designed using previously prepared **AB**s. This decision could be advantageous for synthesising **ABA**s because it eliminates one step of reaction progression. The reaction conditions were optimised by preparing ***nap*ABA** (**2.13**) starting from ***nap*AB** (**2.10**) because it has the highest yield among **AB**s (Scheme 2.8).

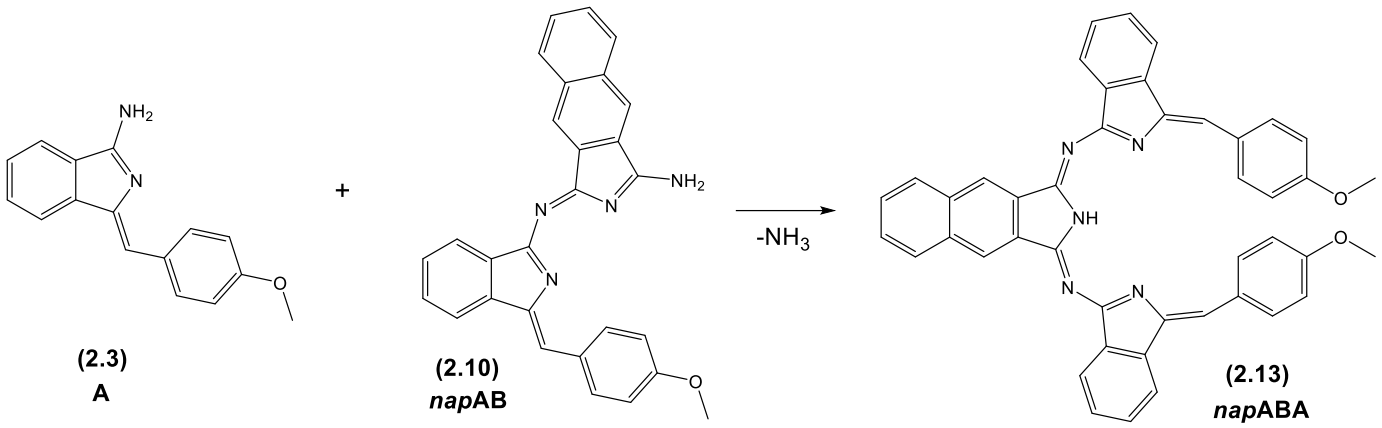

Scheme 2.8synthesis of benzo azatripyrrin (method B)

Aminoisoindoline **A** and ***nap*AB** were reacted with a 1:1 molar ratio. The reaction progression was monitored by TLC and ^{1}H NMR. This method significantly improved the yield of napABA obtained compared to the previous attempts. Table 2.1 illustrates the optimization progression.

No.	solvent	Temperature	Time	Vessel	Yield
1	toluene	reflux	7 days	Round-bottom flask	44%
2	p-xylene	reflux	4 days	Round-bottom flask	48%
3	p-xylene	180 ^{o}C	overnight	Sealed tube	60%
4	p-xylene	180 ^{o}C	2 days	Sealed tube	42%

Table 2-1 Reaction conditions for the synthesis of azatripyrrin (method B)

Entry 3 from Table 2.1 represents the best reaction conditions with the highest yield. Elevated temperatures are favourable for synthesising ***nap*ABA**. Like the previous method, **AA** was observed. The yield increase of ***nap*ABA** against **AA** would be likely due to the condensation reaction starting from ***nap*AB**. On the other hand, increasing reaction time led to the formation of green residue, which was confirmed by MALDI as naphthalocyanine (*m/z*= 714). Therefore, the obtained yield from reaction conditions of entry 4 of Table 2-1 was lower than entry 3. A minor byproduct was observed with a mass comparable to ***nap*AB**; however, it behaved differently during column chromatography. It was eluted by DCM, while ***nap*AB** elutes by higher polarity solvents (i.e. ethyl acetate). The compound is predicted to result from -NH_2 conversion to carbonyl. Scheme 2.9 illustrates the products of reaction conditions of entry 3 in Table 2.1.

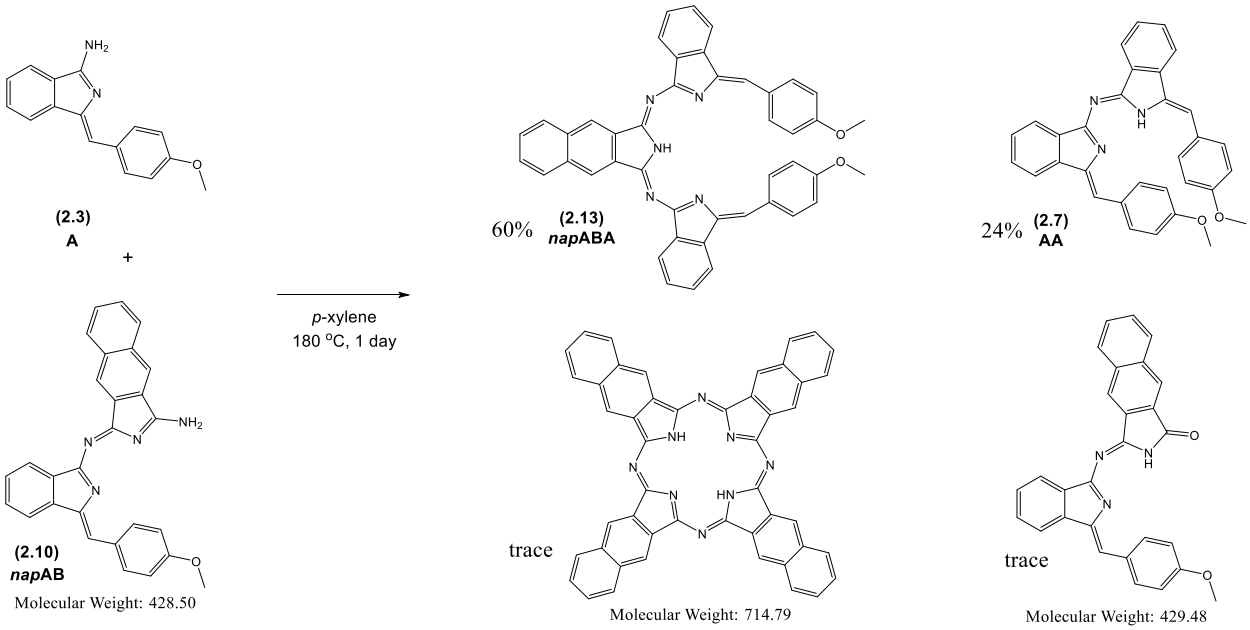

Scheme 2.9 products obtained from the synthesis of ***nap*ABA**

Upon reaction completion, ***nap*ABA** was isolated by column chromatography using DCM. The product was successfully crystallised using a mixture of DCM and petroleum ether. The product was characterised by ^{1}H NMR, ^{13}C NMR, MALDI-TOF, UV-Vis, melting point, and X-ray. NMR confirmed the number of protons and carbons in the product indicating the symmetry of the compound (Figure 2.6).

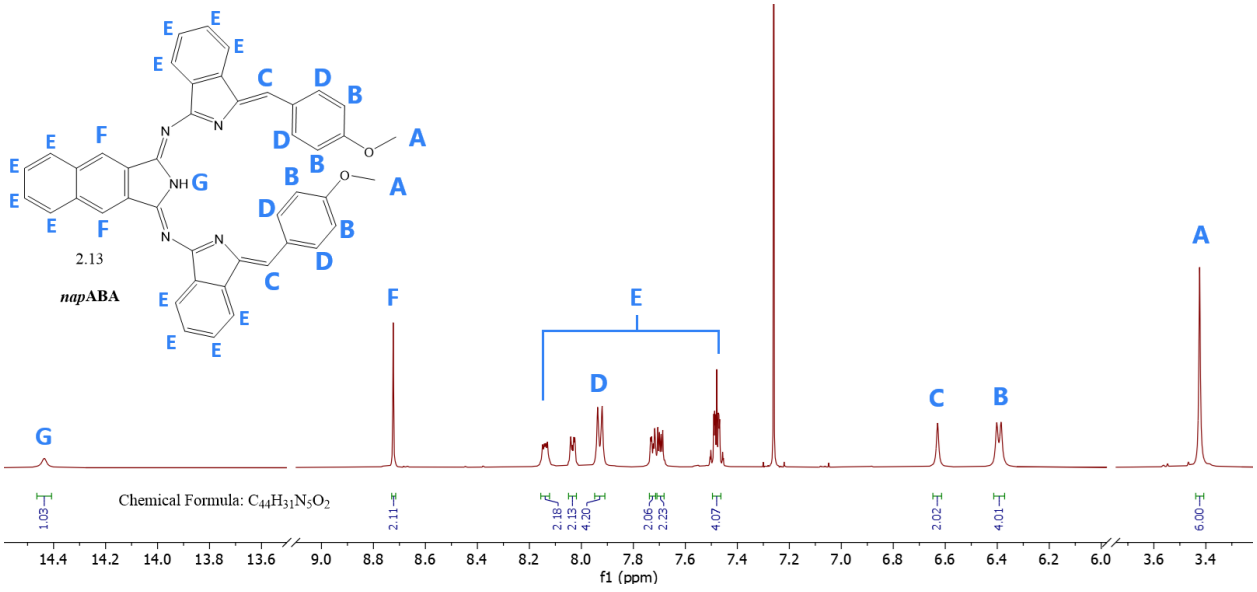

Figure 2.6 ^{1}H NMR of ***nap*ABA**

The crystal structure shows two independent tris-isoindole molecules and two solvent (CH_2Cl_2) molecules in the asymmetric unit. The principal molecules have very similar dimensions and conformations; the only significant differences are in the orientations of one

of the methoxy groups, the methoxy group of O(57)–C(58). The two molecules are mirror images, and the crystals are racemic mixtures. Each molecule forms a spiral chain, from O(31) to C(24), N(14), C(40), C(50) and O(57) in the first molecule and correspondingly from O(131) to O(157) in the second. The phenyl groups in each molecule are essentially parallel and overlapping with interplanar distances *ca* 3.4 Å in both molecules. The central, benzo-isoindole nitrogen atom in each molecule, N(1) and N(101) has a hydrogen attached; these hydrogen atoms form bifurcated hydrogen bonds to the other isoindole N atoms in the molecule. Each solvent molecule donates one hydrogen to a hydrogen bond to a 'bridging' N atom (between isoindole groups). Several instances exist of π…π contacts between parallel (or almost parallel) planes, but stacking appears limited to three (Figure 2.7).

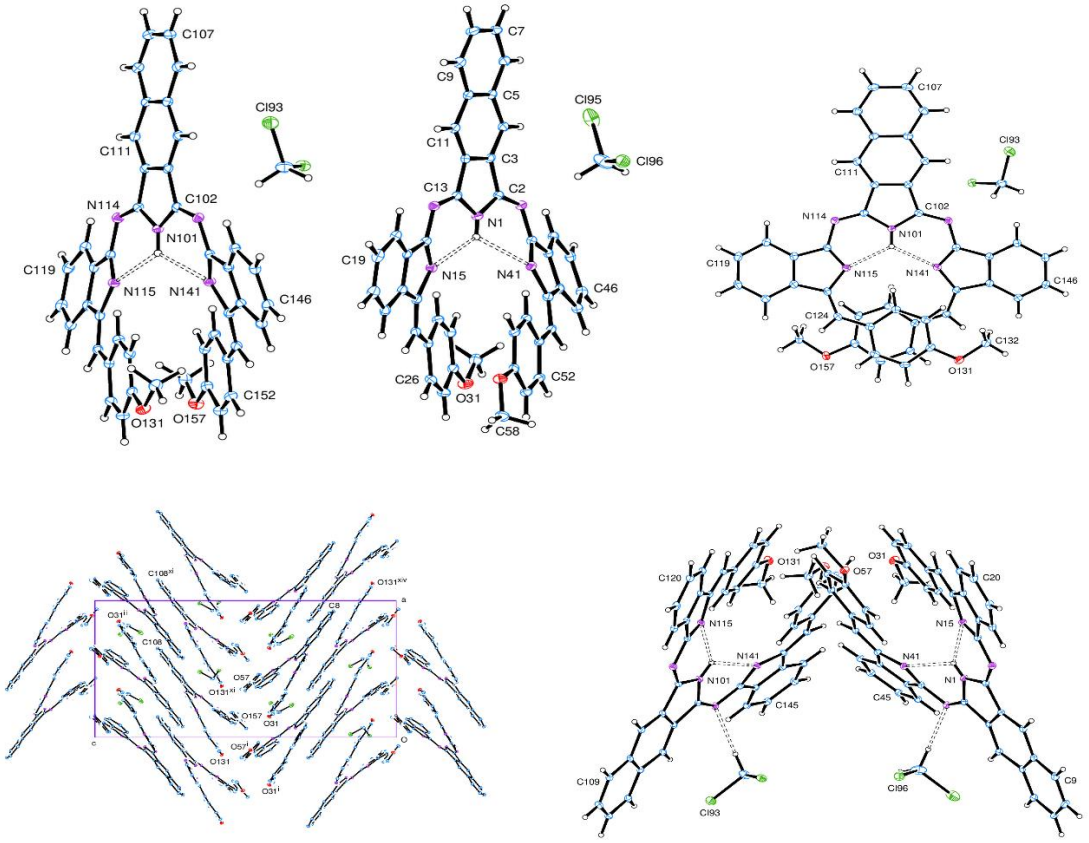

Figure 2.7 X-ray crystallography of ***nap*ABA**

***nap*ABA** is a dark brown compound showing a broad UV-Vis. absorption spectrum (Table 2.2).

A	λ (*nm*)
0.16	464
0.21	429
0.239	399
0.242	379
0.32	320
Ɛ (M^{-1} cm^{-1})	
$0.3.10^4$	
$0.4.10^4$	
$0.45.10^4$	
$0.46.10^4$	
$0.6.10^4$	

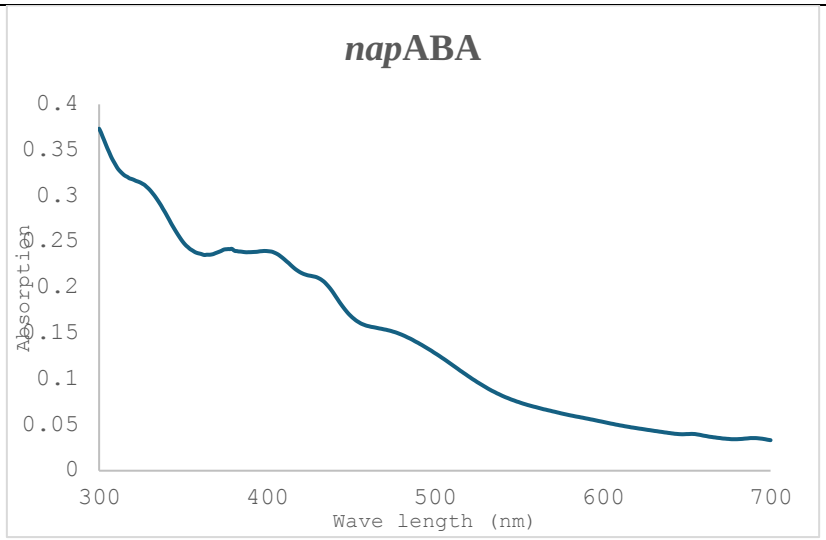

Table 2-2 UV-Vis. absorption of ***nap*ABA**

The reaction procedure of preparing ***nap*ABA** from the condensation of ***nap*AB** and **A** in *p*-xylene at 180 ºC overnight was applied to synthesise **ABA (2.14)** and ***tert*ABA (2.15)** from their **AB** and ***tert*AB** counterparts, respectively. As a result, **ABA** was obtained with a 50% yield and ***tert*ABA** a 55% yield. Similar characterization methods confirmed the synthesis as in ***nap*ABA**, except X-ray imaging was unsuccessful (Figure 2.8).

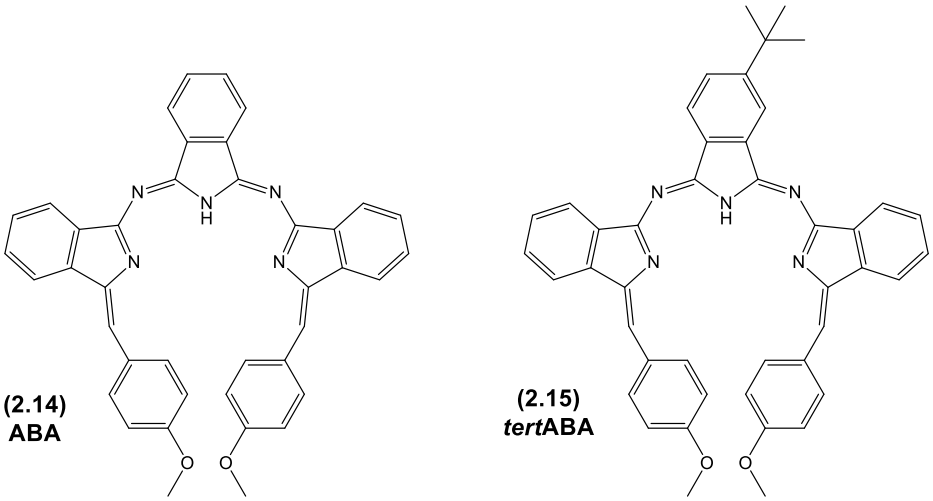

Figure 2.8 **ABA** (2.14) and ***tert*ABA** (2.15)

The first part of the project, preparing symmetrical and unsymmetrical benzo azadipyrrins and benzo azatripyrrins, was successfully achieved. The project then switched course investigating the complexation of these ligands with a target to prepare homoleptic complexes with various metals.

2.5. Complexation Attempts

2.5.1. Benzo Azatripyrrin

The complexations were attempted using ***nap*ABA** because it has the highest production yield compared to **ABA** and ***tert*ABA**. The first target was to obtain a homoleptic ruthenium complex [Ru(*nap*ABA)$_2$], which was inspired by the applications of tris(2,2'-bipyridine)ruthenium(II).[151, 152] The targeted complex was expected to be neutral (figure 2.9).

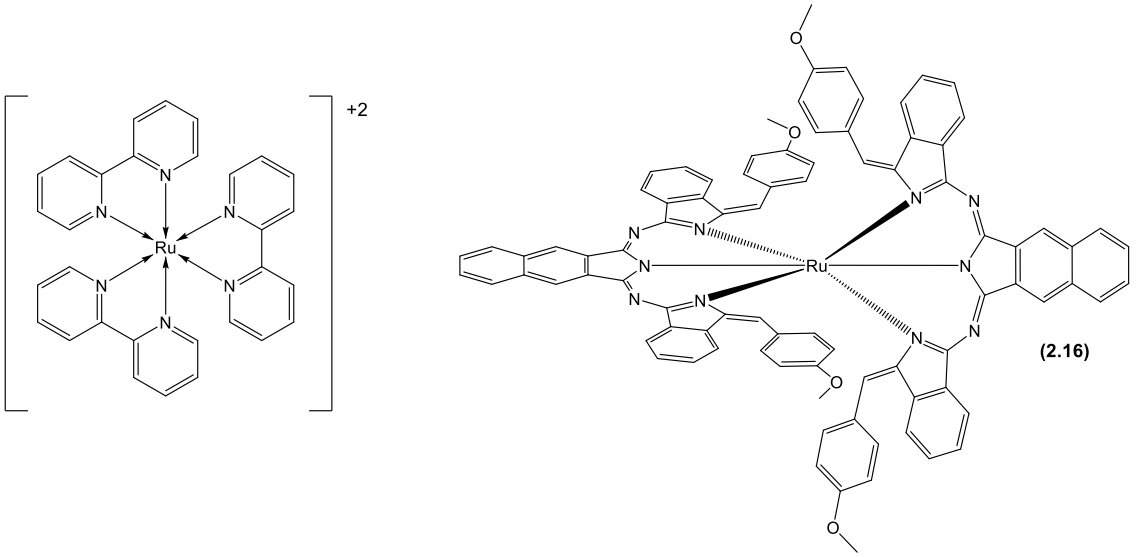

Figure 2.9 tris(2,2'-bipyridine)ruthenium(II) compared to targeted ***nap*ABA** complex

The first attempt was refluxing two equivalents of ***nap*ABA** with one equivalent of $RuCl_3$ in degassed methanol under nitrogen, a commonly reported solvent in the literature.[153] The reaction proceeded for 6 hours without showing any change in the colour of the reaction mixture. Additionally, TLC consistently showed unreacted ***nap*ABA**. Adding a catalytic amount of DBU to promote the complexation via deprotonation of the -NH group in ***nap*ABA** caused the ligand spot to disappear on TLC. Also, many colourless spots were observed on TLC visible under UV lamp. While this was considered a sign of decomposition, MALDI confirmed the idea by showing several low-mass peaks, none exhibiting the isotopic distribution of ruthenium complexes.

Another procedure from the literature showed the preparation of the Ru complexes using a mixture of ethanol and water (8:2).[154] That reaction was carried out under reflux for 3 hours, followed by adding a saturated solution of KPF_6. The last step was necessary to precipitate the charged trisbipyridine complex. When attempting this procedure to prepare [Ru(*nap*ABA)$_2$], the reaction mixture was refluxed for four days with no progression observed

by TLC. Out of desperation, a saturated solution of KPF_6 was added even though the targeted complex was predicted to be neutral. As expected, this addition did not change the outcome.

In 1990, a procedure was reported to prepare tris(2,2'-bipyridyl) ruthenium(II) chloride hexahydrate using $RuCl_3$ in the presence of a reducing agent.[155]

$$RuCl_3 + 3C_{10}H_8N_2 \xrightarrow{NaH_2PO_2/H_2O} [Ru(C_{10}H_8N_2)_3]Cl_2 \cdot 6H_2O$$

$RuCl_3$ was dried for 3 hours in an oven at 120 ^oC before it was grounded and returned to the oven again to dry for one more hour. The reaction started by adding $RuCl_3$ and 2,2'-bipyridyl to water in a round bottom flask. After that, a freshly prepared sodium hypophosphite solution was added to the reaction mixture and refluxed. The colour of the reaction mixture changes from green to brown and then to orange. Finally, the mixture was filtered, and KCl_2 was added to the filtrate, which was then boiled to produce a deep-red solution. Following filtration, washing, and drying, tris(2 2'-bipyridyl) ruthenium(II) chloride hexahydrate was obtained with an 80% yield. This procedure was applied to synthesise [Ru(*nap*ABA)$_2$] up to the addition of sodium hypophosphite solution and reflux. The reaction mixture did not exhibit any colour changes. While the reported procedure was 3 hours long, the reaction was stopped after one day, with one spot showing on TLC (unreacted ***nap*ABA**). A similar procedure was reported using an ethanol and water solvent mixture (1.5:1).[156] Applying this procedure had the same result as the previous attempts. Adding a catalytic amount of DIPEA resulted in spot tailing of ***nap*ABA** on TLC. However, no improvement was observed by MALDI.

As previously discussed, X-ray imaging of ***nap*ABA** shows a helical geometry in which both phenyl methoxy groups cross each other. The structure exhibits a high state of steric crowding. Elevating the temperature could provide energy and promote a less strictly hindered isomer (Figure 2.10). The idea was to make ***nap*ABA** more accessible for metal insertion.

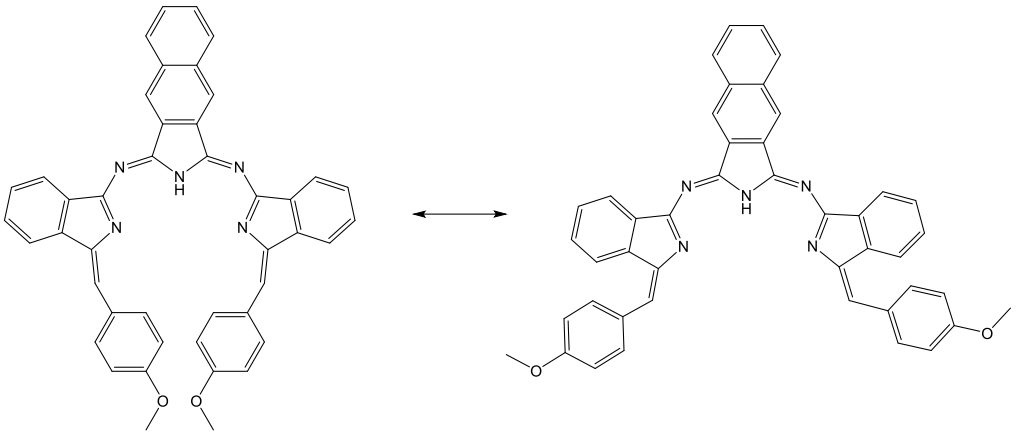

Figure 2.10 Conformational isomers of ***nap*ABA**

In a sealed tube purged with nitrogen, ***nap*ABA** and $RuCl_3$ were dissolved in octanol in the presence of NaH_2PO_2 and DIPEA. For comparison, another sealed tube was prepared with a similar reaction mixture except for $RuCl_3$. Both were heated in an oil bath at 140 ^oC, while the reaction progression was monitored by MALDI and TLC. The mixtures were heated for 8 hours. The control samples always showed a brown spot for ***nap*ABA** on TLC. The TLC of complexation samples did not show the spot of ***nap*ABA**. However, they showed a dominant spot sticking to the baseline. Increasing the polarity of the eluent generated a continuous dark red line fading to green. Several solvent systems were tested for preparative TLC, with every fraction showing an inseparable mixture of compounds confirmed by MALDI. Every fraction contained several peaks with *m/z* < 661 (***nap*ABA**) and many weak peaks of unknown complexes. Attempts of crystallisation failed to isolate the products of this reaction. Two complexation reactions were attempted using these conditions. Fe(*nap*ABA)$_2$ and Zn(*nap*ABA)$_2$ were targeted. As previously described, the reaction mixtures were prepared in two sealed tubes using $ZnCl_2$ and $FeCl_2$. Each reaction mixture contained two equivalent ***nap*ABA**, one equivalent of a metal salt, and a catalytic amount of DIPEA without using NaH_2PO_2. In an oil bath, the reaction mixtures were heated at 140 ^oC for 8 hours, monitored by MALDI and TLC. Samples from both reactions showed a dominant spot on the baseline of TLC. Increasing the polarity of solvent systems generated continuous faint coloured lines. Like Ru complexation, MALDI showed a mixture of several unidentified peaks below 661 *m/z*. However, the TLC of iron complexation samples showed a well-defined red spot when using DCM. This spot was isolated and characterised as a product of self-condensation of aminoisoindoline (**AA**).

Reactions limitations

Unlike bipyridine, ***nap*ABA** is a sterically hindered ligand. Applying the reported reaction conditions of preparing tris(2,2'-bipyridine)ruthenium(II) failed to produce ***nap*ABA** complexes. The use of harsh conditions led to the production of many low-mass compounds. This result indicates the decomposition of materials during the reaction. The generation of **AA** compound during the attempts to prepare Fe(*nap*ABA)$_2$ complex indicates the decomposition and rearrangement of ***nap*ABA**.

The literature reported the limitation of column chromatography in isolating complexes in the synthesis of 1,3-bis(2-pyridylimino)isoindoline complexes.[139] When using column chromatography, the generated complexes were trapped on the baseline. This behaviour was experienced during the attempts to prepare ***nap*ABA** complexes. While the reaction produced several unknown compounds (indicated by MALDI), successful isolation is crucial to identify the obtained products. Several crystallisation attempts failed to overcome this problem.

2.5.2. Benzo Azadipyrrin Complexation Attempts

After the unsuccessful attempts of azatripyrrin complexation, the focus shifted to the symmetrical azadipyrrin **AA**. Both ligands exhibited a symmetrical structure with two 4-methoxyphenyl groups. The bidentate ligand was used to prepare homoleptic complexes (figure 2.11).

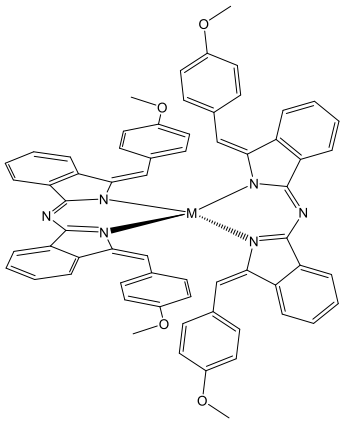

Figure 2.11 The targeted homoleptic complexes structure from symmetrical azadipyrrin

The first attempt was the synthesis of a ruthenium complex. A test reaction was performed using $RuCl_3$ in a 2:1 molar ratio (**AA**: Ru), and methanol was used as a solvent in the presence of TEA. The reaction progression was monitored by TLC and MALDI for three days. This reaction condition was considered a failed attempt, as TLC and MALDI showed

unreacted **AA**. As a result, it was decided to investigate the complexation with Cu(II), Zn(II), and Ni(II). The reported conditions of preparing dipyrrin complexes inspired the attempted complexation reaction conditions.[115, 157, 158] The step of reducing dipyrromethane to dipyrromethene by DDQ was not implemented. While the investigated ligand is an azadipyrromrethtene, only the reported complexation conditions were used. No complexes were successfully isolated from these attempts so that these reactions will be briefly discussed. Table 2.3 summarises the attempted complexation reactions.

No.	**Reactants**	**Solvent**	**Temperature**	**Duration**
1	AA + $CuCl_2.H_2O$ (in methanol)	chloroform	rt – reflux	3 days
2	AA + TEA + $CuCl_2.H_2O$ (in methanol)	chloroform	reflux	2 days
3	AA + TEA + $CuCl_2.H_2O$	methanol	rt – reflux	3 days
4	AA + TEA + $CuCl_2.H_2O$ (in methanol)	DCM	reflux	3 days
5	AA + $Zn(OAc)_2$	methanol	rt – reflux	3 days
6	AA + $Zn(OAc)_2.2H_2O$	methanol	rt – reflux	3 days
7	AA + TEA + $Zn(OAc)_2.2H_2O$	methanol	rt – reflux	3 days
8	AA + TEA + $Zn(OAc)_2.2H_2O$ (in methanol)	toluene	80 ^oC	overnight
9	AA + TEA + $Zn(OAc)_2.2H_2O$ (in methanol)	toluene	reflux	overnight
10	AA + TEA + $Ni(OAc)_2.4H_2O$	DCE	reflux	2 days

Table 2-3 Attempted complexation reaction of symmetrical azadipyrrin

The TEA base was used to deprotonate **AA** by stirring for 30 minutes in a solution mixture before introducing the metal. The reaction conditions from Table 2.3 produced several products observed by MALDI. While some were predicted as 1:2 and 1:1 (M: L) complexes, others could not be identified. The solvents were used based on the solubility of the reactants. Changes in the solvent of some conditions aimed to isolate produced complexes by precipitation. The reactions that started at room temperature did not show any progress overnight. Thus, the temperature was elevated.

MALDI of crude reaction mixtures showed several products. Some were calculated as 1:1 and 2:1 (L: M) complexes, and others were not predicted. Therefore, column chromatography was attempted to isolate the products of these reactions. However, TLC showed a significant spot on the baseline that generates a faint coloured line of overlapping

spots. This finding was observed in every reaction. Column chromatography failed to isolate a pure compound. The crystallisation of these fractions using various solvent mixtures did not successfully purify the obtained products. Furthermore, after the crystallisation attempts, the TLC of nickel and zinc samples started to show a significant spot of **AA** eluted by DCM. Confirmed by MALDI and NMR, this spot was a metal-free starting material. The generation of **AA** is an indication of metal-releasing from nickel and zinc complexes. The inability to attain stable complex geometries with **AA** could be the reason for the instability of these complexes. As a result, the complexation of benzo azadipyrrins continued by investigating unsymmetrical ligands (**AB**).

The unsymmetrical **AB** group has one 4-methoxyphenyl group compared to **AA**, which has two groups. This could be beneficial for obtaining different complex geometries (Figure 2.12).

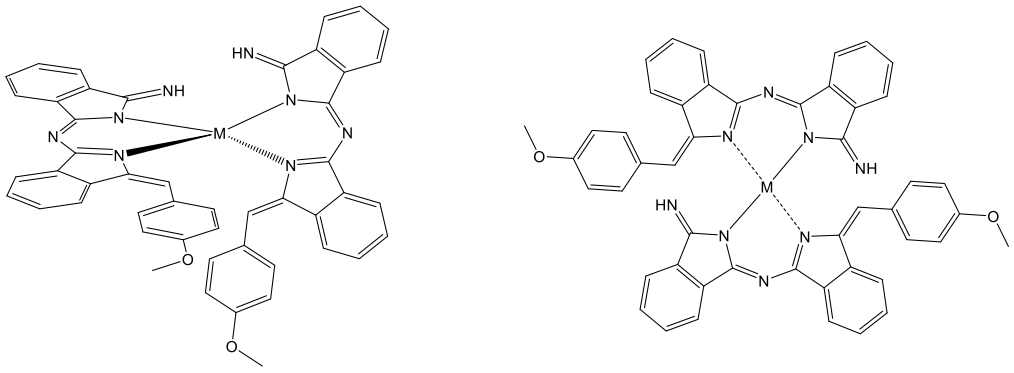

Figure 2.12 The targeted homoleptic complexes structure from unsymmetrical azadipyrrin

The unsymmetrical ***nap*AB** was used to synthesise Zn(II) complexes. As experienced with the complexation of **AA**, the attempts to prepare Zn(***nap*AB**)$_2$ produced several products. Column chromatography resulted in produced complexes being trapped on silica gel. Modifying reaction conditions led to a procedure in which a precipitation of new complexes was observed. At room temperature, two equivalents of ***nap*AB** reacted with one equivalent of $ZnBr_2$ in THF. The reaction proceeded overnight, and a precipitating solid was observed. This solid was filtered and redissolved in acetonitrile. The mass spectrometry of the new solution showed three types of zinc complexes. The first was predicted as a 1:1 complex, while the second and the third were predicted as 2:1 complexes (L: M) with a mass difference of 14 mass units (Figure 2.13).

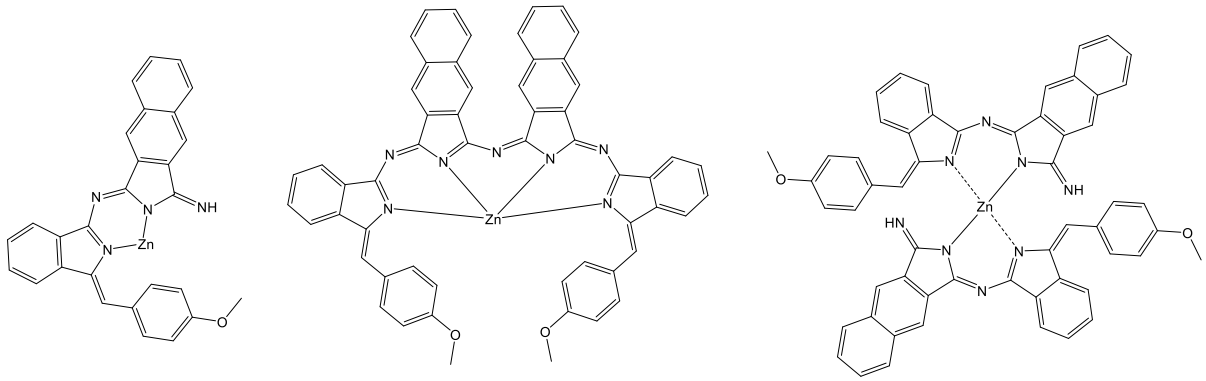

Figure 2.13 Predicted complexes by MALDI of Zn-***nap*AB**

Based on the predictions shown in Figure 2.13, the filtered solid was dissolved in acetonitrile and refluxed. This step aimed to convert complex (2.19) to (2.18) by releasing NH_3. However, by comparing the MALDI results of the solution before and after reflux, the goal was not achieved (Figure 2.14). Moreover, the peak of ***nap*AB** starting material was observed after heating the sample. This finding indicates that the metal was falling off the complexes under reflux.

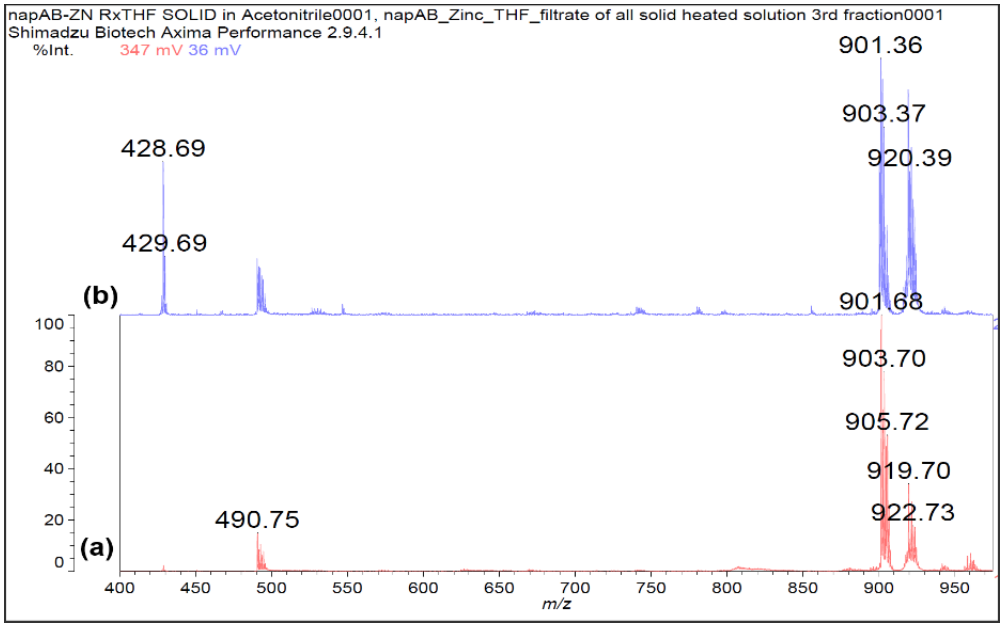

Figure 2.14 MALDI of precipitated solid (a) before reflux in solution, (b) after reflux in solution

Purifying the obtained solid by column chromatography using silica gel and neutral alumina was impossible due to complexes trapped on the baseline. Several crystallisation attempts failed to isolate a pure complex. The problems encountered in the preparation of zinc

complexes were not solved. However, a new challenge arose in the attempt to synthesise nickel complexes.

Unsymmetrical azadipyrrin (**AB**) and nickel (II) acetate were added to a dry acetonitrile solvent in a 2:1 molar ratio. The reaction produced several complexes, which were observed by MALDI. Unlike the previous experience, a new pink spot was observed using neutral alumina TLC. The pink fraction was isolated by column chromatography. However, the fraction was not pure. MALDI and ^{1}H NMR confirmed the presence of several complexes. Upon crystallisation attempts, the soluble pink materials turned into insoluble blue materials. Different solvents failed to redissolve the new material. While the process was not understood, the progress in investigating the complexation of nickel with unsymmetrical azadipyrrin was limited by the formation of the insoluble materials.

Many obstacles limited the success of obtaining new complexes. The attempted reaction conditions produced several products. Therefore, isolation and purification are crucial to identifying these products. Column chromatography, using silica gel or neutral alumina, led to most of the complexes being trapped on the baseline. Also, isolated fractions were not pure. Several crystallisation attempts also failed to obtain clean products. On the other hand, the stability of some complexes was another limiting factor during the investigation. Many test reactions produced similar results. However, the investigation finally turned into a successful trajectory with the complexation of palladium.

2.6. Palladium Complexes

2.6.1. Unsymmetrical Benzo Azadipyrrin-Pd complexes

The investigation initially targeted the synthesis of 2:1 (L: M) complexes. At room temperature, a reaction mixture of AB with palladium(II)chloride in dry acetonitrile was stirred under nitrogen. Using neutral alumina TLC, acetonitrile eluted a new purple spot. The new complex was isolated by column chromatography and crystallised in a solvent mixture of DCM and hexane. The first ^{1}H NMR sample was prepared in deuterated chloroform, which led to complex decomposition. However, a clean ^{1}H NMR spectrum was obtained using deuterated DCM. The predicted compound was a 1:1 (L: M) type complex. Initially, the acetonitrile molecule was expected to coordinate with the palladium metal. However, MALDI showed the complex mass that equals the total mass of [(**AB** + Pd + one acetonitrile molecule) – 1 proton]. Additionally, the isotopic distribution of the calculated mass matched the observed one.

Therefore, the obtained complex was confirmed as a 1:1 type by incorporating an acetonitrile unit into **AB,** turning a diaza ligand into a triaza one. To match the observed mass, palladium metal must be inserted into the phenyl methoxy group. ^{1}H NMR and MALDI data in Figure 2.15 support this prediction. On the other hand, ^{13}C NMR experiments failed to produce a spectrum even with high number of scans. While this could indicate a high relaxation time, however, the issue was not resolved at this stage.

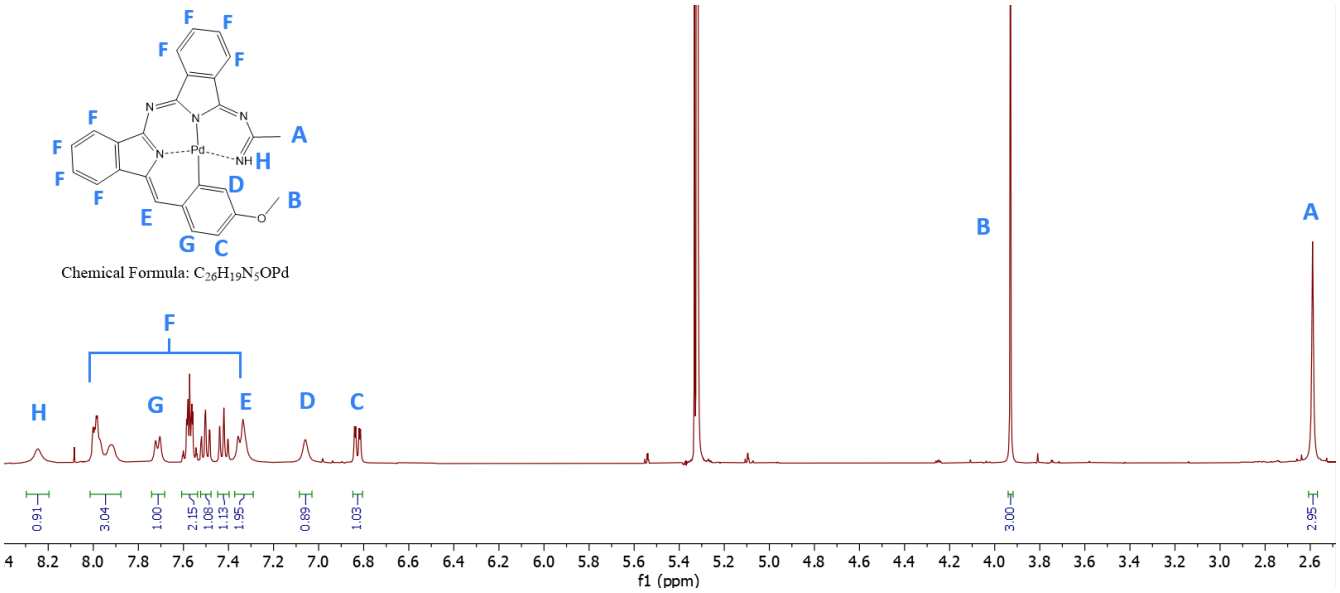

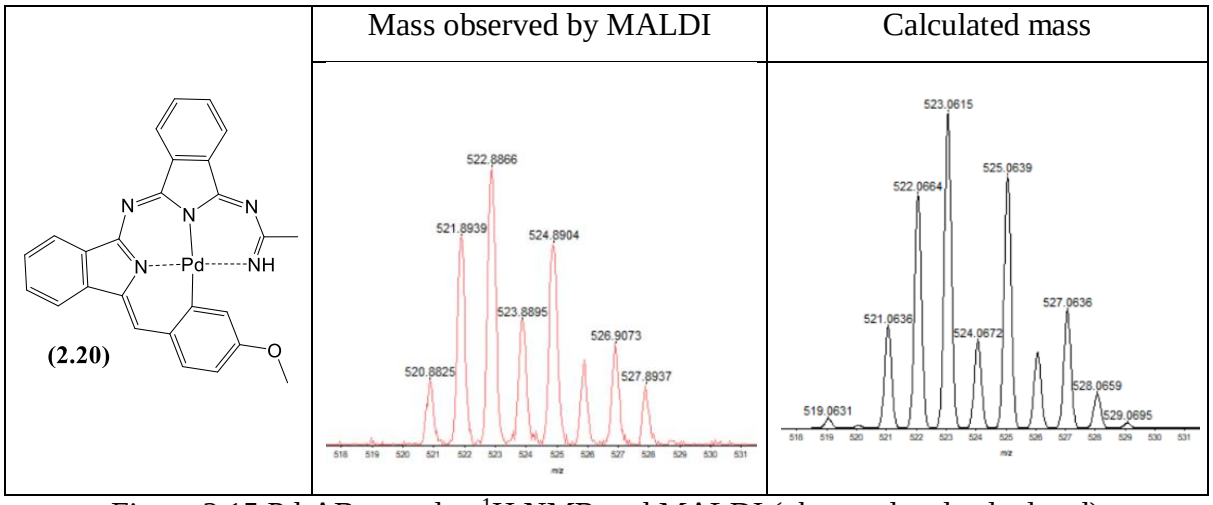

Figure 2.15 Pd-AB complex ^{1}H NMR and MALDI (observed and calculated)

The insertion of palladium into the phenyl methoxy was confirmed by stacking ^{1}H NMR spectra of **AB** and **Pd-AB**. The palladium metal insertion broke the phenyl group's initial symmetry on **AB** (peaks 1 and 2). The doublet peaks had an integration equivalent to four protons on **AB**. Upon metal insertion, three new peaks were observed 1,2, and 3 with an integration corresbondance to 1 proton each (three in total) as showen in Figure 2.16. These new showed a range of splitting, and were assigned based on their *J* values. Several

crystallisation attempts failed to obtain a crystal suitable for X-ray to confirm the complex structure.

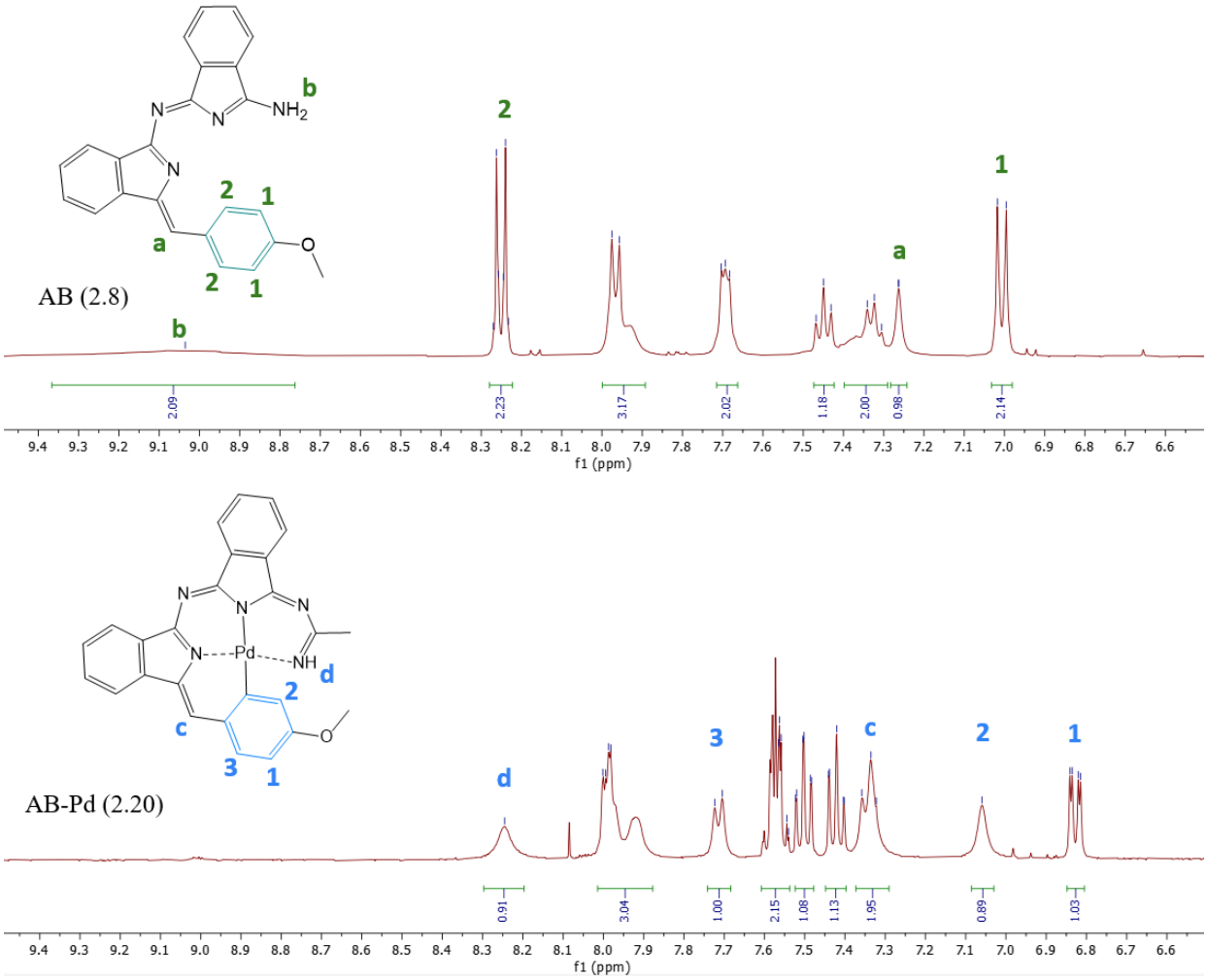

Figure 2.16 ^{1}H NMR of AB-Pd vs AB indicating the insertion of palladium

After this breakthrough, the project's interest shifted to investigating the synthesis of these complexes. Performing the previous reaction using a 1:1 molar ratio of **AB** and $PdCl_2$, the **Pd-AB** complex was obtained with an 87% yield. The reaction proceeded for 7 days to consume **AB** completely under nitrogen at room temperature. Utilising previously prepared unsymmetrical azadipyrrins (***tert*AB** and ***nap*AB**), new palladium complex derivatives were successfully produced with good yields (81% and 89%, respectively). The synthesis was verified by ^{1}H NMR and MALDI, proving the insertion of palladium metal into the phenyl group and the incorporation of an acetonitrile molecule into the ligand (figure 2.17). Finally, the structure of these complexes was determined by X-ray crystallography. This was possible by the recrystallisation of the **Pd-*tert*AB** complex in a mixture of DCM and hexane (figure 2.18).

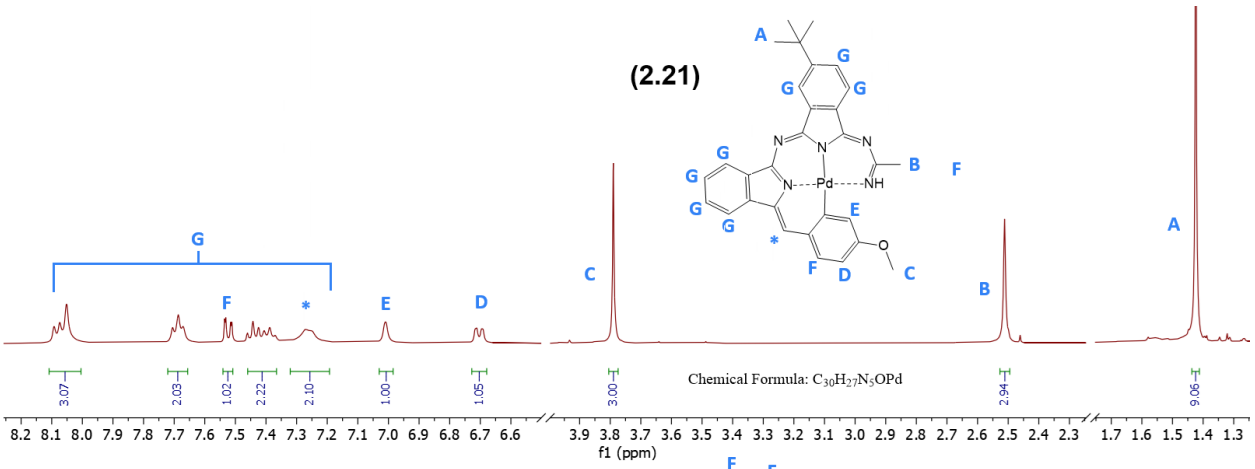

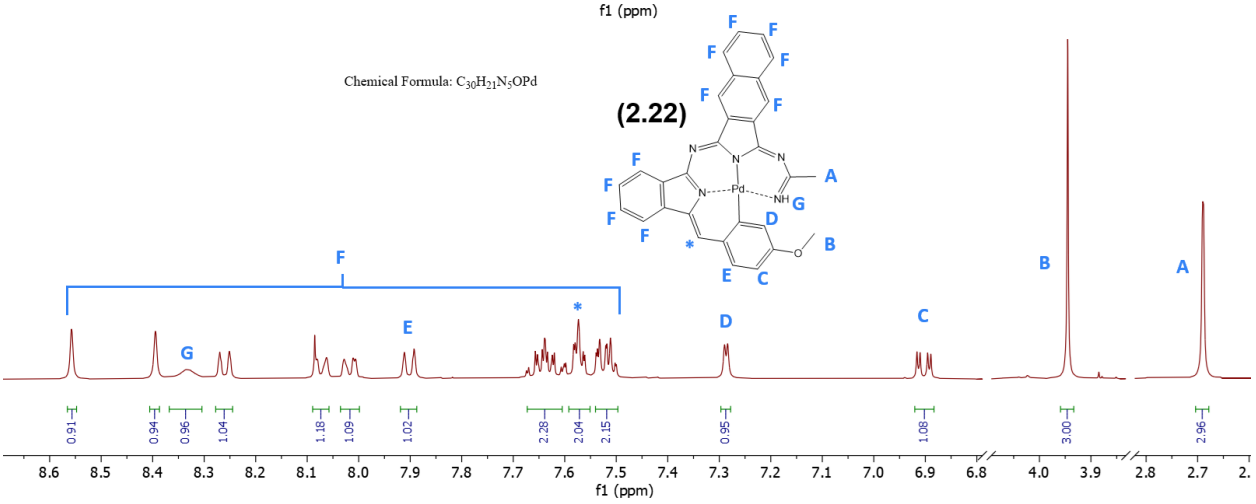

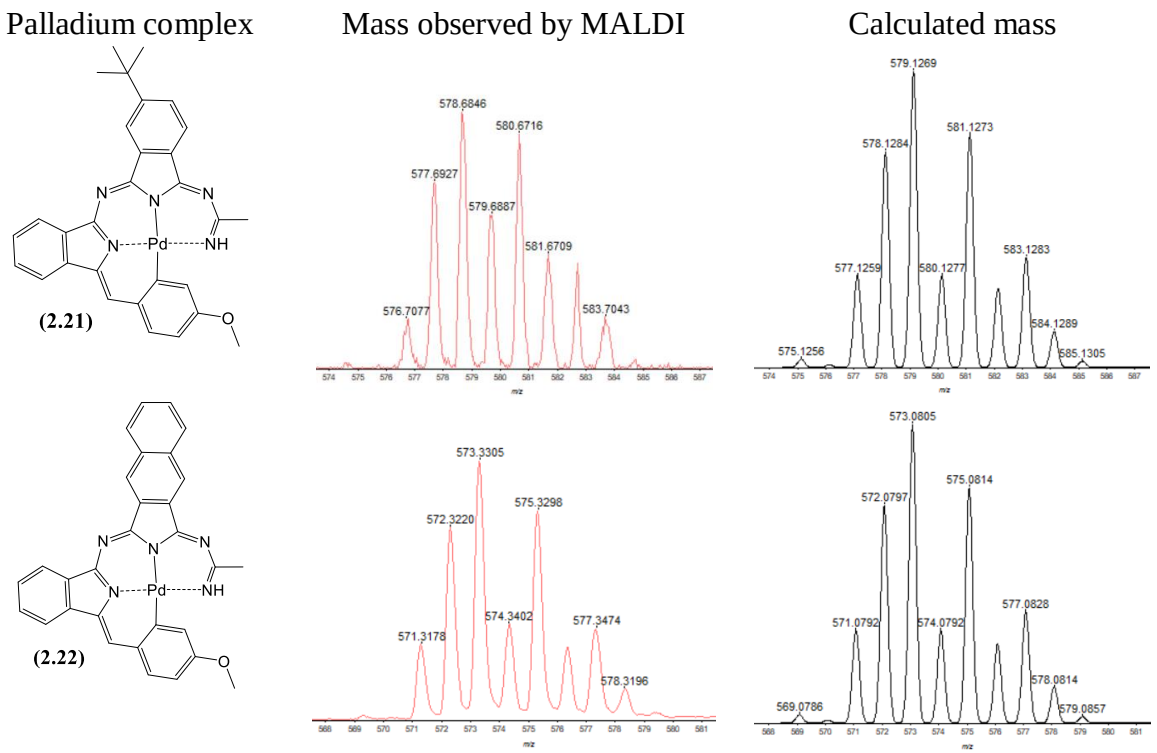

Figure 2.17 Pd-*tert*AB and Pd-*nap*AB complexes ^{1}H NMR and MALDI (observed and calculated)

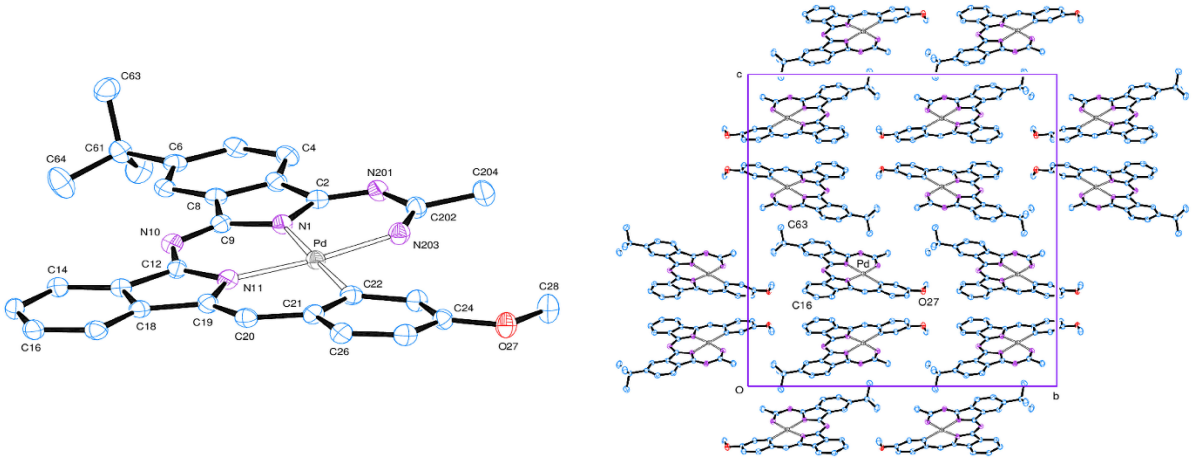

Figure 2.18 X-ray of ***tert*AB-Pd**

X-ray crystallography approved the structure of **Pd-*tert*AB** (**2.21**). The palladium centre exhibited a square planer geometry, which extended across most of the. However, the *t*-butyl and methoxy groups significantly deviated from this plane. Columns of molecules stacked with the NCMeNH group of one complex is lying over the phenyl group of the lower molecule.

Another complex was obtained by performing the reaction in benzonitrile instead of acetonitrile. In this procedure, ***tert*AB** was used. The complex was successfully obtained with an 84% yield. While the reason for using ***tert*AB** was to grow suitable crystals for X-ray crystallography, unfortunately, the goal was not achieved. However, the synthesis was confirmed by ^{1}H NMR and MALDI (figure 2.19).

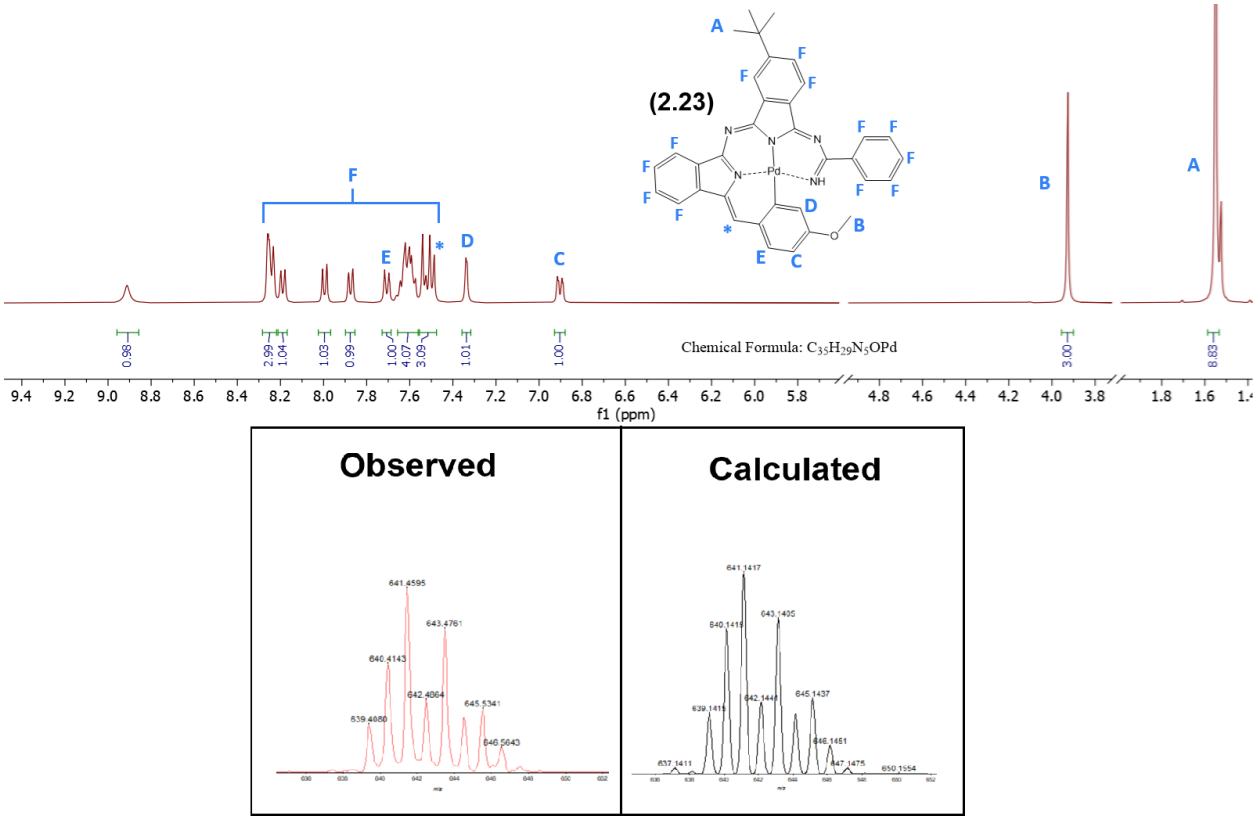

Figure 2.19 Pd-*tert*AB-benzonitrile complex ^{1}H NMR and MALDI (observed and calculated)

Another proof of synthesis is the change in UV-Vis. absorption. The starting ligands are brownish-orange, and the obtained complexes are purple. The starting ligands showed a broad absorption peak around λ ~430 nm. This broad peak is shifted to λ ~530 nm in the obtained complexes. This change in colour and absorption behaviour is related to the electronic environment present by the central palladium and indicates the successful complexation (figure 2.20 and 2.21).[159]

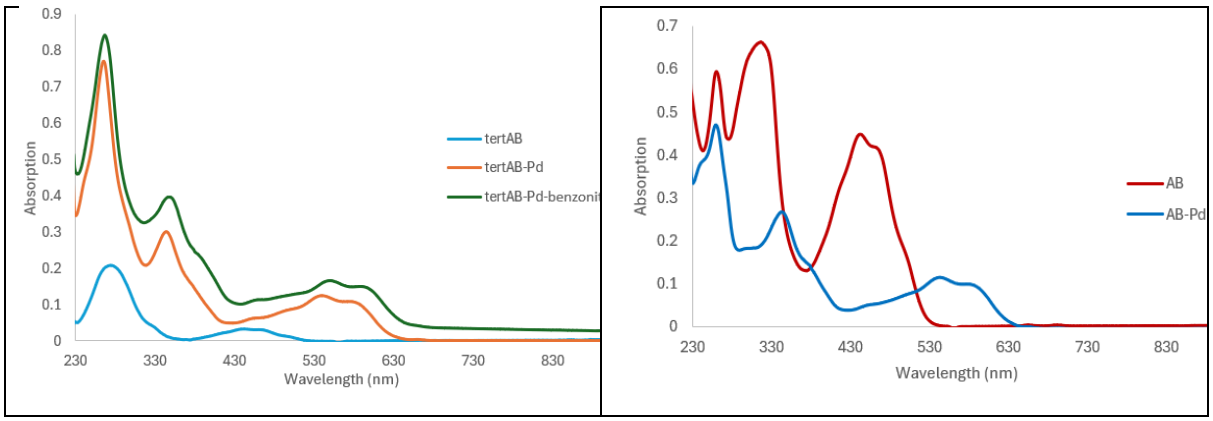

Figure 2.20 UV-Vis absorption of ligands vs complexes (**AB** and ***tert*AB**)

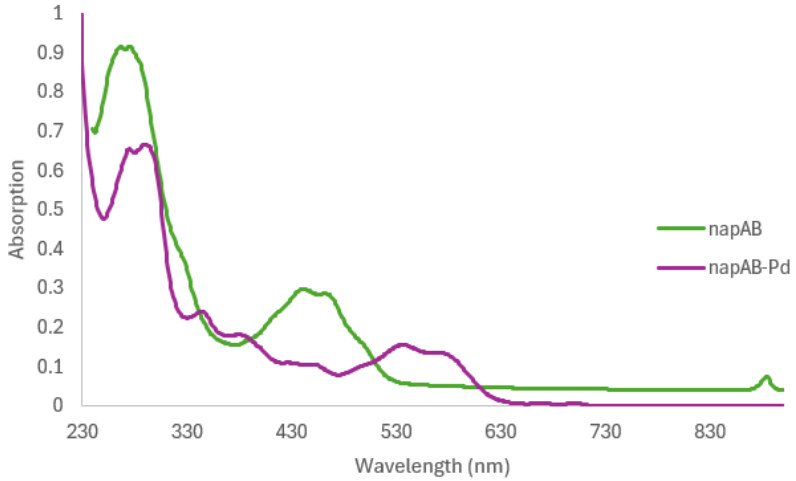

Figure 2.21 UV-Vis absorption of ***nap*AB** vs **Pd-*nap*AB**

The synthetic procedure was inspired by the literature's report on synthesising the palladium(II) complex (Scheme 2.10).[160] While the targeted complex was achieved via a multi-step process, the procedure reported in this project could be valuable in the advancement of synthesizing linear tripyrroles and longer oligopyrrole-based complexes. Achieving this goal could be attributed to the solvent modification that produced **Pd-*tart*AB-benzonitrile** (2.23).

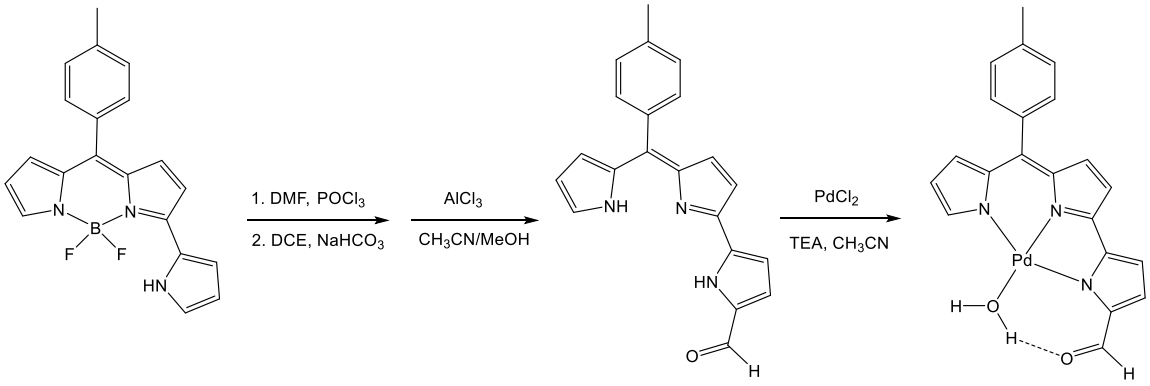

Scheme 2.10 Synthesis, structure, and properties of palladium(II) complex of α-formyl pyrrolyl dipyrromethene.[160]

The example above lacks the insertion behaviour of palladium, which has been witnessed in this project. The synthesis of acetatopalladium(II) 1,3-Bis(2-arylimino)isoindoline was reported with the insertion of palladium metal into an arylimino group. This was selectively achieved using an excess of palladium (II) acetate. However, it was also reported that the ligand's low solubility efficiently supported the product's selective formation (Figure 2.22).[161]

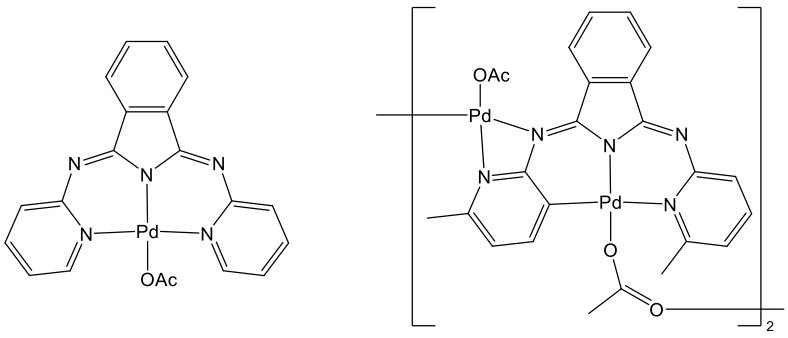

Figure 2.22 Coordination Modes of Acetatopalladium(II) Complexes with 1,3-Bis(2-arylimino)isoindoline Ligands.[161]

2.6.2. Symmetrical Benzo Azadipyrrin-Pd complexes

The successful synthesis of unsymmetrical palladium complexes was followed by applying the same reaction conditions to prepare the symmetrical **Pd-AA** complex. Following the same procedure, **AA** was dissolved in dry acetonitrile, followed by the addition of $PdCl_2$. The reaction proceeded at room temperature under nitrogen. TLC showed the total consumption of **AA** after 5 days, and an insoluble solid formed. After filtration, several solvents were tested to dissolve the obtained solid. However, the insolubility limited the investigation of this reaction. On the other hand, performing the same reaction using $Pd(OAc)_2$ produced a homogeneous reaction solution mixture. The reaction proceeded for 7 days until the consumption of **AA** ligand. Neutral alumina TLC approved the completion of the reaction. While the spot of **AA** disappeared, two new spots were observed using an ethyl acetate eluent. A clean separation between these spots was difficult to attain. 2D TLC indicated the presence of an equilibrium between these compounds. This kind of equilibrium was documented when preparing aza (dibenzo) BODIPYs.[75]

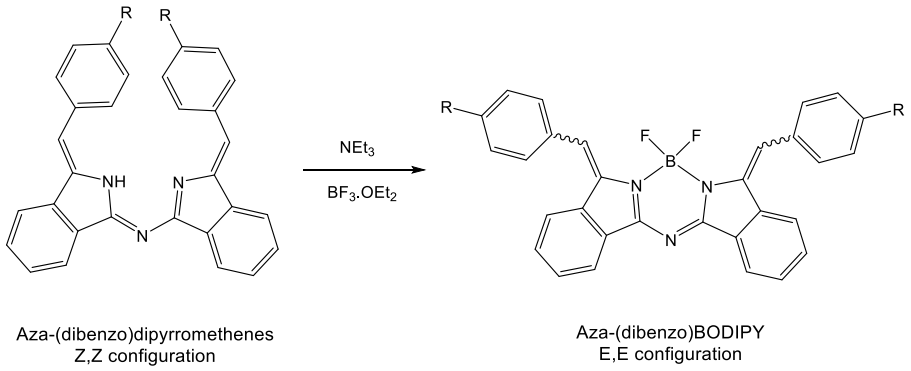

Scheme 2.11 Synthesis of Aza-(dibenzo)BODIPY.[75]

The isolation and characterisation were challenging because the product was a mixture of isomers. While X-ray crystallography confirmed the *E,E* configuration, leaving the sample

in solution at room temperature produced a mixture of *Z* and *E* isomers in equilibrium. NMR also confirmed the presence of the equilibrium.

Returning to the palladium complexation of AA with $Pd(OAc)_2$ in acetonitrile. The attempt to isolate the spots by column chromatography was not successful. However, the ^1H NMR of the collected fraction confirmed the equilibrium by showing different single peaks of a singlet. While using a similar predecessor of the reported Aza-(dibenzo)BODIPY (i.e. **AA**), the observed equilibrium could be related to configurational isomers. However, it is worth mentioning that the spots in equilibrium are red and orange coloured. Two samples of the isolated fractions were separately dissolved in ethyl acetate and acetonitrile. The samples were left overnight, and 2D TLC was performed the next day. The equilibrium was persistent. However, the TLC of the ethyl acetate sample showed a dominant orange spot and a faint red spot. While the equilibrium was not fully understood, the decision was made to perform the complexation reaction in ethyl acetate.

AA and $Pd(OAc)_2$ were dissolved in a 1:1 molar ratio in ethyl acetate. The reaction proceeded for 7 days under nitrogen at room temperature. The neutral alumina TLC showed a single orange spot eluted by ethyl acetate. Upon the complete consumption of **AA**, the product was isolated by column chromatography. Several crystallisation attempts failed to obtain suitable crystals for X-ray crystallography. The isolated product was characterised by MALDI and ^1H NMR. The obtained product exhibited a structural symmetry showing a single singlet peak with an integration corresponding to six protons representing two methoxy groups at 3.8 ppm. A double insertion of palladium into both phenyl groups was predicted by comparing the ^1H NMR spectrum of the palladium complex with the metal-free **AA** ligand. The doublet peak around 6.6 ppm and 7.9 ppm of the **AA** ligand represented 8 protons of the two methoxy phenyl groups. Upon insertion of palladium metal, the two peaks disappeared. Like **AB-Pd,** three new peaks were observed with a total integration value of 6 protons. Exhibiting similar splitting observed previously, the new peaks were assigned and confirmed the synthesis of the new palladium complex. This structure approves the observed symmetry by ^1H NMR. Also, the calculated mass and isotopic distribution matched the observed by MALDI (figure 2.23).

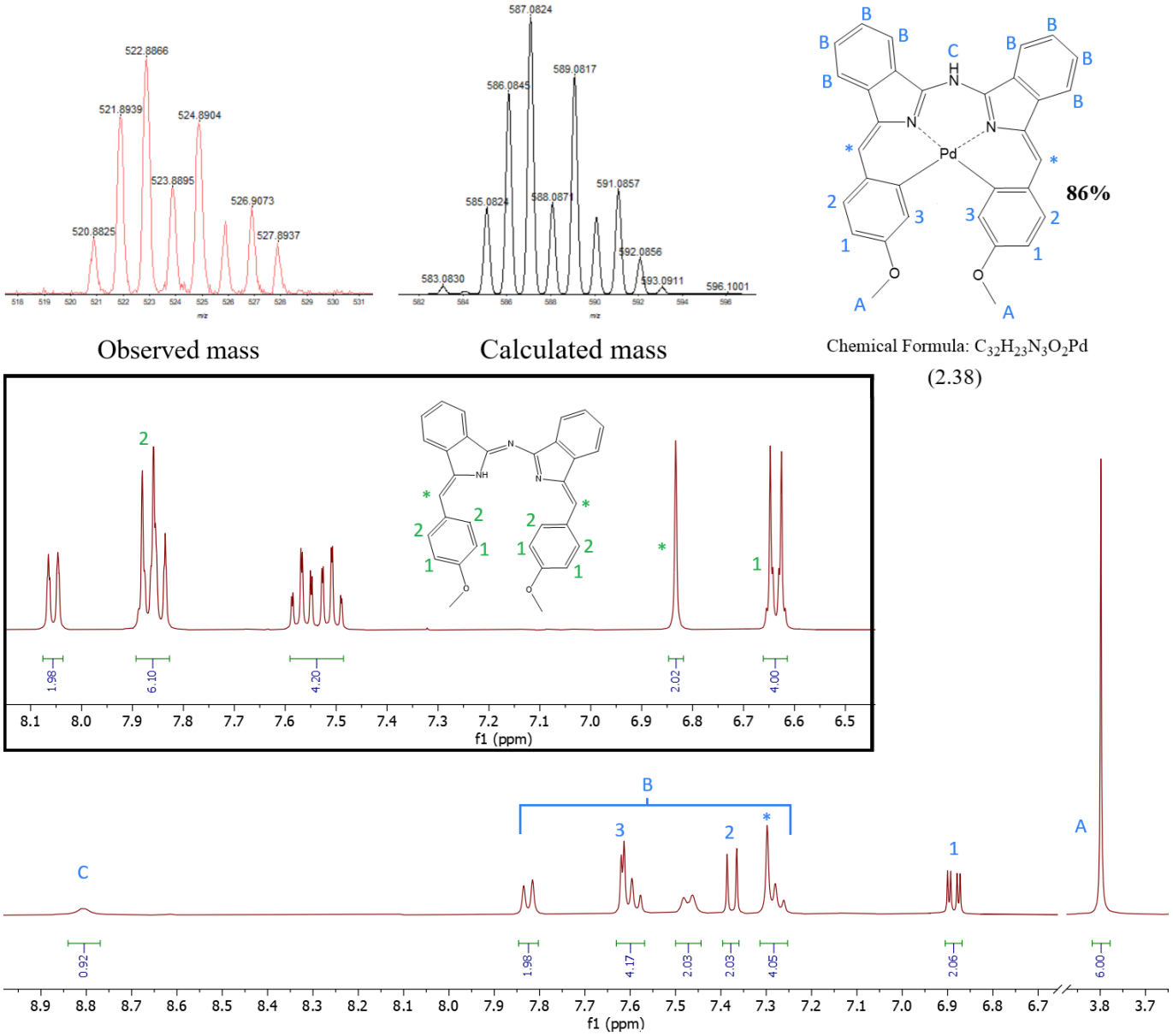

Figure 2.23 Calculated and observed mass of the AA-Pd complex and ^{1}H NMR spectrum of AA-Pd vs AA

The **Pd-AA** (**2.24**) was obtained with an 86% yield. While the new complex was characterised by ^{1}H NMR and MALDI, the ^{13}C NMR experiment did not represent a spectrum similar to the unsymmetrical palladium complexes. The symmetrical complex is described as a dark red (burgundy) compound. The UV-Vis. absorption study of the palladium complex showed two distinguishing peaks at λ = 267 and 404 nm. This absorption differs from the **AA** ligand, where the main absorption peak can be observed at λ = 358 nm. While the absorption in **AA** depends solely on the decolonisation of conjugated π-electrons, the complex has a unique electronic environment in the *d*-orbitals of palladium. The observed effect on UV-Vis.

absorption indicates the presence of palladium metal, thus proving the synthesis of the **Pd-AA** complex (figure 2.24).

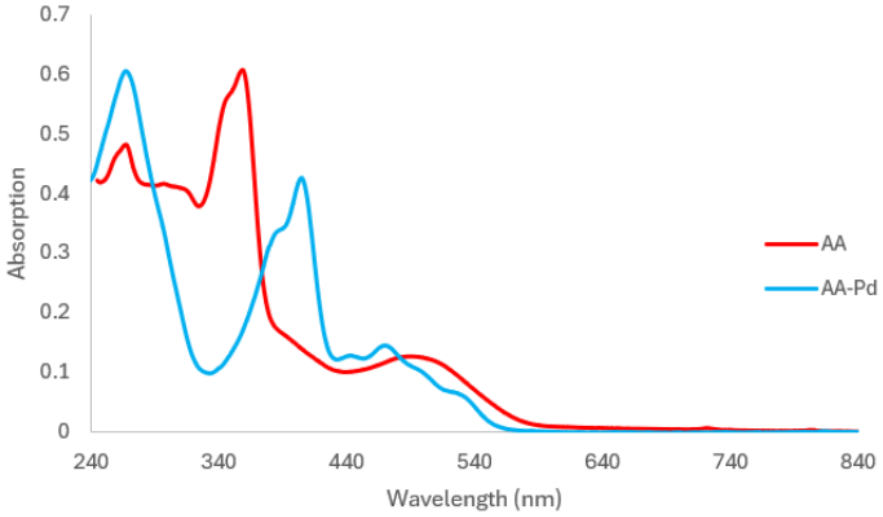

Figure 2.24 UV-Vis absorption of **AA** vs **AA-Pd**

Conclusion

This project initially investigated the synthesis of homoleptic complexes. The main objective was to prepare 2:1 (L: M) type complexes using either symmetrical or unsymmetrical aza (benzo) dipyrromethene. This was the alternative path after the unsuccessful attempts to synthesise homoleptic aza (benzo) tripyrrin complexes. Some metals with several reaction conditions were tried to achieve this goal. Nevertheless, many obstacles prevented the progression of the project, whether the produced complexes' isolation or stability. The 2:1 type complexes were not obtained. However, the successful synthesis of the unsymmetrical palladium (II) complexes directed the project to focus on these complexes. The obtained products are characterised by the incorporation of a solvent molecule into the complexation. Additionally, the palladium was inserted into the phenyl group to produce the complex with square planar geometry. Through the ease of purification and good yield, the derivatives of unsymmetrical palladium (II) complexes were successfully prepared by altering the **B** unit of **AB**s. Also, a unique derivative was prepared using benzonitrile as a solvent instead of acetonitrile. The method of synthesising these complexes was modified to synthesise the symmetrical palladium (II) complex from **AA** and solve the products equilibrium issue. This achievement will open the next part of the investigation, where the complexation of palladium will be studied by altering the **A** units of **AA** and **AB**.

2.7. Ligand Modification

The (Z)-1-(4-Methoxybenzylidene)-1H-isoindol-3-amine (**A**) was the basic unit in the preparation of symmetrical (**AA**) and unsymmetrical (**AB**) azadipyrrins. New ligand derivatives will be synthesised in this part of the project using different aminoisoindoline units and the same **B** unit of phthalonitrile. The previously discussed copper-free Sonogashira cross-coupling procedure will be implemented to synthesise these **A** derivatives. Aiming for thiophenes, ethynyl thiophene was needed to react with 2-bromobenzamidine hydrochloride to obtain the desired aminoisoindoline derivative. Due to their low stability and high cost, TMS-protected ethynyl thiophenes were prepared from 2- or 3-bromothiophene. The TMS-protected ethynyl thiophenes were successfully prepared by reacting a bromothiophene with trimethylsilylacetylene in the presence of TEA, cuprous iodide, and bis(triphenylphosphine)palladium chloride. The reaction mixture was refluxed overnight in THF under nitrogen. Followed by filtration and washing over silica and aqueous extraction by DCM, TMS-protected ethynyl thiophenes were purified by column chromatography. The targeted ethynyl thiophene derivatives were obtained with a good yield (Scheme 2.12).

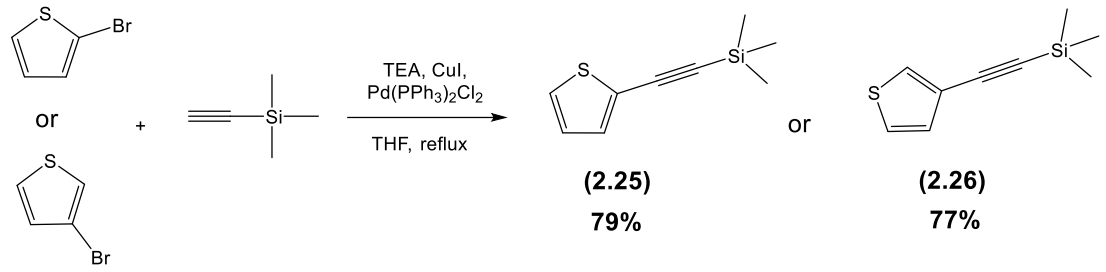

Scheme 2.12 synthesis of TMS-protected ethynylthiophene

These TMS-protected ethynyl thiophenes will be used to synthesise aminoisoindolines. Additionally, two more **A** derivatives were designed using their commercially available acetylenes. These **A** derivatives will be prepared from ethynyl ferrocene and 4-*tert*-butylphenyl acetylene. The new aminoisoindolines were synthesised via a copper-free Sonogashira cross-coupling procedure (Scheme 2.13).

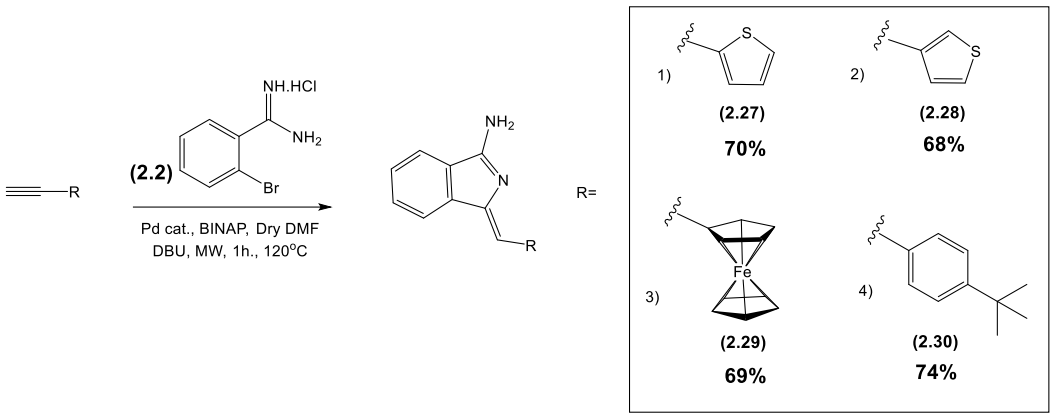

Scheme 2.13 synthesis of thiophene and ferrocene aminoisoindoline derivatives

Like the 4-phenyl methoxy aminoisoindoline, the new derivatives were isolated and purified through aqueous workup, column chromatography, and crystallisation steps. These compounds were proven by ^{1}H NMR and MALDI (Figures 2.25 and 2.26).

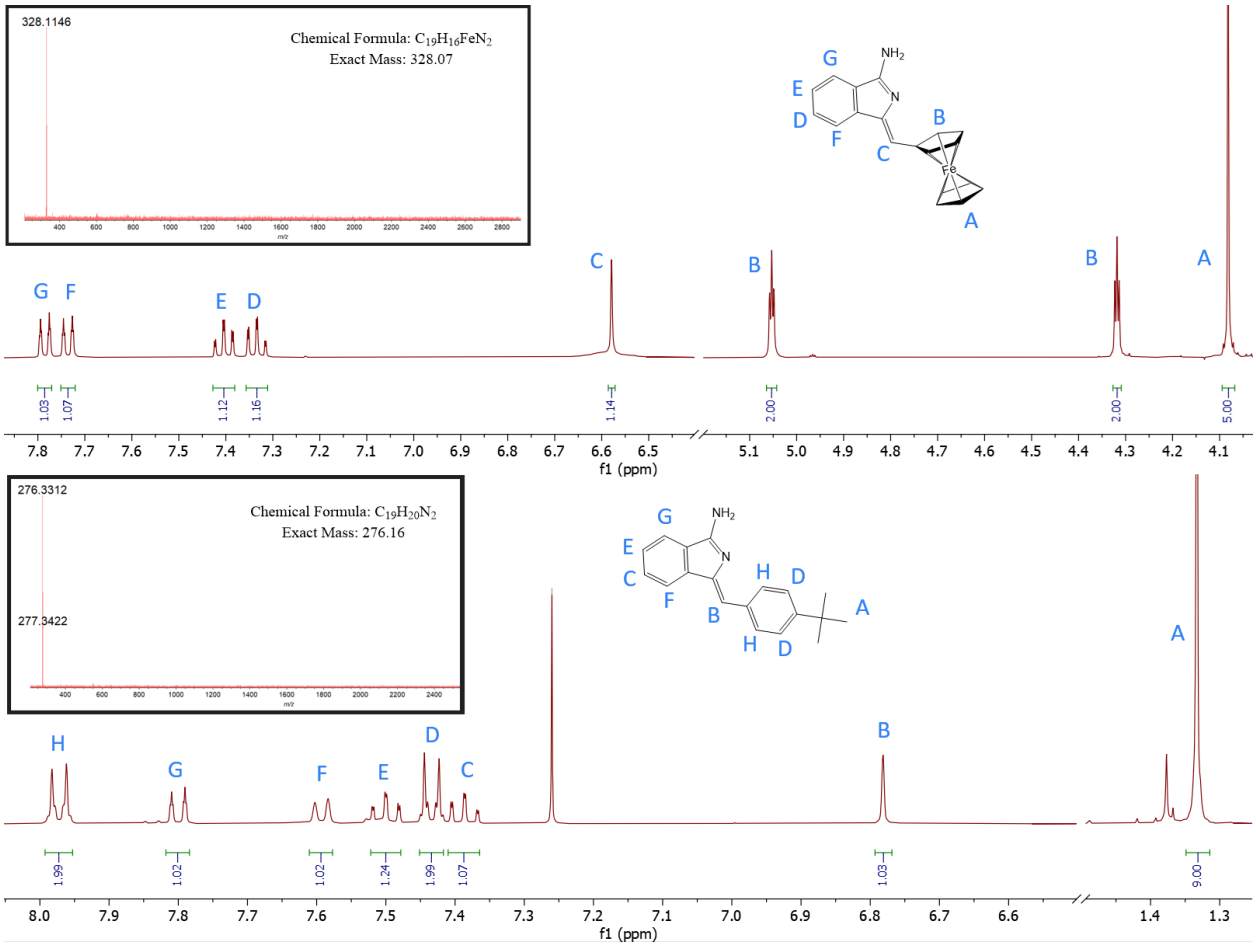

Figure 2.25 MALDI and ^{1}H NMR of ferrocene and tBu-phenyl aminoisoindoline derivatives

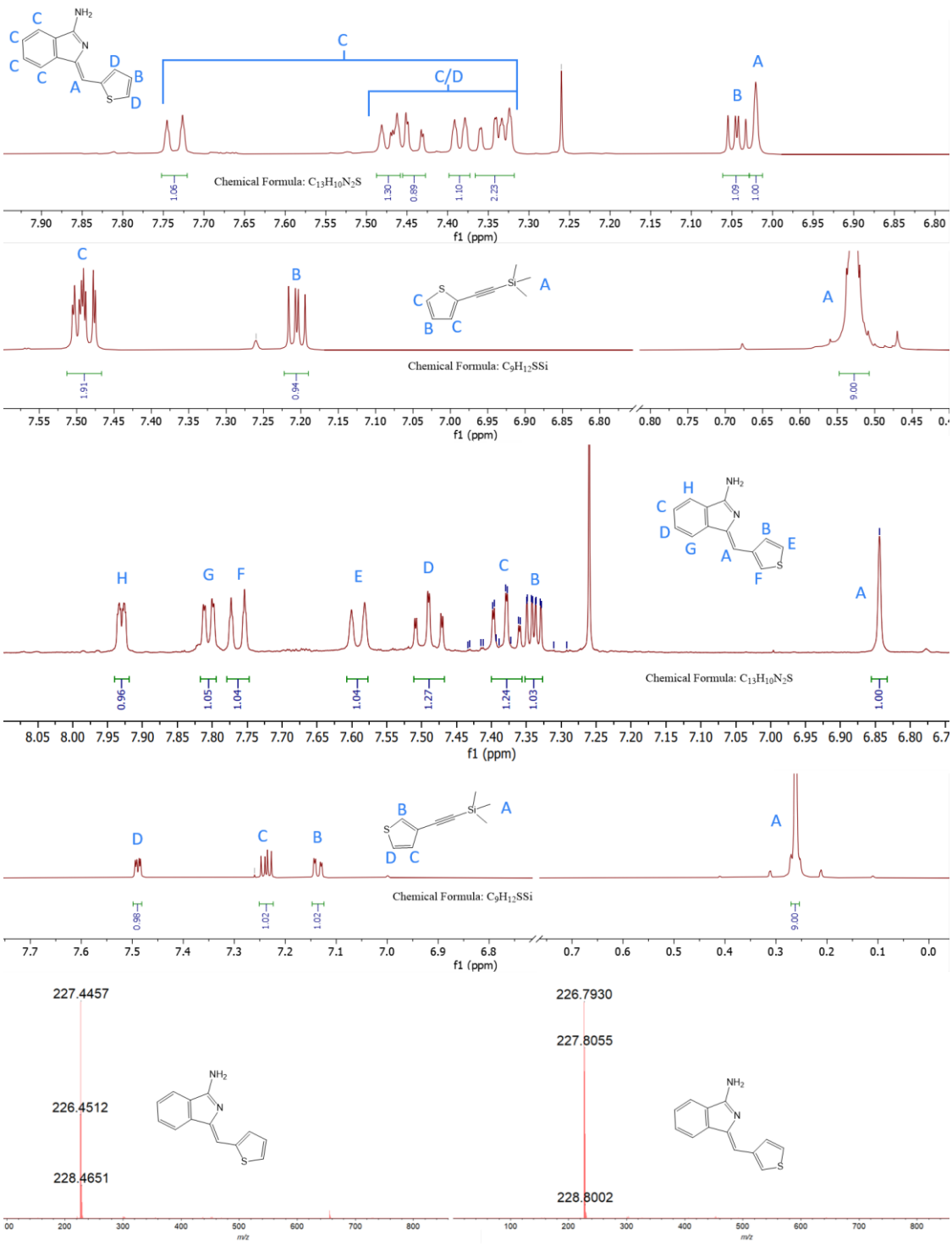

Figure 2.26 MALDI and ^{1}H NMR of thiophene compounds

Symmetrical azadipyrrines were prepared via self-condensation at elevated temperatures. Each of the prepared aminoisoindolines was used to synthesise **AA** derivatives. The thiophenes and the 4-phenyl *tert*butyl symmetrical ligand were accomplished. However, the ferrocene derivative was not attained. The obtained derivatives exhibited a symmetrical

structure observed by ^{1}H NMR. The synthesis of these compounds was proven by NMR, MALDI, and X-ray crystallography (Figures 2.27 and 2.28).

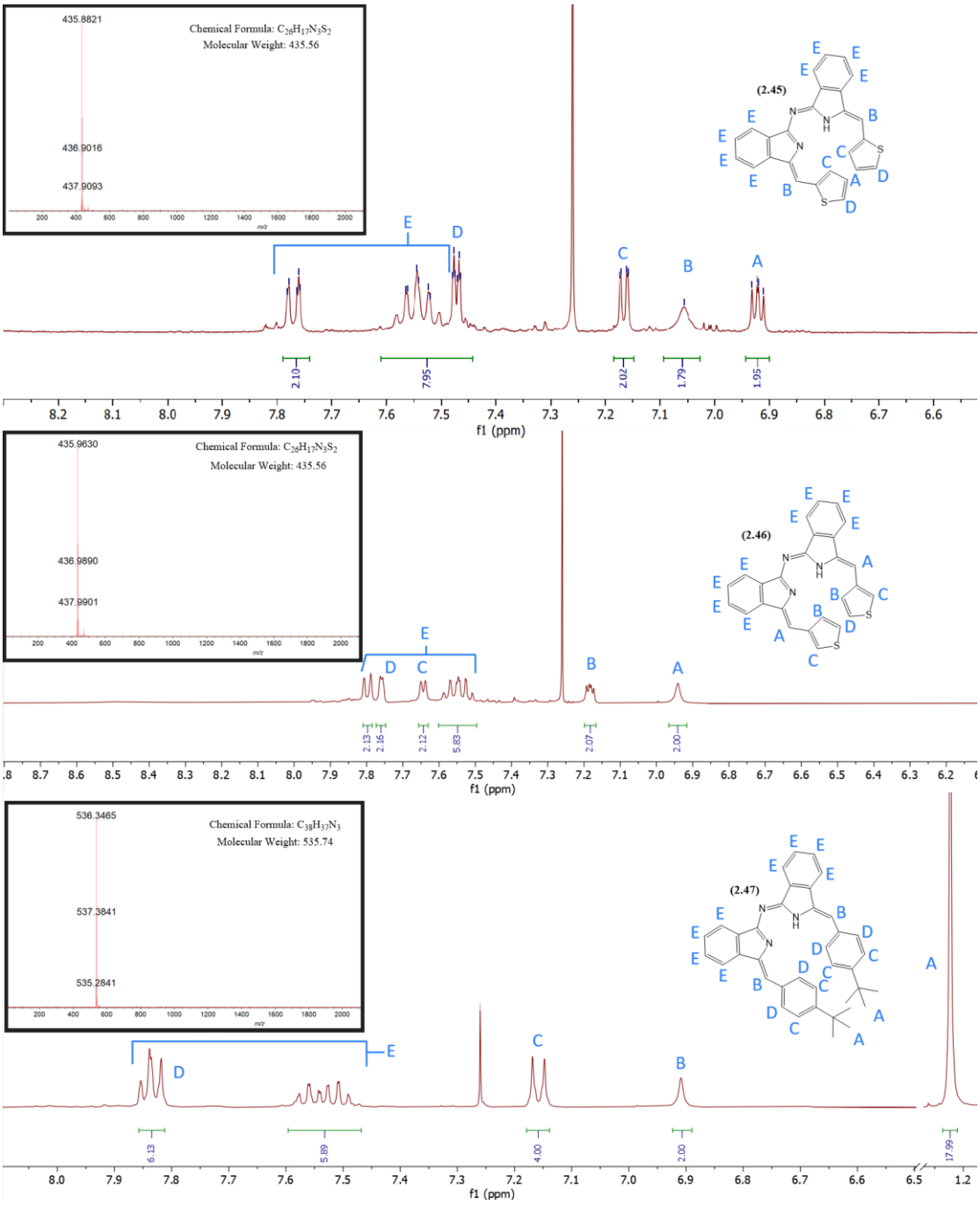

Figure 2.27 MALDI and ^{1}H NMR of the obtained dimers

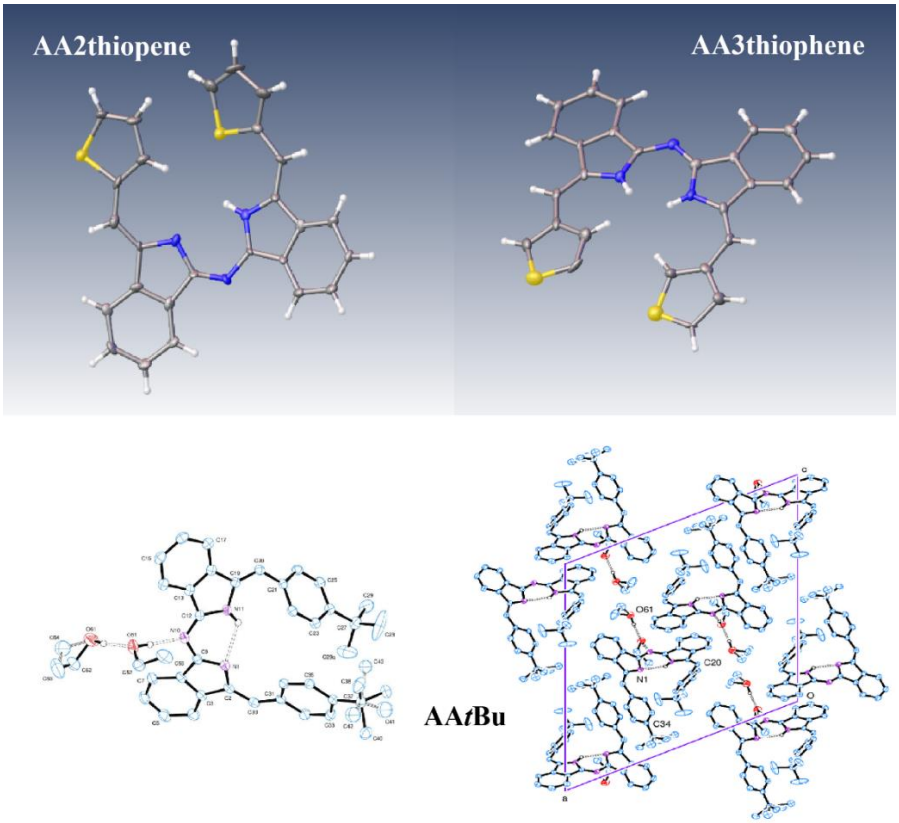

Figure 2.28 X-ray of obtained dimers

The data of **AA*2thiophene*** and **AA*3thiophene*** have not yet been received. While a crystallographer analysed the **AA*t*Bu** sample's data, they noted that the structure comprises the bis-isoindole derivative and two ethanol/solvent molecules. The outermost ethanol molecule is hydrogen bonded to the inner ethanol, which is itself hydrogen bonded to the bis-isoindole molecule. A third intramolecular hydrogen bond is found between the two isoindole units, N(11)-H(11)…N(1). Each isoindole unit and the phenyl groups are essentially planar, but there is rotation in the bridging groups. 10.9° about the C(30)-C(31 bond, 30.1° about C(9)-N(1), and 39.9° about C(20)-C(21), indicating a spiralling of the units to give a significant distortion from a planar molecule. They also found π…π overlaps between the rings, including C(13) and its related neighbour, perpendicular H…π contacts [as H(6) towards the centre of the neighbouring C(21'-26') ring], and van der Waals' contacts [as H(30)…H(42c')].

The synthesis and purification of **AA*2thiophene*** and **AA*3thiophene*** was a straightforward process. On the other hand, **AA*t*Bu** showed different configurational isomers in equilibrium. A slow crystallisation process obtained the *Z, Z* isomer. This symmetrical azadipyrrin derivative was soluble in polar and nonpolar solvents. Thus, the crystallisation was

performed by the slow evaporation of ethanol. By successfully acquiring these symmetrical aza (benzo) dipyrrins, the next step was to prepare the unsymmetrical ligands.

The newly prepared aminoisoindolines (A units) were reacted with phthalonitrile (B units) in methanol at 50 °C in the presence of sodium methoxide. **AB*2thiophene*** (**2.34**) was easily recovered by filtration and washing. On the other hand, this procedure was inefficient for preparing **AB*3thiophene*** (**2.35**) and **AB*ferrocene*** (**2.36**). These reactions produced several products, and the isolation seemed challenging. At the time of the program, it was decided to find an alternative way to achieve the current goal. 1-Imino-3,3-dimethoxyisoindoline (**3.37**) was prepared by reacting phthalonitrile with sodium methoxide in methanol. The reaction mixture was stirred until a precipitate formed. The product was filtered, washed, and dried. This dimethoxy isoindoline was then utilised to prepare **AB*3thiophene*** and **AB*ferrocene*** from their respective aminoisoindoline derivative (Scheme 2.14). The modified procedures were performed overnight at room temperature, and the products were recovered by filtration. The unsymmetrical azadipyrrin derivatives were analysed by NMR and MALDI. It is worth mentioning that the solubility of **AB*2thiophene*** and **AB*3thiophene*** was difficult, even in dimethyl sulfoxide-d6. While DMSO-d6 is the usually used solvent for **AB**s NMR, **AB*ferrocene*** sample decomposed when using this solvent. The NMR data of **AB*ferrocene*** was successfully collected using a deuterated DCM. The mass spectrometry confirmed the synthesis by matching the calculated mass (figure 2.29).

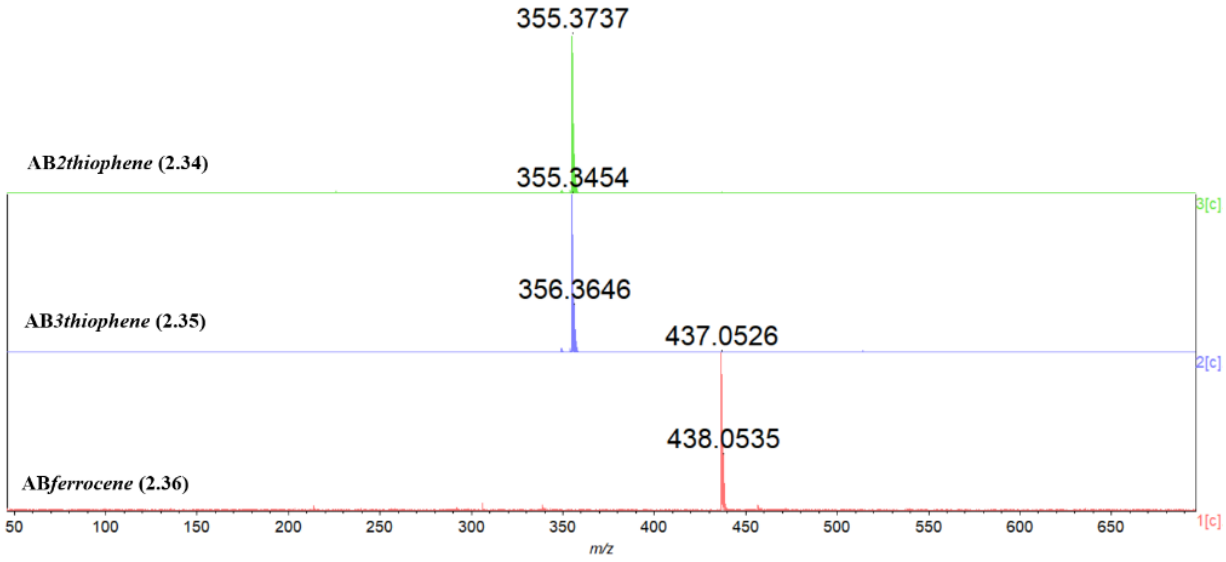

Figure 2.29 MALDI of unsymmetrical azadipyrrin derivatives

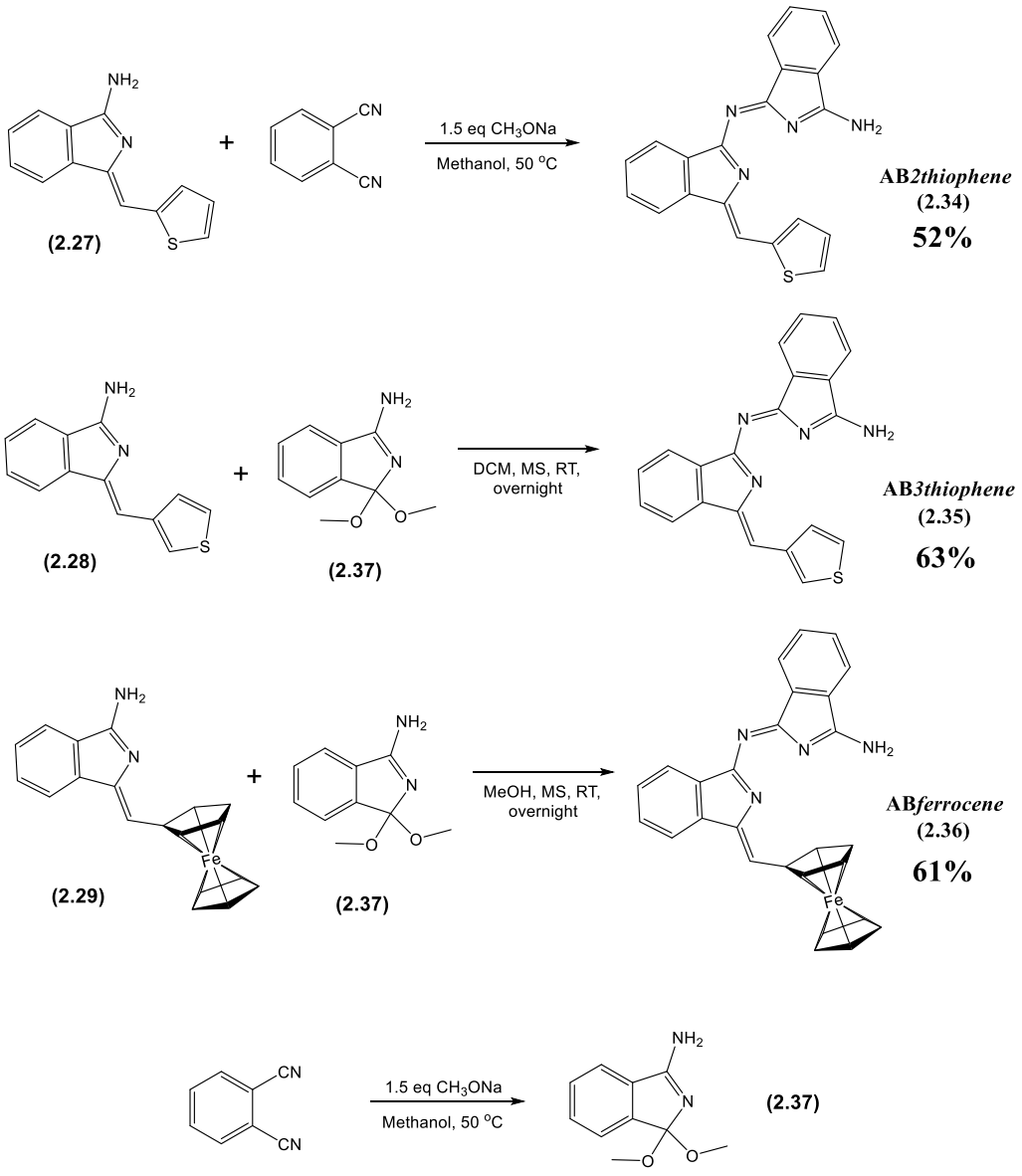

Scheme 2.14 Synthesis of unsymmetrical AB derivatives

These symmetrical and unsymmetrical derivatives will be used in the complexation reactions with Pd(II). Applying the reaction conditions of preparing **Pd-AB** and **Pd-AA** utilising these compounds is expected to produce new derivatives of palladium complexes.

2.7.1. Symmetrical Pd Complexes Derivatives

According to the procedure for synthesising the **Pd-AA** complex (**2.24**), the new complex derivatives were prepared by reacting an equivalent molar ratio of **AA*2thiophene***, **AA*3thiophene***, or **AA*t*Bu** with $Pd(OAc)_2$ in ethyl acetate. These reactions were performed under nitrogen at room temperature. Monitored by TLC and MALDI, the reaction time ranged from 5 to 7 days. The new complexes were isolated using neutral alumina column chromatography with good yields (86% **Pd-AA*2thiophene***, 88% **Pd-AA*3thiophene***, 76% **Pd-**

AA*t*Bu). The crystallisation of thiophene complexes produced a dark red solid. Several attempts were made to grow suitable crystals for X-ray crystallography; however, this was not achieved. The reason for creating a tertiary butyl derivative was to promote crystal growth for X-ray. The aminoisoindoline *t*Bu-derivative was easily crystallised. Even though **AA*t*Bu** is soluble in every tested solvent, good crystals were obtained by slow solvent evaporation. **Pd-AA*t*Bu** complex retained the solubility of its predecessor, but the crystallisation was not successful. Several attempts produced tiny but good-looking crystals in two to three weeks of crystallisation. While they seemed promising initially, the crystallographer could not process the samples because they were not good enough. MALDI proved these complexes by matching the calculated and the observed mass and isotopic distribution (Figure 2.30).

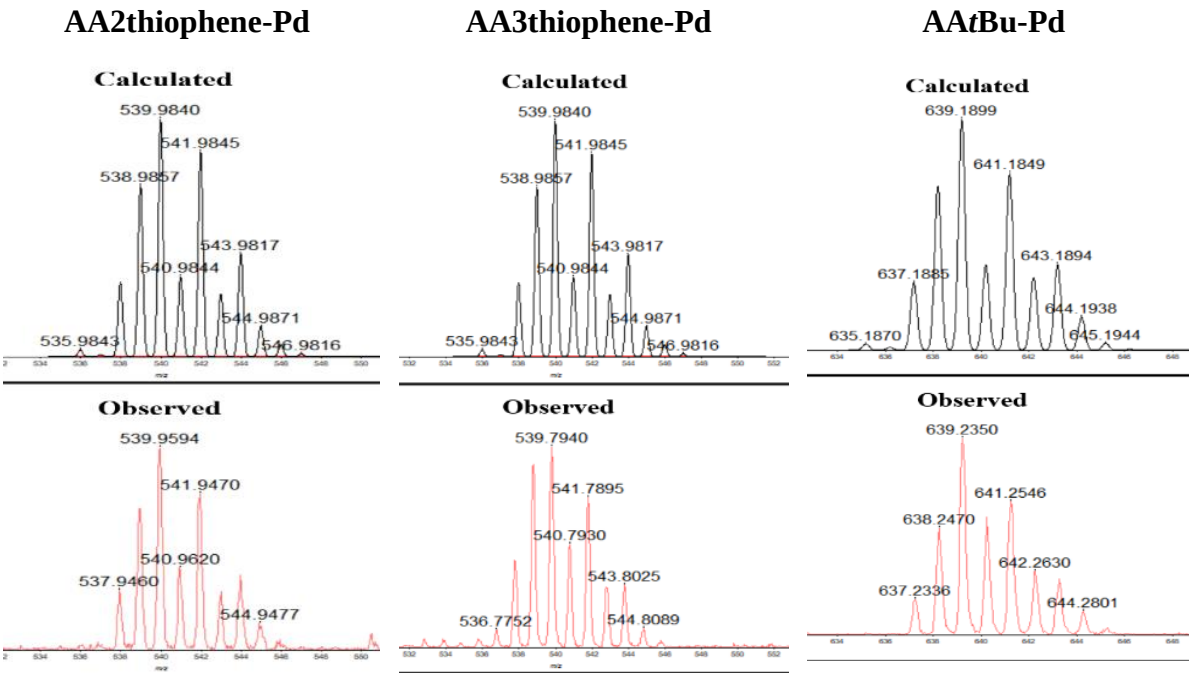

Figure 2.30 Calculated vs. observed mass by MALDI for symmetrical palladium complexes

^{1}H NMR predicted the symmetrical structure of these complexes, and the double insertion of palladium was observed in a similar fashion to that in **Pd-AA** (figure 2.31).

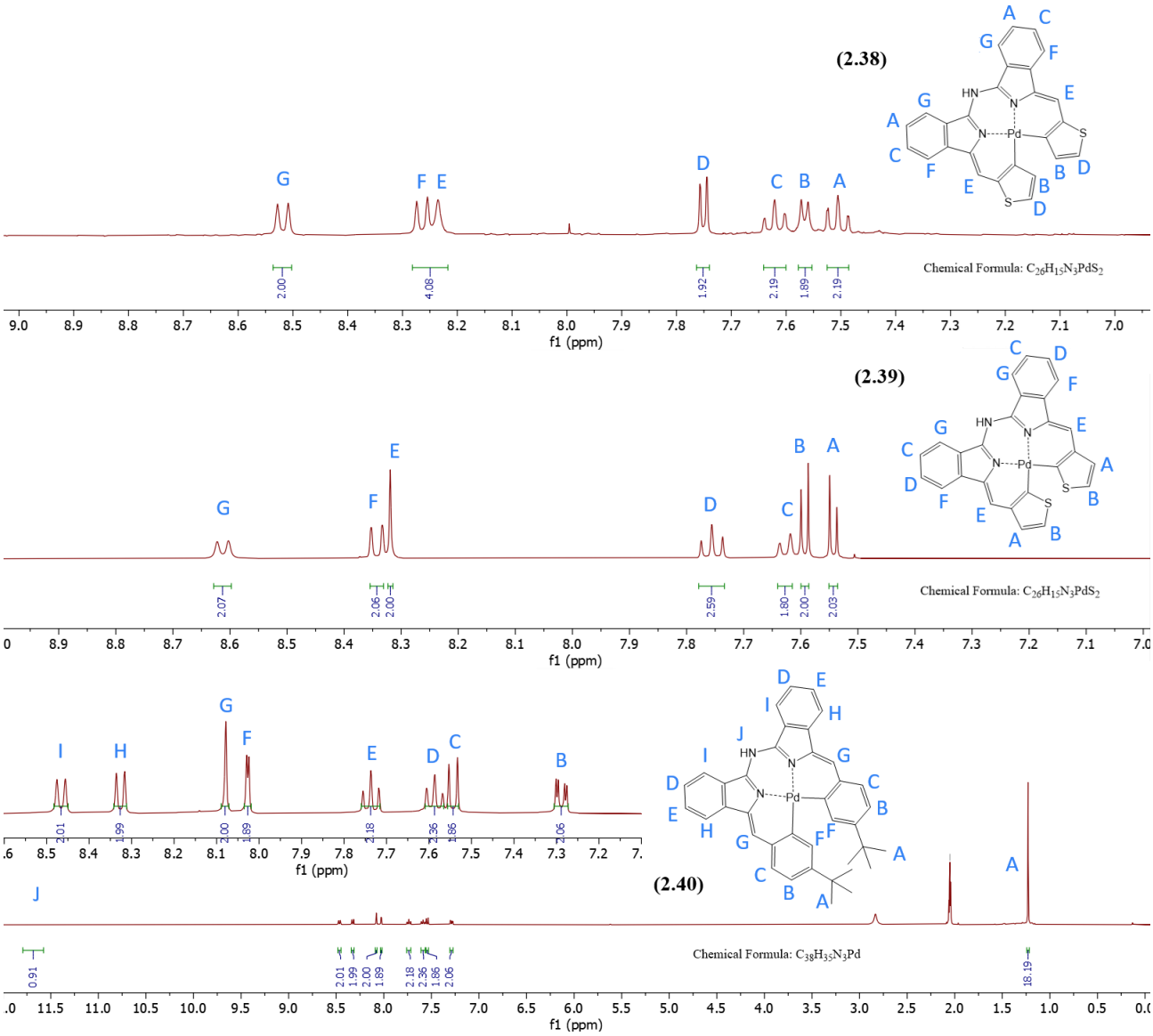

Figure 2.31 ^{1}H NMR of palladium complexes; **AA2thiophene-Pd**, **AA3thiophene-Pd**, and **AAtBu-Pd**

2.7.2. Unsymmetrical Pd Complexes Derivatives

According to the procedure for synthesising the **Pd-AB** complex (**2.20**), the new complex derivatives were prepared by reacting an equivalent molar ratio of **AB*2thiophene***, **AB*3thiophene***, or **AB*ferrocene*** with $PdCl_2$ in dry acetonitrile. These reactions were performed under nitrogen at room temperature. Monitored by TLC and MALDI, the reaction time was 7 days for thiophene derivatives and 2 days for ferrocene. The new complex derivatives were isolated by column chromatography using neutral alumina. These products were obtained as purple solids after crystallisation with good yield (87% **Pd-AB*2thiophene***, 85% **Pd-AB*3thiophene***, 58% **Pd-AB*ferrocene***). MALDI proved these complexes by matching the calculated and the observed mass and isotopic distribution (Figure 2.32).

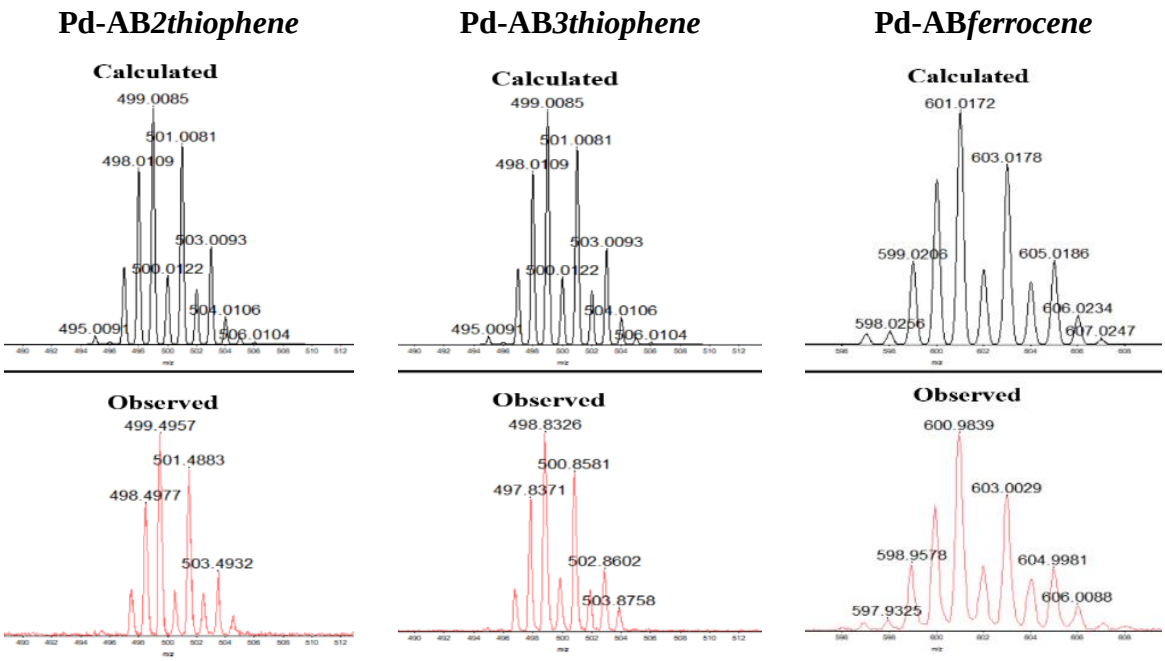

Figure 2.32 Calculated vs. observed mass by MALDI for unsymmetrical palladium complexes

The ^{1}H NMR analysis confirmed the predicted structure of the complexes, showing the incorporation of an acetonitrile molecule in the final product. The thiophene derivatives were difficult to solubilise in deuterated solvents. By increasing the number of scans, clean spectra were obtained. the total peak integration matched the number of predicted protons (figure 2.33).

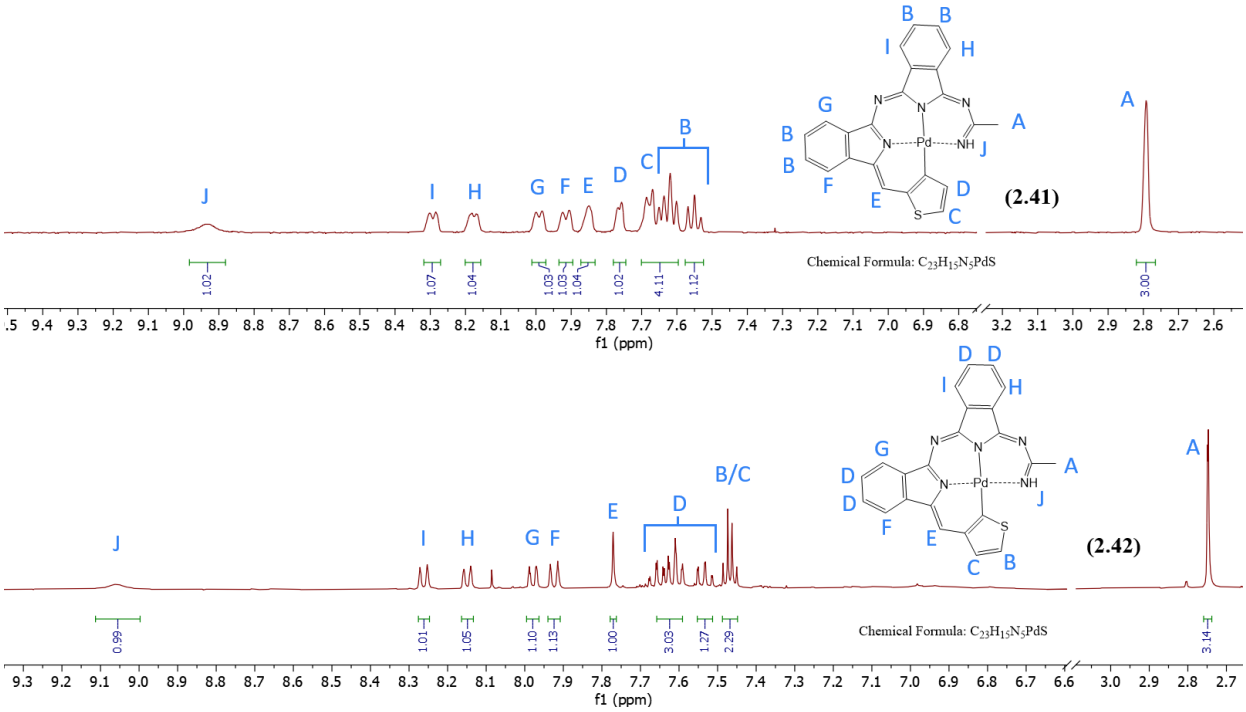

Figure 2.33 ^{1}H NMR of **AB2thiophene** and **AB3thiophene** palladium complexes

Unlike thiophene derivatives, the ferrocene compounds produced clear spectra with proton NMR (figure 2.34). The spectrum of the **AB*ferrocene*** complex shows the exact predicted number of protons. Moreover, the acetonitrile unit appears in the compound, as previously discussed in the complexes of thiophene derivatives. However, the insertion of palladium can be interpreted from the spectra in Figure 2.34. The Ferrocene group shows three instinct peaks in aminoisoindoline. The free side of the ferrocene is represented by a singlet peak corresponding to five protons, and two triplet peaks integrate into four protons on the linked side. These three peaks also exist in the NMR spectrum **AB*ferrocene***, representing nine protons (4 on the linked side and 5 on the free one). In the palladium complex, the metal is expected to be inserted into the ferrocene group's linked side. Instead of two triplets, a triplet and two doublets are formed. The integration of the newly formed peaks corresponds to three protons, which proves the insertion of palladium. By comparing the predicted compound by NMR with the mass observed, the synthesis of the **AB*ferrocene*** palladium complex is confirmed.

The palladium complexes of thiophene derivatives were obtained with high yields (87% Pd-AB2thiophene, 85% Pd-AB3thiophene), and the reactions were completed in 7 days. On the other hand, the ferrocene substituted complex was prepared in 2 days. This reaction consumed the starting materials in the shortest period of time compared to the other palladium

complexes, but it had the lowest yield (58%). An insoluble black material formed during the reaction. The forming of this unknown material is linked to the low yield compared to the other complexes. Also, the colour of Pd-ABferrocene is orange. All of the dimer-like palladium complexes are grads of purple. This difference in colouration could be caused by iron in ferrocene. Thiophene-substituted complexes showed different colours in the solid form. While purple is in solution, the colour becomes dark green when dried, and the purple colour can be retained when dissolved in solution.

The UV-Vis. absorption of the prepared complexes was compared to that of their significant ligand. The absorption of the ligands depends on the presence of the delocalisation of π-electrons distributed around the compounds. While this delocalisation is present in the obtained complexes, the unique electronic environment in the d-orbitals of palladium metal affected the UV-Vis. absorption (Figure 2.35 and 2.36).

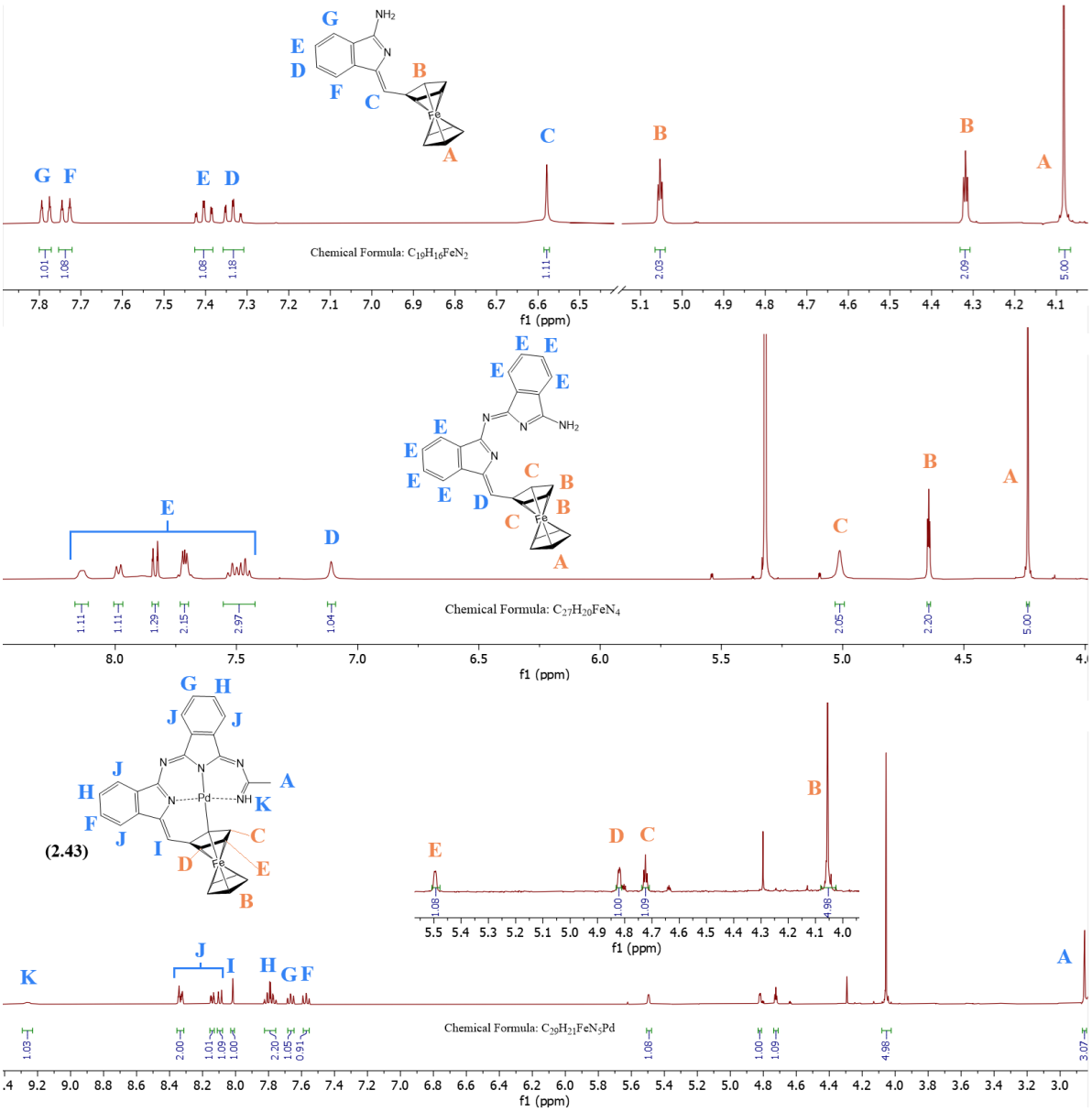

Figure 2.34 ^{1}H NMR of ferrocene derivative compounds

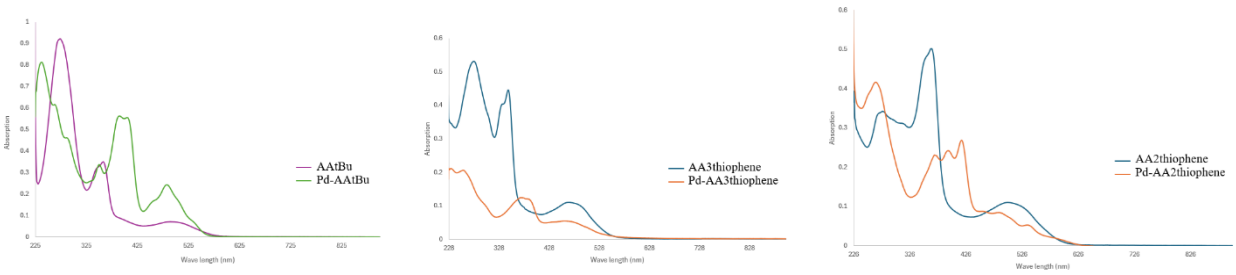

Figure 2.35 UV-Vis. absorption of palladium complexes vs ligands (symmetrical derivatives)

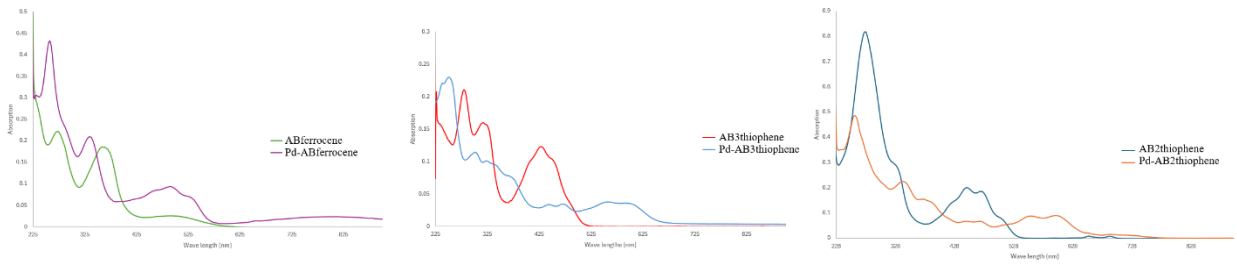

Figure 2.36 UV-Vis. absorption of palladium complexes vs ligands (unsymmetrical derivatives)

2.8. Conclusions

The project's progress and direction were shaped by the obstacles encountered. The first objective was to synthesize aza (benzo) tripyrrin compounds. The structure of these compounds was initially identified and isolated as a byproduct in the synthesis of SubTBDAP hybrids. When this project started, the methods of synthesizing trimers were not fully integrated. Therefore, the initial work focused on optimizing the synthesis. The study led to synthesizing the azatripyrrin derivatives at ~50 % yield. After achieving the first goal, the next objective was to prepare their complexes.

The investigation was conducted on several metals to synthesize azatripyrrin complexes. The study considered the reaction conditions published for similar compounds. This part of the project failed to reach its aim. The main issue, other than successful synthesis, was the isolation and purification of products. The goal was then extended to prepare complexes using benzo azadipyrrins. The symmetrical and unsymmetrical azadipyrrins ligand were altered to avoid the strictly hindered azatripyrrin and to use structurally related compounds. The utilization of these alternative compounds sped up the investigation because their preparation has fewer steps than trimer-like compounds.

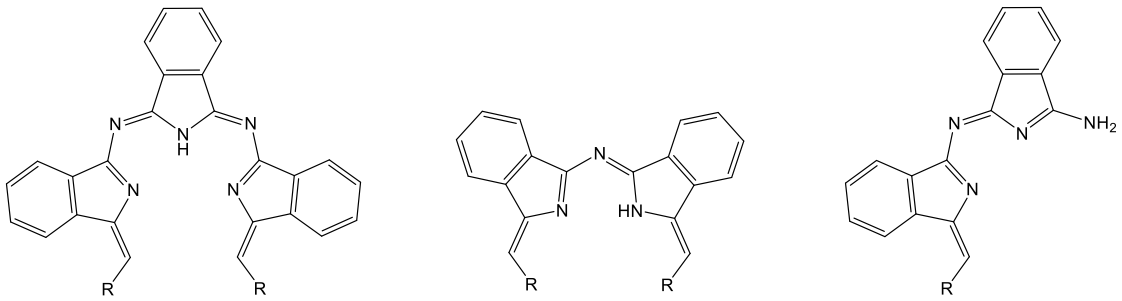

Benzo (aza) tripyrrin

Symmetrical
benzo (aza) dipyrrin

Unsymmetrical
benzo (aza) dipyrrin

Like azatripyrrin, the investigation into the synthesis of dipyrrins complexes was based on a 2:1 ligand-to-metal ratio. The study covered several metals with a variety of reaction conditions. While the initial findings were more promising than the trimer's path, more problems were encountered (*e.g.*, product stability). However, isolating new complexes remained an issue in this work. A new complex was synthesized, successfully isolated, and characterized through. Unlike the targeted 2:1 type complex, the first successfully obtained complex was a 1:1 palladium (II) **AB**. This stable square planer compound was formed through the coordination and insertion of palladium metal and the caption of one acetonitrile unit in the complex. This result guided the project toward these complexes. By modifying this procedure, the palladium complex of the symmetrical azadipyrrin was successfully synthesized.

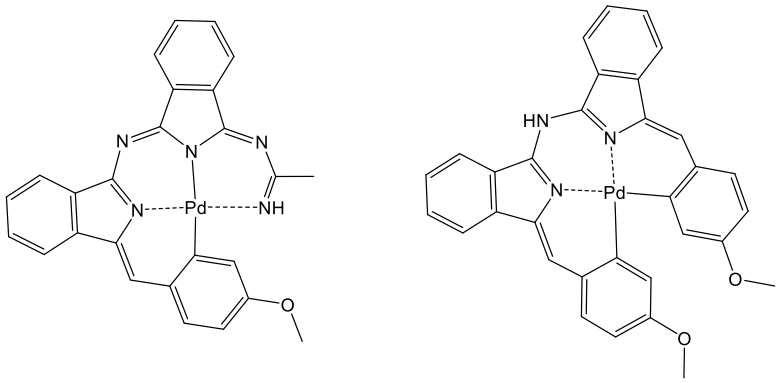

From this point, the project focused on the synthesis of these complexes. Several derivatives were synthesised. Unlike the difficult experiences encountered at the beginning of the project, all of the targeted complexes were successfully obtained with good yields. After the successful synthesis and characterisation, these methods were applied to the complexation of azatripyrrin compounds. Due to time limitations, these attempts were not completed. However, these preliminary results are the basis for future work. Additionally, the palladium complexation conditions were tested on zinc and platinum. While the results are inconclusive, these conditions must be fully covered in future work. These preliminary results will be presented as incomplete work.

2.9. Future work

The highlight of this project is the palladium complexes. Many ideas are based on understanding their synthesis. The first question would be the effect of replacing palladium (II) chloride with bis(acetonitrile)dichloropalladium(II) in the synthesis of **AB** complexes. While

the reaction took 7 days to complete, it could be faster in acetonitrile. Based on the outcome of this reaction, if successful in producing the same complex, it would be interesting to investigate this reaction with other solvents. If these ideas can produce the same type of complexes, this will open the gate to using modified acetonitrile palladium complexes. This idea was briefly tested, and the benzonitrile-caped ***tert*AB** palladium complex was successfully produced. This proposed concept aims to cut the dependence on the solvent, acetonitrile, to cap the complex. While this project focuses on the synthesis, the properties of these complexes should be studied.

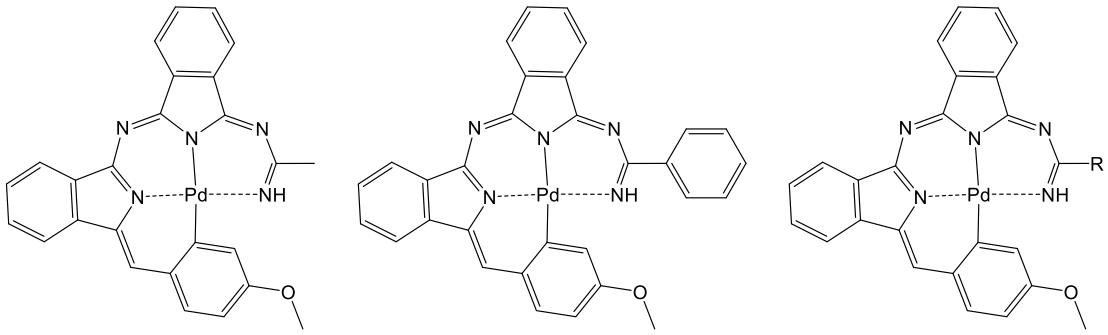

Other metals should be used to study the conditions that produce **Pd-AA** and **Pd-AB** complexes. Additionally, these conditions should be tested using benzo azatripyrrins. For that, some test reactions were performed. At the end of the project's time, the tests were not fully completed.

2.9.1. Preliminary results of incompleted experiments

The first test reaction was the palladium complexation of azatripyrrin using the acetonitrile condition. In this reaction, $PdCl_2$ was used to prepare **Pd-ABA**. Neutral alumina TLC indicated the full consumption of the ligand on day 6. Three new spots were eluted by a mixture of DCM and acetonitrile (2:1). In the order from the top to the bassline, the spots were grey (*faint*), red (*dominant*), and green. All the spots were tailing while the TLC. MALDI of the crude reaction mixture observed several peaks with isotopic distribution resampling palladium complexes. The observed masses did not match the predicted target complex. Column chromatography was performed using neutral alumina to isolate the formed products. Starting with DCM to remove any undetected residual **ABA**, the new spots were eluted by a mixture of DCM and acetonitrile. The data obtained from MALDI showed several peaks in every fraction. While some of these peaks were present in the crude sample, new peaks were observed after isolation. Moreover, the mass of **ABA** was observed in all fractions. This could indicate demetallation during column chromatography or the instability of the complex. Unfortunately, crystallisation attempts failed to produce a single compound and clean NMR.

The second test reaction was performed using the complexation conditions of **Pd-AA**. In ethyl acetate, **ABA** was stirred with $Pd(OAc)_2$ under nitrogen at room temperature. When comparing the MALDI, a different outcome of this condition was noticed (Figure 2.37).

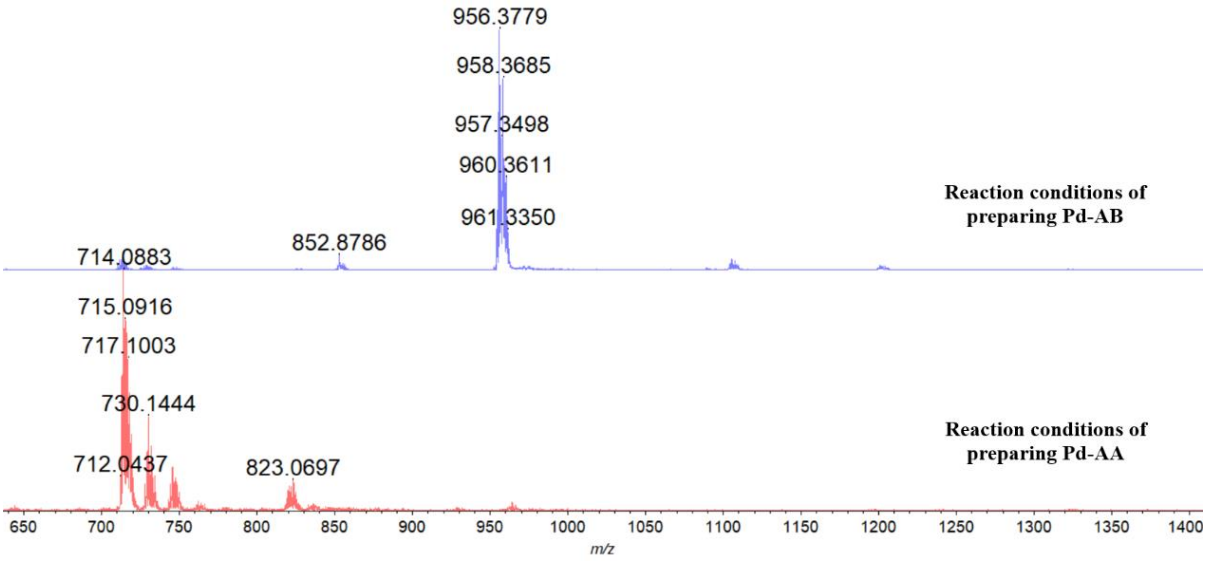

Figure 2.37 MALDI of crude reaction mixtures in the attempts to prepare **Pd-ABA**

This method produced predominant peaks in the 700 m/z region compared to the previous procedure, which produced the main peak at 956 m/z. This was a promising finding until the 700 region was expanded for further analysis (figure 2.38).

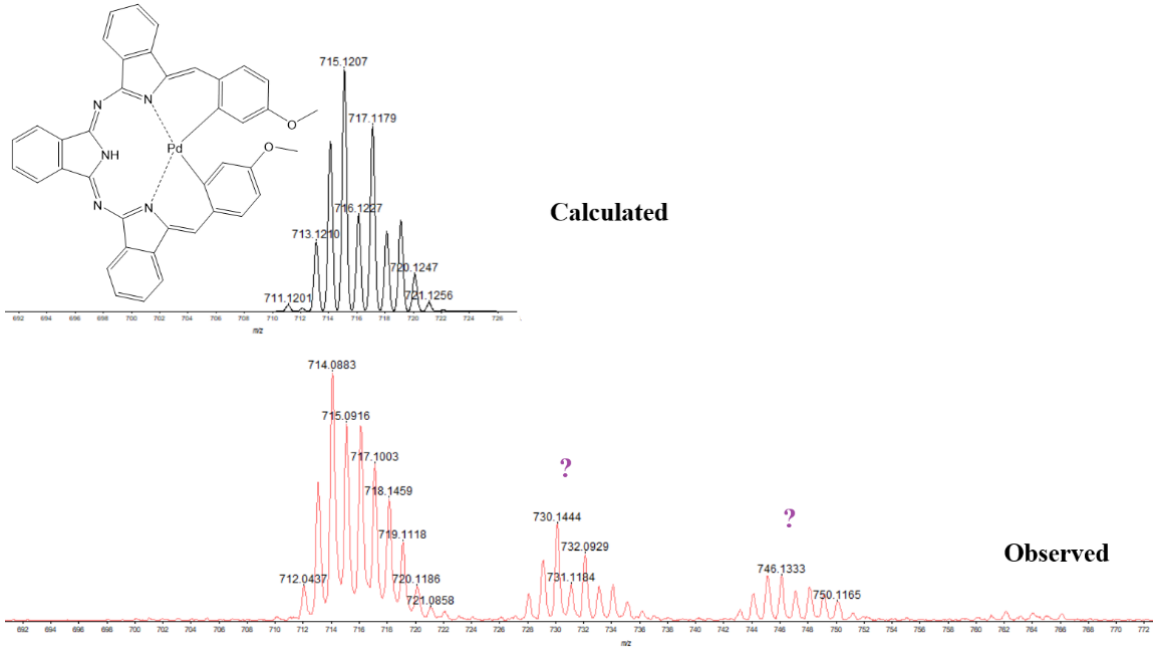

Figure 2.38 Expanded MALDI compared to the calculated mass of predicted complexes

The predicted complex's mass is very close to the observed but does not match the isotopic distribution. Additionally, the masses observed at m/z= 730 and 746 are unknown. TLC showed a faint grey spot eluted first by a mixture of DCM ethyl acetate (1:2) followed by a large green tailing spot. Two-dimensional TLC confirmed that these spots are not in equilibrium. Based on previous experience, the decision was made to avoid column chromatography and rely on crystallisation. This purification method provided a relatively clean ^{1}H NMR (figure 2.39). The first observation was the complex seemed to be unsymmetrical. However, the complete structure was not determined. Unfortunately, several crystallisation attempts failed to grow suitable crystals for X-ray crystallography.

On the other hand, three test reactions were performed: the synthesis of **Zn-AA** using $Zn(OAc)_2$ in ethyl acetate, the synthesis of **Zn-AB** using $ZnCl_2$ in acetonitrile, and the synthesis of **Pt-AB** using K_2PtCl_4 in acetonitrile. The starting materials were not fully consumed for the limited time spent on these reactions. Each reaction produced several products. While some were predicted, others were unknown.

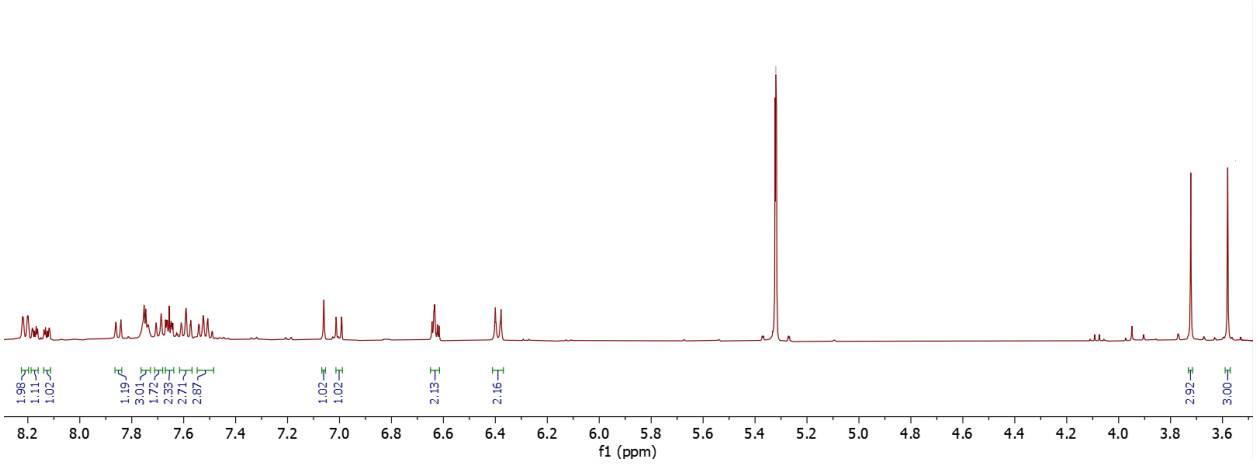

Figure 2.39 ^{1}H NMR of recrystallized materials obtained from **Pd-ABA** complexation

3. Experimental

General Methods

Reagents and solvents were obtained commercially from suppliers, and the department provided the dry solvents (DCM, THF, and acetonitrile). Phthalonitrile was used after recrystallization in xylene. Reactions sensitive to air and water were performed under nitrogen. Liquid-liquid extractions were carried out using distilled water or a saturated sodium hydrogen carbonate solution, and anhydrous magnesium sulfate was used to dry the organic layers. Solvents were removed under reduced pressure using a Büchi rotary evaporator.

Thin-layer chromatography was carried out on coated aluminum sheets. TLC of organic compounds was performed using unmodified silica gel Alugram® Sil G/UV254, and column chromatography was executed using silica gel 60Å mesh 70-230. TLC of complexes was performed using Supelco® Neutral aluminum oxide 60Å coated with fluorescent indicator F_{254}, and column chromatography was executed using neutral Al_2O_3 Brockmann l, 4, -60 mesh powder, S.A. 205m^2/g. UV light (254 or 365 nm) was used to visualize the compounds on TLC. Column chromatography was performed at ambient temperature, and the solvent ratios were calculated based on volume (v:v).

In Norell S500 or 508 quartz NMR tubes, ^{1}H NMR spectra were obtained by either the Ultrashield Plus^{TM} 400 spectrometer or the Bruker Ascend^{TM} 500 spectrometer at 400 MHz and 500 MHz, respectively. Downfield from TMS (δ= 0), the peaks were referred to in ppm (δ) and the coupling constant in Hertz (*J*). ^{13}C NMR spectra were obtained at 101 MHz and 126 MHz. NMR analyses were performed at 298 K using deuterated solvents (i.e., acetone, acetonitrile, chloroform, DCM, DMSO, and methanol).

The Hitachi U-3310 Spectrophotometer was used to measure UV-Vis. absorption and the molar absorption coefficient (ε) was calculated from the known solution concentration (M). Compounds' masses were obtained from MALDI-TOF mass spectroscopy using the Shimadzu AXIMA Performance instrument. The Biotage Initiator+ instrument was used to perform microwave reactions. The Reichart Thermovar microscope with a thermopar-based temperature control was used to determine the melting points.

3.1. Synthesis of 2,3-Dicyanonaphthalene (3.1)

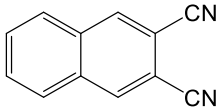

α,α,α′,α′-Tetrabromo-o-xylene (10 g, 23.71 mmol), fumaronitrile (3.2 g, 40.99 mmol), and sodium iodide (10 g, 66.72 mmol) were dissolved in dry DMF(100 mL). The reaction was stirred under nitrogen at 75 °C. After 5.5 h, the solution was allowed to cool to 65 °C and quenched with a mixture of ice and water (150 mL). Sodium bisulfite (3.4 g, 32.67 mmol) was added to the mixture and stirred for 30 minutes. The dark red solution turned into a yellow-tan suspension. The product was filtered, washed, and recrystallised from DCM and PE (3.18 g, 75%).[1]

Chemical Formula and molecular weight: $C_{12}H_6N_2$, 178.19 g.mol^{-1}

^{1}H NMR (400 MHz, DMSO-d_6) δ 8.88 (s, 2H), 8.24 – 8.15 (m, 2H), 7.95 – 7.86 (m, 2H).

MS (MALDI-TOF): m/z = 178.05 $[M]^+$

Melting point: 255 °C (lit. 251 °C)[2]

3.2. Synthesis of TMS Protected Ethynyl Thiophene

3.2.1. 2-Thiophene Derivative (3.2)

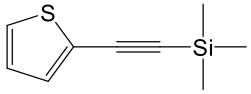

2-Bromothiophene (2.07 g, 1.2 mL, 12.65 mmol), TEA (5 mL), $Pd(PPh_3)_4$ (50 mg, 0.04 mmol), CuI (40 mg, 0.21 mmol), and trimethylsilylacetylene (1.85 g, 2.8 mL, 18.8 mmol) were dissolved in dry THF (15 mL). The reaction was stirred and refluxed overnight under nitrogen. Then, the reaction mixture was passed through a bed of silica and washed through with THF. The solvent was removed under vacuum via a rotary evaporator and redissolved in DCM (70 mL). The solution was extracted with a saturated aqueous solution of NH_4Cl (3 x 150 mL). The organic layer was dried using $MgSO_4$ and filtered, and the solvent was removed under vacuum.

The product was isolated by column chromatography using hexane as a yellow liquid (2.01 g, 88%).[3]

Chemical Formula and molecular weight: $C_9H_{12}SSi$, 180.34 g.mol^{-1}

^{1}H NMR (400 MHz, Chloroform-*d*) δ 7.28 – 7.20 (m, 2H), 6.95 (dd, *J* = 5.2, 3.6 Hz, 1H), 0.27 (s, 9H).

Rf: 0.2 (hexane, silica)

3.2.2. 3-Thiophene Derivative (3.3)

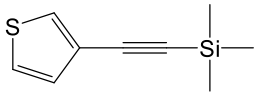

3-Bromothiophene (2.05 g, 1.18 mL, 12.57 mmol), TEA (5 mL), $Pd(PPh_3)_4$ (50 mg, 0.04 mmol), CuI (40 mg, 0.21 mmol), and Trimethylsilylacetylene (1.85 g, 2.8 mL, 18.8 mmol) were dissolved in dry THF (15 mL). The reaction was stirred and refluxed overnight under nitrogen. Then, the reaction mixture was passed through a bed of silica and washed through with THF. The solvent was removed under vacuum via a rotary evaporator and redissolved in DCM (70 mL). The solution was extracted with a saturated aqueous solution of NH_4Cl (3 x 150 mL). The organic layer was dried using $MgSO_4$ and filtered, and the solvent was removed under vacuum. The product was isolated by column chromatography using hexane as a yellow liquid (2.01 g, 88%).[4]

Chemical Formula and molecular weight: $C_9H_{12}SSi$, 180.34 g.mol^{-1}

^{1}H NMR (400 MHz, Chloroform-*d*) δ 7.49 (dd, *J* = 3.0, 1.2 Hz, 1H), 7.24 (dd, *J* = 5.0, 3.0 Hz, 1H), 7.14 (dd, *J* = 5.0, 1.2 Hz, 1H), 0.26 (s, 9H).

^{13}C NMR (101 MHz, Methylene Chloride-d_2) δ 130.2, 129.6, 125.2, 122.4, 100.1, 93.9, 0.1.

Rf: 0.2 (hexane, silica)

3.3. Synthesis of Dimethoxyisoindoline

3.3.1. 1-Imino-3,3-dimethoxyisoindoline (3.4)

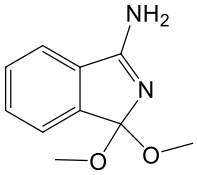

Sodium metal (2 g, 86.99 mmol) was carefully dissolved in methanol (70 mL). When the solution temperature cooled to room temperature, phthalonitrile (10 g, 78.05 mmol) was added. The reaction mixture was stirred for 6 hours until a precipitate formed. The product was filtered, washed with distilled water, and dried under a vacuum. The targeted compound was a pale green solid (8.2 g, 55%).[5]

Chemical Formula and molecular weight: $C_{10}H_{12}N_2O_2$, 192.22 g.mol^{-1}

^{1}H NMR (400 MHz, DMSO-d_6) δ 7.70 – 7.65 (m, 1H), 7.44 – 7.39 (m, 3H), 7.12 (s, 2H), 3.19 (s, 6H).

Melting point: Decomposes

3.3.2. 1-Imino-3,3-dimethoxybenzoisoindoline (3.5)

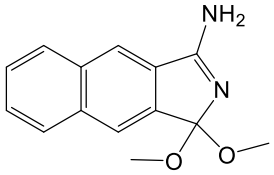

Sodium metal (2 g, 86.99 mmol) was carefully dissolved in methanol (70 mL). When the solution temperature cooled to room temperature, naphthalonitrile (13.8 g, 77.51 mmol) was added. The reaction mixture was stirred for 6 hours, and the product was filtered, washed with distilled water, and dried under a vacuum. The targeted compound was a pale yellow solid (15.2 g, 81%).[5]

Chemical Formula and molecular weight: $C_{14}H_{14}N_2O_2$, 242.28 g.mol^{-1}

^{1}H NMR (400 MHz, DMSO-d_6) δ 8.18 (s, 1H), 8.03 (dd, J = 7.3, 1.9 Hz, 1H), 7.94 (d, 2H), 7.64 – 7.53 (m, 2H), 7.21 (s, 2H), 3.25 (s, 6H).

^{13}C NMR (101 MHz, DMSO-d_6) δ 163.5, 142.7, 133.9, 133.7, 133.1, 129.4, 129.3, 129.3, 127.7, 127.1, 121.0, 119.9, 118.2, 50.6.

Melting point: Decomposes

3.4. Synthesis of 2-Bromobenzamidine hydrochloride (3.6)

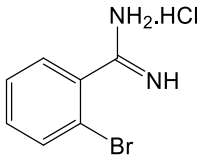

2-Bromobenzonitrile (18 g, 98.89 mmol) was dissolved in dry THF (15 mL). A $LiN(SiMe_3)_2$ solution in anhydrous THF (1 M, 100 ml, 100 mmol) was added to the reaction mixture. After 4 hours of stirring at room temperature, the reaction was cooled using an ice bath, and 5N HCl solution in isopropanol (100 mL) was slowly added. The reaction mixture was stirred overnight, and a white precipitate was filtered and washed with diethyl ether to give colorless crystals (18.6 g, 80%).[6]

Chemical formula and molecular weight: $C_7H_8BrClN_2$, 235.51 g.mol^{-1}

^{1}H NMR (400 MHz, Methanol-d_4) δ 7.81 (dd, J = 7.5, 1.6 Hz, 1H), 7.64 – 7.50 (m, 3H).

Melting point: > 300 ºC (lit. > 250 ºC) [7]

3.5. Synthesis of Aminoisoindoline

3.5.1. General Procedure

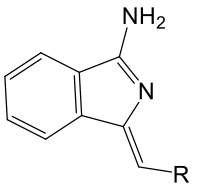

In a sealed microwave vessel purged with nitrogen, a mixture of 2-bromobenzamidine hydrochloride **(3.6)** (1 eq.), BINAP (0.05 eq.), bis(acetonitrile)dichloropalladium(II) (0.05 eq.), and R-ethynyl compound (1.2 eq.) was dissolved in dry DMF. DBU (2.5 eq.) was finally added, and the reaction mixture was stirred at room temperature for 10 min. under nitrogen before being irradiated in a microwave reactor for 1 hour at 120 ºC. The reaction mixture was diluted in ethyl acetate at room temperature and extracted by saturated aqueous solution of sodium

hydrogen carbonate (3-5 times). The organic layer dried over $MgSO_4$ filtered, and the solvent was removed under vacuum via a rotary evaporator. The product was isolated by column chromatography using an eluent mixture of petroleum ether and ethyl acetate (1:1) followed by ethyl acetate. Products were recrystallized, after removing the solvent, in a mixture of DCM and PE.[8]

3.5.2. 4-Methoxyphenyl Derivative (3.7) A

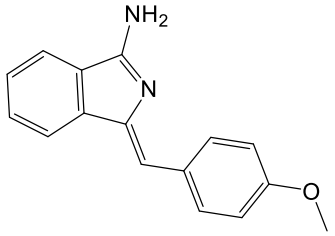

2-Bromobenzamidine hydrochloride **(3.6)** (1 g, 4.25 mmol), BINAP (0.13 g, 0.21 mmol), $PdCl_2(MeCN)_2$ (0.06 mg, 0.21 mmol) and 4-ethynylanisole (0.67 g, 5.1 mmol) were dissolved in dry DMF (14 mL) in a microwave vessel containing magnetic stirrer. The vessel was sealed and purged with nitrogen and DBU (1.62 g, 1.6 mL, 10.62 mmol) added. The reaction and the workup were performed as described in the general procedure. The product was recrystallized to recover needle-like yellow crystals (820 mg, 77%).[9]

Chemical Formula and molecular weight: $C_{16}H_{14}N_2O$, 250.30 $g.mol^{-1}$

^{1}H NMR (400 MHz, DMSO-d_6) δ 8.17 (d, 2H), 7.86 – 7.77 (m, 2H), 7.50 (s, 2H), 7.43 (td, J = 7.4, 1.1 Hz, 1H), 7.35 (td, J = 7.3, 1.0 Hz, 1H), 6.93 (d, 2H), 6.65 (s, 1H), 3.78 (s, 3H).

^{13}C NMR (126 MHz, Chloroform-d) δ 164.4, 159.1, 145.8, 143.2, 132.0, 130.7, 129.6, 128.9, 126.7, 119.5, 118.7, 115.6, 114.0, 55.3.

MS (MALDI-TOF): m/z = 250.1 $[M]^+$

Melting point: 155 ºC (lit. 156-157 ºC)[9]

3.5.3. 4-tert-butylphenyl Derivative (3.8) A*t*Bu

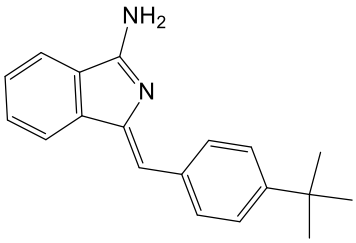

2-Bromobenzamidine hydrochloride **(3.6)** (1 g, 4.25 mmol), BINAP (0.13 g, 0.21 mmol), $PdCl_2(MeCN)_2$ (0.06 mg, 0.21 mmol), 4-tert-Butylphenylacetylene (0.8 g, 5.1 mmol) were dissolved in dry DMF (14 mL) in a microwave vessel containing magnetic stirrer. The vessel was sealed and purged with nitrogen and DBU (1.62 g, 1.6 mL, 10.62 mmol). The reaction and the workup were performed as described in the general procedure. The product was recrystallized to recover needles-like yellow crystals (0.86 g, 73%).

Chemical Formula and molecular weight: $C_{19}H_{20}N_2$, 276.38 $g.mol^{-1}$

^{1}H NMR (400 MHz, Chloroform-*d*) δ 8.02 – 7.95 (m, 2H), 7.80 (dt, *J* = 7.7, 0.9 Hz, 1H), 7.56 – 7.51 (m, 1H), 7.49 (td, *J* = 8.0, 7.0 Hz, 1H), 7.45 – 7.40 (m, 2H), 7.38 (td, *J* = 7.4, 0.9 Hz, 1H), 6.77 (s, 1H), 1.34 (s, 9H).

^{13}C NMR (101 MHz, Chloroform-d) δ 164.9, 150.5, 146.9, 143.1, 134.0, 131.1, 130.3, 129.1, 127.1, 125.5, 119.8, 118.9, 115.4, 34.8, 31.4, 31.0.

MS (MALDI-TOF): m/z = 276.16 $[M]^+$

Melting point: 184 ºC

3.5.4. 2-Thiophene Derivative (3.9) A2thiophene

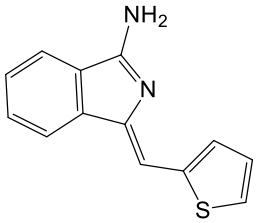

2-Bromobenzamidine hydrochloride **(3.6)** (1 g, 4.25 mmol), BINAP (0.13 mg, 0.21 mmol), $PdCl_2(MeCN)_2$ (0.06 mg, 0.21 mmol), 2-thiophene ethynyl TMS **(3.2)** (0.92 g, 5.1 mmol) were dissolved in dry DMF (14 mL) in a microwave vessel containing magnetic stirrer. The vessel was sealed and purged with nitrogen and DBU (1.62 g, 1.6 mL, 10.62 mmol) added.

The reaction and the workup were performed as described in the general procedure. The product was recrystallized to recover needles-like yellow crystals (0.61 g, 64%).[10]

Chemical Formula and molecular weight: $C_{13}H_{10}N_2S$, 226.30 g.mol^{-1}

^{1}H NMR (400 MHz, Chloroform-*d*) δ 7.74 (dt, *J* = 7.6, 1.0 Hz, 1H), 7.57 – 7.40 (m, 2H), 7.39 (dt, *J* = 5.1, 1.0 Hz, 1H), 7.36 – 7.30 (m, 2H), 7.04 (dd, *J* = 5.1, 3.6 Hz, 1H), 7.02 (s, 1H).

^{13}C NMR (101 MHz, Chloroform-d) δ 164.2, 142.2, 140.2, 131.7, 129.2, 129.0, 128.8, 127.0, 126.9, 119.7, 119.2, 109.8

MS (MALDI-TOF): m/z = 226 [M]$^+$

Melting point: 89.9 °C

3.5.5. 3-Thiophene Derivative (3.10) A3thiophene

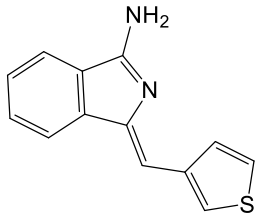

2-Bromobenzamidine hydrochloride **(3.6)** (1 g, 4.25 mmol), BINAP (0.13 g, 0.21 mmol), $PdCl_2(MeCN)_2$ (0.06 g, 0.21 mmol), 3-thiophene ethynyl TMS **(3.2)** (0.92 g, 5.1 mmol) were dissolved in dry DMF (14 mL) in a microwave vessel containing magnetic stirrer. The vessel was sealed and purged with nitrogen and DBU (1.62 g, 1.6 mL, 10.62 mmol). The reaction and the workup were performed as described in the general procedure. The product was recrystallized to recover needles-like yellow crystals (0.62 g, 65%).

Chemical Formula and molecular weight: $C_{13}H_{10}N_2S$, 226.30 g.mol^{-1}

^{1}H NMR (400 MHz, Chloroform-*d*) δ 7.93 (ddd, *J* = 3.0, 1.2, 0.6 Hz, 1H), 7.81 (dd, *J* = 5.0, 1.3 Hz, 1H), 7.76 (dt, *J* = 7.7, 0.9 Hz, 1H), 7.59 (dt, *J* = 7.6, 1.0 Hz, 1H), 7.49 (td, *J* = 7.5, 1.0 Hz, 1H), 7.38 (td, *J* = 7.4, 1.0 Hz, 1H), 7.34 (ddd, *J* = 5.0, 3.0, 0.5 Hz, 1H), 6.84 (s, 1H).

^{13}C NMR (101 MHz, Chloroform-d) δ 164.8, 142.7, 138.1, 131.2, 129.7, 129.2, 127.1, 125.8, 125.3, 119.7, 119.2, 109.7

MS (MALDI-TOF): m/z = 226 [M]$^+$

Melting point: 91.2 °C

3.5.6. Ferrocene Derivative (3.11) *Aferrocene*

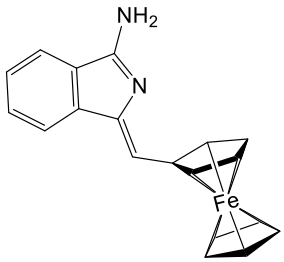

2-Bromobenzamidine hydrochloride **(3.6)** (1 g, 4.25 mmol), BINAP (0.13 g, 0.21 mmol), $PdCl_2(MeCN)_2$ (0.06 mg, 0.21 mmol), ethynylferrocene (1.07 g, 5.1 mmol) were dissolved in dry DMF (14 mL) in a microwave vessel containing magnetic stirrer. The vessel was sealed and purged with nitrogen and DBU (1.62 g, 1.6 mL, 10.62 mmol). The reaction and the workup were performed as described in the general procedure. The product was recrystallized to recover needles-like dark purple crystals (0.85 g, 61%).

Chemical Formula and molecular weight: $C_{19}H_{16}FeN_2$, 328.20 g.mol^{-1}

1H NMR (400 MHz, Acetone-d6) δ 7.79 (dt, J = 7.6, 1.0 Hz, 1H), 7.74 (dt, J = 7.5, 1.0 Hz, 1H), 7.40 (td, *J* = 7.4, 1.1 Hz, 1H), 7.33 (td, *J* = 7.4, 1.0 Hz, 1H), 6.58 (s, 1H), 5.05 (t, *J* = 1.8 Hz, 2H), 4.32 (t, *J* = 1.9 Hz, 2H), 4.08 (s, 5H).

^{13}C NMR (101 MHz, Acetone-d6) δ 164.7, 147.6, 143.5, 132.8, 128.9, 127.0, 120.2, 119.8, 114.7, 69.9, 22.8.

MS (MALDI-TOF): m/z = 328.07 $[M]^+$

Melting point: 94.2 °C

3.5.7. Large Scale Procedure

Aminoisoindoline **(3.7)** was prepared in a two-neck round bottom flask under nitrogen. 2-bromobenzamidine hydrochloride **(3.6)** (5 g, 21.23 mmol, 1 eq.), BINAB (0.66 g, 1.06 mmol, 0.05 eq.), $PdCl_2(MeCN)_2$ (0.28 mg, 1.06 mmol, 0.05 eq.), and 4-methoxyphenylacetylene (3.1 mL, 25.5 mmol, 1.2 eq.) were dissolved in 85 mL of dry DMF followed by the addition of DBU (8 mL, 53.08 mmol, 2.5 eq.). The reaction proceeded under nitrogen for 6 hours at 120 °C. The mixture was diluted with 200 mL ethyl acetate at RT, and the workup was performed as explained previously to obtain needles-like yellow crystals (3.72 g, 70%).

3.6. Synthesis of symmetrical aza (dibenzo) dipyrromethene

3.6.1. General Procedure

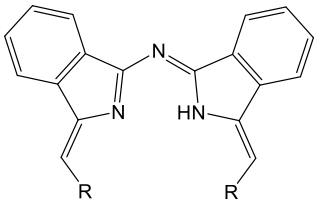

Dimerization reactions were performed by dissolving an aminoisoindoline (200 mg) in toluene (4 mL). The solution was stirred and refluxed overnight. The solvent was allowed to evaporate, and the product was isolated by column chromatography using DCM – DCM/methanol mixture (50:1). The Solvent was removed under a vacuum via a rotary evaporator, and the product was crystallized in a mixture of DCM and methanol.[11]

3.6.2. 4-Methoxyphenyl Derivative (3.12) AA

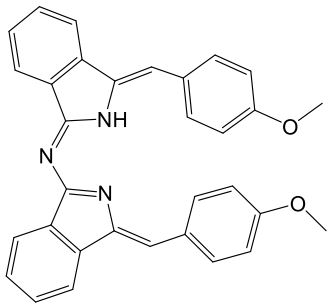

Aminoisoindoline **(3.7)** (200 mg, 0.8 mmol) was used. The reaction and purification steps were performed as described in the general procedure for synthesizing aza (dibenzo) dipyrromethene to obtain needle-like red crystals (141 mg, 73%).[11]

Chemical Formula and molecular weight: $C_{32}H_{25}N_3O_2$, 483.57 g.mol^{-1}

^{1}H NMR (400 MHz, Methylene Chloride-d2) δ 12.99 (s, 1H), 8.06 (dt, J = 7.4, 1.1 Hz, 2H), 7.91 – 7.81 (m, 6H), 7.54 (dtd, J = 23.5, 7.3, 1.2 Hz, 4H), 6.83 (s, 2H), 6.68 – 6.60 (m, 4H), 3.70 (s, 6H).

MS (MALDI-TOF): m/z = 483.19 $[M]^+$

UV-Vis λ_{max} (nm) (Ɛ ($M^{-1}.cm^{-1}$)) = 490 ($1.69.10^4$), 358 ($6.49.10^4$), 267 ($5.24.10^4$)

Melting point: 169-170 ^oC

3.6.3. 4-tert-butylphenyl Derivative (3.13) AA*t*Bu

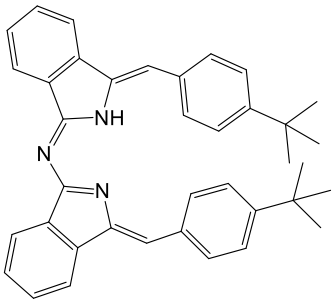

Aminoisoindoline **(3.8)** (200 mg, 0.72 mmol) was used. The reaction and purification steps were performed as described in the general procedure for synthesizing aza (dibenzo) dipyrromethene and crystallized in ethanol to obtain needle-like red crystals (77 mg, 40%).

Chemical Formula and molecular weight: $C_{38}H_{37}N_3$, 535.74 g.mol^{-1}

^{1}H NMR (400 MHz, Chloroform-*d*) δ 12.31 (s, 1H), 7.88 – 7.77 (m, 6H), 7.63 – 7.43 (m, 6H), 7.20 – 7.12 (m, 4H), 6.89 (s, 2H), 1.22 (s, 18H).

^{13}C NMR (101 MHz, Methylene Chloride-d2) δ 165.5, 159.2, 140.0, 139.7, 134.5, 131.1, 129.9, 128.3, 127.9, 121.9, 119.2, 114.6, 114.0, 54.9, 53.8, 50.4.

MS (MALDI-TOF): m/z = 536.3 $[M]^+$

UV-Vis λ_{max} (nm) (Ɛ ($M^{-1}.cm^{-1}$)) = 489 ($1.4.10^4$), 358 (7.10^4), 273 ($1.84.10^5$)

Melting point: 210^{o}C

3.6.4. 2-Thiophene Derivative (3.14) AA2thiophene

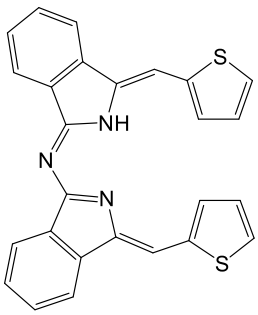

Aminoisoindoline **(3.9)** (200 mg, 0.88 mmol) was used. The reaction and purification steps were performed as described in the general procedure for synthesizing aza (dibenzo) dipyrromethene to obtain needle-like red crystals (134 mg, 70%).[11]

Chemical Formula and molecular weight: $C_{26}H_{17}N_3S_2$, 435.56 g.mol^{-1}

^{1}H NMR (400 MHz, Chloroform-*d*) δ 7.84 – 7.74 (m, 2H), 7.63 – 7.48 (m, 6H), 7.47 (dt, *J* = 3.7, 1.0 Hz, 2H), 7.17 (dd, *J* = 5.2, 1.1 Hz, 2H), 7.06 (s, 2H), 6.92 (dd, *J* = 5.1, 3.6 Hz, 2H).

^{13}C NMR (101 MHz, Chloroform-d) δ 164.8, 140.9, 139.0, 138.9, 135.3, 130.2, 128.9, 128.5, 128.2, 128.0, 122.6, 119.3, 107.6, 31.0.

MS (MALDI-TOF): m/z = 435.09 $[M]^{+}$

UV-Vis λ_{max} (nm) (Ɛ ($M^{-1}.cm^{-1}$)) = 500 ($1.1.10^{4}$), 364 (5.10^{4}), 277 ($3.4.10^{4}$)

Melting point: 184-186 ^{o}C

3.6.5. 3-Thiophene Derivative (3.15) AA3thiophene

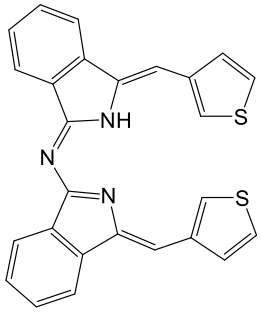

Aminoisoindoline **(3.10)** (200 mg, 0.88 mmol) was used. The reaction and purification steps were performed as described in the general procedure for synthesizing aza (dibenzo) dipyrromethene to obtain needle-like red crystals (137 mg, 71%).

Chemical Formula and molecular weight: $C_{26}H_{17}N_3S_2$, 435.56 $g.mol^{-1}$

^{1}H NMR (400 MHz, Chloroform-*d*) δ 7.83 – 7.77 (m, 2H), 7.76 (d, *J* = 3.0 Hz, 2H), 7.64 (d, *J* = 4.9 Hz, 2H), 7.60 – 7.49 (m, 6H), 7.18 (dd, *J* = 5.1, 3.0 Hz, 2H), 6.94 (s, 2H).

^{13}C NMR (101 MHz, Chloroform-d) δ 165.6, 141.0, 139.5, 137.2, 135.0, 130.2, 128.7, 128.2, 126.7, 125.9, 122.5, 119.3, 108.5

MS (MALDI-TOF): m/z = 435.09 $[M]^{+}$

UV-Vis λ_{max} (nm) (Ɛ ($M^{-1}.cm^{-1}$)) = 467 ($1.1.10^{4}$), 346 ($4.5.10^{4}$), 277 ($5.3.10^{4}$)

Melting point: 191-192 ^{o}C

3.7. Synthesis of unsymmetrical aza (dibenzo) dipyrromethene

3.7.1. Procedure 1

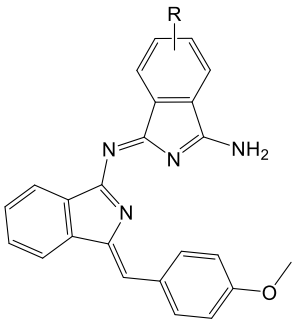

Aminoisoindoline **A (3.7)** (0.3 g, 1.2 mmol, 1 eq.), a dinitrile (1.44 mmol, 1.2 eq.), and NaOMe (0.01 g, 1.8 mmol, 1.5 eq.) reacted in methanol (20 mL) overnight at 50 °C. The precipitated product was filtered and washed with cold methanol.

3.7.2. Phthalonitrile Precursor (3.16) AB

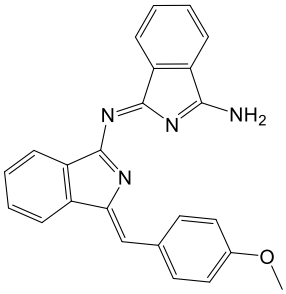

Phthalonitrile (0.18 g, 1.44 mmol, 1.2 eq.) reacted with aminoisoindoline **A (3.7)** according to **Procedure 1**. An orange solid was recovered (0.3 mg, 66%).

Chemical Formula and molecular weight: $C_{24}H_{18}N_4O$, 378.44 g.mol^{-1}

^{1}H NMR (400 MHz, DMSO-d6) δ 9.01 (s, 2H), 8.29 – 8.21 (m, 2H), 7.97 (d, J = 7.4 Hz, 3H), 7.70 (d, J = 5.8 Hz, 2H), 7.45 (t, J = 7.4 Hz, 1H), 7.33 (d, J = 7.0 Hz, 2H), 7.26 (s, 1H), 7.01 (d, J = 8.5 Hz, 2H), 3.81 (s, 3H).

^{13}C NMR (125.7 MHz, DMSO-d6) δ 160.1, 154.3, 153.9, 146.9, 144.1, 128.4, 123.3, 119.8, 119.0, 118.2, 117.4, 117.2, 116.8, 113.4, 55.7

MS (MALDI-TOF): m/z = 378.15 $[M]^+$

UV-Vis λ_{max} (nm) (Ɛ ($M^{-1}.cm^{-1}$)) = 442 ($2.25.10^4$), 316 ($3.3.10^4$), 260 ($2.95.10^4$)

Melting point: 234 °C

3.7.3. 4-tert-butylphthalonitrile Precursor (3.17) *tert*AB

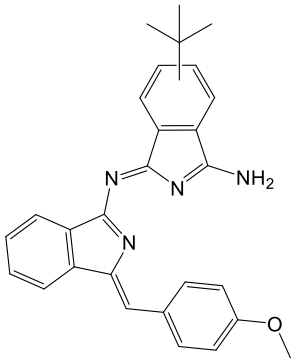

4-tert-Butylphthalonitrile (0.27 g, 1.44 mmol, 1.2 eq.) reacted with aminoisoindoline **A (3.7)** according to **Procedure 1**. An orange solid was recovered (0.31 g, 59%)

Chemical Formula and molecular weight: $C_{28}H_{26}N_4O$, 434.54 g.mol^{-1}

^{1}H NMR (400 MHz, DMSO-d_6) δ 8.89 (s, 2H), 8.25 (d, J = 8.6 Hz, 2H), 7.96 (d, J = 7.5 Hz, 1H), 7.89 (d, J = 11.9 Hz, 2H), 7.74 (s, 1H), 7.44 (d, J = 7.6 Hz, 1H), 7.32 (s, 2H), 7.25 (s, 1H), 7.00 (d, J = 8.4 Hz, 2H), 3.81 (s, 3H), 1.38 (s, 9H).

^{13}C NMR (101 MHz, DMSO-d_6) δ 31.0.

MS (MALDI-TOF): m/z = 434.21 $[M]^+$

UV-Vis λ_{max} (nm) (Ɛ ($M^{-1}.cm^{-1}$)) = 441 ($0.15.10^4$), 274 ($1.05.10^4$)

Melting point: 249 °C

3.7.4. Naphthalonitrile Precursor (3.18) *nap*AB

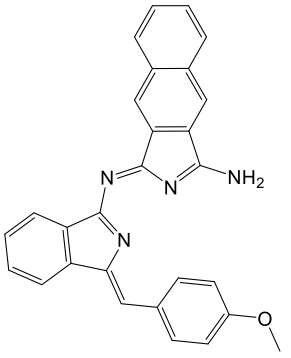

2,3-Dicyanonaphthalene **(3.1)** (0.26 g, 1.44 mmol, 1.2 eq.) reacted with aminoisoindoline **A (3.7)** according to **Procedure 1**. A brownish-orange solid was recovered (0.35 g, 68%).

Chemical Formula and molecular weight: $C_{28}H_{20}N_4O$, 428.50 g.mol^{-1}

^{1}H NMR (500 MHz, DMSO-d_6) δ 8.95 (s, 2H), 8.48 (d, *J* = 14.7 Hz, 2H), 8.30 – 8.21 (m, 3H), 8.14 – 8.08 (m, 1H), 7.96 (d, *J* = 7.6 Hz, 1H), 7.77 – 7.68 (m, 2H), 7.44 (t, *J* = 7.4 Hz, 1H), 7.37 (d, *J* = 7.6 Hz, 1H), 7.32 (t, *J* = 7.3 Hz, 1H), 7.24 (s, 1H), 7.00 (d, *J* = 9.1 Hz, 2H), 3.81 (s, 3H).

^{13}C NMR (101 MHz, DMSO-d_6) δ 142.0, 134.2, 132.9, 129.9, 129.6, 128.9, 128.2, 128.0, 119.3, 114.0, 55.2.

MS (MALDI-TOF): m/z = 428.16 $[M]^+$

UV-Vis λ_{max} (nm) (Ɛ ($M^{-1}.cm^{-1}$)) = 441 (.10^4), 275 (.10^4)

Melting point: 221 ^oC

3.7.5. Procedure 2

The following experiments were performed by altering the starting aminoisoindoline. Either by reacting with phthalonitrile or 1-Imino-3,3-dimethoxyisoindoline **(3.4)**, the targeted compounds were prepared as follows:

3.7.6. 2-Thiophene Derivative (3.19) AB2thiophene

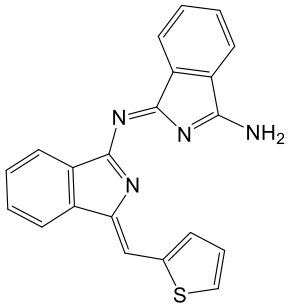

A2thiophene (3.9) (0.3 g, 1.33 mmol, 1 eq.), phthalonitrile (0.2 g, 1.59 mmol, 1.2 eq.), and NaOMe (0.11 mg, 1.99 mmol, 1.5 eq.) reacted in methanol (20 mL) overnight at 50 ^oC. The precipitated brown product was filtered and washed with cold methanol (0.29 g, 61%).[10]

Chemical Formula and molecular weight: $C_{21}H_{14}N_4S$, 354.43g.mol^{-1}

^{1}H NMR (400 MHz, DMSO-d_6) δ 8.06 (s, 1H), 7.98 (d, *J* = 7.7 Hz, 1H), 7.74 (s, 5H), 7.54 – 7.45 (m, 2H), 7.39 (s, 2H), 7.16 (s, 1H).

MS (MALDI-TOF): m/z = 354.09 $[M]^+$

UV-Vis λ_{max} (nm) (ε ($M^{-1}.cm^{-1}$)) = 655 ($0.5.10^3$), 448 (1.10^4), 276 ($4.1.10^4$)

Melting point: 219-221 °C

3.7.7. 3-Thiophene Derivative (3.20) AB3thiophene

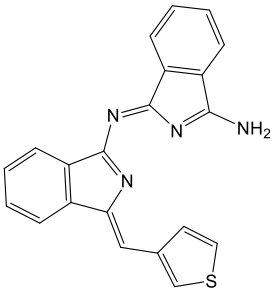

A3thiophene (3.10) (0.3 g, 1.33 mmol) and 1-Imino-3,3-dimethoxyisoindoline **(3.4)** (0.26 g, 1.33 mmol) were dissolved in DCM (20 mL) in the presence of molecular sieve. The reaction proceeded overnight at RT. The precipitated yellowish-orange product was filtered and washed with cold DCM (0.32 g, 69%).

Chemical Formula and molecular weight: $C_{21}H_{14}N_4S$, 354.43g.mol^{-1}

^{1}H NMR (500 MHz, DMSO-d_6) δ 8.88 (s, 2H), 8.12 (s, 1H), 8.04 (s, 1H), 7.94 (d, J = 8.5 Hz, 3H), 7.69 (s, 2H), 7.59 (s, 1H), 7.45 (s, 1H), 7.34 (s, 3H).

^{13}C NMR (101 MHz, DMSO-d_6) δ 137.9, 129.7, 128.4, 127.2, 126.2, 121.5, 119.4.

MS (MALDI-TOF): m/z = 354.09 $[M]^+$

UV-Vis λ_{max} (nm) (ε ($M^{-1}.cm^{-1}$)) = 428 ($1.2.10^4$), 316 ($1.6.10^4$), 279 ($2.1.10^4$)

Melting point: 238-241 °C

3.7.8. Ferrocene Derivative (3.21) AB*ferrocene*

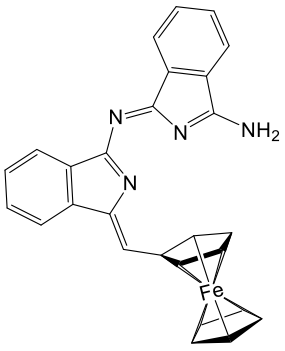

Method A:

Aferrocene **(3.11)** (0.15 g, 0.46 mmol) and 1-Imino-3,3-dimethoxyisoindoline **(3.4)** (0.6 g, 0.46 mmol) were dissolved in DCM (10 mL) in the presence of molecular sieve. The reaction proceeded overnight at RT. The product was isolated by column chromatography using a mixture eluent of DCM/ethyl acetate (8:1). The targeted compound recovered by crystallization in DCM/PE as a dark red solid (0.1 g, 50%).

Method B:

Aferrocene **(3.11)** (0.15 g, 0.46 mmol) and 1-Imino-3,3-dimethoxyisoindoline **(3.4)** (0.6 g, 0.46 mmol) were dissolved in methanol (10 mL). The reaction proceeded overnight at RT. The precipitated dark red product was filtered and washed with cold methanol (0.13 g, 62%).

Chemical Formula and molecular weight: $C_{27}H_{20}FeN_4$, 456.33 $g.mol^{-1}$

^{1}H NMR (400 MHz, Methylene Chloride-d_2) δ 8.71 (s, 1H), 8.14 (d, J = 6.0 Hz, 1H), 7.99 (d, J = 7.3 Hz, 1H), 7.89 (s, 2H), 7.83 (dt, J = 7.5, 1.0 Hz, 1H), 7.76 – 7.66 (m, 2H), 7.56 – 7.42 (m, 2H), 7.11 (s, 1H), 5.01 (s, 2H), 4.65 (t, J = 1.9 Hz, 2H), 4.24 (s, 5H).

^{13}C NMR (101 MHz, Acetone-d_6) δ 70.6.

MS (MALDI-TOF): m/z = 456.1 $[M]^+$

UV-Vis λ_{max} (nm) (Ɛ ($M^{-1}.cm^{-1}$)) = 359 ($1.9.10^4$), 273 ($2.2.10^4$), 224 ($5.8.10^4$), 221 ($1.4.10^4$), 213 ($5.5.10^4$), 208 ($1.01.10^5$).

Melting point: 269-271 ^oC

Rf: 0.5 (DCM 8:1 ethyl acetate, silica)

3.8. Benzo Azatripyrrins

3.8.1. ABA (3.22)

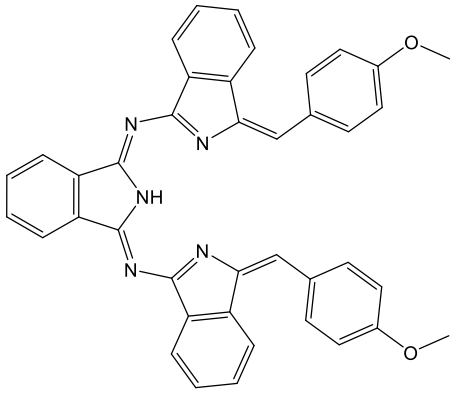

AB (3.16) dimer (100 mg, 0.26 mmol) and aminoisoindoline **A (3.7)** (67 mg, 0.27 mmol) were added to a sealed tube and dissolved in 10 mL of p-xylene. After purging with nitrogen, the reaction mixture was heated to 180 ºC in an oil bath overnight. The solvent was removed under vacuum by a rotary evaporator. The targeted molecule was separated from the crude mixture by column chromatography using DCM. The pure fraction of **ABA (3.22)** was crystallized by DCM and petroleum ether (81 mg, 50%).[13]

Chemical Formula and molecular weight: $C_{40}H_{29}N_5O_2$, 611.71 g.mol^{-1}

^{1}H NMR (400 MHz, Chloroform-*d*) δ 14.21 (s, 1H), 8.19 (dd, *J* = 5.6, 3.1 Hz, 2H), 7.99 – 7.96 (m, 2H), 7.93 (d, *J* = 8.7 Hz, 4H), 7.71 (ddd, *J* = 7.1, 4.7, 2.1 Hz, 4H), 7.53 – 7.40 (m, 4H), 6.61 (s, 2H), 6.40 (d, *J* = 8.3 Hz, 4H), 3.43 (s, 6H).

^{13}C NMR (101 MHz, Chloroform-*d*) δ 159.9, 156.8, 145.9, 142.5, 135.4, 134.4, 133.3, 132.4, 128.9, 128.7, 127.2, 126.3, 123.7, 123.3, 121.3, 118.9, 113.6, 55.0.

MS (MALDI-TOF): m/z = 611.23 $[M]^+$

UV-Vis.: λ_{max} (nm) (Ɛ ($M^{-1}.cm^{-1}$)) = 470 ($1.23.10^4$), 396 ($2.46.10^4$), 334 ($4.46.10^4$), 266 ($4.23.10^4$)

Melting point: 199-202 ºC

Rf: 0.4 (DCM, silica)

3.8.2. *tert*ABA (3.23)

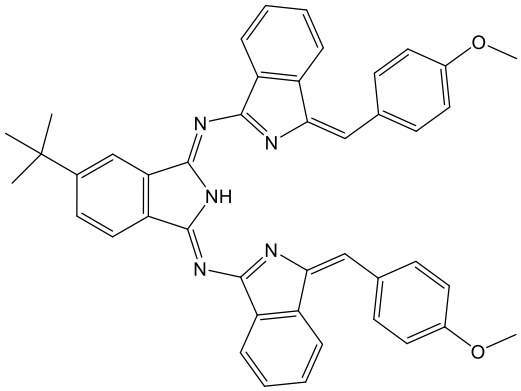

***tert*AB (3.17)** dimer (100 mg, 0.23 mmol) and aminoisoindoline **A (3.7)** (58 mg, 0.23 mmol) were added to a sealed tube and dissolved in 10 mL of p-xylene. After purging with nitrogen, the reaction mixture was heated to 180 ºC in an oil bath overnight. The solvent was removed under vacuum by a rotary evaporator. The targeted molecule was separated from the crude mixture by column chromatography using DCM. The pure fraction of ***tert*ABA (3.23)** was crystallized by DCM and petroleum ether (85 mg, 55%).

Chemical Formula and molecular weight: $C_{44}H_{37}N_5O_2$, 667.81 g.mol^{-1}

^{1}H NMR (400 MHz, Chloroform-*d*) δ 14.13 (s, 1H), 8.20 (d, *J* = 1.8 Hz, 1H), 8.09 (d, *J* = 8.1 Hz, 1H), 8.06 – 8.00 (m, 1H), 8.00 – 7.95 (m, 1H), 7.92 (d, *J* = 8.4 Hz, 4H), 7.76 (dd, *J* = 8.0, 1.7 Hz, 1H), 7.73 – 7.67 (m, 2H), 7.52 – 7.40 (m, 4H), 6.61 (s, 2H), 6.39 (d, *J* = 8.3 Hz, 4H), 3.43 (s, 6H), 1.49 (s, 9H).

^{13}C NMR (101 MHz, Chloroform-*d*) δ 169.3, 159.9, 156.8, 145.9, 145.9, 142.5, 135.4, 133.3, 129.9, 128.9, 128.9, 128.7, 127.1, 126.0, 123.1, 121.3, 121.3, 120.2, 118.9, 113.6, 55.0, 35.8, 31.5.

MS (MALDI-TOF): m/z = 667.29 $[M]^+$

UV-Vis.: λ_{max} (nm) (Ɛ ($M^{-1}.cm^{-1}$)) = 536 ($1.19.10^4$), 343 ($1.78.10^4$), 290 ($4.96.10^4$), 274 ($4.81.10^4$)

Melting point: 187-189 ºC

Rf: 0.4 (DCM, silica)

3.8.3. *nap*ABA (3.24)

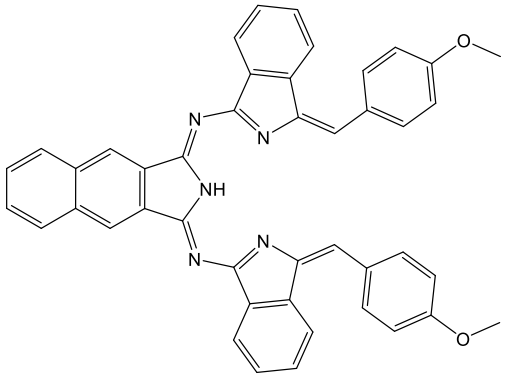

***nap*AB (3.18)** dimer (100 mg, 0.23 mmol) and aminoisoindoline **A (3.7)** (59 mg, 0.24 mmol) were added to a sealed tube and dissolved in 10 mL of p-xylene. After purging with nitrogen, the reaction mixture was heated to 180 ºC in an oil bath overnight. The solvent was removed under vacuum by a rotary evaporator. The targeted molecule was separated from the crude mixture by column chromatography using DCM. The pure fraction of ***nap*ABA (3.24)** was crystallized by DCM and petroleum ether (92 mg, 60%).

Chemical Formula and molecular weight: $C_{44}H_{31}N_5O_2$, 661.77 g.mol^{-1}

^{1}H NMR (500 MHz, Chloroform-*d*) δ 14.44 (s, 1H), 8.72 (s, 2H), 8.14 (dd, *J* = 6.2, 3.4 Hz, 2H), 8.06 – 8.01 (m, 2H), 7.93 (d, *J* = 8.4 Hz, 4H), 7.77 – 7.67 (m, 4H), 7.52 – 7.44 (m, 4H), 6.63 (s, 2H), 6.39 (d, *J* = 8.3 Hz, 4H), 3.42 (s, 6H).

^{13}C NMR (101 MHz, Chloroform-*d*) δ 169.1, 159.8, 156.6, 145.7, 142.4, 135.3, 135.2, 133.1, 131.5, 130.0, 128.8, 128.5, 128.3, 127.0, 125.6, 124.1, 121.2, 118.8, 113.5, 54.9.

MS (MALDI-TOF): m/z = 661.25 $[M]^+$

UV-Vis.: λ_{max} (nm) (Ɛ ($M^{-1}.cm^{-1}$)) = 536 ($0.46.10^4$), 343 ($0.69.10^4$), 290 ($1.91.10^4$), 274 ($1.86.10^4$)

Melting point: 184-186 ºC

Rf: 0.4 (DCM, silica)

3.9. Palladium Complexes of aza (dibenzo) dipyrromethene Compounds

3.9.1. Pd-AA (3.25)

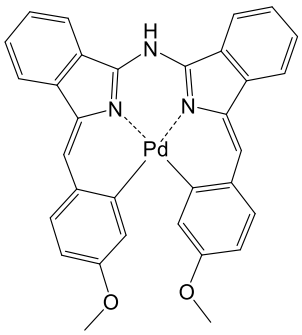

AA (3.12) dimer (80 mg, 0.17 mmol) and palladium (II) acetate (37 mg, 0.17 mmol) were dissolved in ethyl acetate (10 mL) under nitrogen. The reaction was stirred at room temperature for 7 days. The solvent was removed under vacuum via a rotary evaporator. Column chromatography was performed using neutral alumina, starting with DCM and then eluting by ethyl acetate. The solvent was removed, and a mixture of DCM and methanol recrystallized the complex to obtain a dark red solid (84 mg, 86%).

Chemical Formula and molecular weight: $C_{32}H_{23}N_3O_2Pd$, 587.98 g.mol^{-1}

^{1}H NMR (400 MHz, Methylene Chloride-d_2) δ 8.81 (s, 1H), 7.83 (d, *J* = 7.8 Hz, 2H), 7.64 – 7.55 (m, 4H), 7.47 (d, *J* = 7.8 Hz, 2H), 7.38 (d, *J* = 8.5 Hz, 2H), 7.29 (d, *J* = 7.1 Hz, 4H), 6.89 (dd, *J* = 8.4, 2.7 Hz, 2H), 3.80 (s, 6H).

MS (MALDI-TOF): m/z = 587.86 $[M]^+$

UV-Vis.: λ_{max} (nm) (Ɛ ($M^{-1}.cm^{-1}$)) = 470 ($1.4.10^4$), 404 ($4.2.10^4$), 267 ($6.6.10^4$)

Melting point: 290 ºC

Rf: 0.7 (ethyl acetate, neutral alumina)

3.9.2. Pd-AA*t*Bu (3.26)

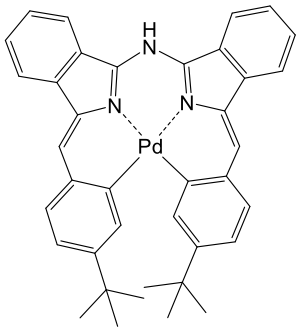

AA*t*Bu (3.13) dimer (45 mg, 0.08 mmol) and palladium (II) acetate (19 mg, 0.08 mmol) were dissolved in ethyl acetate (5 mL) under nitrogen. The reaction was stirred at room temperature for 5 days. The solvent was removed under vacuum via a rotary evaporator. Column chromatography was performed using neutral alumina, starting with DCM and then eluting by ethyl acetate. The solvent was removed, and the complex was recrystallized from ethanol to obtain an orange solid (40 mg, 76%).

Chemical Formula and molecular weight: $C_{38}H_{35}N_3Pd$, 640.14 g.mol^{-1}

^{1}H NMR (400 MHz, Acetone-d_6) δ 11.68 (s, 1H), 8.47 (d, *J* = 7.8 Hz, 2H), 8.33 (d, *J* = 7.8 Hz, 2H), 8.08 (s, 2H), 8.03 (d, *J* = 2.1 Hz, 2H), 7.78 – 7.69 (m, 2H), 7.61 – 7.56 (m, 2H), 7.54 (d, *J* = 8.1 Hz, 2H), 7.29 (dd, *J* = 8.1, 2.2 Hz, 2H), 1.23 (s, 18H).

MS (MALDI-TOF): m/z = 639.23 $[M]^+$

UV-Vis.: λ_{max} (nm) (Ɛ ($M^{-1}.cm^{-1}$)) = 482 ($2.4.10^4$), 390 ($5.6.10^4$), 350 ($3.4.10^4$), 237 ($8.1.10^4$)

Melting point: > 300 ºC

Rf: 0.7 (ethyl acetate, neutral alumina)

3.9.3. Pd-AA2thiophene (3.27)

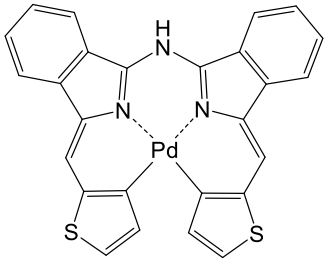

AA2thiophene (3.14) dimer (50 mg, 0.11 mmol) and palladium (II) acetate (26 mg, 0.12 mmol) were dissolved in ethyl acetate (5 mL) under nitrogen. The reaction was stirred at room temperature for 7 days. The solvent was removed under vacuum via a rotary evaporator. Column chromatography was performed using neutral alumina, starting with DCM and then eluting by ethyl acetate. The solvent was removed, and a mixture of DCM and methanol recrystallized the complex to obtain a dark red solid (53 mg, 86%).

Chemical Formula and molecular weight: $C_{26}H_{15}N_3PdS_2$, 539.97 g.mol^{-1}

^{1}H NMR (400 MHz, Acetone-d_6) δ 8.52 (d, *J* = 7.8 Hz, 2H), 8.26 (d, *J* = 7.8 Hz, 2H), 8.24 (s, 2H), 7.75 (dd, *J* = 5.0, 0.7 Hz, 2H), 7.62 (t, *J* = 7.4 Hz, 2H), 7.57 (d, *J* = 4.9 Hz, 2H), 7.54 – 7.46 (m, 2H).

MS (MALDI-TOF): m/z = 539.96 $[M]^+$

UV-Vis.: λ_{max} (nm) (Ɛ ($M^{-1}.cm^{-1}$)) = 418 ($1.7.10^4$), 394 ($1.4.10^4$), 370 ($2.3.10^4$), 265 ($4.2.10^4$)

Melting point: 246 ºC

Rf: 0.7 (ethyl acetate, neutral alumina)

3.9.4. Pd-AA3thiophene (3.28)

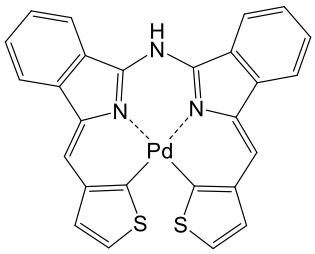

AA2thiophene (3.14) dimer (50 mg, 0.11 mmol) and palladium (II) acetate (26 mg, 0.12 mmol) were dissolved in ethyl acetate (5 mL) under nitrogen. The reaction was stirred at room temperature for 7 days. The solvent was removed under vacuum via a rotary evaporator. Column chromatography was performed using neutral alumina, starting with DCM and then eluting by ethyl acetate. The solvent was removed, and a mixture of DCM and methanol recrystallized the complex to obtain a dark red solid (54 mg, 88%).

Chemical Formula and molecular weight: $C_{26}H_{15}N_3PdS_2$, 539.97 g.mol^{-1}

^{1}H NMR (400 MHz, Chloroform-*d*) δ 7.82 – 7.77 (m, 2H), 7.76 (d, *J* = 3.0 Hz, 2H), 7.64 (d, *J* = 4.8 Hz, 2H), 7.61 – 7.48 (m, 4H), 7.18 (dd, *J* = 5.1, 3.0 Hz, 2H), 6.94 (s, 2H).

MS (MALDI-TOF): m/z = 539.79 $[M]^+$

UV-Vis.: λ_{max} (nm) (Ɛ ($M^{-1}.cm^{-1}$)) = 460 ($0.5.10^4$), 374 ($1.2.10^4$), 257 (2.10^4), 231 ($2.1.10^4$)

Melting point: 242 °C

Rf: 0.7 (ethyl acetate, neutral alumina)

3.10. Palladium Complexes of Unsymmetrical azadipyrrins

3.10.1. Pd-AB (2.29)

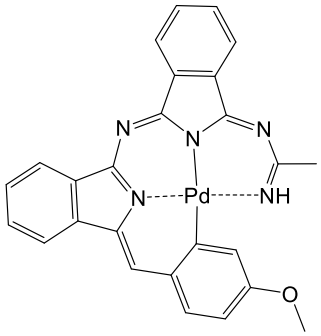

AB dimer (**3.16)** (100 mg, 0.26 mmol) was dissolved in dry acetonitrile (200 ml). Palladium (II) chloride (46 mg, 0.26 mmol) was added, and the reaction was stirred at room temperature for 7 days. The solvent was removed under vacuum via a rotary evaporator, and the residual was separated by column chromatography on neutral alumina, eluting with acetonitrile. The solvent evaporated, and the complex was crystallized from a mixture of DCM and hexane to give a purple solid (122 mg, 87%).

Chemical Formula and molecular weight: $C_{26}H_{19}N_5OPd$, 523.89 $g.mol^{-1}$

^{1}H NMR (400 MHz, Methylene Chloride-d_2) δ 8.25 (s, 1H), 7.99 (dd, *J* = 5.3, 2.6 Hz, 2H), 7.92 (s, 1H), 7.71 (d, *J* = 7.6 Hz, 1H), 7.61 – 7.54 (m, 2H), 7.50 (td, *J* = 7.4, 1.1 Hz, 1H), 7.43 (t, 1H), 7.35 (d, *J* = 9.1 Hz, 2H), 7.06 (s, 1H), 6.83 (dd, *J* = 8.3, 2.4 Hz, 1H), 3.93 (s, 3H), 2.59 (s, 3H).

MS (MALDI-TOF): m/z = 522.65 $[M]^+$

UV-Vis.: λ_{max} (nm) (ε ($M^{-1}.cm^{-1}$)) = 543 ($1.0.10^4$), 343. ($2.45.10^4$), 259 ($4.27.10^4$)

Melting point: 217 ºC

Rf: 0.7 (acetonitrile, neutral alumina)

3.10.2. Pd-*tert*AB (2.30)

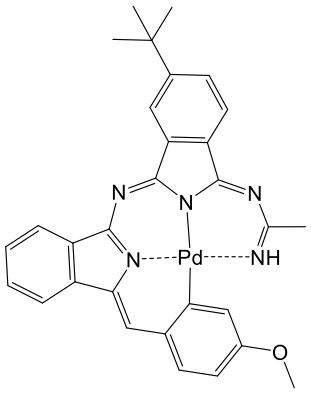

***tert*AB** dimer **(3.17)** (100 mg, 0.23 mmol) was dissolved in dry acetonitrile (200 ml). Palladium (II) chloride (41 mg, 0.23 mmol) was added, and the reaction was stirred at room temperature for 7 days. The solvent was removed under vacuum via a rotary evaporator, and the residual was separated by column chromatography on neutral alumina, eluting with acetonitrile. The solvent evaporated, and the complex was crystallized from a mixture of DCM and hexane to give a purple solid (108 mg, 81%).

Chemical Formula and molecular weight: $C_{30}H_{27}N_5OPd$, 580.00 $g.mol^{-1}$

^{1}H NMR (400 MHz, Methylene Chloride-d_2) δ 8.53 (s, 1H), 8.39 – 8.30 (m, 2H), 7.98 (d, *J* = 8.4 Hz, 3H), 7.71 (d, *J* = 8.1 Hz, 2H), 7.68 – 7.55 (m, 2H), 7.38 (s, 1H), 6.94 (s, 1H), 3.97 (s, 3H), 2.79 (s, 3H), 1.51 (s, 9H).

MS (MALDI-TOF): m/z = 578.68 $[M]^+$

UV-Vis.: λ_{max} (nm) (ε ($M^{-1}.cm^{-1}$)) = 540 ($1.2.10^4$), 344. (3.10^4), 265 ($7.7.10^4$)

Melting point: 219 ºC

Rf: 0.7 (acetonitrile, neutral alumina)

3.10.3. Pd-*nap*AB (2.31)

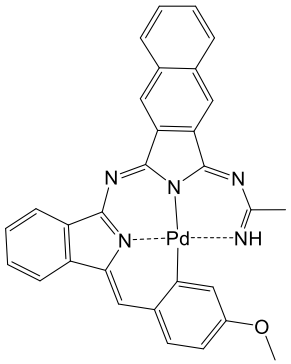

***nap*AB** dimer **(3.18)** (100 mg, 0.23 mmol) was dissolved in dry acetonitrile (200 ml). Palladium (II) chloride (41 mg, 0.23 mmol) was added, and the reaction was stirred at room temperature for 7 days. The solvent was removed under vacuum via a rotary evaporator, and the residual was separated by column chromatography on neutral alumina, eluting with acetonitrile. The solvent evaporated, and the complex was crystallized from a mixture of DCM and hexane to give a purple solid (119 mg, 89%).

Chemical Formula and molecular weight: $C_{30}H_{21}N_5OPd$, 573.95 g.mol^{-1}

^{1}H NMR (400 MHz, Methylene Chloride-d_2) δ 8.51 (s, 1H), 8.35 (s, 1H), 8.28 (s, 1H), 8.23 (d, *J* = 7.4 Hz, 1H), 8.05 (d, *J* = 7.1 Hz, 1H), 7.99 (d, *J* = 7.1 Hz, 1H), 7.87 (d, *J* = 7.5 Hz, 1H), 7.68 – 7.46 (m, 6H), 7.26 (d, *J* = 2.5 Hz, 1H), 6.88 (dd, *J* = 8.3, 2.5 Hz, 1H), 3.93 (s, 3H), 2.66 (d, *J* = 1.0 Hz, 3H).

MS (MALDI-TOF): m/z = 573.28 $[M]^+$

UV-Vis.: λ_{max} (nm) (Ɛ ($M^{-1}.cm^{-1}$)) = 536 ($1.6.10^4$), 343. ($2.4.10^4$), 290 ($6.7.10^4$), 274 ($6.5.10^4$)

Melting point: 223 ^oC

Rf: 0.7 (acetonitrile, neutral alumina)

3.10.4. Pd-AB2thiophene (3.32)

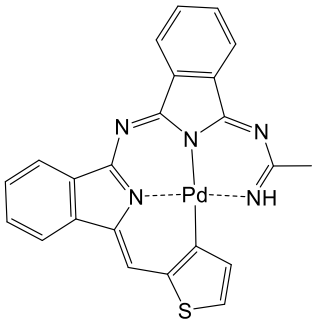

AB2thiophene dimer **(3.19)** (50 mg, 0.14 mmol) was dissolved in dry acetonitrile (100 ml). Palladium (II) chloride (25 mg, 0.14 mmol) was added, and the reaction was stirred at room temperature for 7 days. The solvent was removed under vacuum via a rotary evaporator, and the residual was separated by column chromatography on neutral alumina, eluting with acetonitrile. The solvent evaporated, and the complex was crystallized from a mixture of DCM and hexane to give a purple solid (61 mg, 87%).

Chemical Formula and molecular weight: $C_{23}H_{15}N_5PdS$, 499.89 g.mol^{-1}

^{1}H NMR (400 MHz, Methylene Chloride-d_2) δ 8.88 (s, 1H), 8.27 (d, *J* = 7.5 Hz, 1H), 8.15 (d, *J* = 7.2 Hz, 1H), 7.97 (d, *J* = 7.2 Hz, 1H), 7.89 (d, *J* = 7.6 Hz, 1H), 7.81 (s, 1H), 7.74 (d, *J* = 4.9 Hz, 1H), 7.68 – 7.57 (m, 4H), 7.54 (td, *J* = 7.5, 1.0 Hz, 1H), 2.77 (s, 3H).

MS (MALDI-TOF): m/z = 499.29 $[M]^+$

UV-Vis.: λ_{max} (nm) (Ɛ ($M^{-1}.cm^{-1}$)) = 599 ($0.9.10^4$), 341. ($2.2.10^4$), 258 ($4.9.10^4$)

Melting point: >300 ºC

Rf: 0.7 (acetonitrile, neutral alumina)

3.10.5. Pd-AB3thiophene (3.33)

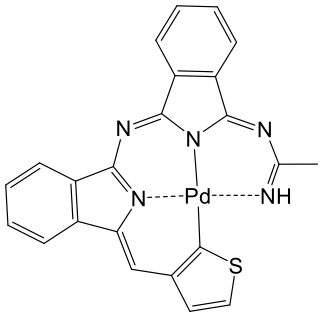

AB3thiophene dimer **(3.20)** (50 mg, 0.14 mmol) was dissolved in dry acetonitrile (100 ml). Palladium (II) chloride (25 mg, 0.14 mmol) was added, and the reaction was stirred at room temperature for 7 days. The solvent was removed under vacuum via a rotary evaporator, and the residual was separated by column chromatography on neutral alumina, eluting with acetonitrile. The solvent evaporated, and the complex was crystallized from a mixture of DCM and hexane to give a purple solid (60 mg, 85%).

Chemical Formula and molecular weight: $C_{23}H_{15}N_5PdS$, 499.89 g.mol^{-1}

^{1}H NMR (400 MHz, Methylene Chloride-d_2) δ 9.06 (s, 1H), 8.26 (td, *J* = 7.6, 1.1 Hz, 1H), 8.14 (d, *J* = 6.9 Hz, 1H), 8.00 – 7.96 (m, 1H), 7.92 (d, *J* = 7.7 Hz, 1H), 7.77 (s, 1H), 7.68 – 7.58 (m, 3H), 7.53 (td, *J* = 7.4, 1.0 Hz, 1H), 7.47 (q, *J* = 4.9 Hz, 2H), 2.75 (s, 3H).

MS (MALDI-TOF): m/z = 498.83 $[M]^+$

UV-Vis.: λ_{max} (nm) (Ɛ ($M^{-1}.cm^{-1}$)) = 557 ($0.4.10^4$), 381. ($1.1.10^4$), 250 ($2.3.10^4$)

Melting point: >300 ºC

Rf: 0.7 (acetonitrile, neutral alumina)

3.10.6. Pd-ABferrocene (3.34)

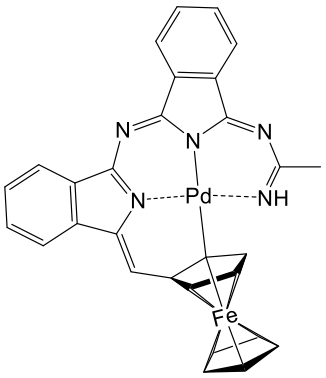

AB*ferrocene* dimer **(3.21)** (50 mg, 0.11 mmol) was dissolved in dry acetonitrile (100 ml). Palladium (II) chloride (19 mg, 0.11 mmol) was added, and the reaction was stirred at room temperature for 3 days. The solvent was removed under vacuum via a rotary evaporator, and the residual was separated by column chromatography on neutral alumina, eluting with acetonitrile. The solvent evaporated, and the complex was crystallized from a mixture of DCM and hexane to give a purple solid (38 mg, 58%).

Chemical Formula and molecular weight: $C_{29}H_{21}FeN_5Pd$, 601.79 g.mol^{-1}

^{1}H NMR (400 MHz, Acetone-d_6) δ 9.26 (s, 1H), 8.37 – 8.30 (m, 2H), 8.16 – 8.12 (m, 1H), 8.09 (dt, *J* = 7.7, 0.9 Hz, 1H), 8.02 (s, 1H), 7.85 – 7.73 (m, 2H), 7.67 (td, *J* = 7.4, 1.1 Hz, 1H), 7.57 (td, *J* = 6.5, 0.8 Hz, 1H), 5.50 (d, *J* = 2.4 Hz, 1H), 4.82 (dd, *J* = 2.4, 1.1 Hz, 1H), 4.72 (t, *J* = 2.4 Hz, 1H), 4.06 (s, 5H), 2.85 (s, 3H).

MS (MALDI-TOF): m/z = 600.98 $[M]^+$

UV-Vis.: λ_{max} (nm) (Ɛ ($M^{-1}.cm^{-1}$)) = 490 ($0.9.10^4$), 335. ($2.1.10^4$), 257 ($4.3.10^4$)

Melting point: >300 ºC

Rf: 0.7 (acetonitrile, neutral alumina)

3.10.7. Pd-*tert*AB-benzonitrile (2.35)

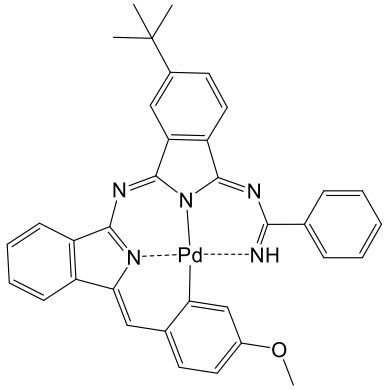

***tert*AB** dimer **(3.17)** (50 mg, 0.12 mmol) was dissolved in dry acetonitrile (100 ml). Palladium (II) chloride (20 mg, 0.12 mmol) was added, and the reaction was stirred at room temperature for 7 days. The solvent was removed under vacuum via a rotary evaporator, and the residual was separated by column chromatography on neutral alumina, eluting with acetonitrile. The solvent evaporated, and the complex was crystallized from a mixture of DCM and hexane to give a purple solid (62 mg, 84%).

Chemical Formula and molecular weight: $C_{35}H_{29}N_5OPd$, 642.07 $g.mol^{-1}$

^{1}H NMR (400 MHz, Methylene Chloride-d_2) δ 8.91 (s, 1H), 8.28 – 8.21 (m, 3H), 8.19 (d, *J* = 7.6 Hz, 1H), 8.03 – 7.96 (m, 1H), 7.87 (d, *J* = 7.8 Hz, 1H), 7.71 (dt, *J* = 7.9, 1.6 Hz, 1H), 7.67 – 7.56 (m, 4H), 7.53 (d, *J* = 6.2 Hz, 1H), 7.50 (d, *J* = 8.0 Hz, 2H), 7.34 (d, *J* = 2.4 Hz, 1H), 6.90 (dt, *J* = 8.4, 1.9 Hz, 1H), 3.93 (s, 3H), 1.55 (s, 9H).

MS (MALDI-TOF): m/z = 641.35 $[M]^+$

UV-Vis.: λ_{max} (nm) (Ɛ ($M^{-1}.cm^{-1}$)) = 550 ($1.7.10^4$), 347. (4.10^4), 267 ($8.3.10^4$)

Melting point: 220 ^{o}C

Rf: 0.7 (acetonitrile, neutral alumina)

References

(1) Moss, G. Nomenclature of tetrapyrroles (Recommendations 1986). *Pure and Applied Chemistry* **1987**, *59* (6), 779-832.

(2) Al-Sheikh-Ali, A.; Cameron, K. S.; Cameron, T. S.; Robertson, K. N.; Thompson, A. Highly diastereoselective templated complexation of dipyrromethenes. *Organic letters* **2005**, *7* (21), 4773-4775.

(3) Porter, C. R. 74. The stereochemistry of metallic derivatives of pyrromethenes. *Journal of the Chemical Society (Resumed)* **1938**, 368-372.

(4) Thoresen, L. H.; Kim, H.; Welch, M. B.; Burghart, A.; Burgess, K. Synthesis of 3, 5-Diaryl-4, 4-difluoro-4-bora-3a, 4a-diaza-s-indacene (BODIPY®) dyes. *Synlett* **1998**, *1998* (11), 1276-1278.

(5) Wood, T. E.; Thompson, A. Advances in the chemistry of dipyrrins and their complexes. *Chemical reviews* **2007**, *107* (5), 1831-1861.

(6) Longo, F. R.; Thorne, E. J.; Adler, A. D.; Dym, S. Notes on the synthesis of porphin. *Journal of Heterocyclic Chemistry* **1975**, *12* (6), 1305-1309.

(7) Piloty, O.; Stock, J.; Dormann, E. Zur Konstitution des Blutfarbstoffs; Dipyrrylmethan-Derivate mit Farbstoff-Charakter. *Berichte der deutschen chemischen Gesellschaft* **1914**, *47* (1), 400-406.

(8) Fischer, H.; Orth, H. Die Chemie des Pyrrols, I; Akad. *Verlagsges: Leipzig, Germany* **1937**.

(9) Loudet, A.; Burgess, K. BODIPY dyes and their derivatives: syntheses and spectroscopic properties. *Chemical reviews* **2007**, *107* (11), 4891-4932.

(10) Singh, R. S.; Paitandi, R. P.; Gupta, R. K.; Pandey, D. S. Recent developments in metal dipyrrin complexes: Design, synthesis, and applications. *Coordination Chemistry Reviews* **2020**, *414*, 213269.

(11) Kowada, T.; Maeda, H.; Kikuchi, K. BODIPY-based probes for the fluorescence imaging of biomolecules in living cells. *Chemical Society Reviews* **2015**, *44* (14), 4953-4972.

(12) Boens, N.; Leen, V.; Dehaen, W. Fluorescent indicators based on BODIPY. *Chemical Society Reviews* **2012**, *41* (3), 1130-1172.

(13) King, E. R.; Betley, T. A. C− H bond amination from a ferrous dipyrromethene complex. *Inorganic chemistry* **2009**, *48* (6), 2361-2363.

(14) King, E. R.; Hennessy, E. T.; Betley, T. A. Catalytic C− H bond amination from high-spin iron imido complexes. *Journal of the American Chemical Society* **2011**, *133* (13), 4917-4923.

(15) Murphy, D. L.; Malachowski, M. R.; Campana, C. F.; Cohen, S. M. A chiral, heterometallic metal-organic framework derived from a tris (chelate) coordination complex. *Chemical communications* **2005**, (44), 5506-5508.

(16) Baudron, S. A. Dipyrrin based homo-and hetero-metallic infinite architectures. *CrystEngComm* **2010**, *12* (8), 2288-2295.

(17) Béziau, A.; Baudron, S. A.; Hosseini, M. W. Heterometallic coordination polymers incorporating dipyrrin based heteroleptic copper and cobalt complexes: to Ag–π or not? *Dalton Transactions* **2012**, *41* (24), 7227-7234.

(18) Béziau, A.; Baudron, S. A.; Guenet, A.; Hosseini, M. W. Luminescent Coordination Polymers Based on Self-Assembled Cadmium Dipyrrin Complexes. *Chemistry–A European Journal* **2013**, *19* (9), 3215-3223.

(19) Do, L.; Halper, S. R.; Cohen, S. M. Helical coordination polymers and cyclic dimers formed from heteroleptic thioether-dipyrrinato copper (ii) complexes. *Chemical communications* **2004**, (23), 2662-2663.

(20) King, E. R.; Sazama, G. T.; Betley, T. A. Co (III) imidos exhibiting spin crossover and C–H bond activation. *Journal of the American Chemical Society* **2012**, *134* (43), 17858-17861.

(21) Scharf, A. B.; Betley, T. A. Electronic perturbations of iron dipyrrinato complexes via ligand β-halogenation and meso-fluoroarylation. *Inorganic Chemistry* **2011**, *50* (14), 6837-6845.

(22) Filatov, M. A.; Lebedev, A. Y.; Mukhin, S. N.; Vinogradov, S. A.; Cheprakov, A. V. π-Extended dipyrrins capable of highly fluorogenic complexation with metal ions. *Journal of the American Chemical Society* **2010**, *132* (28), 9552-9554.

(23) Kamkaew, A.; Lim, S. H.; Lee, H. B.; Kiew, L. V.; Chung, L. Y.; Burgess, K. BODIPY dyes in photodynamic therapy. *Chemical Society Reviews* **2013**, *42* (1), 77-88.

(24) Cohen, S. M.; Halper, S. R. Dipyrromethene complexes of iron. *Inorganica chimica acta* **2002**, *341*, 12-16.

(25) Stork, J. R.; Thoi, V. S.; Cohen, S. M. Rare examples of transition-metal− main-group metal heterometallic metal− organic frameworks from gallium and indium dipyrrinato complexes and silver salts: synthesis and framework variability. *Inorganic chemistry* **2007**, *46* (26), 11213-11223.

(26) Yu, L.; Muthukumaran, K.; Sazanovich, I. V.; Kirmaier, C.; Hindin, E.; Diers, J. R.; Boyle, P. D.; Bocian, D. F.; Holten, D.; Lindsey, J. S. Excited-state energy-transfer dynamics in self-assembled triads composed of two porphyrins and an intervening bis (dipyrrinato) metal complex. *Inorganic chemistry* **2003**, *42* (21), 6629-6647.

(27) Arsenault, G.; Bullock, E.; MacDonald, S. Pyrromethanes and porphyrins therefrom1. *Journal of the American Chemical Society* **1960**, *82* (16), 4384-4389.

(28) Dolphin, D. The Porphyrins Academic Press. *New York* **1978**.

(29) Lash, T. D.; Chen, S. Syntheses of per-15N labeled etioporphyrins I–IV and a related tetrahydrobenzoporphyrin for applications in organic geochemistry and vibrational spectroscopy. *Tetrahedron* **2005**, *61* (49), 11577-11600.

(30) Bari, S. E.; Iturraspe, J.; Frydman, B. Synthesis of biliverdins with stable extended conformations. Part II. *Tetrahedron* **1995**, *51* (8), 2255-2266.

(31) Brückner, C.; Karunaratne, V.; Rettig, S. J.; Dolphin, D. Synthesis of meso-phenyl-4, 6-dipyrrins, preparation of their Cu (II), Ni (II), and Zn (II) chelates, and structural characterization of bis [meso-phenyl-4, 6-dipyrrinato] Ni (II). *Canadian journal of chemistry* **1996**, *74* (11), 2182-2193.

(32) Wagner, R. W.; Lindsey, J. S. A molecular photonic wire. *Journal of the American Chemical Society* **1994**, *116* (21), 9759-9760.

(33) Gryko, D. T.; Gryko, D.; Lee, C.-H. 5-Substituted dipyrranes: synthesis and reactivity. *Chemical Society Reviews* **2012**, *41* (10), 3780-3789.

(34) Littler, B. J.; Miller, M. A.; Hung, C.-H.; Wagner, R. W.; O'Shea, D. F.; Boyle, P. D.; Lindsey, J. S. Refined synthesis of 5-substituted dipyrromethanes. *The Journal of Organic Chemistry* **1999**, *64* (4), 1391-1396.

(35) Jean-Gérard, L.; Vasseur, W.; Scherninski, F.; Andrioletti, B. Recent advances in the synthesis of [a]-benzo-fused BODIPY fluorophores. *Chemical Communications* **2018**, *54* (92), 12914-12929.

(36) Treibs, A.; Kreuzer, F. H. Difluorboryl-komplexe von di-und tripyrrylmethenen. *Justus Liebigs Annalen der Chemie* **1968**, *718* (1), 208-223.

(37) Haugland, H. C. K. a. R. P. 1995.

(38) Knorr, L. Synthese von Furfuranderivaten aus dem Diacetbernsteinsäureester. *Berichte der deutschen chemischen Gesellschaft* **1884**, *17* (2), 2863-2870.

(39) Paal, C. Ueber die Derivate des Acetophenonacetessigesters und des Acetonylacetessigesters. *Berichte der deutschen chemischen Gesellschaft* **1884**, *17* (2), 2756-2767.

(40) Kotali, A.; Tsoungas, P. G. Oxidation of N-Aroylhydrazones of o-hydroxyaryl ketones withlead (IV) acetate: A facile route to aromatic o-diketones. *Tetrahedron letters* **1987**, *28* (37), 4321-4322.

(41) Kubo, Y.; Minowa, Y.; Shoda, T.; Takeshita, K. Synthesis of a new type of dibenzopyrromethene–boron complex with near-infrared absorption property. *Tetrahedron Letters* **2010**, *51* (12), 1600-1602.

(42) Yamazawa, S.; Nakashima, M.; Suda, Y.; Nishiyabu, R.; Kubo, Y. 2, 3-naphtho-fused BODIPYs as near-infrared absorbing dyes. *The Journal of Organic Chemistry* **2016**, *81* (3), 1310-1315.

(43) Kubo, Y.; Watanabe, K.; Nishiyabu, R.; Hata, R.; Murakami, A.; Shoda, T.; Ota, H. Near-infrared absorbing boron-dibenzopyrromethenes that serve as light-harvesting sensitizers for polymeric solar cells. *Organic letters* **2011**, *13* (17), 4574-4577.

(44) Lash, T. D.; Thompson, M. L.; Werner, T. M.; Spence, J. D. Synthesis of novel pyrrolic compounds from nitroarenes and isocyanoacetates using a phosphazene superbase. *Synlett* **2000**, *2000* (02), 213-216.

(45) Ono, N.; Hironaga, H.; Ono, K.; Kaneko, S.; Murashima, T.; Ueda, T.; Tsukamura, C.; Ogawa, T. A new synthesis of pyrroles and porphyrins fused with aromatic rings. *Journal of the Chemical Society, Perkin Transactions 1* **1996**, (5), 417-423.

(46) Filatov, M. A.; Cheprakov, A. V.; Beletskaya, I. P. A Facile and Reliable Method for the Synthesis of Tetrabenzoporphyrin from 4, 7-Dihydroisoindole. Wiley Online Library: 2007.

(47) Descalzo, A. B.; Xu, H.-J.; Xue, Z.-L.; Hoffmann, K.; Shen, Z.; Weller, M. G.; You, X.-Z.; Rurack, K. Phenanthrene-fused boron− dipyrromethenes as bright long-wavelength fluorophores. *Organic letters* **2008**, *10* (8), 1581-1584.

(48) Novak, B. H.; Lash, T. D. Porphyrins with exocyclic rings. 11.1 Synthesis and characterization of phenanthroporphyrins, a new class of modified porphyrin chromophores. *The Journal of Organic Chemistry* **1998**, *63* (12), 3998-4010.

(49) Ito, S.; Murashima, T.; Ono, N. A new synthesis of pyrroles fused with polycyclic skeletons. *Journal of the Chemical Society, Perkin Transactions 1* **1997**, (21), 3161-3166.

(50) Wada, M.; Ito, S.; Uno, H.; Murashima, T.; Ono, N.; Urano, T.; Urano, Y. Synthesis and optical properties of a new class of pyrromethene–BF2 complexes fused with rigid bicyclo rings and benzo derivatives. *Tetrahedron Letters* **2001**, *42* (38), 6711-6713.

(51) Tomimori, Y.; Okujima, T.; Yano, T.; Mori, S.; Ono, N.; Yamada, H.; Uno, H. Synthesis of π-expanded O-chelated boron–dipyrromethene as an NIR dye. *Tetrahedron* **2011**, *67* (18), 3187-3193.

(52) von Dobeneck, H.; Reinhard, H.; Deubel, H.; Wolkenstein, D. Isoindole, I. *Chemische Berichte* **1969**, *102* (4), 1357-1362.

(53) Bonnett, R.; McManus, K. A. Approaches to the stepwise synthesis of benzoporphyrins and phthalocyanines. Part 1. Synthesis of opp-dibenzoporphyrins (dibenzo [g, q] porphyrins). *Journal of the Chemical Society, Perkin Transactions 1* **1996**, (20), 2461-2466.

(54) Jiao, L.; Yu, C.; Liu, M.; Wu, Y.; Cong, K.; Meng, T.; Wang, Y.; Hao, E. Synthesis and functionalization of asymmetrical benzo-fused BODIPY dyes. *The Journal of Organic Chemistry* **2010**, *75* (17), 6035-6038.

(55) Yu, C.; Xu, Y.; Jiao, L.; Zhou, J.; Wang, Z.; Hao, E. Isoindole-BODIPY Dyes as Red to Near-Infrared Fluorophores. *Chemistry–A European Journal* **2012**, *18* (21), 6437-6442.

(56) Yu, C.; Jiao, L.; Tan, X.; Wang, J.; Xu, Y.; Wu, Y.; Yang, G.; Wang, Z.; Hao, E. Straightforward Acid-Catalyzed Synthesis of Pyrrolyldipyrromethenes. *Angewandte Chemie-International Edition* **2012**, *51* (31), 7688.

(57) Maeda, C.; Todaka, T.; Ema, T. Carbazole-based boron dipyrromethenes (BODIPYs): facile synthesis, structures, and fine-tunable optical properties. *Organic letters* **2015**, *17* (12), 3090-3093.

(58) Wang, J.; Wu, Q.; Xu, Y.; Yu, C.; Wei, Y.; Mu, X.; Hao, E.; Jiao, L. Synthesis, structure and photophysical properties of near-infrared 3, 5-diarylbenzoBODIPY fluorophores. *RSC advances* **2016**, *6* (57), 52180-52188.

(59) Killoran, J.; Allen, L.; Gallagher, J. F.; Gallagher, W. M.; Donal, F. Synthesis of BF 2 chelates of tetraarylazadipyrromethenes and evidence for their photodynamic therapeutic behaviour. *Chemical Communications* **2002**, (17), 1862-1863.

(60) Donyagina, V. F.; Shimizu, S.; Kobayashi, N.; Lukyanets, E. A. Synthesis of N, N-difluoroboryl complexes of 3, 3′-diarylazadiisoindolylmethenes. *Tetrahedron Letters* **2008**, *49* (42), 6152-6154.

(61) Rogers, M. A. T. 156. 2: 4-Diarylpyrroles. Part I. Synthesis of 2: 4-diarylpyrroles and 2: 2′: 4: 4′-tetra-arylazadipyrromethines. *Journal of the Chemical Society (Resumed)* **1943**, 590-596.

(62) Davies, W.; Rogers, M. A. 46. 2: 4-Diarylpyrroles. Part IV. The formation of acylated 5-amino-2: 4-diphenylpyrroles from β-benzoly-α-phenylpropionitrile and some notes on the Leuckart reaction. *Journal of the Chemical Society (Resumed)* **1944**, 126-131.

(63) Gorman, A.; Killoran, J.; O'Shea, C.; Kenna, T.; Gallagher, W. M.; O'Shea, D. F. In vitro demonstration of the heavy-atom effect for photodynamic therapy. *Journal of the American Chemical Society* **2004**, *126* (34), 10619-10631.

(64) Ge, Y.; O'Shea, D. F. Azadipyrromethenes: from traditional dye chemistry to leading edge applications. *Chemical Society Reviews* **2016**, *45* (14), 3846-3864.

(65) Hall, M. J.; McDonnell, S. O.; Killoran, J.; O'Shea, D. F. A modular synthesis of unsymmetrical tetraarylazadipyrromethenes. *The Journal of Organic Chemistry* **2005**, *70* (14), 5571-5578.

(66) Bredereck, H.; Vollmann, H. W. Synthesen in der heterocyclischen Reihe, XV. Über 1-[3-Aryl-isoindolyl-(1)-imino]-3-aryl-1H-isoindole. *Chemische Berichte* **1972**, *105* (7), 2271-2283.

(67) Zhao, W.; Carreira, E. M. Conformationally restricted aza-bodipy: a highly fluorescent, stable, near-infrared-absorbing dye. *Angewandte Chemie* **2005**, *117* (11), 1705-1707.

(68) Wang, J.; Yu, C.; Hao, E.; Jiao, L. Conformationally restricted and ring-fused aza-BODIPYs as promising near infrared absorbing and emitting dyes. *Coordination Chemistry Reviews* **2022**, *470*, 214709.

(69) Herold, D. A.; Rieke, R. D. Synthesis of 1, 2-disubstituted acenaphthylenes. *The Journal of Organic Chemistry* **1979**, *44* (8), 1359-1361.

(70) Majumdar, P.; Mack, J.; Nyokong, T. Synthesis, characterization and photophysical properties of an acenaphthalene fused-ring-expanded NIR absorbing aza-BODIPY dye. *RSC advances* **2015**, *5* (95), 78253-78258.

(71) Krizan, T. D.; Martin, J. Directed ortho lithiation of isophthalonitrile. New methodology for the synthesis of 1, 2, 3-trisubstituted benzenes. *The Journal of Organic Chemistry* **1982**, *47* (13), 2681-2682.

(72) Mckeown, G. R.; Manion, J. G.; Lough, A. J.; Seferos, D. S. Synthesis of fused-ring aza-dipyrromethenes from aromatic nitriles. *Chemical Communications* **2018**, *54* (64), 8893-8896.

(73) Zheng, W.; Wang, B. B.; Li, C. H.; Zhang, J. X.; Wan, C. Z.; Huang, J. H.; Liu, J.; Shen, Z.; You, X. Z. Asymmetric Donor–π-Acceptor-Type Benzo-Fused Aza-BODIPYs: Facile Synthesis and Colorimetric Properties. *Angewandte Chemie* **2015**, *127* (31), 9198-9202.

(74) Hellal, M.; Cuny, G. D. Microwave assisted copper-free Sonogashira coupling/5-exo-dig cycloisomerization domino reaction: access to 3-(phenylmethylene) isoindolin-1-ones and related heterocycles. *Tetrahedron letters* **2011**, *52* (42), 5508-5511.

(75) Díaz-Moscoso, A.; Emond, E.; Hughes, D. L.; Tizzard, G. J.; Coles, S. J.; Cammidge, A. N. Synthesis of a class of core-modified aza-BODIPY derivatives. *The Journal of Organic Chemistry* **2014**, *79* (18), 8932-8936.

(76) Hsieh, A.; Rogers, C.; West, B. Synthesis, properties and long range 203,205 Tl-13C couplings in the 13C NMR spectrum of an unusual dimethylthallium (III) complex of 4, 4'-Diethoxycarbonyl-3, 3', 5, 5'-tetramethyldipyrromethene. *Australian Journal of Chemistry* **1976**, *29* (1), 49-54.

(77) March, F. C.; Couch, D.; Emerson, K.; Fergusson, J.; Robinson, W. T. Dipyrromethene complexes of transition metals. Part II. Stereochemistry of complexes of cobalt (II), nickel (II), copper (II), zinc (II), cadmium (II), mercury (II), and palladium (II) and crystal structure analysis of the palladium complex. *Journal of the Chemical Society A: Inorganic, Physical, Theoretical* **1971**, 440-448.

(78) Murakami, Y.; Matsuda, Y.; Sakata, K.; Harada, K. Transition-metal Complexes of Pyrrole Pigments. IX. Divalent and Trivalent Iron Chelates of Dipyrromethenes. *Bulletin of the Chemical Society of Japan* **1974**, *47* (2), 458-462.

(79) Ruffin, H.; Baudron, S. A.; Salazar-Mendoza, D.; Hosseini, M. W. A Silver Bite: Crystalline Heterometallic Architectures Based on Ag–π Interactions with a Bis-Dipyrrin Zinc Helicate. *Chemistry–A European Journal* **2014**, *20* (9), 2449-2453.

(80) Béziau, A.; Baudron, S. A.; Pogozhev, D.; Fluck, A.; Hosseini, M. W. Stepwise construction of grid-type Cu (II)–Cd (II) heterometallic MOFs based on an imidazole-appended dipyrrin ligand. *Chemical Communications* **2012**, *48* (83), 10313-10315.

(81) Pogozhev, D.; Baudron, S. A.; Hosseini, M. W. Combination of hydrogen and coordination bonding for the construction of one-dimensional networks based on a 7-azaindole appended dipyrrin. *CrystEngComm* **2010**, *12* (7), 2238-2244.

(82) Brückner, C.; Zhang, Y.; Rettig, S. J.; Dolphin, D. Synthesis, derivatization and structural characterization of octahedral tris (5-phenyl-4, 6-dipyrrinato) complexes of cobalt (III) and iron (III). *Inorganica chimica acta* **1997**, *263* (1-2), 279-286.

(83) Halper, S. R.; Cohen, S. M. Synthesis, Structure, and Spectroscopy of Phenylacetylenylene Rods Incorporating meso-Substituted Dipyrrin Ligands. *Chemistry–A European Journal* **2003**, *9* (19), 4661-4669.

(84) Thoi, V. S.; Stork, J. R.; Magde, D.; Cohen, S. M. Luminescent dipyrrinato complexes of trivalent group 13 metal ions. *Inorganic chemistry* **2006**, *45* (26), 10688-10697.

(85) Miao, Q.; Shin, J.-Y.; Patrick, B. O.; Dolphin, D. Self-assembly of oligomeric linear dipyrromethene metal complexes. *Chemical communications* **2009**, (18), 2541-2543.

(86) Guseva, G.; Antina, E.; Berezin, M.; V'yugin, A. Influence of metal cation on chromophore properties of complexes of some d metals with α, α-dipyrrolylmethene. *Russian journal of general chemistry* **2004**, *74*, 1282-1285.

(87) Hall, M. J.; Allen, L. T.; O'Shea, D. F. PET modulated fluorescent sensing from the BF 2 chelated azadipyrromethene platform. *Organic & Biomolecular Chemistry* **2006**, *4* (5), 776-780.

(88) Coskun, A.; Yilmaz, M. D.; Akkaya, E. U. Bis (2-pyridyl)-substituted boratriazaindacene as an NIR-emitting chemosensor for Hg (II). *Organic Letters* **2007**, *9* (4), 607-609.

(89) Teets, T. S.; Partyka, D. V.; Esswein, A. J.; Updegraff, J. B.; Zeller, M.; Hunter, A. D.; Gray, T. G. Luminescent, three-coordinate azadipyrromethene complexes of d10 copper, silver, and gold. *Inorganic chemistry* **2007**, *46* (16), 6218-6220.

(90) Teets, T. S.; Updegraff III, J. B.; Esswein, A. J.; Gray, T. G. Three-coordinate, phosphine-ligated azadipyrromethene complexes of univalent group 11 metals. *Inorganic chemistry* **2009**, *48* (17), 8134-8144.

(91) Teets, T. S.; Partyka, D. V.; Updegraff Iii, J. B.; Gray, T. G. Homoleptic, four-coordinate azadipyrromethene complexes of d10 zinc and mercury. *Inorganic chemistry* **2008**, *47* (7), 2338-2346.

(92) Partyka, D. V.; Deligonul, N.; Washington, M. P.; Gray, T. G. fac-Tricarbonyl rhenium (I) azadipyrromethene complexes. *Organometallics* **2009**, *28* (20), 5837-5840.

(93) Madhu, S.; Kumar, S.; Chatterjee, T.; Ravikanth, M. Synthesis, X-ray structure, spectral and electrochemical properties of a β-meso covalently linked BODIPY–Ru (II) dipyrrin complex. *New Journal of Chemistry* **2014**, *38* (11), 5551-5558.

(94) Bronner, C.; Baudron, S. A.; Hosseini, M. W.; Strassert, C. A.; Guenet, A.; De Cola, L. Dipyrrin based luminescent cyclometallated palladium and platinum complexes. *Dalton Transactions* **2010**, *39* (1), 180-184.

(95) Gresser, R.; Hoyer, A.; Hummert, M.; Hartmann, H.; Leo, K.; Riede, M. Homoleptic Co (II), Ni (II), Cu (II), Zn (II) and Hg (II) complexes of bis-(phenyl)-diisoindol-aza-methene. *Dalton Transactions* **2011**, *40* (14), 3476-3483.

(96) Bessette, A.; Ferreira, J. G.; Giguere, M.; Belanger, F.; Desilets, D.; Hanan, G. S. Azadipyrromethene dye derivatives in coordination chemistry: the structure–property relationship in homoleptic metal (II) complexes. *Inorganic chemistry* **2012**, *51* (22), 12132-12141.

(97) Senevirathna, W.; Sauvé, G. Introducing 3D conjugated acceptors with intense red absorption: homoleptic metal (ii) complexes of di (phenylacetylene) azadipyrromethene. *Journal of Materials Chemistry C* **2013**, *1* (40), 6684-6694.

(98) Deligonul, N.; Gray, T. G. Azadipyrromethene complexes of d8 metal centers: Rhodium (I), iridium (I), palladium (II), and platinum (II). *Inorganic Chemistry* **2013**, *52* (22), 13048-13057.

(99) Deligonul, N.; Browne, A. R.; Golen, J. A.; Rheingold, A. L.; Gray, T. G. Cyclometalated iridium (III) complexes of azadipyrromethene chromophores. *Organometallics* **2014**, *33* (3), 637-643.

(100) Nazeeruddin, M. K.; Pechy, P.; Renouard, T.; Zakeeruddin, S. M.; Humphry-Baker, R.; Comte, P.; Liska, P.; Cevey, L.; Costa, E.; Shklover, V. Engineering of efficient panchromatic sensitizers for nanocrystalline TiO2-based solar cells. *Journal of the American Chemical Society* **2001**, *123* (8), 1613-1624.

(101) Smalley, S. J.; Waterland, M. R.; Telfer, S. G. Heteroleptic dipyrrin/bipyridine complexes of ruthenium (II). *Inorganic Chemistry* **2009**, *48* (1), 13-15.

(102) Weston, M.; Reade, T. J.; Handrup, K.; Champness, N. R.; O'Shea, J. N. Adsorption of dipyrrin-based dye complexes on a rutile TiO2 (110) surface. *The Journal of Physical Chemistry C* **2012**, *116* (34), 18184-18192.

(103) Hewat, T. E.; Yellowlees, L. J.; Robertson, N. Neutral copper (I) dipyrrin complexes and their use as sensitizers in dye-sensitized solar cells. *Dalton Transactions* **2014**, *43* (10), 4127-4136.

(104) Mei, Y.; Bentley, P. A. A ratiometric fluorescent sensor for Zn2+ based on internal charge transfer (ICT). *Bioorganic & medicinal chemistry letters* **2006**, *16* (12), 3131-3134.

(105) Sutton, J. M.; Rogerson, E.; Wilson, C. J.; Sparke, A. E.; Archibald, S. J.; Boyle, R. W. Synthesis and structural characterisation of novel bimetallic dipyrromethene complexes: rotational locking of the 5-aryl group. *Chemical communications* **2004**, (11), 1328-1329.

(106) Ding, Y.; Xie, Y.; Li, X.; Hill, J. P.; Zhang, W.; Zhu, W. Selective and sensitive "turn-on" fluorescent Zn 2+ sensors based on di-and tripyrrins with readily modulated emission wavelengths. *Chemical Communications* **2011**, *47* (19), 5431-5433.

(107) Ducloiset, C.; Jouin, P.; Paredes, E.; Guillot, R.; Sircoglou, M.; Orio, M.; Leibl, W.; Aukauloo, A. Monoanionic dipyrrin–pyridine ligands: synthesis, structure and photophysical properties. *European Journal of Inorganic Chemistry* **2015**, *2015* (32), 5405-5410.

(108) Guski, S.; Albrecht, M.; Willms, T.; Nabeshima, T.; Pan, F.; Puttreddy, R.; Rissanen, K. Extended dipyrrin ligands: candidates for optical metal ion detection under competitive conditions. *Chemical Communications* **2017**, *53* (22), 3213-3215.

(109) Baudron, S. A. Luminescent dipyrrin based metal complexes. *Dalton Transactions* **2013**, *42* (21), 7498-7509.

(110) Maeda, H.; Bando, Y. Recent progress in research on anion-responsive pyrrole-based π-conjugated acyclic molecules. *Chemical Communications* **2013**, *49* (39), 4100-4113.

(111) Wang, Q.; Xie, Y.; Ding, Y.; Li, X.; Zhu, W. Colorimetric fluoride sensors based on deprotonation of pyrrole–hemiquinone compounds. *Chemical communications* **2010**, *46* (21), 3669-3671.

(112) Deliomeroglu, M. K.; Lynch, V. M.; Sessler, J. L. Conformationally switchable non-cyclic tetrapyrrole receptors: Synthesis of tetrakis (1 H-pyrrole-2-carbaldehyde) derivatives and their anion binding properties. *Chemical Communications* **2014**, *50* (80), 11863-11866.

(113) Wojaczyński, J.; Maciołek, J.; Chmielewski, P. J. Dipyrrin-Bis (N-Confused Porphyrin) Conjugate: Synthesis, Synergetic Ligation and Chirality Sensing. *Chemistry–An Asian Journal* **2017**, *12* (6), 643-647.

(114) Artigau, M.; Bonnet, A.; Ladeira, S.; Hoffmann, P.; Vigroux, A. A free-base dipyrrin capable of forming extended architectures comparable to those of its metal (ii) complex counterparts. *CrystEngComm* **2011**, *13* (23), 7149-7152.

(115) Halper, S. R.; Malachowski, M. R.; Delaney, H. M.; Cohen, S. M. Heteroleptic copper dipyrromethene complexes: synthesis, structure, and coordination polymers. *Inorganic chemistry* **2004**, *43* (4), 1242-1249.

(116) Pogozhev, D.; Baudron, S. A.; Hosseini, M. W. Assembly of heteroleptic copper complexes with silver salts: from discrete trinuclear complexes to infinite networks. *Inorganic chemistry* **2010**, *49* (1), 331-338.

(117) Béziau, A.; Baudron, S. A.; Rasoloarison, D.; Hosseini, M. W. Rigid yet flexible heteroleptic Co (III) dipyrrin complexes for the construction of heterometallic 1-and 2-D coordination polymers. *CrystEngComm* **2014**, *16* (23), 4973-4980.

(118) Baudron, S. A. Luminescent metal–organic frameworks based on dipyrromethene metal complexes and BODIPYs. *CrystEngComm* **2016**, *18* (25), 4671-4680.

(119) Bronner, C.; Baudron, S. A.; Hosseini, M. W. Carboxylic acid appended dipyrrin for the formation of a hexanuclear iridium/copper paddlewheel complex. *Inorganic chemistry* **2010**, *49* (19), 8659-8661.

(120) Rio, Y.; Sánchez-García, D.; Seitz, W.; Torres, T.; Sessler, J. L.; Guldi, D. M. A Bisfullerene–Bis (dipyrrinato) zinc Complex: Electronic Coupling and Charge Separation in an Easy-to-Assemble Synthetic System. *Chemistry–A European Journal* **2009**, *15* (16), 3956-3959.

(121) Matsuoka, R.; Toyoda, R.; Sakamoto, R.; Tsuchiya, M.; Hoshiko, K.; Nagayama, T.; Nonoguchi, Y.; Sugimoto, K.; Nishibori, E.; Kawai, T. Bis (dipyrrinato) metal (II) coordination polymers: crystallization, exfoliation into single wires, and electric conversion ability. *Chemical Science* **2015**, *6* (5), 2853-2858.

(122) Sakamoto, R.; Hoshiko, K.; Liu, Q.; Yagi, T.; Nagayama, T.; Kusaka, S.; Tsuchiya, M.; Kitagawa, Y.; Wong, W.-Y.; Nishihara, H. A photofunctional bottom-up bis (dipyrrinato) zinc (II) complex nanosheet. *Nature communications* **2015**, *6* (1), 6713.

(123) Singh, S. K.; Pandey, D. S. Multifaceted half-sandwich arene–ruthenium complexes: interactions with biomolecules, photoactivation, and multinuclearity approach. *RSC Advances* **2014**, *4* (4), 1819-1840.

(124) Furrer, J.; Smith, G. S.; Therrien, B. Metal Complexes as Enzyme Inhibitors and Catalysts in Living Cells. *Inorganic Chemical Biology: Principles, Techniques and Applications* **2014**, 341-371.

(125) Gupta, R. K.; Dubey, M.; Li, P. Z.; Xu, Q.; Pandey, D. S. Size-controlled synthesis of Ag nanoparticles functionalized by heteroleptic dipyrrinato complexes having meso-pyridyl substituents and their catalytic applications. *Inorganic Chemistry* **2015**, *54* (6), 2500-2511.

(126) Gupta, R. K.; Kumar, V.; Srivastava, A.; Pandey, D. S. Dipyrrin complex assisted in situ synthesis of ultra-small gold nanoparticles decorated on a partially reduced graphene oxide nanocomposite for efficient catalytic reduction of Cr (vi) to Cr (iii). *RSC advances* **2016**, *6* (47), 40911-40915.

(127) Hennessy, E. T.; Betley, T. A. Complex N-heterocycle synthesis via iron-catalyzed, direct C–H bond amination. *Science* **2013**, *340* (6132), 591-595.

(128) Kleinlein, C.; Zheng, S.-L.; Betley, T. A. Ground State and Excited State Tuning in Ferric Dipyrrin Complexes Promoted by Ancillary Ligand Exchange. *Inorganic chemistry* **2017**, *56* (10), 5892-5901.

(129) Elvidge, J.; Golden, J. 138. Conjugated macrocycles. Part XXVIII. Adducts from di-iminoisoindoline and arylene-m-diamines, and a new type of crossconjugated macrocycle with three-quarters of the chromophore of phthalocyanine. *Journal of the Chemical Society (Resumed)* **1957**, 700-709.

(130) Soji, S. Core-modified phthalocyanines and subphthalocyanines: a synthetic strategy towards core-modification and novel properties arising from the inner ring-expansion. *Макрогетероциклы* **2015**, *8* (4), 332-342.

(131) Siegl, W. O. A template type synthesis using phthalonitrile. Metal complexes of 1, 3-bis (2-pyridylimnio) isoindolines. *Inorganic and Nuclear Chemistry Letters* **1974**, *10* (10), 825-829.

(132) Siegl, W. O. Metal ion activation of nitriles. Syntheses of 1, 3-bis (arylimino) isoindolines. *The Journal of Organic Chemistry* **1977**, *42* (11), 1872-1878.

(133) de La Torre, G.; Torres, T. Stepwise Synthesis of Substituted Dicyanotriazolehemiporphyrazines. A Regioselective Approach to Unsymmetrically Substituted Hemiporphyrazines. *The Journal of Organic Chemistry* **1996**, *61* (18), 6446-6449.

(134) Danilova, E. A.; Melenchuk, T. V.; Melekhonova, E. E.; Tyutina, M. A.; Islyaikin, M. K. Three-unit products from condensation of 3-alkylsubstituted 2, 5-diamino-1, 3, 4-thiadiazoles with 1, 1-dime-thoxy-3-iminoisoindoline. *Macroheterocycles* **2009**, *2* (3-4), 246.

(135) Makarova, A. S.; Kibireva, Y. E.; Vasina, M. V.; Islyaikin, M. K. Microwave-Assisted Approach to Hemiporphyrazine Synthesis.

(136) Kustova, T.; Danilova, E.; Mileeva, M. Triazoleand Thiadiazolecontaining Macroheterocycles: Review of Main Achievements for Last Decade. *Макрогетероциклы* **2020**, *13* (3), 234-239.

(137) Balogh-Hergovich, É.; Speier, G.; Réglier, M.; Giorgi, M.; Kuzmann, E.; Vértes, A. Synthesis, structure and spectral properties of a novel stable homoleptic iron (II) complex of 1, 3-bis (2′-pyridylimino) isoindoline, Fe (ind) 2. *Inorganic Chemistry Communications* **2005**, *8* (5), 457-459.

(138) Meder, M.; Galka, C. H.; Gade, L. H. Bis (2-pyridylimino) isoindole (BPI) ligands with novel linker units: synthesis and characterization of their palladium and platinum complexes. *Monatshefte für Chemie/Chemical Monthly* **2005**, *136*, 1693-1706.

(139) Dang, J. D.; Bender, T. P. Boron, aluminum, gallium, and indium complexes of 1, 3-bis (2-pyridylimino) isoindoline (BPI). *Inorganic Chemistry Communications* **2013**, *30*, 147-151.

(140) Reshma, G.; Padmanabhan, V.; Varma, A. R.; Gouri, M.; Nair, U. R.; Parvathy, P.; Kulkarni, N. V.; Senthurpandi, D. Synthesis and structure of mono and bis {1, 3-bis (2-pyridylimino) isoindoline} supported 3d transition metal complexes. *Journal of Molecular Structure* **2021**, *1226*, 129344.

(141) Dalai, S.; Belov, V. N.; Nizamov, S.; Rauch, K.; Finsinger, D.; de Meijere, A. Access to Variously Substituted 5, 6, 7, 8-Tetrahydro-3H-quinazolin-4-ones via Diels–Alder Adducts of Phenyl Vinyl Sulfone to Cyclobutene-Annelated Pyrimidinones. Wiley Online Library: 2006.

(142) Wheeler, B. L.; Nagasubramanian, G.; Bard, A. J.; Schechtman, L. A.; Kenney, M. E. A silicon phthalocyanine and a silicon naphthalocyanine: synthesis, electrochemistry, and electrogenerated chemiluminescence. *Journal of the American Chemical Society* **1984**, *106* (24), 7404-7410.

(143) Cammidge, A. N.; Cook, M. J.; Hughes, D. L.; Nekelson, F.; Rahman, M. A remarkable side-product from the synthesis of an octaalkylphthalocyanine: formation of a tetrabenzotriazaporphyrin. *Chemical communications* **2005**, (7), 930-932.

(144) Cammidge, A. N.; Chambrier, I.; Cook, M. J.; Hughes, D. L.; Rahman, M.; Sosa-Vargas, L. Phthalocyanine Analogues: Unexpectedly Facile Access to Non-Peripherally

Substituted Octaalkyl Tetrabenzotriazaporphyrins, Tetrabenzodiazaporphyrins, Tetrabenzomonoazaporphyrins and Tetrabenzoporphyrins. *Chemistry–A European Journal* **2011**, *17* (11), 3136-3146.

(145) Mack, J.; Sosa-Vargas, L.; Coles, S. J.; Tizzard, G. J.; Chambrier, I.; Cammidge, A. N.; Cook, M. J.; Kobayashi, N. Synthesis, characterization, MCD spectroscopy, and TD-DFT calculations of copper-metalated nonperipherally substituted octaoctyl derivatives of tetrabenzotriazaporphyrin, cis-and trans-tetrabenzodiazaporphyrin, tetrabenzomonoazaporphyrin, and tetrabenzoporphyrin. *Inorganic chemistry* **2012**, *51* (23), 12820-12833.

(146) Alharbi, N.; Díaz-Moscoso, A.; Tizzard, G. J.; Coles, S. J.; Cook, M. J.; Cammidge, A. N. Improved syntheses of meso-aryl tetrabenzotriazaporphyrins (TBTAPs). *Tetrahedron* **2014**, *70* (40), 7370-7379.

(147) Gretton, J. Phthalocyanine and Subphthalocyanine hybrid macrocycles: improved accessibility and synthetic control via new intermediates. University of East Anglia, 2022.

(148) Remiro Buenamanana, S. Contracted phthalocyanine macrocycles: Conjugation with nanoparticles and the first synthesis of meso-substituted Boron SubTriBenzoDiAzaPorphyrin hybrids (SubTBDAPs). University of East Anglia, 2015.

(149) Newman, M. S.; Lednicer, D. The synthesis and resolution of hexahelicene1. *Journal of the American Chemical Society* **1956**, *78* (18), 4765-4770.

(150) Amemiya, R.; Yamaguchi, M. Chiral recognition in noncovalent bonding interactions between helicenes: right-handed helix favors right-handed helix over left-handed helix. *Organic & biomolecular chemistry* **2008**, *6* (1), 26-35.

(151) Zhou, M.; Robertson, G. P.; Roovers, J. Comparative study of ruthenium (II) tris (bipyridine) derivatives for electrochemiluminescence application. *Inorganic chemistry* **2005**, *44* (23), 8317-8325.

(152) Balzani, V.; Ceroni, P.; Credi, A.; Venturi, M. Ruthenium tris (bipyridine) complexes: Interchange between photons and electrons in molecular-scale devices and machines. *Coordination Chemistry Reviews* **2021**, *433*, 213758.

(153) Borgström, M.; Johansson, O.; Lomoth, R.; Baudin, H. B.; Wallin, S.; Sun, L.; Åkermark, B.; Hammarström, L. Electron Donor− Acceptor Dyads and Triads Based on Tris (bipyridine) ruthenium (II) and Benzoquinone: Synthesis, Characterization, and Photoinduced Electron Transfer Reactions. *Inorganic chemistry* **2003**, *42* (17), 5173-5184.

(154) Amar, A.; Savel, P.; Akdas-Kilig, H.; Katan, C.; Meghezzi, H.; Boucekkine, A.; Malval, J. P.; Fillaut, J. L. Photoisomerisation in Aminoazobenzene-Substituted Ruthenium (II) Tris (bipyridine) Complexes: Influence of the Conjugation Pathway. *Chemistry–A European Journal* **2015**, *21* (22), 8262-8270.

(155) Broomhead, J. A.; Young, C. G.; Hood, P. Tris (2, 2 ″-Bipyridine) Ruthenium (II) Dichloride Hexahydrate. *Inorganic Syntheses: Reagents for transition metal complex and organometallic syntheses* **1990**, *28*, 338-340.

(156) Nagao, H.; Nishimura, H.; Kitanaka, Y.; Howell, F. S.; Mukaida, M.; Kakihana, H. Selective formation of ruthenium (IV) complexes with a monooxygen ligand: trans-[RuX (O)(py) 4]+(X= Cl, ONO). *Inorganic Chemistry* **1990**, *29* (9), 1693-1700.

(157) Alqahtani, N. Z.; Blevins, T. G.; McCusker, C. E. Quantifying triplet state formation in zinc dipyrrin complexes. *The Journal of Physical Chemistry A* **2019**, *123* (46), 10011-10018.

(158) Wang, Y.; Xue, Z.; Dong, Y.; Zhu, W. Synthesis and electrochemistry of meso-substitutes dipyrromethene nickel (II) complexes. *Polyhedron* **2015**, *102*, 578-582.

(159) Kohtoku, M.; Honma, H.; Takai, O. Electroless Plating Catalyst Performance of a Cationic Moiety Bearing Palladium Complex. *Journal of the Electrochemical Society* **2014**, *161* (14), D806.

(160) Panchavarnam, S.; Sengupta, R.; Ravikanth, M. Synthesis, structure, and properties of palladium (II) complex of α-formyl pyrrolyl dipyrromethene. *Dalton Transactions* **2022**, *51* (14), 5587-5595.

(161) Bröring, M.; Kleeberg, C.; Cónsul Tejero, E. Syntheses, Structures and Coordination Modes of Acetatopalladium (II) Complexes with 1, 3-Bis (2-arylimino) isoindoline Ligands of Different Steric Influence. Wiley Online Library: 2007.

Experimental references

1- B. L. Wheeler, G. Nagasubramaniai, A. J. Bard, L. A. Schechtman, D. R. Dininny, M. E. Kenney, *J. Am. Chem. Soc*., **1984**, *106*, 7404 - 7410.

2- E. I. Kovshev, V. A. Puchnova, E. A. Luk'yanets, *J. Org. Chem. USSR (Engl. Transl.)*, **1971**, *7*, 364 - 369.

3- Y. Appiarius, P. J. Gliese, S. A. W. Segler, P. Rusch, J. Zhang, P. J. Gates, R. Pal, L. A. Malaspina, K. Sugimoto, T. Neudecker, N. C. Bigall, S. Grabowsky, A. A. Bakulin, . A. Staubitz, *J. Phys. Chem. C*, **2022**, *126*, 4563-4576.

4- V. Claus, M.l Schukin, S. Harrer, M. Rudolph, F. Rominger, A. M. Asiri, J. Xie, A. S. K. Hashmi, *Angew. Chem. Int. Ed.*, **2018**, *57*, 12966-12970

5- I. Chambrier and M. J. Cook, *Journal of Chemical Research, Synopses*, **1990**, *10*, 322-323.

6- R. T. Boer´e, R. T. Oakley and R. W. Reed, *Journal of Organometallic Chemistry*, **1987**, *331*, 161-167.

7- V. Wentworth, O. L. Brady, *Journal of the Chemical Society*, *Perkin Transactions 1*, **1920**, *117*, 1040-1045.

8- M. Hellal and G. D. Cuny, *Tetrahedron Letters*, **2011**, *52*, 5508-5511.

9- A. Díaz-Moscoso, G. J. Tizzard, S. J. Coles, A. N. Cammidge, *Angew. Chem. Int. Ed*. **2013**, *52*, 10784 -10787.

10- Norah A. A. 2022. Multidecker assemblies from Porphyrin and Phthalocyanine derivatives. Ph.D. thesis, University of East Anglia.

11- Budur N. A. 2023. Synthesis of novel symmetrical and unsymmetrical aza BODIPY analogues. Ph.D. thesis, University of East Anglia.

12- A. Díaz-Moscoso, E. Emond, D. L. Hughes, G. J. Tizzard, S. J. Coles, A. N. Cammidge, *The Journal of Organic Chemistry*, **2014**, *79*, 8932-8936.

13- Jacob G. 2022. Phthalocyanine and Subphthalocyanine Hybrid Macrocycles: Improved Accessibility and Synthetic Control via new Intermediates. Ph.D. thesis, University of east Anglia.

Appendix

Crystal data and structure refinement for $HNC_{12}H_6$-{N-(isoindole)-CH-C_6H_4-OMe}$_2$.CH_2Cl_2

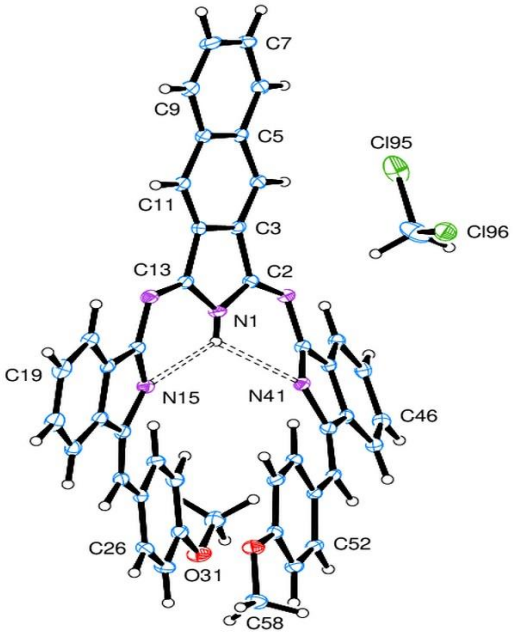

Identification code	isabf1197
Elemental formula	2(C44 H30 N5 O2, C H2 Cl2)
Formula weight	1493.32
Crystal system, space group	Orthorhombic, $Pca2_1$ (no. 29)
Unit cell dimensions	a = 16.1812(3) Å α = 90 ° b = 14.6930(3) Å β = 90 ° c = 30.2522(6) Å γ = 90 °
Volume	7192.5(2) $Å^3$
Z, Calculated density	4, 1.379 Mg/m^3
F(000)	3104
Absorption coefficient	2.004 mm^{-1}
Temperature	106(2) K
Wavelength	1.54184 Å
Crystal colour, shape	dark orange block
Crystal size	0.72 x 0.45 x 0.43 mm

Crystal mounting: on a small loop, in oil, fixed in cold N_2 stream

On the diffractometer:

Theta range for data collection	2.921 to 72.479 °
Limiting indices	-19<=h<=15, -17<=k<=17, -36<=l<=36
Completeness to theta = 67.684	99.7 %
Absorption correction	Semi-empirical from equivalents
Max. and min. transmission	1.00000 and 0.24577
Reflections collected (not including absences)	29676
No. of unique reflections	11425 [R(int) for equivalents = 0.041]
No. of 'observed' reflections (I > 2σI)	10830
Structure determined by:	dual methods, in SHELXT
Refinement:	Full-matrix-block least-squares on F^2, in SHELXL
Data / restraints / parameters	11425 / 1 / 985
Goodness-of-fit on F^2	1.055
Final R indices ('observed' data)	R_1 = 0.039, wR_2 = 0.102
Final R indices (all data)	R_1 = 0.041, wR_2 = 0.103
Reflections weighted: $w = [\sigma^2(Fo^2)+(0.0652P)^2+0.8113P]^{-1}$ where $P=(Fo^2+2Fc^2)/3$	
Absolute structure parameter	0.104(8)
Extinction coefficient	n/a
Largest diff. peak and hole	0.48 and -0.43 e.Å^{-3}
Location of largest difference peak	near Cl(95)

Table 1. Atomic coordinates (x 10^5) and equivalent isotropic displacement parameters ($Å^2$ x 10^4). U(eq) is defined as one third of the trace of the orthogonalized Uij tensor. E.s.ds are in parentheses.

	x	y	z	U(eq)
N(1)	56869(16)	89989(17)	33454(9)	210(5)
C(2)	59699(17)	81120(20)	33438(10)	207(6)
C(3)	66745(18)	80960(20)	30346(10)	209(6)
C(4)	71875(18)	73980(20)	29072(10)	228(6)
C(5)	78512(18)	76020(20)	26171(10)	228(6)
C(6)	84056(19)	69140(20)	24732(10)	269(7)
C(7)	90730(20)	71200(20)	22153(11)	311(7)
C(8)	92130(20)	80240(30)	20803(11)	333(8)
C(9)	86850(20)	87020(20)	22036(11)	300(7)
C(10)	79910(18)	85140(20)	24731(10)	239(6)
C(11)	74329(18)	92120(20)	26049(10)	236(6)
C(12)	67938(17)	89930(20)	28801(10)	213(6)
C(13)	61484(17)	95620(20)	30736(10)	220(6)
N(14)	60604(15)	104204(17)	29938(9)	238(5)
N(15)	47433(15)	105640(17)	33629(9)	239(5)
C(16)	54133(18)	109050(20)	31744(10)	226(6)
C(17)	54007(18)	118960(20)	31591(10)	229(6)
C(18)	59520(20)	125280(20)	29906(10)	266(7)
C(19)	57440(20)	134420(20)	30207(11)	314(7)
C(20)	50110(20)	137020(20)	32240(11)	322(7)
C(21)	44600(20)	130760(20)	33954(11)	276(7)
C(22)	46583(19)	121500(20)	33573(10)	247(6)
C(23)	42353(18)	113050(20)	34783(10)	229(6)
C(24)	34779(18)	112480(20)	36681(10)	238(6)
C(25)	29956(18)	104520(20)	37912(10)	229(6)
C(26)	22882(18)	105710(20)	40540(11)	274(7)
C(27)	18177(19)	98450(20)	41903(12)	316(7)
C(28)	20309(18)	89680(20)	40620(10)	268(7)
C(29)	27207(18)	88270(20)	37974(11)	265(6)
C(30)	31966(18)	95590(20)	36667(10)	253(6)
O(31)	15250(14)	82882(17)	42148(9)	352(5)
C(32)	17180(20)	73750(20)	40917(12)	334(7)
N(40)	56942(14)	74170(17)	35591(9)	219(5)
N(41)	49049(15)	82650(17)	40958(9)	219(5)
C(42)	51006(17)	75130(20)	38839(10)	209(6)
C(43)	46515(17)	67210(20)	40520(10)	206(6)
C(44)	46312(17)	58060(20)	39249(10)	223(6)
C(45)	41197(18)	52250(20)	41577(11)	249(6)
C(46)	36427(18)	55420(20)	45124(11)	262(7)
C(47)	36690(18)	64440(20)	46407(11)	246(6)
C(48)	41712(17)	70410(20)	44034(10)	212(6)
C(49)	43286(17)	80270(20)	44241(10)	217(6)
C(50)	39384(17)	86150(20)	47037(10)	215(6)
C(51)	40017(16)	95940(20)	47450(10)	202(6)
C(52)	34162(18)	100460(20)	50070(10)	235(6)
C(53)	34143(19)	109900(20)	50484(10)	253(6)
C(54)	40155(18)	114940(20)	48295(10)	228(6)

C(55)	46143(17)	110570(20)	45745(10)	235(6)
C(56)	45992(18)	101250(20)	45256(10)	219(6)
O(57)	40710(13)	124219(15)	48393(8)	284(5)
C(58)	35130(20)	128900(20)	51270(12)	323(7)
C(94)	68380(20)	56740(30)	39158(18)	541(12)
Cl(95)	73368(7)	50726(7)	34861(4)	590(3)
Cl(96)	74838(6)	64997(6)	41571(3)	398(2)
N(101)	29432(15)	38882(16)	66597(8)	191(5)
C(102)	32265(17)	30040(20)	66752(10)	196(6)
C(103)	39364(17)	30010(20)	69785(10)	196(6)
C(104)	44416(18)	23140(20)	71189(10)	216(6)
C(105)	51140(17)	25250(20)	74015(10)	229(6)
C(106)	56731(19)	18500(20)	75529(10)	268(7)
C(107)	63453(19)	20700(20)	78011(11)	301(7)
C(108)	64980(20)	29840(20)	79216(11)	321(7)
C(109)	59641(19)	36560(20)	77890(11)	279(7)
C(110)	52610(18)	34500(20)	75291(10)	229(6)
C(111)	47065(17)	41470(20)	73867(10)	225(6)
C(112)	40608(17)	39060(20)	71223(10)	202(6)
C(113)	34103(16)	44710(20)	69223(10)	203(6)
N(114)	33263(15)	53285(17)	69885(9)	233(5)
N(115)	19900(14)	54523(16)	66382(8)	221(5)
C(116)	26664(17)	57950(20)	68097(10)	205(6)
C(117)	26551(19)	67940(20)	68223(10)	228(6)
C(118)	32256(18)	74270(20)	69741(10)	238(6)
C(119)	30050(20)	83380(20)	69495(11)	278(7)
C(120)	22400(20)	85940(20)	67744(11)	275(7)
C(121)	16772(19)	79610(20)	66195(10)	248(6)
C(122)	18928(18)	70490(20)	66450(10)	221(6)
C(123)	14649(18)	61859(19)	65294(10)	208(6)
C(124)	7023(18)	61220(20)	63502(10)	214(6)
C(125)	2189(17)	53280(20)	62239(10)	221(6)
C(126)	4338(18)	44300(20)	63322(10)	235(6)
C(127)	-399(18)	36990(20)	61988(10)	243(6)
C(128)	-7439(17)	38450(20)	59462(10)	235(6)
C(129)	-9708(18)	47280(20)	58337(11)	268(7)
C(130)	-4997(18)	54540(20)	59752(10)	256(6)
O(131)	-12542(13)	31660(15)	57901(8)	299(5)
C(132)	-10090(20)	22510(20)	58741(12)	307(7)
N(140)	29500(15)	22965(16)	64657(8)	206(5)
N(141)	20996(14)	31194(16)	59417(9)	215(5)
C(142)	23490(16)	23700(20)	61441(10)	195(6)
C(143)	19623(17)	15594(19)	59592(10)	201(6)
C(144)	20350(17)	6400(20)	60625(10)	215(6)
C(145)	15839(18)	270(20)	58099(11)	237(6)
C(146)	10855(18)	3220(20)	54645(11)	249(6)
C(147)	10196(17)	12410(20)	53560(10)	227(6)
C(148)	14611(17)	18606(19)	56141(10)	209(6)
C(149)	15553(17)	28559(19)	56036(10)	198(6)
C(150)	11806(17)	34140(20)	53087(10)	217(6)
C(151)	12307(17)	43920(20)	52545(10)	205(6)
C(152)	6559(19)	48180(20)	49772(10)	246(6)
C(153)	6363(19)	57490(20)	49290(11)	266(7)
C(154)	12094(18)	62860(20)	51552(11)	246(6)
C(155)	18067(17)	58810(20)	54208(10)	225(6)
C(156)	18064(18)	49440(20)	54722(10)	232(6)

O(157)	11207(13)	72010(14)	50960(8)	299(5)
C(158)	17270(20)	77800(20)	52914(12)	291(7)
C(91)	42840(20)	6860(30)	60925(14)	380(8)
Cl(92)	48854(4)	15841(5)	58830(3)	307(2)
Cl(93)	47888(5)	710(6)	65162(3)	396(2)

Table 2. Molecular dimensions. Bond lengths are in Ångstroms, angles in degrees. E.s.ds are in parentheses.

N(1)-C(2)	1.381(4)	C(43)-C(44)	1.398(4)
N(1)-C(13)	1.385(4)	C(43)-C(48)	1.398(4)
N(1)-H(1)	0.78(4)	C(44)-C(45)	1.382(4)
C(2)-N(40)	1.291(4)	C(45)-C(46)	1.402(5)
C(2)-C(3)	1.475(4)	C(46)-C(47)	1.381(4)
C(3)-C(4)	1.374(4)	C(47)-C(48)	1.394(4)
C(3)-C(12)	1.413(4)	C(48)-C(49)	1.473(4)
C(4)-C(5)	1.419(4)	C(49)-C(50)	1.363(4)
C(5)-C(6)	1.421(4)	C(50)-C(51)	1.448(4)
C(5)-C(10)	1.426(4)	C(51)-C(52)	1.402(4)
C(6)-C(7)	1.367(5)	C(51)-C(56)	1.408(4)
C(7)-C(8)	1.408(5)	C(52)-C(53)	1.392(5)
C(8)-C(9)	1.364(5)	C(53)-C(54)	1.390(4)
C(9)-C(10)	1.416(4)	C(54)-O(57)	1.367(4)
C(10)-C(11)	1.423(4)	N(101)-C(102)	1.378(4)
C(11)-C(12)	1.366(4)	N(101)-C(113)	1.391(4)
C(12)-C(13)	1.460(4)	N(101)-H(101)	0.88(4)
C(13)-N(14)	1.293(4)	C(102)-N(140)	1.297(4)
N(14)-C(16)	1.379(4)	C(102)-C(103)	1.470(4)
N(15)-C(16)	1.323(4)	C(103)-C(104)	1.366(4)
N(15)-C(23)	1.408(4)	C(103)-C(112)	1.414(4)
C(16)-C(17)	1.458(4)	C(104)-C(105)	1.418(4)
C(17)-C(18)	1.385(4)	C(105)-C(106)	1.418(4)
C(17)-C(22)	1.394(4)	C(105)-C(110)	1.433(4)
C(18)-C(19)	1.388(5)	C(106)-C(107)	1.361(5)
C(19)-C(20)	1.389(5)	C(107)-C(108)	1.412(5)
C(20)-C(21)	1.383(5)	C(108)-C(109)	1.372(5)
C(21)-C(22)	1.402(4)	C(109)-C(110)	1.416(4)
C(22)-C(23)	1.465(4)	C(110)-C(111)	1.428(4)
C(23)-C(24)	1.356(4)	C(111)-C(112)	1.363(4)
C(24)-C(25)	1.455(4)	C(112)-C(113)	1.471(4)
C(25)-C(30)	1.403(4)	C(113)-N(114)	1.283(4)
C(25)-C(26)	1.404(4)	N(114)-C(116)	1.380(4)
C(26)-C(27)	1.374(5)	N(115)-C(116)	1.312(4)
C(27)-C(28)	1.389(5)	N(115)-C(123)	1.411(4)
C(28)-O(31)	1.371(4)	C(116)-C(117)	1.468(4)
C(28)-C(29)	1.389(4)	C(117)-C(118)	1.389(4)
C(29)-C(30)	1.381(4)	C(117)-C(122)	1.396(4)
O(31)-C(32)	1.428(4)	C(118)-C(119)	1.388(4)
N(40)-C(42)	1.381(4)	C(119)-C(120)	1.398(5)
N(41)-C(42)	1.316(4)	C(120)-C(121)	1.384(5)
N(41)-C(49)	1.406(4)	C(121)-C(122)	1.387(4)
C(42)-C(43)	1.463(4)	C(122)-C(123)	1.486(4)

C(123)-C(124)	1.351(4)	C(146)-C(147)	1.393(4)
C(124)-C(125)	1.455(4)	C(147)-C(148)	1.397(4)
C(125)-C(130)	1.397(4)	C(148)-C(149)	1.471(4)
C(125)-C(126)	1.403(4)	C(149)-C(150)	1.355(4)
C(126)-C(127)	1.380(4)	C(150)-C(151)	1.448(4)
C(127)-C(128)	1.388(4)	C(151)-C(156)	1.400(4)
C(128)-O(131)	1.378(4)	C(151)-C(152)	1.400(4)
C(128)-C(129)	1.391(4)	C(152)-C(153)	1.377(4)
C(129)-C(130)	1.379(5)	C(153)-C(154)	1.396(4)
O(131)-C(132)	1.424(4)	C(154)-O(157)	1.364(4)
N(140)-C(142)	1.380(4)	C(54)-C(55)	1.395(4)
N(141)-C(142)	1.323(4)	C(55)-C(56)	1.378(4)
N(141)-C(149)	1.404(4)	O(57)-C(58)	1.431(4)
C(142)-C(143)	1.457(4)		
C(143)-C(144)	1.392(4)	C(154)-C(155)	1.390(4)
C(143)-C(148)	1.394(4)	C(155)-C(156)	1.386(4)
C(144)-C(145)	1.388(4)	O(157)-C(158)	1.427(4)
C(145)-C(146)	1.389(5)		
C(2)-N(1)-C(13)	112.5(3)	C(24)-C(23)-N(15)	125.8(3)
C(2)-N(1)-H(1)	125(3)	C(24)-C(23)-C(22)	125.5(3)
C(13)-N(1)-H(1)	123(3)	N(15)-C(23)-C(22)	108.7(3)
N(40)-C(2)-N(1)	129.0(3)	C(23)-C(24)-C(25)	130.0(3)
N(40)-C(2)-C(3)	125.1(3)	C(30)-C(25)-C(26)	117.2(3)
N(1)-C(2)-C(3)	105.9(3)	C(30)-C(25)-C(24)	124.0(3)
C(4)-C(3)-C(12)	121.4(3)	C(26)-C(25)-C(24)	118.8(3)
C(4)-C(3)-C(2)	131.1(3)	C(27)-C(26)-C(25)	121.7(3)
C(12)-C(3)-C(2)	107.5(3)	C(26)-C(27)-C(28)	119.9(3)
C(3)-C(4)-C(5)	118.2(3)	O(31)-C(28)-C(27)	115.7(3)
C(4)-C(5)-C(6)	121.1(3)	O(31)-C(28)-C(29)	124.4(3)
C(4)-C(5)-C(10)	120.5(3)	C(27)-C(28)-C(29)	119.9(3)
C(6)-C(5)-C(10)	118.4(3)	C(30)-C(29)-C(28)	119.8(3)
C(7)-C(6)-C(5)	121.1(3)	C(29)-C(30)-C(25)	121.5(3)
C(6)-C(7)-C(8)	120.1(3)	C(28)-O(31)-C(32)	117.8(3)
C(9)-C(8)-C(7)	120.6(3)	C(102)-N(101)-C(113)	112.3(2)
C(8)-C(9)-C(10)	120.8(3)	C(102)-N(101)-H(101)	125(2)
C(9)-C(10)-C(11)	121.6(3)	C(113)-N(101)-H(101)	123(2)
C(9)-C(10)-C(5)	119.0(3)	N(140)-C(102)-N(101)	128.6(3)
C(11)-C(10)-C(5)	119.4(3)	N(140)-C(102)-C(103)	124.9(3)
C(12)-C(11)-C(10)	118.8(3)	N(101)-C(102)-C(103)	106.5(2)
C(11)-C(12)-C(3)	121.7(3)	C(104)-C(103)-C(112)	120.9(3)
C(11)-C(12)-C(13)	130.7(3)	C(104)-C(103)-C(102)	131.6(3)
C(3)-C(12)-C(13)	107.7(3)	C(112)-C(103)-C(102)	107.5(2)
N(14)-C(13)-N(1)	129.4(3)	C(103)-C(104)-C(105)	119.0(3)
N(14)-C(13)-C(12)	124.2(3)	C(104)-C(105)-C(106)	122.1(3)
N(1)-C(13)-C(12)	106.4(3)	C(104)-C(105)-C(110)	119.8(3)
C(13)-N(14)-C(16)	120.9(3)	C(106)-C(105)-C(110)	118.1(3)
C(16)-N(15)-C(23)	107.0(3)	C(107)-C(106)-C(105)	121.4(3)
N(15)-C(16)-N(14)	126.7(3)	C(106)-C(107)-C(108)	120.5(3)
N(15)-C(16)-C(17)	112.3(3)	C(109)-C(108)-C(107)	119.9(3)
N(14)-C(16)-C(17)	120.9(3)	C(108)-C(109)-C(110)	120.9(3)
C(18)-C(17)-C(22)	122.3(3)	C(109)-C(110)-C(111)	121.2(3)
C(18)-C(17)-C(16)	132.3(3)	C(109)-C(110)-C(105)	119.1(3)
C(22)-C(17)-C(16)	105.5(3)	C(111)-C(110)-C(105)	119.7(3)
C(17)-C(18)-C(19)	117.9(3)	C(112)-C(111)-C(110)	118.2(3)
C(18)-C(19)-C(20)	120.2(3)	C(111)-C(112)-C(103)	122.3(3)
C(21)-C(20)-C(19)	122.2(3)	C(111)-C(112)-C(113)	130.0(3)
C(20)-C(21)-C(22)	117.8(3)	C(103)-C(112)-C(113)	107.6(2)
C(17)-C(22)-C(21)	119.6(3)	N(114)-C(113)-N(101)	129.5(3)
C(17)-C(22)-C(23)	106.4(3)	N(114)-C(113)-C(112)	124.5(3)
C(21)-C(22)-C(23)	134.0(3)	N(101)-C(113)-C(112)	106.1(2)

C(113)-N(114)-C(116)	120.6(3)	C(50)-C(49)-C(48)	124.7(3)
C(116)-N(115)-C(123)	107.5(2)	N(41)-C(49)-C(48)	109.2(2)
N(115)-C(116)-N(114)	127.6(3)	C(49)-C(50)-C(51)	130.5(3)
N(115)-C(116)-C(117)	112.6(3)	C(52)-C(51)-C(56)	117.9(3)
N(114)-C(116)-C(117)	119.8(3)	C(52)-C(51)-C(50)	118.1(3)
C(118)-C(117)-C(122)	122.3(3)	C(56)-C(51)-C(50)	123.9(3)
C(118)-C(117)-C(116)	132.1(3)	C(53)-C(52)-C(51)	121.6(3)
C(122)-C(117)-C(116)	105.6(3)	C(54)-C(53)-C(52)	119.1(3)
C(119)-C(118)-C(117)	117.2(3)	O(57)-C(54)-C(53)	124.6(3)
C(118)-C(119)-C(120)	120.5(3)	O(57)-C(54)-C(55)	115.2(3)
C(121)-C(120)-C(119)	122.0(3)	C(53)-C(54)-C(55)	120.3(3)
C(120)-C(121)-C(122)	117.7(3)	C(56)-C(55)-C(54)	120.3(3)
C(121)-C(122)-C(117)	120.2(3)	C(55)-C(56)-C(51)	120.8(3)
C(121)-C(122)-C(123)	133.9(3)	C(54)-O(57)-C(58)	116.8(3)
C(117)-C(122)-C(123)	105.9(3)		
C(124)-C(123)-N(115)	126.2(3)	C(102)-N(140)-C(142)	121.6(3)
C(124)-C(123)-C(122)	125.4(3)	C(142)-N(141)-C(149)	107.4(2)
N(115)-C(123)-C(122)	108.4(2)	N(141)-C(142)-N(140)	127.3(3)
C(123)-C(124)-C(125)	130.7(3)	N(141)-C(142)-C(143)	111.8(3)
C(130)-C(125)-C(126)	117.2(3)	N(140)-C(142)-C(143)	120.6(3)
C(130)-C(125)-C(124)	118.8(3)	C(144)-C(143)-C(148)	121.7(3)
C(126)-C(125)-C(124)	124.0(3)	C(144)-C(143)-C(142)	132.1(3)
C(127)-C(126)-C(125)	121.7(3)	C(148)-C(143)-C(142)	106.1(2)
C(126)-C(127)-C(128)	119.7(3)	C(145)-C(144)-C(143)	117.5(3)
O(131)-C(128)-C(127)	124.6(3)	C(144)-C(145)-C(146)	121.1(3)
O(131)-C(128)-C(129)	115.7(3)	C(145)-C(146)-C(147)	121.6(3)
C(127)-C(128)-C(129)	119.7(3)	C(146)-C(147)-C(148)	117.5(3)
C(130)-C(129)-C(128)	120.0(3)	C(143)-C(148)-C(147)	120.6(3)
C(129)-C(130)-C(125)	121.6(3)	C(143)-C(148)-C(149)	105.8(2)
C(128)-O(131)-C(132)	117.1(2)	C(147)-C(148)-C(149)	133.6(3)
C(2)-N(40)-C(42)	121.2(3)	C(150)-C(149)-N(141)	126.4(3)
C(42)-N(41)-C(49)	107.2(2)	C(150)-C(149)-C(148)	124.7(3)
N(41)-C(42)-N(40)	126.8(3)	N(141)-C(149)-C(148)	108.9(2)
N(41)-C(42)-C(43)	112.3(3)	C(149)-C(150)-C(151)	130.5(3)
N(40)-C(42)-C(43)	120.8(3)	C(156)-C(151)-C(152)	117.7(3)
C(44)-C(43)-C(48)	121.3(3)	C(156)-C(151)-C(150)	124.0(3)
C(44)-C(43)-C(42)	132.9(3)	C(152)-C(151)-C(150)	118.3(3)
C(48)-C(43)-C(42)	105.8(3)	C(153)-C(152)-C(151)	121.6(3)
C(45)-C(44)-C(43)	117.9(3)	C(152)-C(153)-C(154)	119.6(3)
C(44)-C(45)-C(46)	121.0(3)	O(157)-C(154)-C(155)	124.7(3)
C(47)-C(46)-C(45)	121.1(3)	O(157)-C(154)-C(153)	115.0(3)
C(46)-C(47)-C(48)	118.4(3)	C(155)-C(154)-C(153)	120.3(3)
C(47)-C(48)-C(43)	120.3(3)	C(156)-C(155)-C(154)	119.3(3)
C(47)-C(48)-C(49)	134.2(3)	C(155)-C(156)-C(151)	121.6(3)
C(43)-C(48)-C(49)	105.5(2)	C(154)-O(157)-C(158)	117.4(2)
C(50)-C(49)-N(41)	126.0(3)		
C(91)-Cl(92)	1.758(4)	C(94)-Cl(96)	1.759(4)
C(91)-Cl(93)	1.769(4)	C(94)-Cl(95)	1.767(5)
Cl(92)-C(91)-Cl(93)	112.89(18)	Cl(96)-C(94)-Cl(95)	112.3(2)

Table 3. Anisotropic displacement parameters (Å^2 x 10^4) for the expression:

$$\exp\{-2\pi^2(h^2a^{*2}U_{11} + \ldots + 2hka^*b^*U_{12})\}$$

E.s.ds are in parentheses.

	U_{11}	U_{22}	U_{33}	U_{23}	U_{13}	U_{12}
N(1)	214(12)	214(12)	201(13)	-6(10)	48(11)	12(10)
C(2)	209(13)	235(14)	176(14)	-30(12)	-16(12)	11(11)
C(3)	224(13)	261(15)	143(14)	-28(12)	-12(11)	-9(12)
C(4)	252(13)	246(15)	187(14)	-21(12)	-10(12)	30(12)
C(5)	236(13)	305(16)	144(14)	-35(12)	-28(12)	20(12)
C(6)	306(15)	282(16)	218(16)	-49(13)	-16(13)	45(13)
C(7)	298(15)	401(18)	234(16)	-80(14)	28(14)	108(14)
C(8)	290(15)	460(20)	248(17)	-20(15)	96(14)	12(14)
C(9)	301(15)	344(17)	255(16)	23(14)	21(14)	6(14)
C(10)	240(13)	306(15)	172(14)	-4(12)	-6(12)	12(12)
C(11)	254(14)	258(15)	197(15)	5(12)	3(12)	0(12)
C(12)	206(13)	262(15)	172(14)	-2(12)	-20(12)	28(11)
C(13)	222(13)	266(16)	172(14)	0(12)	-1(12)	-12(12)
N(14)	251(12)	250(13)	213(13)	30(10)	38(11)	-2(10)
N(15)	268(12)	235(13)	215(13)	8(10)	19(11)	39(10)
C(16)	261(14)	242(15)	177(14)	-5(12)	13(12)	-6(12)
C(17)	285(14)	265(15)	136(13)	-16(12)	-19(12)	13(12)
C(18)	325(15)	270(16)	203(15)	5(13)	-9(13)	-32(13)
C(19)	418(18)	262(16)	261(17)	14(13)	-42(15)	-88(14)
C(20)	524(19)	182(15)	259(16)	-25(13)	-27(16)	-10(14)
C(21)	394(17)	237(15)	197(15)	-16(12)	-29(14)	61(13)
C(22)	325(15)	246(15)	170(14)	-7(12)	-20(13)	5(13)
C(23)	300(14)	210(14)	177(14)	9(12)	0(13)	29(12)
C(24)	282(14)	233(14)	200(14)	-6(12)	-28(12)	63(12)
C(25)	207(13)	308(16)	172(14)	-10(12)	-37(12)	35(12)
C(26)	232(14)	310(17)	281(17)	-10(13)	-18(13)	63(12)
C(27)	198(14)	439(19)	310(18)	-6(15)	44(14)	32(13)
C(28)	201(13)	386(18)	216(15)	37(13)	-7(12)	-16(13)
C(29)	258(14)	291(16)	245(16)	-10(13)	-18(13)	10(12)
C(30)	230(14)	311(16)	217(15)	-25(13)	18(12)	24(12)
O(31)	306(11)	378(13)	373(14)	31(11)	100(10)	-55(10)
C(32)	310(16)	376(19)	316(18)	37(15)	-6(15)	-52(14)
N(40)	229(11)	230(12)	199(12)	-9(10)	20(10)	0(10)
N(41)	241(11)	221(12)	194(13)	21(10)	20(10)	22(10)
C(42)	219(13)	228(14)	179(14)	3(12)	-7(12)	5(11)
C(43)	189(12)	241(14)	186(14)	-3(12)	-37(11)	-1(11)
C(44)	218(13)	249(15)	203(14)	-16(12)	-19(12)	-2(11)
C(45)	264(14)	215(14)	267(16)	0(13)	-88(13)	-29(12)
C(46)	230(14)	279(16)	277(16)	49(13)	-24(13)	-51(12)
C(47)	238(13)	269(15)	231(15)	14(13)	-14(13)	9(12)
C(48)	201(13)	257(15)	178(14)	32(12)	-37(12)	5(11)
C(49)	196(13)	247(14)	209(15)	18(12)	2(12)	2(11)
C(50)	202(13)	292(15)	151(14)	15(12)	0(11)	-15(11)
C(51)	173(12)	278(15)	154(14)	-11(12)	1(11)	9(11)
C(52)	215(13)	303(16)	188(14)	-22(12)	19(12)	-24(12)
C(53)	252(14)	290(16)	217(15)	-40(13)	19(12)	25(12)
C(54)	244(14)	248(14)	192(14)	-7(12)	-34(12)	14(12)
C(55)	209(13)	307(16)	190(15)	-4(12)	18(12)	-16(12)
C(56)	200(13)	266(15)	191(14)	-16(12)	-4(12)	19(12)
O(57)	312(10)	233(10)	307(12)	-49(9)	44(10)	10(9)
C(58)	331(16)	277(16)	360(19)	-54(14)	26(15)	78(13)

C(94)	293(17)	410(20)	920(40)	80(20)	30(20)	-28(16)
Cl(95)	704(7)	350(5)	715(7)	-115(5)	-324(6)	64(4)
Cl(96)	462(4)	338(4)	393(5)	-5(4)	3(4)	74(4)
N(101)	191(11)	198(12)	183(12)	3(10)	-33(10)	2(9)
C(102)	217(13)	223(14)	149(13)	18(11)	29(12)	8(11)
C(103)	206(13)	232(14)	150(13)	16(11)	24(11)	-18(11)
C(104)	237(13)	215(14)	195(14)	17(12)	28(12)	14(11)
C(105)	218(13)	293(16)	177(14)	33(12)	18(12)	20(12)
C(106)	336(16)	276(16)	191(15)	44(13)	21(13)	67(13)
C(107)	274(15)	396(18)	234(16)	61(14)	-5(13)	104(14)
C(108)	285(15)	440(20)	241(16)	-22(15)	-73(14)	42(14)
C(109)	293(15)	345(17)	200(15)	-19(13)	-23(13)	47(13)
C(110)	222(13)	318(16)	148(14)	6(12)	-7(12)	15(12)
C(111)	247(13)	234(14)	194(14)	-12(12)	10(12)	5(11)
C(112)	228(13)	221(14)	156(14)	12(11)	0(12)	11(11)
C(113)	197(13)	241(14)	170(14)	2(12)	-8(11)	5(11)
N(114)	245(11)	228(12)	226(13)	-13(10)	-17(11)	5(10)
N(115)	237(11)	216(12)	210(12)	1(10)	-29(10)	36(10)
C(116)	232(13)	220(14)	162(14)	-27(11)	3(12)	17(11)
C(117)	291(14)	231(15)	161(14)	-22(12)	37(12)	0(12)
C(118)	274(14)	247(15)	194(14)	-12(12)	20(12)	-28(12)
C(119)	350(15)	263(16)	223(15)	-30(13)	8(14)	-66(13)
C(120)	407(17)	192(14)	225(16)	11(12)	40(14)	20(13)
C(121)	293(14)	263(15)	188(15)	7(12)	0(13)	22(12)
C(122)	275(14)	238(14)	151(13)	-17(12)	32(12)	22(12)
C(123)	271(14)	182(13)	171(14)	-4(11)	40(12)	26(11)
C(124)	267(14)	195(13)	180(14)	23(11)	43(12)	49(11)
C(125)	224(13)	265(15)	174(14)	-1(12)	29(12)	24(11)
C(126)	220(13)	271(15)	213(15)	10(12)	-19(12)	11(12)
C(127)	258(14)	269(15)	202(15)	31(12)	21(12)	20(12)
C(128)	226(13)	296(15)	184(15)	-15(12)	26(12)	-38(12)
C(129)	212(14)	348(17)	244(16)	17(13)	-71(13)	40(12)
C(130)	243(14)	280(15)	245(16)	21(13)	12(13)	60(12)
O(131)	303(11)	303(11)	290(12)	-10(10)	-76(10)	-46(9)
C(132)	331(16)	295(16)	294(17)	-21(14)	-11(15)	-49(13)
N(140)	243(12)	186(12)	189(12)	8(10)	-7(10)	-1(9)
N(141)	225(11)	200(12)	219(13)	11(10)	-20(10)	19(9)
C(142)	186(13)	207(14)	193(14)	2(11)	37(12)	-5(11)
C(143)	186(12)	214(14)	204(15)	-7(12)	20(12)	-11(11)
C(144)	223(13)	205(14)	218(14)	1(12)	25(12)	-9(11)
C(145)	263(14)	198(13)	249(15)	-10(12)	37(13)	-16(11)
C(146)	258(14)	234(14)	256(16)	-52(12)	4(13)	-41(12)
C(147)	213(13)	250(15)	218(15)	-6(12)	-2(12)	-10(11)
C(148)	183(13)	220(14)	224(15)	-19(12)	19(12)	0(11)
C(149)	196(13)	209(14)	187(14)	-26(11)	5(11)	-11(11)
C(150)	196(12)	243(15)	211(15)	-18(12)	2(12)	-5(11)
C(151)	202(12)	219(14)	194(14)	-7(12)	15(12)	-15(11)
C(152)	253(14)	251(15)	234(15)	15(12)	-33(13)	-30(12)
C(153)	247(14)	259(15)	290(17)	29(13)	-46(13)	2(12)
C(154)	272(14)	218(15)	247(16)	22(12)	30(13)	-9(12)
C(155)	234(13)	237(15)	204(15)	-19(12)	24(12)	-61(12)
C(156)	228(14)	267(15)	201(14)	23(12)	-15(12)	-14(11)
O(157)	327(11)	179(10)	391(13)	6(9)	-37(10)	-12(9)
C(158)	344(15)	214(15)	314(17)	-40(13)	32(15)	-53(13)
C(91)	292(16)	373(19)	480(20)	49(17)	-112(16)	-46(14)
Cl(92)	286(3)	255(3)	380(4)	-10(3)	-70(3)	5(3)
Cl(93)	442(4)	338(4)	409(5)	58(4)	-6(4)	65(3)

Table 4. Hydrogen coordinates (x 10^4) and isotropic displacement parameters ($Å^2$ x 10^3). All hydrogen atoms were included in idealised positions with U(iso)'s set at 1.2*U(eq) or, for the methyl group hydrogen atoms, 1.5*U(eq) of the parent carbon atoms.

	x	y	z	U(iso)
H(1)	5300(20)	9170(20)	3477(12)	18(9)
H(4)	7100	6795	3011	27
H(6)	8311	6300	2558	32
H(7)	9444	6652	2127	37
H(8)	9679	8163	1902	40
H(9)	8785	9308	2107	36
H(11)	7504	9819	2503	28
H(18)	6458	12341	2859	32
H(19)	6103	13891	2902	38
H(20)	4885	14332	3246	39
H(21)	3962	13266	3534	33
H(24)	3223	11816	3730	29
H(26)	2131	11168	4140	33
H(27)	1347	9942	4372	38
H(29)	2865	8229	3707	32
H(30)	3671	9456	3488	30
H(32A)	1741	7329	3769	50
H(32B)	1290	6964	4205	50
H(32C)	2254	7204	4217	50
H(44)	4959	5591	3686	27
H(45)	4091	4602	4076	30
H(46)	3295	5130	4667	31
H(47)	3352	6653	4885	30
H(50)	3564	8336	4904	26
H(52)	3011	9700	5160	28
H(53)	3008	11285	5224	30
H(55)	5034	11404	4434	28
H(56)	4997	9836	4342	26
H(58A)	2943	12760	5038	48
H(58B)	3614	13547	5108	48
H(58C)	3600	12685	5432	48
H(94A)	6339	5975	3796	65
H(94B)	6659	5238	4146	65
H(101)	2510(20)	4070(20)	6507(13)	23(9)
H(104)	4344	1704	7028	26
H(106)	5576	1230	7479	32
H(107)	6715	1606	7894	36
H(108)	6969	3133	8094	39
H(109)	6068	4269	7873	34
H(111)	4786	4762	7474	27
H(118)	3745	7244	7090	29
H(119)	3377	8791	7052	33
H(120)	2103	9222	6761	33
H(121)	1161	8145	6500	30
H(124)	438	6689	6298	26
H(126)	918	4323	6502	28
H(127)	115	3098	6279	29
H(129)	-1450	4832	5659	32

H(130)	-668	6055	5902	31
H(13A)	-471	2137	5736	46
H(13B)	-1421	1834	5750	46
H(13C)	-968	2154	6194	46
H(144)	2380	439	6297	26
H(145)	1617	-604	5874	28
H(146)	782	-113	5298	30
H(147)	687	1438	5116	27
H(150)	827	3115	5104	26
H(152)	270	4456	4818	30
H(153)	235	6025	4743	32
H(155)	2211	6244	5566	27
H(156)	2206	4670	5660	28
H(15A)	1717	7706	5613	44
H(15B)	1606	8415	5216	44
H(15C)	2276	7616	5179	44
H(91A)	4145	265	5848	46
H(91B)	3759	936	6210	46

Table 5. Torsion angles, in degrees. E.s.ds are in parentheses.

C(13)-N(1)-C(2)-N(40)	179.4(3)	C(16)-N(15)-C(23)-C(22)	-1.7(3)
C(13)-N(1)-C(2)-C(3)	-1.1(3)	C(113)-N(101)-C(102)-N(140)	-178.4(3)
N(40)-C(2)-C(3)-C(4)	-0.7(5)	C(113)-N(101)-C(102)-C(103)	0.7(3)
N(1)-C(2)-C(3)-C(4)	179.7(3)	N(140)-C(102)-C(103)-C(104)	-1.6(5)
N(40)-C(2)-C(3)-C(12)	-178.1(3)	N(101)-C(102)-C(103)-C(104)	179.2(3)
N(1)-C(2)-C(3)-C(12)	2.3(3)	N(140)-C(102)-C(103)-C(112)	177.5(3)
C(12)-C(3)-C(4)-C(5)	0.5(4)	N(101)-C(102)-C(103)-C(112)	-1.7(3)
C(2)-C(3)-C(4)-C(5)	-176.6(3)	C(112)-C(103)-C(104)-C(105)	-2.0(4)
C(3)-C(4)-C(5)-C(6)	179.9(3)	C(102)-C(103)-C(104)-C(105)	177.0(3)
C(3)-C(4)-C(5)-C(10)	1.7(4)	C(103)-C(104)-C(105)-C(106)	-178.7(3)
C(4)-C(5)-C(6)-C(7)	-176.0(3)	C(103)-C(104)-C(105)-C(110)	-1.0(4)
C(10)-C(5)-C(6)-C(7)	2.1(4)	C(104)-C(105)-C(106)-C(107)	175.8(3)
C(5)-C(6)-C(7)-C(8)	-1.2(5)	C(110)-C(105)-C(106)-C(107)	-2.0(4)
C(6)-C(7)-C(8)-C(9)	-0.1(5)	C(105)-C(106)-C(107)-C(108)	1.1(5)
C(7)-C(8)-C(9)-C(10)	0.6(5)	C(106)-C(107)-C(108)-C(109)	0.2(5)
C(8)-C(9)-C(10)-C(11)	-179.9(3)	C(107)-C(108)-C(109)-C(110)	-0.4(5)
C(8)-C(9)-C(10)-C(5)	0.4(5)	C(108)-C(109)-C(110)-C(111)	-179.5(3)
C(4)-C(5)-C(10)-C(9)	176.5(3)	C(108)-C(109)-C(110)-C(105)	-0.5(5)
C(6)-C(5)-C(10)-C(9)	-1.7(4)	C(104)-C(105)-C(110)-C(109)	-176.1(3)
C(4)-C(5)-C(10)-C(11)	-3.2(4)	C(106)-C(105)-C(110)-C(109)	1.7(4)
C(6)-C(5)-C(10)-C(11)	178.6(3)	C(104)-C(105)-C(110)-C(111)	2.8(4)
C(9)-C(10)-C(11)-C(12)	-177.3(3)	C(106)-C(105)-C(110)-C(111)	-179.4(3)
C(5)-C(10)-C(11)-C(12)	2.4(4)	C(109)-C(110)-C(111)-C(112)	177.4(3)
C(10)-C(11)-C(12)-C(3)	-0.2(4)	C(105)-C(110)-C(111)-C(112)	-1.6(4)
C(10)-C(11)-C(12)-C(13)	178.5(3)	C(110)-C(111)-C(112)-C(103)	-1.5(4)
C(4)-C(3)-C(12)-C(11)	-1.3(4)	C(110)-C(111)-C(112)-C(113)	-178.8(3)
C(2)-C(3)-C(12)-C(11)	176.4(3)	C(104)-C(103)-C(112)-C(111)	3.4(4)
C(4)-C(3)-C(12)-C(13)	179.7(3)	C(102)-C(103)-C(112)-C(111)	-175.8(3)
C(2)-C(3)-C(12)-C(13)	-2.6(3)	C(104)-C(103)-C(112)-C(113)	-178.7(3)
C(2)-N(1)-C(13)-N(14)	179.7(3)	C(102)-C(103)-C(112)-C(113)	2.1(3)
C(2)-N(1)-C(13)-C(12)	-0.5(3)	C(102)-N(101)-C(113)-N(114)	-179.8(3)
C(11)-C(12)-C(13)-N(14)	2.9(5)	C(102)-N(101)-C(113)-C(112)	0.5(3)
C(3)-C(12)-C(13)-N(14)	-178.3(3)	C(111)-C(112)-C(113)-N(114)	-3.7(5)
C(11)-C(12)-C(13)-N(1)	-176.9(3)	C(103)-C(112)-C(113)-N(114)	178.7(3)
C(3)-C(12)-C(13)-N(1)	1.9(3)	C(111)-C(112)-C(113)-N(101)	176.0(3)
N(1)-C(13)-N(14)-C(16)	-3.0(5)	C(103)-C(112)-C(113)-N(101)	-1.6(3)
C(12)-C(13)-N(14)-C(16)	177.2(3)	N(101)-C(113)-N(114)-C(116)	4.5(5)
C(23)-N(15)-C(16)-N(14)	-177.1(3)	C(112)-C(113)-N(114)-C(116)	-175.8(3)
C(23)-N(15)-C(16)-C(17)	1.0(3)	C(123)-N(115)-C(116)-N(114)	175.5(3)
C(13)-N(14)-C(16)-N(15)	-14.4(5)	C(123)-N(115)-C(116)-C(117)	-1.0(3)
C(13)-N(14)-C(16)-C(17)	167.7(3)	C(113)-N(114)-C(116)-N(115)	14.3(5)
N(15)-C(16)-C(17)-C(18)	-179.0(3)	C(113)-N(114)-C(116)-C(117)	-169.3(3)
N(14)-C(16)-C(17)-C(18)	-0.8(5)	N(115)-C(116)-C(117)-C(118)	179.7(3)
N(15)-C(16)-C(17)-C(22)	0.1(3)	N(114)-C(116)-C(117)-C(118)	2.9(5)
N(14)-C(16)-C(17)-C(22)	178.3(3)	N(115)-C(116)-C(117)-C(122)	0.7(3)
C(22)-C(17)-C(18)-C(19)	-0.5(5)	N(114)-C(116)-C(117)-C(122)	-176.1(3)
C(16)-C(17)-C(18)-C(19)	178.5(3)	C(122)-C(117)-C(118)-C(119)	0.9(4)
C(17)-C(18)-C(19)-C(20)	1.5(5)	C(116)-C(117)-C(118)-C(119)	-177.9(3)
C(18)-C(19)-C(20)-C(21)	-1.1(5)	C(117)-C(118)-C(119)-C(120)	-0.5(4)
C(19)-C(20)-C(21)-C(22)	-0.3(5)	C(118)-C(119)-C(120)-C(121)	-0.1(5)
C(18)-C(17)-C(22)-C(21)	-0.9(5)	C(119)-C(120)-C(121)-C(122)	0.4(5)
C(16)-C(17)-C(22)-C(21)	179.8(3)	C(120)-C(121)-C(122)-C(117)	0.0(4)
C(18)-C(17)-C(22)-C(23)	178.1(3)	C(120)-C(121)-C(122)-C(123)	178.1(3)
C(16)-C(17)-C(22)-C(23)	-1.2(3)	C(118)-C(117)-C(122)-C(121)	-0.7(5)
C(20)-C(21)-C(22)-C(17)	1.3(5)	C(116)-C(117)-C(122)-C(121)	178.5(3)
C(20)-C(21)-C(22)-C(23)	-177.4(3)	C(118)-C(117)-C(122)-C(123)	-179.2(3)
C(16)-N(15)-C(23)-C(24)	178.0(3)	C(116)-C(117)-C(122)-C(123)	-0.1(3)

C(116)-N(115)-C(123)-C(124)	-179.1(3)	C(54)-C(55)-C(56)-C(51)	-2.5(4)
C(116)-N(115)-C(123)-C(122)	0.9(3)	C(52)-C(51)-C(56)-C(55)	1.1(4)
C(17)-C(22)-C(23)-C(24)	-177.9(3)	C(50)-C(51)-C(56)-C(55)	178.9(3)
C(21)-C(22)-C(23)-C(24)	0.9(6)	C(121)-C(122)-C(123)-C(124)	1.3(5)
C(17)-C(22)-C(23)-N(15)	1.8(3)	C(117)-C(122)-C(123)-C(124)	179.5(3)
C(21)-C(22)-C(23)-N(15)	-179.4(3)	C(121)-C(122)-C(123)-N(115)	-178.8(3)
N(15)-C(23)-C(24)-C(25)	-1.3(5)	C(117)-C(122)-C(123)-N(115)	-0.5(3)
C(22)-C(23)-C(24)-C(25)	178.3(3)	N(115)-C(123)-C(124)-C(125)	0.2(5)
C(23)-C(24)-C(25)-C(30)	-10.4(5)	C(122)-C(123)-C(124)-C(125)	-179.8(3)
C(23)-C(24)-C(25)-C(26)	168.9(3)	C(123)-C(124)-C(125)-C(130)	-169.2(3)
C(30)-C(25)-C(26)-C(27)	1.0(5)	C(123)-C(124)-C(125)-C(126)	10.0(5)
C(24)-C(25)-C(26)-C(27)	-178.4(3)	C(130)-C(125)-C(126)-C(127)	0.2(4)
C(25)-C(26)-C(27)-C(28)	-1.0(5)	C(124)-C(125)-C(126)-C(127)	-179.0(3)
C(26)-C(27)-C(28)-O(31)	179.9(3)	C(125)-C(126)-C(127)-C(128)	0.8(5)
C(26)-C(27)-C(28)-C(29)	0.2(5)	C(126)-C(127)-C(128)-O(131)	179.0(3)
O(31)-C(28)-C(29)-C(30)	-179.0(3)	C(126)-C(127)-C(128)-C(129)	-0.7(4)
C(27)-C(28)-C(29)-C(30)	0.7(5)	O(131)-C(128)-C(129)-C(130)	179.9(3)
C(28)-C(29)-C(30)-C(25)	-0.7(5)	C(127)-C(128)-C(129)-C(130)	-0.4(5)
C(26)-C(25)-C(30)-C(29)	-0.1(4)	C(128)-C(129)-C(130)-C(125)	1.4(5)
C(24)-C(25)-C(30)-C(29)	179.3(3)	C(126)-C(125)-C(130)-C(129)	-1.3(4)
C(27)-C(28)-O(31)-C(32)	179.9(3)	C(124)-C(125)-C(130)-C(129)	178.0(3)
C(29)-C(28)-O(31)-C(32)	-0.3(4)	C(127)-C(128)-O(131)-C(132)	-3.8(4)
N(1)-C(2)-N(40)-C(42)	-8.9(5)	C(129)-C(128)-O(131)-C(132)	175.9(3)
C(3)-C(2)-N(40)-C(42)	171.6(3)	N(101)-C(102)-N(140)-C(142)	7.4(5)
C(49)-N(41)-C(42)-N(40)	-174.5(3)	C(103)-C(102)-N(140)-C(142)	-171.6(3)
C(49)-N(41)-C(42)-C(43)	1.2(3)	C(149)-N(141)-C(142)-N(140)	172.8(3)
C(2)-N(40)-C(42)-N(41)	-19.3(5)	C(149)-N(141)-C(142)-C(143)	-1.7(3)
C(2)-N(40)-C(42)-C(43)	165.4(3)	C(102)-N(140)-C(142)-N(141)	14.9(4)
N(41)-C(42)-C(43)-C(44)	177.4(3)	C(102)-N(140)-C(142)-C(143)	-171.0(3)
N(40)-C(42)-C(43)-C(44)	-6.7(5)	N(141)-C(142)-C(143)-C(144)	179.8(3)
N(41)-C(42)-C(43)-C(48)	-2.0(3)	N(140)-C(142)-C(143)-C(144)	4.9(5)
N(40)-C(42)-C(43)-C(48)	173.9(3)	N(141)-C(142)-C(143)-C(148)	1.4(3)
C(48)-C(43)-C(44)-C(45)	0.0(4)	N(140)-C(142)-C(143)-C(148)	-173.5(2)
C(42)-C(43)-C(44)-C(45)	-179.3(3)	C(148)-C(143)-C(144)-C(145)	-0.4(4)
C(43)-C(44)-C(45)-C(46)	-0.6(4)	C(142)-C(143)-C(144)-C(145)	-178.6(3)
C(44)-C(45)-C(46)-C(47)	-0.1(5)	C(143)-C(144)-C(145)-C(146)	0.6(4)
C(45)-C(46)-C(47)-C(48)	1.2(5)	C(144)-C(145)-C(146)-C(147)	0.3(5)
C(46)-C(47)-C(48)-C(43)	-1.7(4)	C(145)-C(146)-C(147)-C(148)	-1.3(4)
C(46)-C(47)-C(48)-C(49)	176.6(3)	C(144)-C(143)-C(148)-C(147)	-0.7(4)
C(44)-C(43)-C(48)-C(47)	1.1(4)	C(142)-C(143)-C(148)-C(147)	177.9(3)
C(42)-C(43)-C(48)-C(47)	-179.4(3)	C(144)-C(143)-C(148)-C(149)	-179.1(3)
C(44)-C(43)-C(48)-C(49)	-177.6(3)	C(142)-C(143)-C(148)-C(149)	-0.5(3)
C(42)-C(43)-C(48)-C(49)	1.9(3)	C(146)-C(147)-C(148)-C(143)	1.6(4)
C(42)-N(41)-C(49)-C(50)	-176.7(3)	C(146)-C(147)-C(148)-C(149)	179.4(3)
C(42)-N(41)-C(49)-C(48)	0.1(3)	C(142)-N(141)-C(149)-C(150)	-177.8(3)
C(47)-C(48)-C(49)-C(50)	-3.0(5)	C(142)-N(141)-C(149)-C(148)	1.4(3)
C(43)-C(48)-C(49)-C(50)	175.5(3)	C(143)-C(148)-C(149)-C(150)	178.7(3)
C(47)-C(48)-C(49)-N(41)	-179.8(3)	C(147)-C(148)-C(149)-C(150)	0.6(5)
C(43)-C(48)-C(49)-N(41)	-1.3(3)	C(143)-C(148)-C(149)-N(141)	-0.5(3)
N(41)-C(49)-C(50)-C(51)	-0.4(5)	C(147)-C(148)-C(149)-N(141)	-178.6(3)
C(48)-C(49)-C(50)-C(51)	-176.7(3)	N(141)-C(149)-C(150)-C(151)	0.5(5)
C(49)-C(50)-C(51)-C(52)	168.5(3)	C(148)-C(149)-C(150)-C(151)	-178.5(3)
C(49)-C(50)-C(51)-C(56)	-9.3(5)	C(149)-C(150)-C(151)-C(156)	10.4(5)
C(56)-C(51)-C(52)-C(53)	0.6(4)	C(149)-C(150)-C(151)-C(152)	-167.8(3)
C(50)-C(51)-C(52)-C(53)	-177.3(3)	C(156)-C(151)-C(152)-C(153)	-2.0(4)
C(51)-C(52)-C(53)-C(54)	-1.0(5)	C(150)-C(151)-C(152)-C(153)	176.3(3)
C(52)-C(53)-C(54)-O(57)	179.0(3)	C(151)-C(152)-C(153)-C(154)	1.1(5)
C(52)-C(53)-C(54)-C(55)	-0.4(4)	C(152)-C(153)-C(154)-O(157)	-178.0(3)
O(57)-C(54)-C(55)-C(56)	-177.3(3)	C(152)-C(153)-C(154)-C(155)	1.2(5)
C(53)-C(54)-C(55)-C(56)	2.1(4)	O(157)-C(154)-C(155)-C(156)	176.7(3)

C(153)-C(154)-C(155)-C(156)	-2.5(4)	C(53)-C(54)-O(57)-C(58)	5.8(4)
C(154)-C(155)-C(156)-C(151)	1.5(4)	C(55)-C(54)-O(57)-C(58)	-174.8(3)
C(152)-C(151)-C(156)-C(155)	0.7(4)	C(155)-C(154)-O(157)-C(158)	5.5(4)
C(150)-C(151)-C(156)-C(155)	-177.5(3)	C(153)-C(154)-O(157)-C(158)	-175.3(3)

Table 6. Hydrogen bonds, in Angstroms and degrees.

D-H...A	d(D-H)	d(H...A)	d(D...A)	<(DHA)
C(55)-H(55)...O(31)#1	0.95	2.54	3.416(4)	153.0
C(94)-H(94A)...N(40)	0.99	2.47	3.339(5)	146.6
C(91)-H(91B)...N(140)	0.99	2.51	3.396(5)	148.4
N(1)-H(1)...N(15)	0.78(4)	2.26(4)	2.761(4)	122(3)
N(1)-H(1)...N(41)	0.78(4)	2.39(4)	2.814(4)	116(3)
N(101)-H(101)...N(115)	0.88(4)	2.24(4)	2.768(3)	119(3)
N(101)-H(101)...N(141)	0.88(4)	2.31(4)	2.803(3)	116(3)

Symmetry transformation used to generate equivalent atoms:
#1 : x+½, 2-y, z

Crystal structure analysis of $HNC_{12}H_6$-{N-(isoindole)-CH-C_6H_4-OMe}$_2$.CH_2Cl_2

Crystal data: 2(C_{44} H_{30} N_5 O_2, CH_2 Cl_2), M = 1493.32. Orthorhombic, space group $Pca2_1$ (no. 29), a = 16.1812(3), b = 14.6930(3), c = 30.2522(6) Å, α = 90, β = 90, γ = 90 °, V = 7192.5(2) $Å^3$. Z = 4, Dc = 1.379 g cm^{-3}, F(000) = 3104, T = 106(2) K, μ(Cu-Kα) = 20.0 cm^{-1}, λ(Cu-Kα) = 1.54184 Å.

The crystal was a dark orange block. From a sample under oil, one, *ca* 0.43 x 0.45 x 0.72 mm, was mounted on a small loop and fixed in the cold nitrogen stream on a Rigaku Oxford Diffraction XtaLAB Synergy diffractometer, equipped with Cu-Kα radiation, HyPix detector and mirror monochromator. Intensity data were measured by thin-slice ω-scans. Total no. of reflections recorded, to θ_{max} = 72.5°, was 29,676 of which 11,425 were unique (Rint = 0.041); 10,830 were 'observed' with $I > 2\sigma_I$.

Data were processed using the CrysAlisPro-CCD and -RED (1) programs. The structure was determined by the intrinsic phasing routines in the SHELXT program (2A) and refined by full-matrix least-squares methods, on F^2's, in SHELXL (2B). There are two organic molecules and two solvent, CH_2Cl_2 molecules in the asymmetric unit. The non-hydrogen atoms were refined with anisotropic thermal parameters. The hydrogen atoms on N(1) and N(101 were located in a difference map and were refined freely. The remaining hydrogen atoms were included in idealised positions and their Uiso values were set to ride on the Ueq values of the parent carbon atoms. At the conclusion of the refinement, wR_2 = 0.103 and R_1 = 0.041 (2B) for all 11,425 reflections weighted $w = [\sigma^2(F_o^2) + (0.0625\ P)^2 + 0.8113\ P]^{-1}$ with $P = (F_o^2 + 2F_c^2)/3$; for the 'observed' data only, R_1 = 0.039. The Flack x parameter is 0.104(8) and the diagrams show the correct absolute configuration.

In the final difference map, the highest peak (*ca* 0.5 $eÅ^{-3}$) was near Cl(95).

Scattering factors for neutral atoms were taken from reference (3). Computer programs used in this analysis have been noted above, and were run through WinGX (4) on a Dell Optiplex 780 PC at the University of East Anglia.

References

(1) Programs CrysAlisPro, Rigaku Oxford Diffraction Ltd., Abingdon, UK (2018).

(2) G. M. Sheldrick, Programs for crystal structure determination (SHELXT), *Acta Cryst.* (2015) A**71**, 3-8, and refinement (SHELXL), *Acta Cryst.* (2008) A**64**, 112-122 and (2015) C**71**, 3-8.

(3) *'International Tables for X-ray Crystallography'*, Kluwer Academic Publishers, Dordrecht (1992). Vol. C, pp. 500, 219 and 193.

(4) L. J. Farrugia, *J. Appl. Cryst.* (2012) **45**, 849–854.

Legends for Figures

Figure 1 a and b. Views of the two independent tris-isoindole molecules, indicating the atom numbering scheme. Thermal ellipsoids are drawn at the 30% probability level.

Figure 2. View on to the plane of the benzo-isoindole group of one of the independent molecules, showing how the spiralling of the chain leads to the overlap of the phenyl groups

Figure 3. View of the two independent molecules and solvent molecules, showing the hydrogen bonds.

Figure 4. View of the packing of molecules, along the *b* axis, showing the potential for π...π interactions.

Notes on the structure

The crystal structure analysis shows two independent, tris-isoindole molecules and two solvent (CH_2Cl_2) molecules in the asymmetric unit. The principal molecules have very similar dimensions and conformations; the only significant differences are in the orientations of one of the methoxy groups; the methoxy group of O(57)–C(58) is the odd one out, Figure 1a and 1b. The two molecules are mirror images, Figure 1, and the crystals are therefore racemic mixtures.

Each molecule forms a spiral chain, from O(31) to C(24), N(14), C(40), C(50) and O(57) in the first molecule and correspondingly from O(131) to O(157) in the second. The phenyl groups in each molecule are essentially parallel and overlapping with interplanar distances *ca* 3.4 Å in both molecules, e.g. Figure 2.

The central, benzo-isoindole nitrogen atom in each molecule, N(1) and N(101), has a hydrogen attached; these hydrogen atoms form bifurcated hydrogen bonds to the other isoindole N atoms in the molecule. Each solvent molecule donates one hydrogen to a hydrogen bond to a 'bridging' N atom (between isoindole groups), Figure 3. There are several instances of π…π contacts between parallel (or almost parallel) planes but stacking appears to be limited to three planes; Figure 4 shows the packing of the molecules and the alignment of the aromatic groups.

Crystal data and structure refinement for
[Pd {$MeOC_6H_3$-CH-isoindole-N-(^{t}Bu-isoindole)-NCMeNH}]

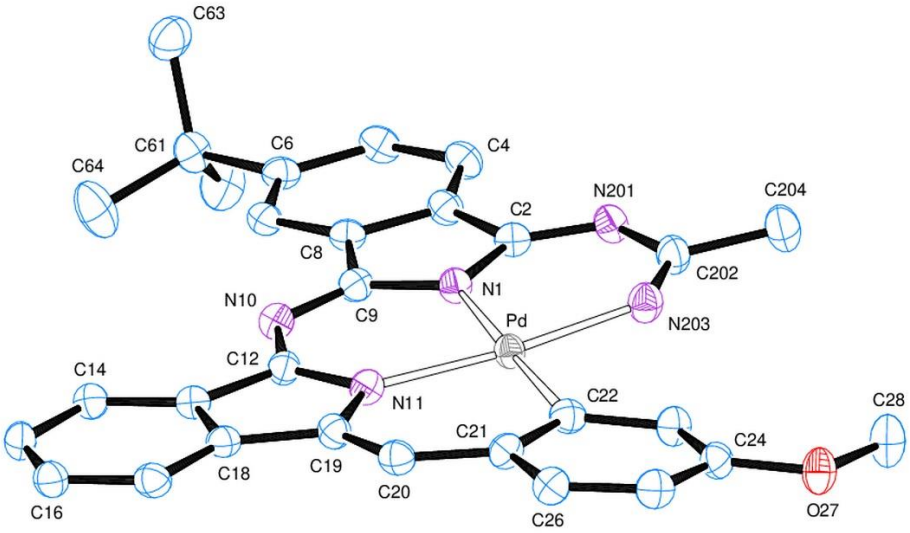

Identification code	isabf1586
Elemental formula	C30 H27 N5 O Pd
Formula weight	579.96
Crystal system, space group	Orthorhombic, Pbca (no. 61)
Unit cell dimensions	a = 6.48179(10) Å α = 90 ° b = 26.7151(5) Å β = 90 ° c = 29.1342(6) Å γ = 90 °
Volume	5044.93(16) $Å^3$
Z, Calculated density	8, 1.527 Mg/m^3
F(000)	2368
Absorption coefficient	6.198 mm^{-1}
Temperature	100(2) K
Wavelength	1.54184 Å
Crystal colour, shape	dark red needle
Crystal size	0.40 x 0.04 x 0.04 mm

Crystal mounting: on a small loop, in oil, fixed in cold N_2 stream

On the diffractometer:

Theta range for data collection	7.663 to 72.487 °
Limiting indices	-6<=h<=8, -33<=k<=21, -35<=l<=36
Completeness to theta = 67.684	99.5 %

Absorption correction	Semi-empirical from equivalents
Max. and min. transmission	1.00000 and 0.51965
Reflections collected (not including absences)	19408
No. of unique reflections	4843 [R(int) for equivalents = 0.035]
No. of 'observed' reflections ($I > 2\sigma_I$)	4429
Structure determined by:	dual methods, in SHELXT
Refinement:	Full-matrix least-squares on F^2, in SHELXL
Data / restraints / parameters	4843 / 0 / 358
Goodness-of-fit on F^2	1.082
Final R indices ('observed' data)	R1 = 0.030, wR2 = 0.081
Final R indices (all data)	R1 = 0.032, wR2 = 0.083
Reflections weighted: $w = [\sigma^2(Fo^2)+(0.0435P)^2+3.8822P]^{-1}$ where $P=(Fo^2+2Fc^2)/3$	
Extinction coefficient	n/a
Largest diff. peak and hole	0.56 and -0.67 e.Å^{-3}
Location of largest difference peak	near the Pd atom

Table 1. Atomic coordinates (x 10^5) and equivalent isotropic displacement parameters ($Å^2$ x 10^4). U(eq) is defined as one third of the trace of the orthogonalized Uij tensor. E.s.ds are in parentheses.

	x	y	z	U(eq)
Pd	30247(2)	37315(2)	36030(2)	192.9(8)
N(1)	14520(30)	31756(7)	39293(7)	215(4)
C(2)	-3360(40)	32320(8)	41739(8)	216(5)
C(3)	-10430(40)	27361(8)	43305(8)	228(5)
C(4)	-27510(40)	25782(9)	45783(9)	252(5)
C(5)	-29580(40)	20663(9)	46512(8)	256(5)
C(6)	-15390(40)	17142(9)	44899(8)	234(5)
C(7)	1910(40)	18842(8)	42485(8)	221(5)
C(8)	3960(30)	23916(8)	41743(8)	210(4)
C(9)	19550(30)	26786(9)	39194(8)	214(5)
N(10)	35290(30)	24639(7)	37204(7)	222(4)
N(11)	50670(30)	32216(7)	33955(7)	219(4)
C(12)	49660(40)	27277(8)	34819(8)	213(5)
C(13)	67360(30)	24736(9)	32877(8)	215(5)
C(14)	72770(40)	19674(9)	32780(8)	238(5)
C(15)	91130(40)	18404(9)	30608(8)	261(5)
C(16)	103630(40)	22080(9)	28636(8)	258(5)
C(17)	98260(40)	27109(9)	28727(8)	247(5)
C(18)	79790(30)	28386(9)	30874(8)	216(5)
C(19)	69200(30)	33149(9)	31580(8)	219(5)
C(20)	75610(40)	37738(8)	30291(9)	232(5)
C(21)	65180(40)	42455(8)	30831(8)	220(5)
C(22)	45270(40)	43013(8)	32822(8)	231(5)
C(23)	36570(40)	47835(8)	32577(8)	239(5)
C(24)	47230(40)	51936(8)	30832(8)	237(5)
C(25)	67160(40)	51378(9)	29129(9)	253(5)
C(26)	75750(40)	46678(9)	29062(8)	243(5)
O(27)	39390(30)	56695(6)	30551(6)	280(4)
C(28)	19280(40)	57615(10)	32332(11)	338(6)
C(61)	-18670(40)	11552(10)	45883(9)	266(5)
C(62)	-41180(40)	10117(10)	44898(11)	379(6)
C(63)	-13940(50)	10604(10)	50928(10)	356(6)
C(64)	-4480(50)	8261(10)	42977(11)	424(7)
N(201)	-13520(30)	36423(7)	42691(7)	241(4)
C(202)	-6980(40)	41012(9)	41189(9)	255(5)
N(203)	9200(30)	41903(8)	38690(7)	256(4)
C(204)	-20610(40)	45241(10)	42686(11)	327(6)

Table 2. Molecular dimensions. Bond lengths are in Ångstroms, angles in degrees. E.s.ds are in parentheses.

Pd-N(203)	1.991(2)	N(203)-Pd-N(11)	173.61(8)
Pd-N(11)	1.9933(19)	N(203)-Pd-C(22)	92.66(9)
Pd-C(22)	2.034(2)	N(11)-Pd-C(22)	93.09(9)
Pd-N(1)	2.0367(19)	N(203)-Pd-N(1)	85.66(8)
		N(11)-Pd-N(1)	88.60(8)
		C(22)-Pd-N(1)	178.30(9)
N(1)-C(9)	1.367(3)	C(18)-C(19)	1.460(3)
N(1)-C(2)	1.369(3)	C(19)-C(20)	1.348(3)
C(2)-N(201)	1.308(3)	C(20)-C(21)	1.439(3)
C(2)-C(3)	1.474(3)	C(21)-C(26)	1.417(3)
C(3)-C(4)	1.387(3)	C(21)-C(22)	1.422(3)
C(3)-C(8)	1.388(3)	C(22)-C(23)	1.408(3)
C(4)-C(5)	1.390(4)	C(23)-C(24)	1.391(3)
C(5)-C(6)	1.397(3)	C(23)-H(23)	0.91(3)
C(6)-C(7)	1.400(3)	C(24)-O(27)	1.372(3)
C(6)-C(61)	1.535(3)	C(24)-C(25)	1.392(3)
C(7)-C(8)	1.379(3)	C(25)-C(26)	1.374(3)
C(8)-C(9)	1.470(3)	O(27)-C(28)	1.424(3)
C(9)-N(10)	1.306(3)	C(61)-C(63)	1.523(4)
N(10)-C(12)	1.359(3)	C(61)-C(64)	1.528(4)
N(11)-C(12)	1.345(3)	C(61)-C(62)	1.535(4)
N(11)-C(19)	1.409(3)	N(201)-C(202)	1.369(3)
C(12)-C(13)	1.448(3)	C(202)-N(203)	1.299(3)
C(13)-C(18)	1.393(3)	C(202)-C(204)	1.499(3)
C(13)-C(14)	1.397(3)	N(203)-H(203)	0.85(3)
C(14)-C(15)	1.390(4)	C(204)-H(20A)	0.95(3)
C(15)-C(16)	1.397(4)	C(204)-H(20B)	0.95(4)
C(16)-C(17)	1.388(3)	C(204)-H(20C)	0.99(4)
C(17)-C(18)	1.393(3)		
C(9)-N(1)-C(2)	108.64(19)	N(11)-C(12)-N(10)	129.6(2)
C(9)-N(1)-Pd	125.37(16)	N(11)-C(12)-C(13)	110.4(2)
C(2)-N(1)-Pd	125.90(15)	N(10)-C(12)-C(13)	120.0(2)
N(201)-C(2)-N(1)	128.9(2)	C(18)-C(13)-C(14)	121.6(2)
N(201)-C(2)-C(3)	122.1(2)	C(18)-C(13)-C(12)	107.1(2)
N(1)-C(2)-C(3)	109.00(19)	C(14)-C(13)-C(12)	131.3(2)
C(4)-C(3)-C(8)	120.4(2)	C(15)-C(14)-C(13)	117.4(2)
C(4)-C(3)-C(2)	133.0(2)	C(14)-C(15)-C(16)	120.8(2)
C(8)-C(3)-C(2)	106.6(2)	C(17)-C(16)-C(15)	121.8(2)
C(3)-C(4)-C(5)	117.1(2)	C(16)-C(17)-C(18)	117.5(2)
C(4)-C(5)-C(6)	123.2(2)	C(17)-C(18)-C(13)	120.9(2)
C(5)-C(6)-C(7)	118.6(2)	C(17)-C(18)-C(19)	132.9(2)
C(5)-C(6)-C(61)	120.1(2)	C(13)-C(18)-C(19)	106.20(19)
C(7)-C(6)-C(61)	121.4(2)	C(20)-C(19)-N(11)	124.1(2)
C(8)-C(7)-C(6)	118.4(2)	C(20)-C(19)-C(18)	127.5(2)
C(7)-C(8)-C(3)	122.4(2)	N(11)-C(19)-C(18)	108.42(19)
C(7)-C(8)-C(9)	131.2(2)	C(19)-C(20)-C(21)	128.4(2)
C(3)-C(8)-C(9)	106.38(19)	C(26)-C(21)-C(22)	120.2(2)
N(10)-C(9)-N(1)	128.5(2)	C(26)-C(21)-C(20)	115.5(2)
N(10)-C(9)-C(8)	122.1(2)	C(22)-C(21)-C(20)	124.2(2)
N(1)-C(9)-C(8)	109.39(19)	C(23)-C(22)-C(21)	116.0(2)
C(9)-N(10)-C(12)	122.3(2)	C(23)-C(22)-Pd	121.07(18)
C(12)-N(11)-C(19)	107.87(19)	C(21)-C(22)-Pd	122.91(17)
C(12)-N(11)-Pd	125.55(16)	C(24)-C(23)-C(22)	122.7(2)
C(19)-N(11)-Pd	126.48(15)	C(24)-C(23)-H(23)	116.3(18)

C(22)-C(23)-H(23)	121.0(18)	C(2)-N(201)-C(202)	121.8(2)
O(27)-C(24)-C(23)	124.6(2)	N(203)-C(202)-N(201)	126.4(2)
O(27)-C(24)-C(25)	115.0(2)	N(203)-C(202)-C(204)	120.1(2)
C(23)-C(24)-C(25)	120.5(2)	N(201)-C(202)-C(204)	113.6(2)
C(26)-C(25)-C(24)	118.6(2)	C(202)-N(203)-Pd	131.21(17)
C(25)-C(26)-C(21)	121.8(2)	C(202)-N(203)-H(203)	113(2)
C(24)-O(27)-C(28)	118.51(19)	Pd-N(203)-H(203)	116(2)
C(63)-C(61)-C(64)	108.5(2)	C(202)-C(204)-H(20A)	109.4(17)
C(63)-C(61)-C(6)	108.3(2)	C(202)-C(204)-H(20B)	110(2)
C(64)-C(61)-C(6)	111.9(2)	H(20A)-C(204)-H(20B)	111(3)
C(63)-C(61)-C(62)	109.3(2)	C(202)-C(204)-H(20C)	108(2)
C(64)-C(61)-C(62)	108.9(2)	H(20A)-C(204)-H(20C)	109(3)
C(6)-C(61)-C(62)	109.8(2)	H(20B)-C(204)-H(20C)	109(3)

Table 3. Anisotropic displacement parameters ($Å^2$ x 10^4) for the expression:

$$\exp\{-2\pi^2(h^2a^{*2}U_{11} + \ldots + 2hka^*b^*U_{12})\}$$

E.s.ds are in parentheses.

	U_{11}	U_{22}	U_{33}	U_{23}	U_{13}	U_{12}
Pd	186.8(12)	174.6(12)	217.5(12)	1.2(6)	19.4(6)	0.2(6)
N(1)	213(9)	202(9)	231(10)	3(7)	19(8)	1(8)
C(2)	207(11)	231(11)	211(11)	5(9)	1(9)	-22(9)
C(3)	224(11)	229(11)	232(11)	-23(9)	0(9)	-10(9)
C(4)	228(11)	274(12)	255(12)	-32(10)	39(9)	-13(10)
C(5)	235(12)	286(12)	249(12)	-25(10)	43(9)	-51(9)
C(6)	263(11)	244(11)	195(11)	-7(9)	-15(9)	-40(10)
C(7)	240(11)	221(11)	202(11)	-20(9)	-5(9)	-2(9)
C(8)	207(11)	238(11)	185(10)	-3(9)	-8(9)	-24(9)
C(9)	223(12)	206(11)	214(12)	2(9)	-14(9)	-15(9)
N(10)	193(9)	225(9)	246(10)	10(8)	-4(8)	-11(8)
N(11)	210(9)	211(9)	234(10)	14(7)	-3(8)	-9(8)
C(12)	219(11)	194(10)	227(11)	-11(9)	-33(9)	15(9)
C(13)	218(11)	226(11)	201(11)	2(9)	-2(9)	-4(9)
C(14)	259(11)	223(11)	233(12)	-3(9)	1(10)	6(9)
C(15)	275(12)	231(11)	279(12)	-16(9)	-23(10)	69(10)
C(16)	229(11)	304(12)	242(12)	-16(9)	13(9)	57(10)
C(17)	231(11)	290(12)	219(11)	2(9)	19(9)	6(10)
C(18)	224(12)	239(12)	185(11)	-7(9)	-17(8)	7(9)
C(19)	195(11)	231(12)	232(11)	-9(9)	2(9)	9(8)
C(20)	206(11)	267(13)	221(13)	4(8)	29(10)	-8(10)
C(21)	216(11)	208(11)	237(11)	25(9)	0(9)	-19(9)
C(22)	242(11)	227(11)	223(11)	-16(9)	-14(9)	-28(9)
C(23)	214(12)	211(11)	291(12)	9(9)	14(10)	-13(9)
C(24)	268(12)	188(11)	254(12)	-24(9)	-20(10)	5(9)
C(25)	260(12)	218(11)	282(12)	15(9)	8(10)	-62(9)
C(26)	204(10)	260(12)	266(12)	5(9)	0(10)	-11(10)
O(27)	248(8)	188(8)	402(10)	15(7)	27(8)	-16(7)
C(28)	269(14)	235(12)	510(17)	23(11)	65(12)	21(10)
C(61)	263(13)	224(11)	311(13)	-18(10)	33(10)	-38(9)
C(62)	337(15)	265(13)	536(18)	16(12)	-49(13)	-95(11)
C(63)	422(15)	287(13)	360(15)	61(11)	-19(13)	-8(12)
C(64)	498(17)	226(12)	549(18)	-71(12)	218(15)	-91(12)
N(201)	243(10)	215(9)	264(10)	-14(8)	42(9)	0(8)
C(202)	249(12)	240(11)	276(12)	0(9)	38(10)	36(10)
N(203)	255(10)	216(10)	296(11)	28(8)	34(9)	4(8)
C(204)	376(16)	230(13)	376(16)	10(11)	131(12)	31(11)

Table 4. Hydrogen coordinates (x 10^4) and isotropic displacement parameters (A^2 x 10^3). The hydrogens close to N(203) were located in a difference map and were refined freely. All remaining hydrogen atoms were included in idealised positions with U(iso)'s set at 1.2*U(eq) or, for the methyl group hydrogen atoms, 1.5*U(eq) of the parent carbon atoms.

	x	y	z	U(iso)
H(4)	-3737	2810	4693	30
H(5)	-4120	1950	4819	31
H(7)	1199	1656	4138	27
H(14)	6423	1720	3415	29
H(15)	9523	1499	3046	31
H(16)	11615	2111	2719	31
H(17)	10685	2959	2738	30
H(20)	8872	3788	2884	28
H(25)	7466	5419	2803	30
H(26)	8914	4625	2780	29
H(28A)	923	5554	3069	51
H(28B)	1578	6115	3192	51
H(28C)	1899	5679	3561	51
H(62A)	-4468	1103	4174	57
H(62B)	-5030	1190	4703	57
H(62C)	-4293	650	4530	57
H(63A)	-1607	705	5163	53
H(63B)	-2314	1264	5284	53
H(63C)	42	1151	5157	53
H(64A)	-741	882	3972	64
H(64B)	-687	473	4373	64
H(64C)	993	912	4362	64
H(20A)	-2040(40)	4547(11)	4593(11)	26(7)
H(20B)	-1600(50)	4826(13)	4133(12)	47(9)
H(20C)	-3490(60)	4454(12)	4163(12)	46(9)
H(203)	1080(50)	4500(13)	3810(11)	40(9)
H(23)	2330(50)	4840(11)	3347(11)	31(8)

Table 5. Torsion angles, in degrees. E.s.ds are in parentheses.

C(9)-N(1)-C(2)-N(201)	179.6(2)	C(16)-C(17)-C(18)-C(13)	0.5(3)
Pd-N(1)-C(2)-N(201)	-3.5(4)	C(16)-C(17)-C(18)-C(19)	-179.1(2)
C(9)-N(1)-C(2)-C(3)	-0.3(3)	C(14)-C(13)-C(18)-C(17)	-0.6(4)
Pd-N(1)-C(2)-C(3)	176.50(15)	C(12)-C(13)-C(18)-C(17)	179.5(2)
N(201)-C(2)-C(3)-C(4)	1.4(4)	C(14)-C(13)-C(18)-C(19)	179.2(2)
N(1)-C(2)-C(3)-C(4)	-178.6(3)	C(12)-C(13)-C(18)-C(19)	-0.8(3)
N(201)-C(2)-C(3)-C(8)	-179.4(2)	C(12)-N(11)-C(19)-C(20)	-177.7(2)
N(1)-C(2)-C(3)-C(8)	0.6(3)	Pd-N(11)-C(19)-C(20)	-1.2(3)
C(8)-C(3)-C(4)-C(5)	-1.3(4)	C(12)-N(11)-C(19)-C(18)	1.5(3)
C(2)-C(3)-C(4)-C(5)	177.8(2)	Pd-N(11)-C(19)-C(18)	178.09(15)
C(3)-C(4)-C(5)-C(6)	0.3(4)	C(17)-C(18)-C(19)-C(20)	-1.5(4)
C(4)-C(5)-C(6)-C(7)	0.9(4)	C(13)-C(18)-C(19)-C(20)	178.8(2)
C(4)-C(5)-C(6)-C(61)	179.5(2)	C(17)-C(18)-C(19)-N(11)	179.3(2)
C(5)-C(6)-C(7)-C(8)	-1.1(3)	C(13)-C(18)-C(19)-N(11)	-0.4(3)
C(61)-C(6)-C(7)-C(8)	-179.6(2)	N(11)-C(19)-C(20)-C(21)	-2.9(4)
C(6)-C(7)-C(8)-C(3)	0.1(3)	C(18)-C(19)-C(20)-C(21)	178.0(2)
C(6)-C(7)-C(8)-C(9)	-176.8(2)	C(19)-C(20)-C(21)-C(26)	-179.2(3)
C(4)-C(3)-C(8)-C(7)	1.1(4)	C(19)-C(20)-C(21)-C(22)	-1.5(4)
C(2)-C(3)-C(8)-C(7)	-178.2(2)	C(26)-C(21)-C(22)-C(23)	4.7(3)
C(4)-C(3)-C(8)-C(9)	178.7(2)	C(20)-C(21)-C(22)-C(23)	-172.9(2)
C(2)-C(3)-C(8)-C(9)	-0.6(2)	C(26)-C(21)-C(22)-Pd	-173.49(18)
C(2)-N(1)-C(9)-N(10)	179.5(2)	C(20)-C(21)-C(22)-Pd	8.9(3)
Pd-N(1)-C(9)-N(10)	2.6(4)	C(21)-C(22)-C(23)-C(24)	-4.9(3)
C(2)-N(1)-C(9)-C(8)	-0.1(3)	Pd-C(22)-C(23)-C(24)	173.28(19)
Pd-N(1)-C(9)-C(8)	-176.92(15)	C(22)-C(23)-C(24)-O(27)	-179.7(2)
C(7)-C(8)-C(9)-N(10)	-1.8(4)	C(22)-C(23)-C(24)-C(25)	1.5(4)
C(3)-C(8)-C(9)-N(10)	-179.1(2)	O(27)-C(24)-C(25)-C(26)	-176.7(2)
C(7)-C(8)-C(9)-N(1)	177.7(2)	C(23)-C(24)-C(25)-C(26)	2.2(4)
C(3)-C(8)-C(9)-N(1)	0.5(3)	C(24)-C(25)-C(26)-C(21)	-2.4(4)
N(1)-C(9)-N(10)-C(12)	0.1(4)	C(22)-C(21)-C(26)-C(25)	-1.2(4)
C(8)-C(9)-N(10)-C(12)	179.6(2)	C(20)-C(21)-C(26)-C(25)	176.6(2)
C(19)-N(11)-C(12)-N(10)	176.4(2)	C(23)-C(24)-O(27)-C(28)	2.8(4)
Pd-N(11)-C(12)-N(10)	-0.2(4)	C(25)-C(24)-O(27)-C(28)	-178.4(2)
C(19)-N(11)-C(12)-C(13)	-2.0(3)	C(5)-C(6)-C(61)-C(63)	-73.2(3)
Pd-N(11)-C(12)-C(13)	-178.64(15)	C(7)-C(6)-C(61)-C(63)	105.3(3)
C(9)-N(10)-C(12)-N(11)	-1.5(4)	C(5)-C(6)-C(61)-C(64)	167.2(2)
C(9)-N(10)-C(12)-C(13)	176.9(2)	C(7)-C(6)-C(61)-C(64)	-14.3(3)
N(11)-C(12)-C(13)-C(18)	1.8(3)	C(5)-C(6)-C(61)-C(62)	46.1(3)
N(10)-C(12)-C(13)-C(18)	-176.9(2)	C(7)-C(6)-C(61)-C(62)	-135.4(2)
N(11)-C(12)-C(13)-C(14)	-178.1(2)	N(1)-C(2)-N(201)-C(202)	0.6(4)
N(10)-C(12)-C(13)-C(14)	3.2(4)	C(3)-C(2)-N(201)-C(202)	-179.4(2)
C(18)-C(13)-C(14)-C(15)	0.1(4)	C(2)-N(201)-C(202)-N(203)	0.9(4)
C(12)-C(13)-C(14)-C(15)	-180.0(2)	C(2)-N(201)-C(202)-C(204)	-179.4(2)
C(13)-C(14)-C(15)-C(16)	0.4(4)	N(201)-C(202)-N(203)-Pd	0.7(4)
C(14)-C(15)-C(16)-C(17)	-0.5(4)	C(204)-C(202)-N(203)-Pd	-179.0(2)
C(15)-C(16)-C(17)-C(18)	0.0(4)		

Crystal structure analysis of

[Pd {$MeOC_6H_3$-CH-isoindole-N-(^{t}Bu-isoindole)-NCMeNH}]

Crystal data: $C_{30}H_{27}N_5OPd$, M = 579.96. Orthorhombic, space group Pbca (no. 61), a = 6.48179(10), b = 26.7151(5), c = 29.1342(6) Å, V = 5044.93(16) Å^3. Z = 8, Dc = 1.527 g cm^{-3}, F(000) = 2368, T = 100(2) K, μ(Cu-Kα) = 61.98 cm^{-1}, λ(Cu-Kα) = 1.54184 Å.

The crystal was a dark red needle. From a sample under oil, one, *ca* 0.04 x 0.04 x 0.40 mm, was mounted on a small loop and fixed in the cold nitrogen stream on a Rigaku Oxford Diffraction XtaLAB Synergy diffractometer, equipped with Cu-Kα radiation, HyPix detector and mirror monochromator. Intensity data were measured by thin-slice ω-scans. Total no. of reflections recorded, to θ_{max} = 72.5°, was 19,408 of which 4,843 were unique (Rint = 0.035); 4429 were 'observed' with $I > 2\sigma_I$.

Data were processed using the CrysAlisPro-CCD and -RED (1) programs. The structure was determined by the intrinsic phasing routines in the SHELXT program (2A) and refined by full-matrix least-squares methods, on F^2's, in SHELXL (2B). The non-hydrogen atoms were refined with anisotropic thermal parameters. The hydrogen atom of the amino group, N(203), and neighbouring H atoms were located in difference maps and were refined freely. The remaining hydrogen atoms were included in idealised positions and their Uiso values were set to ride on the Ueq values of the parent carbon atoms. At the conclusion of the refinement, wR_2 = 0.083 and R_1 = 0.032 (2B) for all 4843 reflections weighted w = $[\sigma^2(F_o^2) + (0.0435\ P)^2 + 3.8822\ P]^{-1}$ with P = $(F_o^2 + 2F_c^2)/3$; for the 'observed' data only, R_1 = 0.030.

In the final difference map, the highest peak (*ca* 0.6 eÅ^{-3}) was near the Pd atom.

Scattering factors for neutral atoms were taken from reference (3). Computer programs used in this analysis have been noted above, and were run through WinGX (4) on a Dell Optiplex 780 PC at the University of East Anglia.

References

(5) Programs CrysAlisPro, Rigaku Oxford Diffraction Ltd., Abingdon, UK (2018).

(6) G. M. Sheldrick, Programs for crystal structure determination (SHELXT), *Acta Cryst.* (2015) A**71**, 3-8, and refinement (SHELXL), *Acta Cryst.* (2008) A**64**, 112-122 and (2015) C**71**, 3-8.

(7) *'International Tables for X-ray Crystallography'*, Kluwer Academic Publishers, Dordrecht (1992). Vol. C, pp. 500, 219 and 193.

(8) L. J. Farrugia, *J. Appl. Cryst.* (2012) **45**, 849–854.

Legends for Figures

Figure 1. View of the [Pd {$MeOC_6H_3$-CH-isoindole-N-(^{t}Bu-isoindole)-NCMeNH}] molecule, indicating the atom numbering scheme. Thermal ellipsoids are drawn at the 50% probability level.

Figure 2. The packing of molecules, viewed along the *a* axis.

Figure 3. View showing the overlapping of the right-hand side of the Pd molecule over the left-hand side of the Pd'molecule below.

Notes on the structure

Coordination about the palladium centre is square planar and the planarity extends across most of the molecule; only the *t*-butyl and methoxy groups deviate significantly from this plane, Figure 1. Columns of molecules stack parallel to the *a* axis, (Figure 2) with the isoindole group of N(1) and the NCMeNH group of C(202) lying over the isoindole ligand of N(11) and the phenyl group of the lower molecule, Figure 3.

There are no apparent hydrogen bond acceptor groups for the N(203)-H donor atom, but there are close interactions for H(203), the shortest of which is H(203)…H(23) at 1.75 A. All the H atoms in this region were located as difference peaks; they were initially included with idealised geometries in the refinement process, but were later refined independently and freely. Some of the interatomic distances are, indeed, short, from both approaches

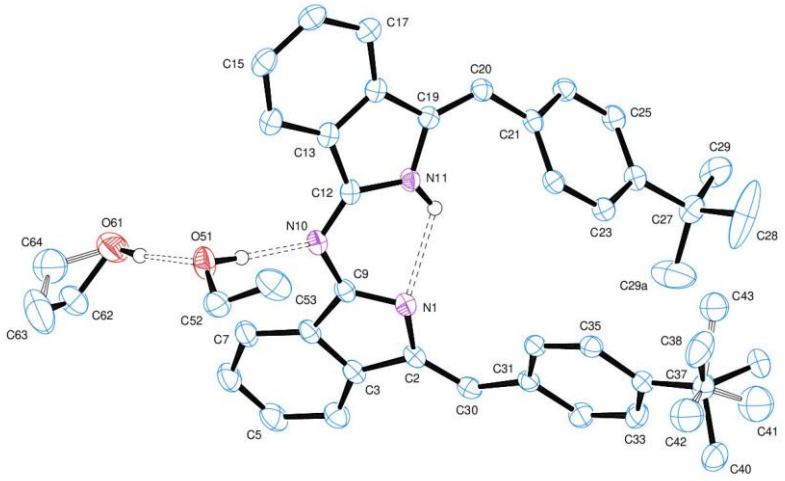

Crystal data and structure refinement for
Bu^t-C_6H_4-CH-isoindole-N-(isoindole-H)-CH-C_6H_4-Bu^t

Identification code	isabf1675
Elemental formula	C38 H37 N3, 2(C2 H6 O)
Formula weight	627.84
Crystal system, space group	Monoclinic, $P2_1/n$ (no. 14)
Unit cell dimensions	a = 21.2122(4) Å α = 90 ° b = 8.49586(12) Å β = 114.313(2) ° c = 22.1333(4) Å γ = 90 °
Volume	3635.02(12) $Å^3$
Z, Calculated density	4, 1.147 Mg/m^3
F(000)	1352
Absorption coefficient	0.543 mm^{-1}
Temperature	100(2) K
Wavelength	1.54184 Å
Crystal colour, shape	orange cuboid
Crystal size	0.93 x 0.21 x 0.18 mm
Crystal mounting:	on a small loop, in oil, fixed in cold N_2 stream
On the diffractometer:	
Theta range for data collection	7.748 to 72.457 °
Limiting indices	-26<=h<=23, -10<=k<=10, -16<=l<=27
Completeness to theta = 67.684	99.7 %
Absorption correction	Semi-empirical from equivalents
Max. and min. transmission	1.00000 and 0.36696
Reflections collected (not including absences)	29580
No. of unique reflections	6998 [R(int) for equivalents = 0.052]
No. of 'observed' reflections ($I > 2\sigma_I$)	6241
Structure determined by:	dual methods, in SHELXT
Refinement:	Full-matrix least-squares on F^2, in SHELXL
Data / restraints / parameters	6998 / 0 / 460
Goodness-of-fit on F^2	1.038
Final R indices ('observed' data)	R_1 = 0.049, wR_2 = 0.126
Final R indices (all data)	R_1 = 0.054, wR_2 = 0.130

Reflections weighted:
$w = [\sigma^2(Fo^2)+(0.0634P)^2+1.4249P]^{-1}$ where $P=(Fo^2+2Fc^2)/3$

Extinction coefficient	n/a
Largest diff. peak and hole	0.33 and -0.36 e.Å^{-3}
Location of largest difference peak	near O(61)

Table 1. Atomic coordinates (x 10^5) and equivalent isotropic displacement parameters ($Å^2$ x 10^4). U(eq) is defined as one third of the trace of the orthogonalized Uij tensor. E.s.ds are in parentheses.

	x	y	z	U(eq)	S.o.f.#
N(1)	67667(6)	38650(14)	40697(5)	236(2)	
C(2)	73817(7)	30214(16)	42027(6)	236(3)	
C(3)	78493(7)	32365(17)	49091(7)	254(3)	
C(4)	84941(8)	26212(19)	53099(7)	318(3)	
C(5)	87938(8)	31010(20)	59686(8)	372(4)	
C(6)	84648(8)	41660(20)	62206(7)	362(4)	
C(7)	78207(8)	47875(19)	58236(7)	300(3)	
C(8)	75180(7)	42991(17)	51633(7)	248(3)	
C(9)	68430(7)	46148(16)	46184(6)	229(3)	
N(10)	63565(6)	55677(14)	46949(5)	237(3)	
N(11)	54317(6)	40418(13)	39154(5)	228(2)	
C(12)	56981(7)	52617(16)	43415(6)	225(3)	
C(13)	51061(7)	60927(16)	43734(6)	236(3)	
C(14)	50721(8)	74409(17)	47175(7)	280(3)	
C(15)	44216(9)	79453(17)	46448(8)	314(3)	
C(16)	38239(8)	71156(18)	42496(7)	311(3)	
C(17)	38580(8)	57530(18)	39170(7)	278(3)	
C(18)	45080(7)	52506(16)	39833(6)	234(3)	
C(19)	47133(7)	38906(16)	37006(6)	220(3)	
C(20)	43228(7)	26874(16)	33469(6)	233(3)	
C(21)	45648(7)	13688(16)	30721(6)	222(3)	
C(22)	50375(7)	15625(16)	27851(6)	230(3)	
C(23)	52392(7)	3035(16)	25093(6)	242(3)	
C(24)	49858(7)	-12155(16)	25106(6)	239(3)	
C(25)	45256(8)	-14104(17)	28085(7)	263(3)	
C(26)	43089(7)	-1468(17)	30725(6)	253(3)	
C(27)	52024(9)	-25588(17)	21746(8)	314(3)	
C(28)	49070(20)	-22440(30)	14347(11)	1023(13)	
C(29)	49411(11)	-41396(19)	22849(11)	450(4)	
C(29A)	59902(12)	-26490(30)	24526(19)	894(10)	
C(30)	75246(7)	22121(17)	37482(7)	251(3)	
C(31)	71334(7)	21207(16)	30285(7)	232(3)	
C(32)	73541(8)	10736(18)	26666(7)	292(3)	
C(33)	70468(8)	10391(18)	19811(7)	302(3)	
C(34)	65047(7)	20582(17)	16187(7)	253(3)	
C(35)	62710(7)	30604(16)	19798(7)	241(3)	
C(36)	65753(7)	31054(16)	26695(7)	235(3)	
C(37)	62081(8)	20732(19)	8575(7)	322(3)	
C(38)	56454(11)	33020(30)	5563(8)	503(6)	0.942(4)
C(39)	59152(10)	4410(30)	5926(9)	414(5)	0.942(4)
C(40)	68008(10)	24360(20)	6460(9)	394(5)	0.942(4)
C(41)	62700(200)	8900(500)	5200(200)	600(100)*	0.058(4)
C(42)	63030(190)	38600(400)	5960(180)	530(90)*	0.058(4)
C(43)	52790(160)	23700(400)	6110(150)	390(70)*	0.058(4)
O(51)	67255(6)	85263(14)	53177(5)	382(3)	
C(52)	69112(9)	95400(20)	49020(8)	376(4)	
C(53)	63959(10)	95030(20)	41981(9)	476(5)	
O(61)	71959(7)	78490(20)	66387(7)	580(4)	
C(62)	78587(12)	84990(30)	69757(11)	492(8)	0.859(8)

C(63)	78842(13)	102480(30)	69390(13)	771(8)	
C(64)	75910(100)	87900(200)	71760(80)	560(50)*	0.141(8)

- site occupancy, if different from 1.
* - U(iso) ($Å^2$ x 10^4)

Table 2. Molecular dimensions. Bond lengths are in ÅAngstroms, angles in degrees. E.s.ds are in parentheses.

N(1)-C(9)	1.3208(18)	C(24)-C(25)	1.394(2)
N(1)-C(2)	1.4093(18)	C(24)-C(27)	1.532(2)
C(2)-C(30)	1.352(2)	C(25)-C(26)	1.388(2)
C(2)-C(3)	1.4780(18)	C(27)-C(29)	1.511(2)
C(3)-C(4)	1.390(2)	C(27)-C(28)	1.517(3)
C(3)-C(8)	1.397(2)	C(27)-C(29A)	1.527(3)
C(4)-C(5)	1.390(2)	C(30)-C(31)	1.4640(19)
C(5)-C(6)	1.392(2)	C(31)-C(36)	1.399(2)
C(6)-C(7)	1.389(2)	C(31)-C(32)	1.400(2)
C(7)-C(8)	1.3956(19)	C(32)-C(33)	1.383(2)
C(8)-C(9)	1.4679(19)	C(33)-C(34)	1.398(2)
C(9)-N(10)	1.3759(18)	C(34)-C(35)	1.3914(19)
N(10)-C(12)	1.3153(18)	C(34)-C(37)	1.5368(19)
N(11)-C(12)	1.3580(17)	C(35)-C(36)	1.3917(19)
N(11)-C(19)	1.4028(18)	C(37)-C(41)	1.29(4)
N(11)-H(11)	0.8800	C(37)-C(38)	1.518(2)
C(12)-C(13)	1.468(2)	C(37)-C(39)	1.534(2)
C(13)-C(14)	1.3937(19)	C(37)-C(40)	1.543(2)
C(13)-C(18)	1.402(2)	C(37)-C(42)	1.67(4)
C(14)-C(15)	1.389(2)	C(37)-C(43)	1.83(3)
C(15)-C(16)	1.399(2)		
C(16)-C(17)	1.390(2)	O(51)-C(52)	1.429(2)
C(17)-C(18)	1.392(2)	O(51)-H(51)	0.94(3)
C(18)-C(19)	1.4631(19)	C(52)-C(53)	1.490(2)
C(19)-C(20)	1.345(2)		
C(20)-C(21)	1.4648(19)	O(61)-C(64)	1.392(17)
C(21)-C(26)	1.398(2)	O(61)-C(62)	1.405(2)
C(21)-C(22)	1.4002(19)	O(61)-H(61)	0.99(3)
C(22)-C(23)	1.3838(19)	C(62)-C(63)	1.491(4)
C(23)-C(24)	1.3985(19)	C(63)-C(64)	1.569(17)
C(9)-N(1)-C(2)	107.50(11)	C(15)-C(14)-C(13)	117.55(14)
C(30)-C(2)-N(1)	125.11(12)	C(14)-C(15)-C(16)	121.21(14)
C(30)-C(2)-C(3)	126.27(13)	C(17)-C(16)-C(15)	121.31(14)
N(1)-C(2)-C(3)	108.57(11)	C(16)-C(17)-C(18)	117.70(14)
C(4)-C(3)-C(8)	120.80(13)	C(17)-C(18)-C(13)	120.96(13)
C(4)-C(3)-C(2)	133.17(14)	C(17)-C(18)-C(19)	130.79(13)
C(8)-C(3)-C(2)	106.03(12)	C(13)-C(18)-C(19)	108.25(12)
C(3)-C(4)-C(5)	117.65(15)	C(20)-C(19)-N(11)	126.12(13)
C(4)-C(5)-C(6)	121.50(14)	C(20)-C(19)-C(18)	128.94(13)
C(7)-C(6)-C(5)	121.24(14)	N(11)-C(19)-C(18)	104.82(11)
C(6)-C(7)-C(8)	117.26(14)	C(19)-C(20)-C(21)	125.85(13)
C(7)-C(8)-C(3)	121.55(13)	C(26)-C(21)-C(22)	117.36(12)
C(7)-C(8)-C(9)	132.74(14)	C(26)-C(21)-C(20)	120.12(12)
C(3)-C(8)-C(9)	105.63(11)	C(22)-C(21)-C(20)	122.50(12)
N(1)-C(9)-N(10)	125.64(12)	C(23)-C(22)-C(21)	121.24(13)
N(1)-C(9)-C(8)	112.09(12)	C(22)-C(23)-C(24)	121.56(13)
N(10)-C(9)-C(8)	122.25(12)	C(25)-C(24)-C(23)	117.07(13)
C(12)-N(10)-C(9)	118.49(12)	C(25)-C(24)-C(27)	123.31(13)
C(12)-N(11)-C(19)	112.87(11)	C(23)-C(24)-C(27)	119.59(12)
N(10)-C(12)-N(11)	126.89(13)	C(26)-C(25)-C(24)	121.66(13)
N(10)-C(12)-C(13)	126.61(12)	C(25)-C(26)-C(21)	121.07(13)
N(11)-C(12)-C(13)	106.31(12)	C(29)-C(27)-C(28)	108.35(18)
C(14)-C(13)-C(18)	121.24(13)	C(29)-C(27)-C(29A)	107.70(16)
C(14)-C(13)-C(12)	131.26(13)	C(28)-C(27)-C(29A)	110.0(2)
C(18)-C(13)-C(12)	107.47(12)	C(29)-C(27)-C(24)	112.36(12)

C(28)-C(27)-C(24)	108.64(14)	C(39)-C(37)-C(34)	109.28(13)
C(29A)-C(27)-C(24)	109.81(14)	C(38)-C(37)-C(40)	108.71(15)
C(2)-C(30)-C(31)	129.51(13)	C(39)-C(37)-C(40)	108.49(14)
C(36)-C(31)-C(32)	117.31(12)	C(34)-C(37)-C(40)	108.51(13)
C(36)-C(31)-C(30)	123.65(12)	C(41)-C(37)-C(42)	117(2)
C(32)-C(31)-C(30)	118.87(13)	C(34)-C(37)-C(42)	109.5(13)
C(33)-C(32)-C(31)	121.56(13)	C(41)-C(37)-C(43)	107(2)
C(32)-C(33)-C(34)	121.39(13)	C(34)-C(37)-C(43)	103.4(9)
C(35)-C(34)-C(33)	116.92(13)	C(42)-C(37)-C(43)	92.3(16)
C(35)-C(34)-C(37)	122.87(13)		
C(33)-C(34)-C(37)	120.19(13)	C(52)-O(51)-H(51)	108.9(15)
C(34)-C(35)-C(36)	122.19(13)	O(51)-C(52)-C(53)	112.49(13)
C(35)-C(36)-C(31)	120.55(12)		
C(38)-C(37)-C(39)	109.41(16)	C(62)-O(61)-H(61)	101.9(16)
C(41)-C(37)-C(34)	122.0(18)	O(61)-C(62)-C(63)	114.4(2)
C(38)-C(37)-C(34)	112.35(13)	O(61)-C(64)-C(63)	110.5(11)

Table 3. Anisotropic displacement parameters ($Å^2$ x 10^4) for the expression:

$$\exp\{-2\pi^2(h^2a^{*2}U_{11} + \ldots + 2hka^*b^*U_{12})\}$$

E.s.ds are in parentheses.

	U_{11}	U_{22}	U_{33}	U_{23}	U_{13}	U_{12}
N(1)	232(6)	227(6)	228(5)	-18(4)	74(4)	-17(5)
C(2)	201(6)	219(7)	247(6)	1(5)	51(5)	-29(5)
C(3)	231(7)	255(7)	239(6)	4(5)	60(5)	-54(6)
C(4)	263(7)	347(8)	298(7)	10(6)	68(6)	13(6)
C(5)	257(8)	464(10)	288(7)	36(7)	5(6)	5(7)
C(6)	323(8)	458(10)	224(7)	-23(6)	32(6)	-57(7)
C(7)	294(8)	326(8)	245(7)	-32(6)	78(6)	-59(6)
C(8)	242(7)	234(7)	238(6)	-2(5)	70(5)	-63(5)
C(9)	243(7)	189(6)	236(6)	-3(5)	79(5)	-51(5)
N(10)	264(6)	209(6)	214(5)	-13(4)	74(5)	-20(5)
N(11)	225(6)	207(6)	228(5)	-37(4)	68(4)	6(5)
C(12)	291(7)	187(6)	185(6)	8(5)	86(5)	-9(5)
C(13)	303(7)	199(7)	208(6)	29(5)	107(5)	11(5)
C(14)	383(8)	207(7)	276(7)	0(5)	162(6)	-15(6)
C(15)	447(9)	208(7)	360(8)	-5(6)	239(7)	32(6)
C(16)	366(8)	265(8)	366(8)	49(6)	214(7)	69(6)
C(17)	301(7)	276(7)	273(7)	31(6)	134(6)	33(6)
C(18)	288(7)	210(7)	206(6)	27(5)	104(5)	8(5)
C(19)	220(7)	225(7)	199(6)	18(5)	70(5)	20(5)
C(20)	212(7)	248(7)	216(6)	10(5)	64(5)	13(5)
C(21)	207(6)	221(7)	190(6)	-5(5)	33(5)	-3(5)
C(22)	238(7)	186(6)	237(6)	8(5)	70(5)	-17(5)
C(23)	258(7)	218(7)	247(6)	12(5)	100(5)	-8(5)
C(24)	270(7)	190(7)	229(6)	19(5)	75(5)	4(5)
C(25)	311(7)	196(7)	270(7)	14(5)	109(6)	-39(6)
C(26)	255(7)	264(7)	243(6)	13(5)	106(5)	-27(6)
C(27)	439(9)	188(7)	368(8)	4(6)	221(7)	6(6)
C(28)	2310(40)	422(12)	469(12)	62(10)	701(19)	468(18)
C(29)	586(11)	199(8)	713(12)	-62(8)	416(10)	-13(7)
C(29A)	516(13)	466(13)	1880(30)	-549(16)	673(17)	-128(10)
C(30)	194(6)	241(7)	289(7)	13(5)	71(5)	0(5)
C(31)	204(6)	217(7)	269(7)	-22(5)	89(5)	-36(5)
C(32)	272(7)	266(7)	325(7)	-12(6)	111(6)	44(6)
C(33)	318(8)	282(8)	320(7)	-58(6)	144(6)	39(6)
C(34)	232(7)	262(7)	266(7)	-42(5)	105(5)	-42(6)
C(35)	209(7)	242(7)	267(7)	1(5)	92(5)	5(5)
C(36)	213(6)	232(7)	260(6)	-31(5)	97(5)	-11(5)
C(37)	339(8)	373(9)	256(7)	-46(6)	124(6)	0(7)
C(38)	528(12)	690(15)	243(8)	33(8)	111(8)	254(11)
C(39)	363(10)	519(12)	322(9)	-150(8)	102(7)	-120(9)
C(40)	470(11)	437(11)	337(9)	-40(7)	227(8)	-54(8)
O(51)	487(7)	295(6)	336(6)	-96(5)	140(5)	-92(5)
C(52)	361(9)	325(8)	472(9)	-87(7)	202(7)	-84(7)
C(53)	459(10)	427(10)	494(10)	131(8)	148(8)	-92(8)
O(61)	434(8)	907(12)	376(7)	-55(7)	143(6)	-210(7)
C(62)	298(12)	688(16)	383(12)	-83(10)	34(9)	-17(10)
C(63)	600(14)	717(17)	698(15)	-297(13)	-35(11)	-5(12)

Table 4. Hydrogen coordinates (x 10^4) and isotropic displacement parameters ($Å^2$ x 10^3). All hydrogen atoms were included in idealised positions with U(iso)'s set at 1.2*U(eq) or, for the methyl group hydrogen atoms, 1.5*U(eq) of the parent carbon atoms.

	x	y	z	U(iso)	S.o.f.#
H(4)	8722	1898	5140	38	
H(5)	9233	2692	6253	45	
H(6)	8685	4473	6673	43	
H(7)	7595	5515	5994	36	
H(11)	5683	3413	3788	27	
H(14)	5479	7995	4992	34	
H(15)	4382	8871	4868	38	
H(16)	3386	7491	4208	37	
H(17)	3452	5184	3654	33	
H(20)	3847	2694	3268	28	
H(22)	5223	2577	2780	28	
H(23)	5557	475	2314	29	
H(25)	4356	-2434	2831	32	
H(26)	3981	-315	3257	30	
H(28A)	5072	-1223	1354	153	
H(28B)	4401	-2233	1257	153	
H(28C)	5057	-3074	1216	153	
H(29A)	5119	-4352	2762	68	
H(29B)	5101	-4963	2071	68	
H(29C)	4434	-4130	2094	68	
H(29D)	6175	-1624	2403	134	
H(29E)	6126	-3450	2210	134	
H(29F)	6175	-2930	2923	134	
H(30)	7940	1615	3921	30	
H(32)	7724	370	2897	35	
H(33)	7207	308	1752	36	
H(35)	5891	3737	1748	29	
H(36)	6403	3811	2898	28	
H(38A)	5831	4344	728	75	0.942(4)
H(38B)	5258	3060	673	75	0.942(4)
H(38C)	5484	3295	73	75	0.942(4)
H(39A)	6275	-356	795	62	0.942(4)
H(39B)	5761	421	110	62	0.942(4)
H(39C)	5522	216	703	62	0.942(4)
H(40A)	7159	1624	822	59	0.942(4)
H(40B)	7001	3466	821	59	0.942(4)
H(40C)	6620	2449	161	59	0.942(4)
H(41A)	5924	958	67	89	0.058(4)
H(41B)	6214	-87	727	89	0.058(4)
H(41C)	6737	913	524	89	0.058(4)
H(42A)	6172	4661	843	79	0.058(4)
H(42B)	6006	3962	122	79	0.058(4)
H(42C)	6787	4019	669	79	0.058(4)
H(43A)	5204	3367	795	58	0.058(4)
H(43B)	5093	1501	779	58	0.058(4)
H(43C)	5042	2406	126	58	0.058(4)
H(52A)	7369	9219	4924	45	
H(52B)	6953	10631	5071	45	
H(53A)	6539	10233	3936	71	

H(53B)	5941	9817	4174	71	
H(53C)	6368	8434	4022	71	
H(62A)	8170	8045	6789	59	0.859(8)
H(62B)	8038	8184	7448	59	0.859(8)
H(63A)	8361	10608	7185	116	0.859(8)
H(63B)	7720	10574	6474	116	0.859(8)
H(63C)	7588	10713	7134	116	0.859(8)
H(63D)	8161	10899	7323	116	0.141(8)
H(63E)	8175	9884	6719	116	0.141(8)
H(63F)	7499	10873	6627	116	0.141(8)
H(64A)	7979	8168	7496	67	0.141(8)
H(64B)	7303	9158	7404	67	0.141(8)
H(51)	6623(13)	7520(30)	5123(12)	66(7)	
H(61)	7055(14)	8290(30)	6186(15)	83(8)	

- site occupancy, if different from 1.

Table 5. Torsion angles, in degrees. E.s.ds are in parentheses.

C(9)-N(1)-C(2)-C(30)	-174.22(14)	C(17)-C(18)-C(19)-N(11)	177.12(13)
C(9)-N(1)-C(2)-C(3)	3.16(15)	C(13)-C(18)-C(19)-N(11)	-2.83(14)
C(30)-C(2)-C(3)-C(4)	-6.6(3)	N(11)-C(19)-C(20)-C(21)	-5.4(2)
N(1)-C(2)-C(3)-C(4)	176.09(15)	C(18)-C(19)-C(20)-C(21)	179.24(12)
C(30)-C(2)-C(3)-C(8)	173.04(14)	C(19)-C(20)-C(21)-C(26)	141.94(14)
N(1)-C(2)-C(3)-C(8)	-4.30(15)	C(19)-C(20)-C(21)-C(22)	-39.9(2)
C(8)-C(3)-C(4)-C(5)	0.0(2)	C(26)-C(21)-C(22)-C(23)	0.42(19)
C(2)-C(3)-C(4)-C(5)	179.58(15)	C(20)-C(21)-C(22)-C(23)	-177.79(12)
C(3)-C(4)-C(5)-C(6)	-0.3(2)	C(21)-C(22)-C(23)-C(24)	-0.6(2)
C(4)-C(5)-C(6)-C(7)	0.3(3)	C(22)-C(23)-C(24)-C(25)	-0.6(2)
C(5)-C(6)-C(7)-C(8)	0.1(2)	C(22)-C(23)-C(24)-C(27)	177.59(13)
C(6)-C(7)-C(8)-C(3)	-0.4(2)	C(23)-C(24)-C(25)-C(26)	2.1(2)
C(6)-C(7)-C(8)-C(9)	175.76(15)	C(27)-C(24)-C(25)-C(26)	-176.01(13)
C(4)-C(3)-C(8)-C(7)	0.4(2)	C(24)-C(25)-C(26)-C(21)	-2.4(2)
C(2)-C(3)-C(8)-C(7)	-179.31(13)	C(22)-C(21)-C(26)-C(25)	1.07(19)
C(4)-C(3)-C(8)-C(9)	-176.72(13)	C(20)-C(21)-C(26)-C(25)	179.33(12)
C(2)-C(3)-C(8)-C(9)	3.62(14)	C(25)-C(24)-C(27)-C(29)	-7.8(2)
C(2)-N(1)-C(9)-N(10)	-179.78(12)	C(23)-C(24)-C(27)-C(29)	174.05(15)
C(2)-N(1)-C(9)-C(8)	-0.86(15)	C(25)-C(24)-C(27)-C(28)	112.0(2)
C(7)-C(8)-C(9)-N(1)	-178.48(15)	C(23)-C(24)-C(27)-C(28)	-66.1(2)
C(3)-C(8)-C(9)-N(1)	-1.88(16)	C(25)-C(24)-C(27)-C(29A)	-127.7(2)
C(7)-C(8)-C(9)-N(10)	0.5(2)	C(23)-C(24)-C(27)-C(29A)	54.2(2)
C(3)-C(8)-C(9)-N(10)	177.09(12)	N(1)-C(2)-C(30)-C(31)	6.2(2)
N(1)-C(9)-N(10)-C(12)	30.1(2)	C(3)-C(2)-C(30)-C(31)	-170.75(13)
C(8)-C(9)-N(10)-C(12)	-148.77(13)	C(2)-C(30)-C(31)-C(36)	10.9(2)
C(9)-N(10)-C(12)-N(11)	2.9(2)	C(2)-C(30)-C(31)-C(32)	-173.85(15)
C(9)-N(10)-C(12)-C(13)	177.17(12)	C(36)-C(31)-C(32)-C(33)	1.7(2)
C(19)-N(11)-C(12)-N(10)	169.89(12)	C(30)-C(31)-C(32)-C(33)	-173.81(14)
C(19)-N(11)-C(12)-C(13)	-5.33(15)	C(31)-C(32)-C(33)-C(34)	0.5(2)
N(10)-C(12)-C(13)-C(14)	6.4(2)	C(32)-C(33)-C(34)-C(35)	-2.6(2)
N(11)-C(12)-C(13)-C(14)	-178.32(13)	C(32)-C(33)-C(34)-C(37)	175.67(14)
N(10)-C(12)-C(13)-C(18)	-171.97(13)	C(33)-C(34)-C(35)-C(36)	2.5(2)
N(11)-C(12)-C(13)-C(18)	3.26(14)	C(37)-C(34)-C(35)-C(36)	-175.66(13)
C(18)-C(13)-C(14)-C(15)	-1.8(2)	C(34)-C(35)-C(36)-C(31)	-0.4(2)
C(12)-C(13)-C(14)-C(15)	179.99(13)	C(32)-C(31)-C(36)-C(35)	-1.8(2)
C(13)-C(14)-C(15)-C(16)	1.0(2)	C(30)-C(31)-C(36)-C(35)	173.52(13)
C(14)-C(15)-C(16)-C(17)	0.3(2)	C(35)-C(34)-C(37)-C(41)	-160(3)
C(15)-C(16)-C(17)-C(18)	-0.8(2)	C(33)-C(34)-C(37)-C(41)	22(3)
C(16)-C(17)-C(18)-C(13)	0.1(2)	C(35)-C(34)-C(37)-C(38)	0.5(2)
C(16)-C(17)-C(18)-C(19)	-179.85(13)	C(33)-C(34)-C(37)-C(38)	-177.60(16)
C(14)-C(13)-C(18)-C(17)	1.2(2)	C(35)-C(34)-C(37)-C(39)	-121.11(16)
C(12)-C(13)-C(18)-C(17)	179.85(12)	C(33)-C(34)-C(37)-C(39)	60.76(18)
C(14)-C(13)-C(18)-C(19)	-178.80(12)	C(35)-C(34)-C(37)-C(40)	120.76(16)
C(12)-C(13)-C(18)-C(19)	-0.19(14)	C(33)-C(34)-C(37)-C(40)	-57.36(19)
C(12)-N(11)-C(19)-C(20)	-171.13(13)	C(35)-C(34)-C(37)-C(42)	58.2(14)
C(12)-N(11)-C(19)-C(18)	5.17(14)	C(33)-C(34)-C(37)-C(42)	-120.0(14)
C(17)-C(18)-C(19)-C(20)	-6.7(2)	C(35)-C(34)-C(37)-C(43)	-39.2(11)
C(13)-C(18)-C(19)-C(20)	173.33(13)	C(33)-C(34)-C(37)-C(43)	142.7(11)

Table 6. Hydrogen bonds, in Ångstroms and degrees.

D-H...A	d(D-H)	d(H...A)	d(D...A)	<(DHA)
N(11)-H(11)...N(1)	0.88	2.15	2.7133(16)	120.9
C(20)-H(20)...O(61)#1	0.95	2.35	3.2666(19)	161.7
O(51)-H(51)...N(10)	0.94(3)	1.88(3)	2.8182(16)	176(2)
O(61)-H(61a)...O(51)	0.99(3)	1.76(3)	2.7340(18)	164(3)

Symmetry transformations used to generate equivalent atoms:
#1 : 1-x, 1-y, 1-z

Crystal structure analysis of Bu^t-C_6H_4-CH-isoindole-N-(isoindole-H)-CH-C_6H_4-Bu^t

Crystal data: $C_{38}\,H_{37}\,N_3$, $2(C_2\,H_6\,O)$, M = . 627.84. Monoclinic, space group $P2_1/n$ (no. 14), a = 21.2122(4), b = 8.49586(12), c = 22.1333(4) Å, β = 114.313(2) °, V = 3635.02(12) $Å^3$. Z = 4, Dc = 1.147 g cm^{-3}, F(000) = 1352, T = 100(2) K, μ(Cu-Kα) = 5.43 cm^{-1}, λ(Cu-Kα) = 1.54184 Å.

The crystal was an orange cuboid. From a sample under oil, one, *ca* 0.18 x 0.21 x 0.93 mm, was mounted on a small loop and fixed in the cold nitrogen stream on a Rigaku Oxford Diffraction XtaLAB Synergy diffractometer, equipped with Cu-Kα radiation, HyPix detector and mirror monochromator. Intensity data were measured by thin-slice ω-scans. Total no. of reflections recorded, to θ_{max} = 72.5°, was 29,580 of which 6,998 were unique (Rint = 0.052); 6,241 were 'observed' with $I > 2\sigma_I$.

Data were processed using the CrysAlisPro-CCD and -RED (1) programs. The structure was determined by the intrinsic phasing routines in the SHELXT program (2A) and refined by full-matrix least-squares methods, on F^2's, in SHELXL (2B). In addition to the principal, bis-indole molecule, there are two ethanol solvate molecules in the asymmetric unit There are two sites of disorder – one in one of the *t*-butyl groups, the other in one of the solvent molecules. The non-hydrogen atoms (excepting the minor components of the disordered groups) were refined with anisotropic thermal parameters. The hydrogen atoms of the methanol solvent molecules were located in difference maps and were refined freely. The remaining hydrogen atoms were included in idealised positions and their Uiso values were set to ride on the Ueq values of the parent carbon atoms. At the conclusion of the refinement, wR_2 = 0.130 and R_1 = 0.054 (2B) for all 6,998 reflections weighted $w = [\sigma^2(F_o^2) + (0.0634\ P)^2 + 1.425\ P]^{-1}$ with $P = (F_o^2 + 2F_c^2)/3$; for the 'observed' data only, R_1 = 0.049.

In the final difference map, the highest peak (*ca* 0.33 $eÅ^{-3}$) was near O(61).

Scattering factors for neutral atoms were taken from reference (3). Computer programs used in this analysis have been noted above, and were run through WinGX (4) on a Dell Optiplex 780 PC at the University of East Anglia.

References

(9) Programs CrysAlisPro, Rigaku Oxford Diffraction Ltd., Abingdon, UK (2018).

(10) G. M. Sheldrick, Programs for crystal structure determination (SHELXT), *Acta Cryst.* (2015) A**71**, 3-8, and refinement (SHELXL), *Acta Cryst.* (2008) A**64**, 112-122 and (2015) C**71**, 3-8.

(11) *'International Tables for X-ray Crystallography'*, Kluwer Academic Publishers, Dordrecht (1992). Vol. C, pp. 500, 219 and 193.

(12) L. J. Farrugia, *J. Appl. Cryst.* (2012) **45**, 849–854.

Legends for Figures

Figure 1. View of the bis-isoindole derivative, with the two associated ethanol solvent molecules, indicating the atom numbering scheme. Thermal ellipsoids are drawn at the 50% probability level.

Figure 2. The packing of molecules, viewed along the *b* axis.

Notes on the structure

The structure comprises the bis-isoindole derivative and two ethanol/solvent molecules. The outermost ethanol molecule is hydrogen bonded to the inner ethanol which is itself hydrogen bonded to the bis-isoindole molecule. A third, intramolecular, hydrogen bond is found between the two isoindole units, N(11)-H(11)…N(1).

Each of the isoindole units and the phenyl groups are essentially planar, but there is rotation in the bridging groups, viz. 10.9° about the C(30)-C(31 bond, 30.1° about C(9)-N(1), and 39.9° about C(20)-C(21), indicating a spiralling of the units to give a significant distortion from a planar molecule.

In addition to the intermolecular hydrogen bonding contacts noted above, we find π…π overlaps between the rings including C(13) and its related neighbour, perpendicular H…π contacts [as H(6) towards the centre of the neighbouring C(21'-26') ring], and van der Waals' contacts [as H(30)…H(42c')].